

ÉCOLE DOCTORALE 414

**Institut de génétique et de biologie moléculaire et cellulaire
(IGBMC)**

CNRS UMR 7104 – INSERM U 964

THÈSE présentée par
Thibaud METZGER

Soutenue le 25 mars 2014

pour obtenir le grade de : **Docteur de l'université de Strasbourg**

Discipline/ Spécialité : Aspects moléculaires de la biologie

**Molecular mechanisms of PLK1 recognition
by CUL3/KLHL22 E3-ubiquitin ligase
controlling mitotic progression**

**Mécanismes moléculaires de reconnaissance de PLK1
par l'E3-ubiquitine ligase CUL3/KLHL22 contrôlant la
progression mitotique**

THÈSE dirigée par :

Mme SUMARA Izabela

Dr., Université de Strasbourg

RAPPORTEURS :

Mme OLIFERENKO Snezhana

Mr PINTARD Lionel

Mr RICCI Romeo

Dr., King's College London, London

Dr., Institut Jacques Monod, Paris

Pr.-PUPH., IGBMC, Strasbourg

Acknowledgments / Remerciements

I could not thank enough all the people that contributed to this work, not only on the scientific but also on the human level, to make this PhD a great experience.

First of all, I would like to thank all jury members, Snezhana, Lionel and Romeo for agreeing to judge my work. I am sure your expertise will provide great insights and help defining future directions of the project.

Iza, I don't even know where to start! Thank you for giving me the opportunity to do my PhD in your lab. The whole setting-up-the-lab period was quite challenging, and I'm glad I was involved in it. Thanks for always being available for discussion. It has not been easy every day, we unfortunately did not achieve all we aimed at, but be sure I had a great time working at your side. You give your students a lot of freedom, supporting self-management and scientific curiosity and for this I am very grateful. Keep up the optimism, the best is yet to come! Good luck with everything!

I thank very warmly all members of the Sumara lab. Each and every one of you brought his own expertise and his own personality, and all this together made the lab a great place to work in. Special thanks goes to Charlotte for the help on my project, our (not always) smart discussions during coffee breaks and for adjusting pH so nicely ;-), and to Steff for scientific guidance, tremendous work on the NICE-4 project (and for coffee breaks!). You both helped me a lot, so thank you so much!

I would like to thank also very warmly Andrea Musacchio, member of my thesis committee for the great inputs and advices on my project, for inviting me to Dortmund to discuss troubleshooting with him and his people and for the Aurora B-INCENP IN box construct he kindly shared with us.

Thanks to the whole Ricci lab for comments during our seminar and to Marie-Laure Diebold, Claire Batisse, Nicolas Levy, Christophe Romier and Marc Ruff from the

Structural Department for the incredible number of questions they answered me during these three years.

Thanks a lot to all IGBMC's common facilities, especially the mass spectrometry, the antibody production and the cloning services and thanks to IGBMC, ATIP-Avenir and UDS for funding this work.

Thanks to all members of our IGBMC-Indoor-football team: we fought hard, battling for power and supremacy, and despite injuries we kept on coming back every Thursday! That's the spirit!

Un immense merci à toute la team du RU, Anne-So, Stéphanie, Léa, Rose, Sarah, David, Thomas, Jérôme, Adrien and Salim. Même si j'ai râlé TOUS les jours du fait de votre ponctualité catastrophique, on se sera quand même bien marré! Portez-vous bien et bonne chance pour la suite!

Je remercie également tous mes amis au sein et en dehors de l'IGBMC qui m'ont permis de rester sain d'esprit et de me changer les idées quand tout ne filait pas droit! Un immense big up à La Meute, toujours là pour représenter!

J'aimerais remercier toute ma famille et ma belle-famille pour leur soutien sans faille. Maman, Papa, c'est grâce à vous si j'en suis là aujourd'hui, merci pour tout! Quant à toi Pépère, tu as enfin la preuve écrite que je n'ai JAMAIS travaillé avec des mouches!

Enfin, un immense merci à Anne-Sophie toujours à me soutenir depuis tant d'années. Je me rappelle il y a six ans tu me faisais déjà apprendre en speed mes exams de génétique. Pendant toute cette thèse tu as continué à m'aider, tous les jours, supportant mon caractère parfois un peu pourri (je l'admets!), mes manips qui ne marchaient pas et mes dimanches au labo. Je ne sais pas où on sera dans 6 mois, mais une chose est sûre, tous les deux, tout ne peut que bien se passer! Merci pour tout!

A ma mamie, Nicole

1 Table of contents

1	Table of contents	1
2	Résumé de thèse	3
3	Summary	6
4	Introduction	8
4.1	Progression through mitosis.....	9
4.2	Control of mitosis.....	10
4.3	Regulation of mitosis by phosphorylation	11
4.3.1	Cyclin-dependent protein kinases (CDKs)/Cyclins:	11
4.3.2	Polo-like kinase family:.....	12
4.3.3	Aurora Kinase family:	17
4.4	Regulation of mitosis by protein ubiquitination.....	20
4.4.1	The ubiquitin-proteasome system	20
4.4.2	Cullin-RING E3-ubiquitin ligases	21
4.4.2.1	The SCF complex	23
4.4.2.2	The APC/C.....	23
4.4.2.3	CUL3 E3-ubiquitin ligases	24
5	Aim of the thesis.....	29
6	Results.....	30
6.1	Results part 1: Manuscript: Ubiquitylation-dependent localization of PLK1 in mitosis.	31
6.2	Results part 2 : How does KLHL22 interact with PLK1 and what about other KELCH/Kinase complexes ?.....	45
6.2.1	Manuscript: CUL3 and protein kinases: insights from PLK1/KLHL22 interaction. ..	45
6.2.2	Unbiased approaches.....	52
6.2.2.1	Peptide array and truncation experiments	52
6.2.2.2	In vitro complex reconstitution of PLK1/KLHL22 and other Kinase/Kelch adaptor complexes	57
6.2.2.3	Reconstitution of PLK1/KLHL22 complex by coexpression	59
6.2.2.4	Reconstitution of PLK1/KLHL22 complex by separate expression.....	60
6.2.2.5	Reconstitution of Aurora B/KLHL21 complex by separate expression	64
6.2.3	Hypothesis-driven approaches.....	74
6.2.3.1	How does KLHL22 interact with the PBD of PLK1?.....	74
6.2.3.2	How does KLHL22 interact with the kinase domain of PLK1?	77

6.3	Results part 3: Identification and characterization of novel components of PLK1/KLHL22 pathway	80
7	Discussion	89
7.1	A general mechanism for kinase recognition by BTB-Kelch adaptors?	89
7.2	Post-translational modifications may not be required for PLK1/KLHL22 interaction.....	89
7.3	The DLG/DFG-motif could constitute a common recognition site between kinases and BTB-Kelch adaptors.....	90
7.4	The PBD-mediated interaction of PLK1 with KLHL22 might ensure specificity of this complex.....	92
7.5	The D-box of PLK1 does not appear to be involved in KLHL22 binding.....	92
7.6	Poor protein stability prevented structural studies.....	94
7.7	The PLK1-PBD shows mitosis-specific interactions with proteins involved in cell cycle regulation	97
7.8	NICE-4 interacts with PLK1-PBD and is involved in faithful mitotic regulation.....	98
8	Materials and methods	101
9	Abbreviations	113
10	References	115
11	Appendix.....	130
11.1	Appendix I. List of the 614 hits found in each of four GST-PLK1-PBD pulldowns. 130	
11.2	Appendix II. List of the 458 hits found in GST-PLK1-PBD-UBI pulldown.	165
11.3	Appendix III. List of the 115 hits identified in both the GST-PLK1-PBD wild-type and the GST-PLK1-PBD-UBI mutant.	190

2 Résumé de thèse

La découverte de l'ubiquitine en 1975 (Goldstein et al., 1975) et la compréhension de son rôle essentiel pour la régulation protéolytique des protéines a entraîné un engouement considérable au sein de la communauté scientifique. Cependant, au cours des dernières années, il est devenu clair que l'ubiquitination des protéines n'a pas pour seule conséquence la dégradation de celles-ci, mais permet aussi de réguler leur signalisation cellulaire. En effet, l'attachement d'ubiquitine peut aussi influencer sur la localisation des protéines, l'assemblage de complexes protéiques et les activités enzymatiques (Li and Ye, 2008). Les E3-ubiquitine ligases sont les membres les plus critiques de la machinerie de conjugaison de l'ubiquitine car elles sont responsables de la spécificité vis-à-vis du substrat. Nos propres études, dans les cellules de mammifères, ont permis d'identifier les E3-ubiquitine ligases à sous-unité de type Cullin3 en tant que nouveaux et importants régulateurs de la mitose (Maerki et al., 2009; Sumara and Peter, 2007; Sumara et al., 2007). Ainsi, notre laboratoire a caractérisé plusieurs complexes à sous-unité Cullin3 qui sont requis pour la progression mitotique et plus particulièrement pour la coordination entre l'alignement des chromosomes, leur ségrégation et l'achèvement de la cytokinèse. De plus, nous avons identifié la protéine à domaines BTB et Kelch, KLHL21, en tant qu'important facteur fonctionnel spécifique de la régulation par CUL3 de la localisation de la kinase Aurora B et de l'accomplissement de la cytokinèse (Maerki et al., 2009).

Le travail de recherche effectué décrit le rôle d'une E3 à CUL3 comprenant une autre protéine adaptatrice à domaine BTB, KLHL22, dans la régulation de la kinase mitotique Polo-Like Kinase 1 (PLK1). En effet, la déplétion de KLHL22 induit de sévères défauts mitotiques et fréquemment une mort cellulaire en prométaphase. Après des expériences de criblage haut-débit, de co-immunoprécipitation et d'interaction *in vitro*, nous avons identifié PLK1 comme interagissant de manière directe avec KLHL22. Comme le niveau de PLK1 dans les cellules déplétées de KLHL22 reste similaire aux conditions sauvages, l'ubiquitination de PLK1 par CUL3/KLHL22 ne conduit pas à une dégradation de la protéine. Au contraire, elle semble réguler la localisation de PLK1 : les cellules déplétées de KLHL22 montrent une localisation plus abondante de PLK1 au niveau des kinétochores des chromosomes. Celle-ci est corrélée à une augmentation de la phosphorylation de BUBRI sur sa sérine 676 (S676), préalablement montrée comme

signalant les attachements incorrects entre les kinétochores et les microtubules en prometa/metaphase (Elowe et al., 2007). Des tests d'ubiquitination *in vitro* ont montré que PLK1 était mono-ubiquitinée par CUL3/KLHL22 au niveau de sa lysine 492 (K492), confirmant ainsi l'hypothèse d'une régulation spatiale et non protéolytique de PLK1. Le mutant de PLK1 K492R mimique parfaitement l'inactivation de KLHL22 par ARN interférence à savoir une rétention de PLK1 au niveau des kinétochores, une hyperphosphorylation de BUBRI, accompagnée d'une délocalisation du senseur d'attachement stables entre les kinétochores et les microtubules, RANGAP1. Ainsi nous concluons que l'addition d'une molécule d'ubiquitine sur la protéine kinase PLK1 par l'E3-ubiquitine ligase CUL3/KLHL22 est nécessaire à son retrait des kinétochores stabilisant leurs contacts avec les microtubules, nécessaires à une ségrégation chromosomique parfaite (Beck et al., 2013).

Dans la continuité de cette étude, nous avons pu démontré que l'activité catalytique de PLK1 n'était pas nécessaire à son interaction avec KLHL22. L'expression de mutants tronqués de PLK1, nous a également permis d'observer que aussi bien son domaine kinase que son domaine Polo (PBD) étaient suffisants à la co-purification de KLHL22, aussi bien à partir de protéines exprimées en bactérie et donc probablement sans modification post-traductionnelle, qu'à partir de cellules mammifères (Metzger et al., 2013). De manière intéressante, le PBD de PLK1 a depuis longtemps été montré comme essentiel à la localisation de la protéine, de part sa capacité à interagir avec des protéines-réceptrices phosphorylées (Elia et al., 2003a; Elowe et al., 2007; Goto et al., 2006; Qi et al., 2006). Des mutations au niveau des résidus H538A/K540M du PBD sont connues pour abroger ces interactions phopsho-dépendentes, mais nos récentes données non-publiées ont pu montrer qu'elles n'influent pas significativement sur l'interaction avec KLHL22. La mutation du tryptophane 414 (W414F), impliqué dans les interactions avec des récepteurs non-phosphorylés, réduit quant-à-elle fortement l'affinité de KLHL22 pour PLK1. Au niveau du domaine kinase, mutant au niveau du motif DFG situé en amont de la boucle d'activation de PLK1 (résidus 194 à 196) semblent influencer sur son interaction avec KLHL22 et nous sommes à l'heure actuelle entrain de caractériser ces effets *in vivo*. Désirant comprendre plus en détails les interactions entre ces deux protéines, nous nous sommes orientés vers des études structurales du complexe. Cependant, dû au caractère agrégé de KLHL22 ou des

différents mutants tronqués testés, nous avons à l'heure actuelle dû abandonner cette approche.

En résumé, notre étude a pu montrer l'importance de l'ubiquitination de PLK1 par CUL3/KLHL22 pour une régulation mitotique parfaite. Bien que les mécanismes sous-jacents de cette interaction soient encore loin d'être parfaitement compris, nous avons ainsi obtenu les premières indications biochimiques du mode d'interaction des E3-ubiquitin ligases à sous-unité CUL3 avec des protéines kinases.

3 Summary

The discovery of ubiquitin in 1975 (Goldstein et al., 1975) and the understanding of its essential role in the proteolytic degradation of proteins generated a great enthusiasm among the scientific community. Over the last decade, it became clear the ubiquitination of proteins not only targets them for degradation but also can regulate signalling pathways. Indeed, ubiquitin conjugation may induce relocalization of substrate proteins, but also participate in the assembly of macro-molecular complexes and regulate enzymatic activities (Li and Ye, 2008). E3-ubiquitin ligases are the most critical members of the ubiquitination machinery as they provide substrate specificity. Our own studies in human cells identified the CUL3-based ubiquitin E3-ligase as a novel and important regulator of mitosis (Maerki et al., 2009; Sumara and Peter, 2007; Sumara et al., 2007). We have characterized several CUL3-based complexes required for mitotic progression in particular for coordination of chromosome alignment and segregation with completion of cytokinesis (Maerki et al., 2009).

Moreover, we identified the BTB- and Kelch-domain containing protein KLHL21 as a functionally important specificity factor for CUL3-dependent regulation of Aurora B kinase localization and completion of cytokinesis. The research presented here describes the role of novel CUL3-based E3-ligase, associating with BTB-Kelch adaptor KLHL22 to regulate major mitotic kinase Polo-Like Kinase 1 (PLK1). Indeed, inactivation of KLHL22 leads to severe mitotic defects and often to apoptotic death in prometaphase. Following high-throughput screening, co-immunoprecipitations and interactions tests *in vitro*, we identified PLK1 as a direct interactor of KLHL22. KLHL22 inactivation did not influence the total level of PLK1, suggesting that CUL3/KLHL22 mediated ubiquitination of PLK1 does not lead to degradation. However, when depleted for KLHL22, we could observe a more abundant localization of the kinase on kinetochores (KT) of chromosomes, and consistently an increased phosphorylation of known substrate of PLK1, BubRI on its serine 676 (S676), which is a marker of unattached kinetochores to the spindle-microtubules in prometa/metaphase (Elowe et al., 2007). *In vitro* ubiquitination tests showed that PLK1 was readily mono-ubiquitinated by CUL3/KLHL22 on its lysine 492 (K492). Expression of PLK1 K492R mutant resembles KLHL22 RNAi phenotype as an increased retention of PLK1 on kinetochores, hyper-phosphorylation of BUBRI and delocalization of the microtubule-kinetochore

attachment sensor RANGAP1 was observed. We thereby concluded that PLK1 ubiquitination by CUL3/KLHL22 E3-ubiquitin ligase is essential for its removal from kinetochore to stabilize their interaction with microtubules, that is essential for proper chromosome segregation (Beck et al., 2013).

Following this study, we could further demonstrate that the catalytic activity of PLK1 was not required for its interaction with KLHL22. Using truncated mutants of PLK1, we could observe that both the kinase and the Polo-Box Domain (PBD) were sufficient to co-purify KLHL22 from bacteria, thus presumably without prior post-translational modification, and from mammalian cells (Metzger et al., 2013). Interestingly, PLK1-PBD has previously been shown to be implicated in the recruitment of the kinase to specific subcellular localization during mitosis thanks to its ability to bind phosphorylated receptor-proteins (Elia et al., 2003a; Elowe et al., 2007; Goto et al., 2006; Qi et al., 2006). Mutations H538A/K540M within the PLK1-PBD are known to abrogate phospho-dependent interactions between PLK1 and its receptors, but did not significantly influence its affinity towards KLHL22. In contrary, mutation of W414F, responsible for interactions with non-phosphorylated receptors, highly decreased KLHL22 binding to PLK1. Within the kinase domain, changes in the DFG-motif, located at the beginning of the activation loop (amino-acids 194-196) seems to influence KLHL22 affinity and we are currently characterizing these effects *in vivo*. In order to understand molecular interaction between PLK1 and KLHL22 in details, we were interested in pursuing crystallographic approaches, as they can provide atomic-resolution of multi-protein complexes. However, due to the aggregated state of KLHL22 and the different truncation mutants tested, we were unable to reconstitute a soluble complex in quantity and quality sufficient for structural studies.

As a summary, our research could demonstrate the importance of PLK1 ubiquitination by CUL3/KLHL22 for faithful completion of mitosis. Although the molecular mechanisms underlying this process are still far from being uncovered, we obtained first biochemical insights into the mode of interaction between CUL3-complexes and kinases.

4 Introduction

Cell reproduction is essential for all living organisms. The highly regulated series of events that mediates cell proliferation is called cell cycle. Its role is to ensure that replicated copies of the genome are properly segregated to the daughter cells. First, DNA is duplicated in *synthetic* or *S phase* and then the two copies are equally distributed between the two daughter cells in *mitosis* or *M phase* (**Fig. 1**). Both are separated by so-called gap phases: *G1* takes place before *S phase*, which is followed by *G2*. Both are mostly preparative stages, in which cells grow in size and produce proteins essential for the following steps. During *G1*, cells lacking optimal growth conditions can also exit temporarily the cell cycle and reach a quiescent stage, *G0*, in which they are neither dividing, nor preparing to divide, but only fulfill their main metabolic functions. Often terminally differentiated cells also reach *G0*, but those hardly re-enter the cell cycle.

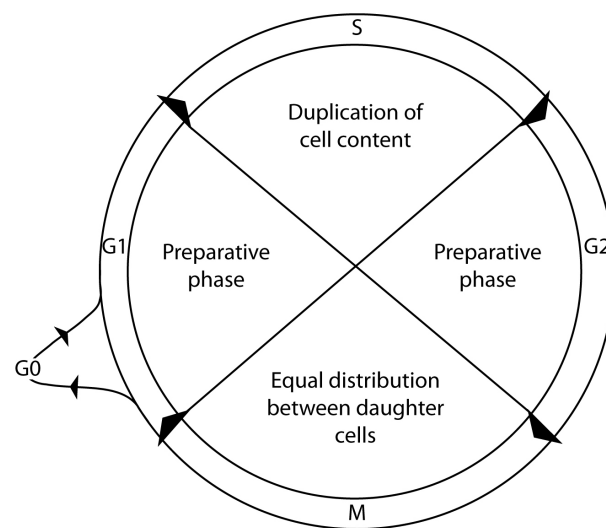


Figure 1. Simplified scheme of the cell cycle. The different phases *G0*, *G1*, *S* (synthetic), *G2* and *M* (mitosis) are represented.

4.1 Progression through mitosis

At the end of S phase, duplicated chromosomes assemble pairs of so-called sister chromatids that are maintained together by a Cohesin complex made of specialized proteins called cohesins. In the first stage of mitosis, prophase, condensation of sister chromatids into chromosomes and breakdown of the nuclear envelope take place. Duplicated centrosomes separate and migrate towards opposite poles of the cell. From them microtubules start to nucleate, that constitute the mitotic spindle. Subsequently, these microtubules attach to specific proteinous structures, called kinetochores, assembled on centromeres of all sister chromatids. This bipolar attachment allows to move and maintain each chromosome to the metaphase plate during prometaphase and metaphase stages. When all chromosomes are correctly attached and aligned, cells can enter anaphase: cohesins are cleaved allowing the paired chromatids to segregate towards opposite poles of the cell. Once chromatids reach centrosomes, cell enters telophase stage, in which nuclear envelope is re-formed around decondensing chromosomes. Cytokinesis then starts, separating the cytoplasm into two daughter cells thanks to formation of the cleavage furrow in the equatorial zone of the cell and its constriction in the midbody (**Fig. 2**).

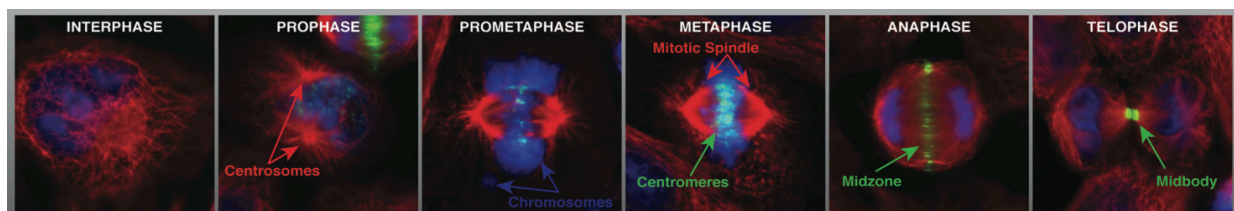


Figure 2. Cell cycle stages of human cells from interphase to mitosis (prophase, prometaphase, metaphase, anaphase and telophase). DNA is represented in blue (DAPI), tubulin in red and green represents localization of Aurora B kinase, a marker of centromeres and midzone. (Adapted from (Fournane et al., 2012))

4.2 Control of mitosis

To ensure the precise spatial and temporal coordination of mitotic events, cells have developed a cell-cycle control system, made of four major checkpoints (Morgan, 1997) (**Fig. 3**). The G1/S checkpoint prevents *S phase* onset as long as environmental conditions are not optimal. The S-phase checkpoint acts during the whole S phase, when the progression of the replication fork becomes stalled in response to stresses like DNA damage or depletion of nucleotides. Its role is to signal and coordinate reparation of the damage as well to protect the integrity of the replication fork. The G2/M or DNA damage checkpoint ensures that the whole genome is replicated and undamaged before mitotic entry, and finally, the Spindle Assembly Checkpoint (SAC), controls the metaphase-to-anaphase transition by ensuring bipolar attachment of kinetochores of all chromosomes to the spindle microtubules before anaphase onset. All these checkpoints are driven by the controlled regulation of major cell cycle protein kinases, phosphorylation of specific substrates and ubiquitination-dependent degradation of key components.

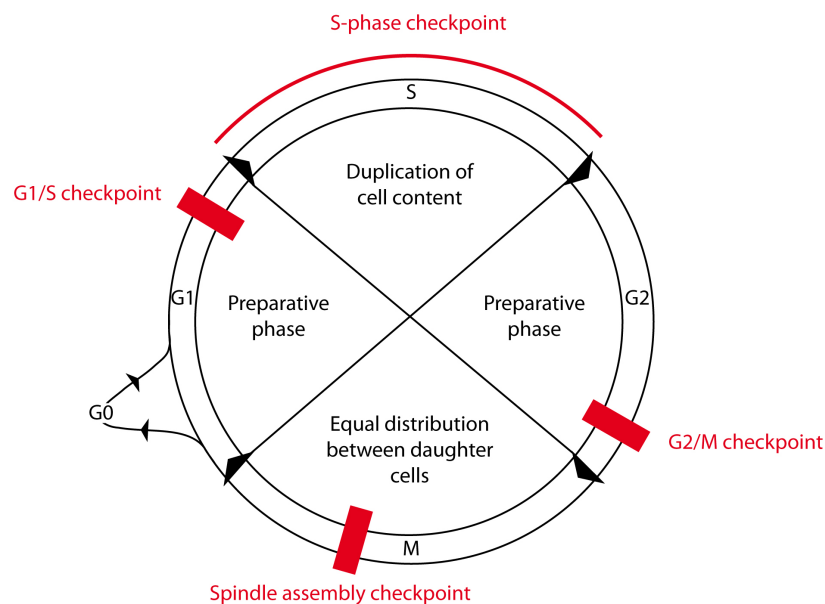


Figure 3. Simplified scheme of the cell cycle and its checkpoints. The different phases G0, G1, S (synthetic), G2 and M (mitosis) are represented in black, whereas red bars mark the different checkpoints ensuring faithful progression through each stage of the cell cycle: the G1/S checkpoint, the S-phase checkpoint, the G2/M checkpoint, and the Spindle Assembly Checkpoint (SAC).

4.3 Regulation of mitosis by phosphorylation

There are several families of protein kinases involved in faithful progression of mitosis. While Cyclin-dependent kinases are undoubtedly the master regulators of cell cycle, two other families of protein kinases have been shown to be essential for progression through mitosis: the Polo-like kinases and the Aurora kinases (Morgan, 1997; Nigg, 2001)

4.3.1 Cyclin-dependent protein kinases (CDKs)/Cyclins:

CDKs are the central components of the cell-cycle control system. Their levels of expression are mostly constant during the cell cycle but their activation depends on association with transcriptionally regulated subunits known as Cyclins. Different CDK/Cyclin complexes are formed throughout the cell cycle, thereby coordinating spatio-temporal regulation and ensuring uni-directionality of the cell cycle progression (**Fig. 4**). In response to growth factors, Cyclin D is synthesized. It interacts with CDK4/6, allowing exit from G₀ and entry into a new cell cycle. This leads to the formation of active CDK2/Cyclin E complex driving progression through the G₁/S checkpoint, entry into S phase when CDK2 associates with Cyclin A triggering the initiation and progression of DNA replication. At the S/G₂ transition, Cyclin A relocates from the nucleus to the centrosomes, where it associates with CDK1 which contributes to the preparation of mitosis. The transcription of Cyclin B is switched on, and concentration of the protein increases during G₂. Perfectly replicated and undamaged chromosomes trigger association of CDK1/Cyclin B at centrosomes (Jackman et al., 2003), that allows silencing of the G₂/M checkpoint and the cell progression through mitosis. During mitosis, numerous substrates of CDK1/Cyclin B were described. For instance, the motor protein EG5 that is essential for proper centrosomes separation (Blangy et al., 1995) and Lamins important for nuclear envelope breakdown (Lüscher et al., 1991; Peter et al., 1990). CDK1/Cyclin B is also essential for proper chromosome condensation in prophase as it phosphorylates Condensin (Abe et al., 2011) and for proper metaphase-to-anaphase transition by regulation of the Anaphase-Promoting Complex/Cyclosome (APC/C) (Kraft et al., 2003). Ultimately, activation of APC/C induces Cyclin B destruction,

and thereby CDKs inactivation. This triggers mitotic exit by disassembling the mitotic spindle, and initiates cytokinesis.

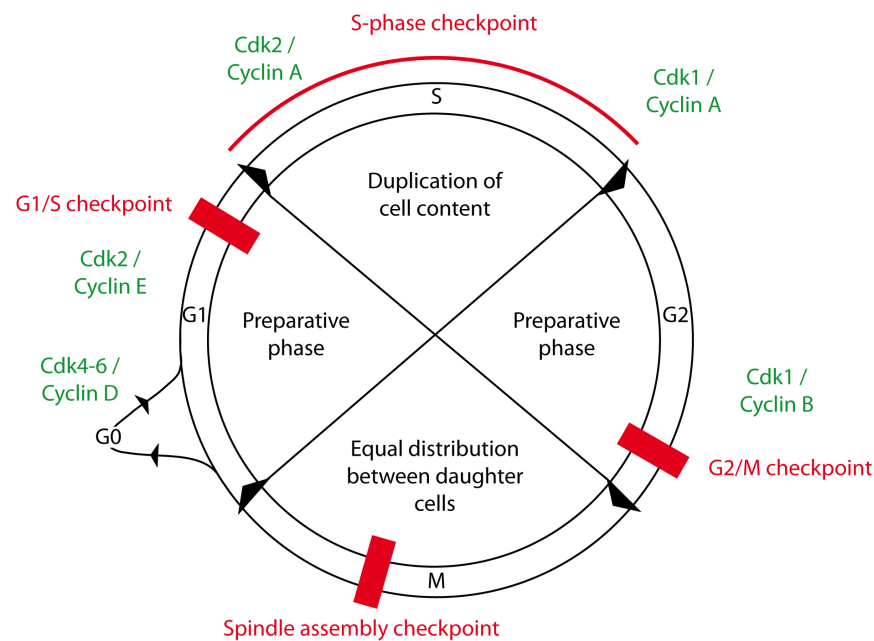


Figure 4. Simplified scheme of the cell cycle control by CDK/Cyclin complexes. The different phases G0, G1, S (synthetic), G2 and M (mitosis) are represented in black, whereas red bars mark the different checkpoint ensuring faithful progression through each stage of the cell cycle. The different CDK/Cyclin complexes regulating progression of the cell cycle are represented in green.

4.3.2 Polo-like kinase family:

Members of the Polo-Like Kinase (PLK) family are defined based on their common architecture: a N-terminal Ser/Thr kinase domain precedes a regulatory domain called Polo-Box Domain (PBD), made of one or two polo-boxes (**Fig. 5A**). To date, it consists of four members that perform crucial but non-overlapping functions during the cell cycle. PLK2 is expressed in G1, where it mediates signaling for entry into S-phase (Ma et al., 2003). During this stage, PLK2 is also required for faithful response to replication stress and DNA damage (Matthew et al., 2007). PLK3 expression is stable throughout the cell cycle and has been shown to be involved in mitosis by regulating microtubules dynamics (Ouyang, 1997; Wang et al., 2002), in DNA damage response (Xie et al., 2001) and in

Golgi dynamics (Xie et al., 2004). To date, PLK4 was only described as being essential for centriole duplication (Habedanck et al., 2005). The most characterized member of the PLK family is PLK1, whose level of expression increases in late G2 and peaks during the whole mitosis (Golsteyn et al., 1995). It displays a very dynamic localization during mitotic progression (**Fig. 5B**). In late G2, PLK1 localizes to centrosomes where it promotes mitotic entry by phosphorylation of Cyclin B1 and CDC25C, leading to increased activity of CDK1 (Toyoshima-morimoto et al., 2001; Toyoshima-Morimoto et al., 2002). This induces CDK1-mediated phosphorylation of BORA in complex with Aurora A (Chan et al., 2008), which in turn phosphorylates PLK1 in its activation loop (on T210) (Seki et al., 2008), resulting in its full activation. PLK1 is also essential for proper centrosome maturation. Indeed, depletion of PLK1 leads to formation of monopolar spindles (Sumara et al., 2004) by altering the recruitment of the γ -Tubulin ring complex (Lane and Nigg, 1996), and by preventing phosphorylation of key factors: KIZUNA, responsible for stabilizing centrosomes when the mitotic spindle is formed (Oshimori et al., 2006), Abnormal Spindle (ASP) (do Carmo Avides et al., 2001) and Ninein-Like Protein (NLP)(Casenghi et al., 2005), both involved in microtubule nucleation, and PERICENTRIN required for the recruitment of γ -Tubulin (Lee and Rhee, 2011).

In prometaphase and metaphase stages, PLK1 localizes to kinetochores of chromosomes, where it regulates their attachment to spindle microtubules. Initial recruitment and maintenance of PLK1 at kinetochores is mediated via its interaction with PBIP (Kang et al., 2006). Formation of the PLK1/PBIP complex actually induces degradation of PBIP, but PLK1 is retained in the vicinity of kinetochores, via interactions with other proteins such as INCENP and components of the SAC BUB1 and BUBRI (Elowe et al., 2007; Goto et al., 2006; Qi et al., 2006). Interestingly, the SAC-induced prometaphase arrest observed in PLK1 depleted cells suggests that PLK1 activity is not essential for the establishment of SAC signaling. Instead, PLK1 appears to be implicated in the stable attachment of kinetochores to microtubules, in a process involving PLK1-dependent phosphorylation of BUBRI and NUDC (Elowe et al., 2007; Nishino et al., 2006).

PLK1 also regulates the removal of Cohesin complexes during mitosis. Whereas in yeast, PLK1 ortholog, CDC5, phosphorylates cohesins to increase their cleavability by separase at anaphase onset (Alexandru et al., 2001), eukaryotes share two distinct pathways: the

majority of Cohesin is removed from chromosomal arms during the early stages of mitosis (prophase/prometaphase) in a PLK1-dependent but separase-independent pathway (Sumara et al., 2000, 2002). At anaphase onset, only the residual amounts of Cohesin is then removed from chromosomes in a Separase-dependent manner (Waizenegger et al., 2000).

After anaphase onset, PLK1 translocates from kinetochores to the spindle midzone via its interaction with PRC1 (Hu et al., 2012) and remains in the midbody during telophase where it is responsible for the formation of the contractile acto-myosin ring. Indeed, PLK1 phosphorylation of CYK-4 induces recruitment of ECT2 to the CENTRALSPINDLIN complex (Wolfe et al., 2009). ECT2-CENTRALSPINDLIN complex will promote activation of the small GTPase RhoA, which drives the assembly of the cleavage furrow (Yüce et al., 2005)

Decrease in PLK1 concentration occurs in late mitosis and in G1 when the destruction-box (D-box; amino-acids 337-RKPL-340) of PLK1 is recognized by the E3-ubiquitin ligase APC/C^{Cdh1}. As a consequence, PLK1 is polyubiquitinated, and thereby targeted for proteasomal degradation (Lindon and Pines, 2004).

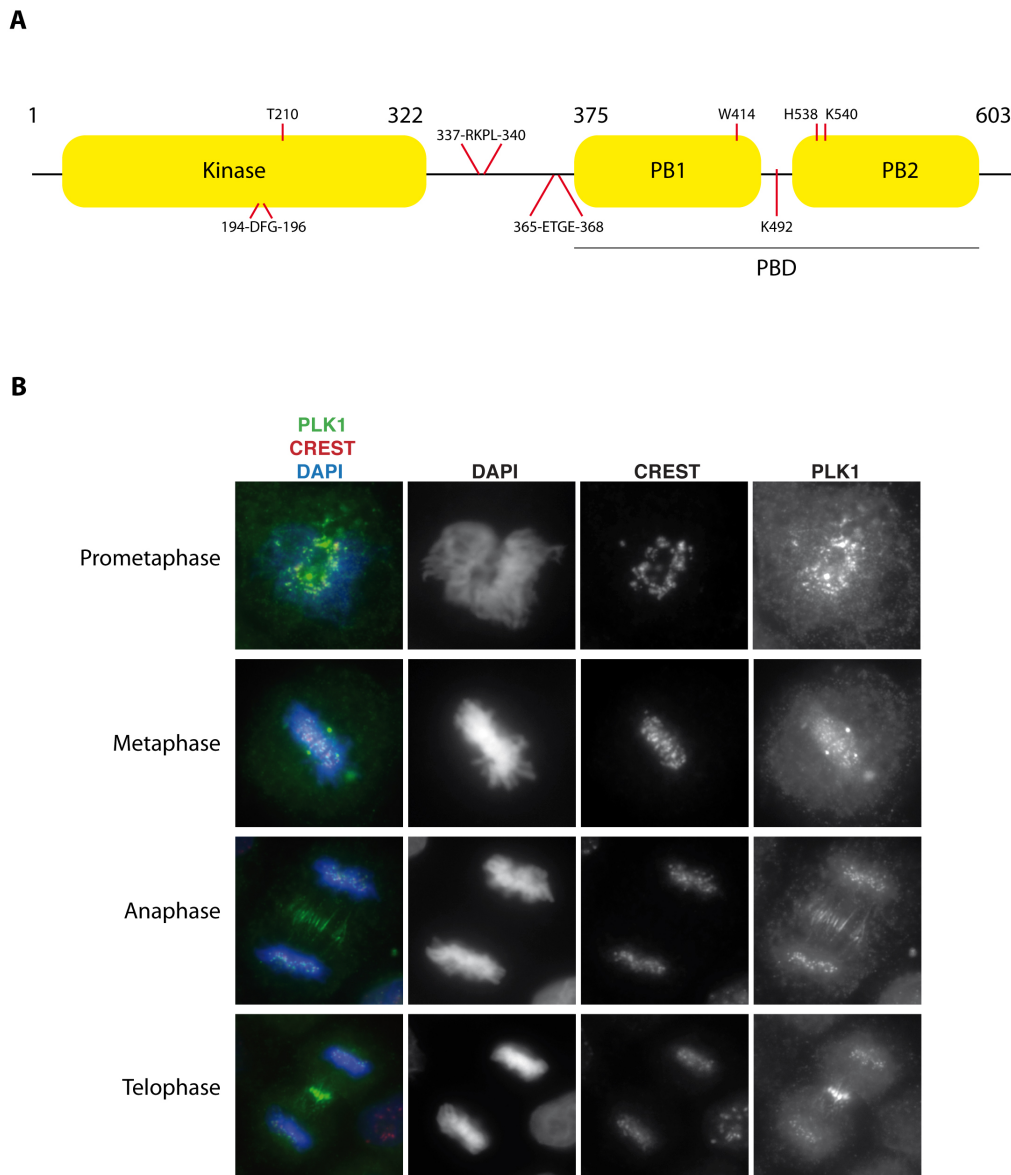


Figure 5. Architecture and localization of PLK1 protein. **A.** Schematic representation of PLK1 protein structure. It is composed of a kinase domain at its amino-terminal side, whereas two polo-boxes constitute the Polo-Box Domain (PBD) at its carboxy-terminus extremity. Key residues that will be subsequently investigated are shown in red. **B.** Localization of PLK1 during mitosis. HeLa cells were fixed, stained with PLK1 and CREST (a marker of kinetochores) antibodies and DAPI to visualize DNA and analyzed by immunofluorescence microscopy. PLK1 localizes to centrosomes in prophase and prometaphase and on kinetochores upon establishment of kinetochore-microtubule attachments. In metaphase, PLK1 is partially removed from kinetochores, and at anaphase onset, it relocates from kinetochores to the spindle midzone and subsequently to the midbody during telophase and cytokinesis.

Interestingly, the recruitment of PLK1 to the different cellular localization during cell cycle is dependent on its PBD domain. Indeed, it was shown that the PBD of PLK1 can act as a phospho-peptide binding motif (Elia et al., 2003b) and thereby suggests a mechanism by which PLK1 can dock to specific phosphorylated targets via its PBD. This involves key residues H538 and K540, both essential for electrostatic interaction with the phosphate group, and W414 required for binding the backbone of the phosphorylated receptor protein (Cheng et al., 2003; Elia et al., 2003a). Interestingly, the optimal consensus sequence recognized by the PBD, -LHSSp/TpP- (Yun et al., 2009), shows partial overlap with the phosphorylation sequences generated by mitotic-Proline directed kinases as CDK1. CDK1 indeed primes early mitotic interactors of PLK1 like INCENP, BUB1 and BUBR1 (Elowe et al., 2007; Goto et al., 2006; Qi et al., 2006). However, PLK1 is also able to create its own docking site, like for PBIP (Kang et al., 2006), or PRC1 (Hu et al., 2012).

Yet other interactions are completely independent of phospho-priming. For instance, interactions between *D. melanogaster* POLO and MAP205 depend on the PBD, but do not require any phosphorylation. Interestingly, CDK1-mediated phosphorylation of MAP205 inhibits PLK1 binding rather than promoting it (Archambault et al., 2008; Xu et al., 2013). The binding of PLK1 to BORA has also been suggested to be phospho-independent, but in this case only the PBD or the kinase domain are sufficient to co-purify BORA (Seki et al., 2008). However, recent data from Dr. Pintard's laboratory indicate that phosphorylation of BORA orthologue in *C. elegans* SPAT-1 is required for interaction with PLK1 and regulation of mitotic entry (Pintard L., personal communication). This strongly suggests that PLK1 is capable of using several binding mechanisms to interact with its substrates and receptors. Future studies are needed to understand these mechanisms.

4.3.3 Aurora Kinase family:

Another group of kinases essential for mitotic progression is the Aurora family. It is composed of three members, Aurora A, B and C, all sharing the same organization: a highly conserved catalytic domain, associated to a more divergent amino-terminal extension (Fig. 6A).

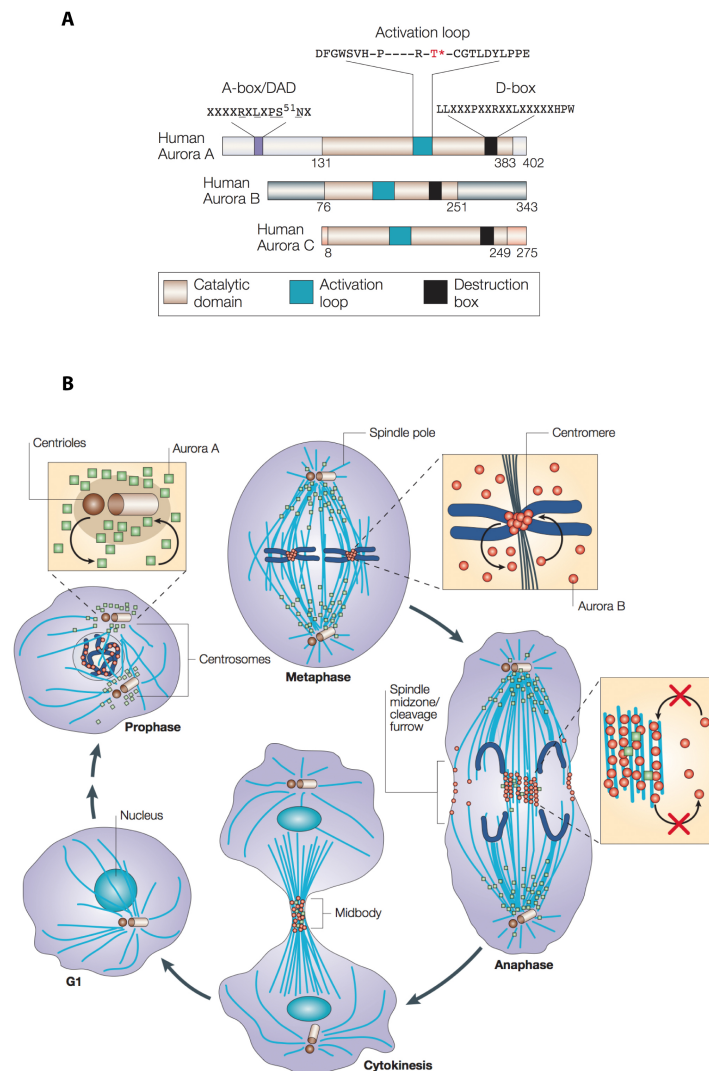


Figure 6. Architecture and localization of Aurora kinases. **A.** Schematic representation of the domain organization of Aurora kinase family. Whereas the kinase domain is highly conserved (more than 70% between Aurora A and B), the amino-terminal extremities exhibit strong divergence. **B.** Schematic representation of the subcellular localization of Aurora A (green squares) and Aurora B (red circles). (Adapted from (Carmena and Earnshaw, 2003))

Aurora A expression and activity peak at the G2/M transition after phosphorylation of its activation loop. This regulation appears to be conferred by its interaction with binding partners, the most characterized ones being BORA and TPX2. As described previously, in early mitosis Aurora A localizes at centrosomes (**Fig. 6B**), where its association with BORA is responsible for PLK1 activation (Toyoshima-morimoto et al., 2001; Toyoshima-Morimoto et al., 2002), and is also important for the recruitment of peri-centriolar material, essential for centrosome separation and maturation (Berdnik and Knoblich, 2002; Hannak et al., 2001). It also phosphorylates CDC25B phosphatase, thereby ensuring faithful mitotic entry (Dutertre et al., 2004). In mitosis, PLK1 mediates degradation of BORA via the E3-ubiquitin ligase SCF (Chan et al., 2008) and Aurora A can subsequently interact with its co-activator TPX2, which drives the complex to the mitotic spindle (Eyers and Maller, 2004). While its function there is not completely understood, its role in the maintenance of stable kinetochore-microtubule (KT-MT) interactions is firmly established, as its inhibition leads to chromosome misalignments and thereby defective chromosome segregation (Lioutas and Vernos, 2013) and its over-expression bypasses SAC-dependent arrest induced by the microtubule-stabilizing drug Taxol (Anand et al., 2003). Aurora A is degraded in an APC/C^{Cdh1} dependent manner in late anaphase and this has been shown to be an important event for reorganization of microtubules during interphase stage (Floyd et al., 2008). However, in human cells, over-expression of GFP-Aurora A leads to a reminiscent pool of the kinase localizing to midbody in late mitosis (Sugimoto et al., 2002), the function of which still has to be understood.

Aurora B expression is similar to the one of Aurora A. It is part of the so-called Chromosomal Passenger Complex (CPC), which includes the proteins INCENP, SURVIVIN and BOREALIN. Upon binding to INCENP, Aurora B is primely activated. It then phosphorylates both INCENP (Bishop and Schumacher, 2002) and the T-loop of its kinase domain (Yasui et al., 2004) *in trans*, resulting in full activation of Aurora B (Sessa et al., 2005). Aurora B and the entire CPC display a very dynamic localization, moving from chromosomes and inner centromeres from prophase to metaphase to the central spindle during anaphase and finally to the midbody during telophase and cytokinesis (**Fig. 2 and 6B**). In early mitosis, two histone phosphorylations, H3T3 and H2AT120 catalyzed by HASPIN and BUB1 respectively, are required for accumulation of the CPC at inner centromeres (Wang et al., 2010; Yamagishi et al., 2010), where its major role is to

control kinetochore-microtubule (KT-MT) attachments. Indeed, incorrect attachment of microtubules to kinetochores of chromosomes (i.e. not bi-oriented) triggers Aurora B phosphorylation of components of the KMN complex (NDC80, MIS12 and KNL1) and of the kinesin-motor MCAK (Lan et al., 2004; Zhang et al., 2007). This induces a decrease in their affinity towards microtubules, destabilizing wrong attachments, and thereby promoting novel, accurate interactions of the mitotic spindle to chromosomes (Cheeseman et al., 2006; Welburn et al., 2010). Aurora B is also required to actively signal the Spindle Assembly Checkpoint (SAC) as, similarly to Aurora A, Aurora B inhibition induces a SAC over-ride in Taxol-treated cells (Hauf et al., 2003). It was shown to be required for the accurate recruitment of the key SAC components (Vigneron et al., 2004). This recruitment, combined to its functions in creating unattached kinetochores makes Aurora B a central player in SAC signaling in mitosis.

Following SAC silencing upon accurate kinetochore-microtubule attachments, cells enter anaphase, where H3T3 is dephosphorylated. This facilitates CPC relocalization to the central midzone, where it mediates, indirectly via phosphorylation of MKLP1, the recruitment of CENTRALSPINDLIN, which contributes to the stabilization of the central spindle (Douglas et al., 2010; Guse et al., 2005). Thereby, by promoting the recruitment of CENTRALSPINDLIN to the midzone, the coordinate action of Aurora B with PLK1 will allow formation of the ECT2- CENTRALSPINDLIN complex, essential for the activation of RhoA GTPase and subsequent ingression of the cleavage furrow, after which, both the A-box and the D-box of Aurora B are recognized by APC/C^{Cdh1} which subsequently catalyses degradation of the kinase (Stewart and Fang, 2005a).

Aurora C is the third and last member of the Aurora family and its functions are to-date only poorly understood. Interestingly, it is only highly expressed in the embryonic stages and in cancer cells, where, like other members of the family, it peaks during G2/M phases. It has been shown to be associated with centrosomes (Induced et al., 2005; Kimura, 1999), but has also been suggested to be a CPC-associated protein (Li et al., 2004; Sasai et al., 2004; Yan et al., 2005), where it can complement Aurora B functions (Sasai et al., 2004; Slattery et al., 2009).

4.4 Regulation of mitosis by protein ubiquitination

4.4.1 The ubiquitin-proteasome system

Progression through mitosis is not only regulated by protein phosphorylation and dephosphorylation, but also by ubiquitin-mediated proteolysis of specific substrates, thereby ensuring uni-directionality of the cell cycle. Ubiquitin is a small 8.5 kDa protein that is covalently attached to lysine residues of other proteins through the sequential actions of three enzymes. E1, the ubiquitin-activating enzyme, which, in an ATP-dependent process, activates ubiquitin by covalently linking its carboxy-terminal glycine to cysteine residue in the active site of the E1. The E1 subsequently transfers the activated ubiquitin to a cysteine residue within the active site of the E2-ubiquitin conjugating enzyme. Finally, ubiquitin is transferred from the E2 to the lysine residue of the substrate protein in an E3-dependent manner (**Fig. 7**). In case of HECT family of E3-ubiquitin ligases, this involves binding of ubiquitin to a cysteine within the active site of the ligase and then this ubiquitin molecule is covalently linked to the substrate, whereas in case of the RING family, there is a direct transfer of ubiquitin from the E2 to the substrate. In most organisms, specificity towards the substrate is provided by the E3-ubiquitin ligase as there is a single E1, several types of E2 enzymes and multiple families of E3 ligases, which are often multiprotein complexes. Substrates can be modified by a single ubiquitin on one or more sites (mono and multi-ubiquitination, respectively) or poly-ubiquitination can occur, in which substrates are modified with chains of ubiquitin thanks to the seven internal lysines within the ubiquitin itself (K6, K11, K27, K29, K33, K48, K63) (**Fig. 7**). This creates a huge plethora of possible ubiquitin signals, all of which appear to have very distinct functions. For instance, while K-11 and K-48 poly-ubiquitinated proteins are usually recognized and degraded by the proteasome (Chau et al., 1989; Jin et al., 2008), K-63 linkage was shown to be important for signal transduction in DNA damage (Spence et al., 1995) and in stress response pathways (Wang et al., 2001). Mono- or multi-ubiquitination serves as a targeting signal in major cellular processes like DNA repair, transcription, endocytosis but also in mitosis (reviewed in (Welchman et al., 2005)). Increased complexity arises from the ability of the Ubiquitin-Domain Binding (UBD) proteins to interact specifically with ubiquitinated proteins, regulating their functions. Also, ubiquitin modifications are counteracted by

specific deubiquitinating enzymes (DUBs), which can thereby rescue substrate proteins from degradation (Rumpf and Jentsch, 2006), allow ubiquitin recycling (Yao and Cohen, 2002) and regulate transcription by altering chromatin structure (Joo et al., 2007; Zhang et al., 2008) and mitosis (reviewed in (Fournane et al., 2012)).

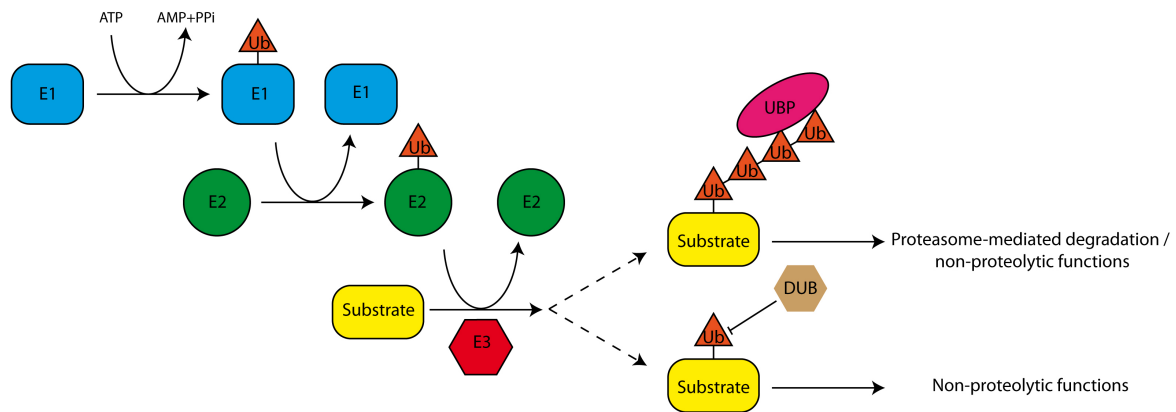


Figure 7. *The ubiquitin conjugation pathway. Conjugation of ubiquitin to substrate proteins involves three enzymes, E1, E2 and E3. Ubiquitination can lead to mono- or polyubiquitination. The latter is more characterized for its proteolytic roles, but may also mediate major signaling functions, similar to mono-ubiquitination. Different types of modifications are recognized by distinct Ubiquitin-Binding Proteins (UBPs). Ubiquitination can be removed from the substrate protein by DeUBiquitinating enzymes (DUBs).*

4.4.2 Cullin-RING E3-ubiquitin ligases

The human genome encodes seven members of the Cullin family: CUL1, CUL2, CUL3, CUL4A, CUL4B, CUL5 and CUL7 and one more distant member, APC2. All of them harbour a very specific architecture: the amino-terminal domain of the Cullins binds substrate adaptor proteins (either directly, or indirectly through a linker), which mediates interaction with the substrate (**Fig. 8**). On the other hand, the carboxy-terminal part of Cullin protein binds a RING-finger protein, usually RBX1, which ensures the recruitment of the E2 enzyme conjugated to ubiquitin, and positions it near the substrate (reviewed in (Sumara et al., 2008)). CRL activity is mostly regulated via neddylation/deneylation cycles, activating (Duda et al., 2008; Pintard et al., 2003a;

Sakata et al., 2007; Wu et al., 2000) or inhibiting (Cope et al., 2002; Lyapina et al., 2001) CRLs respectively.

To date, three major CRL complexes have been shown to be essential for faithful progression of mitosis: one based on CUL1 or so-called the SCF complex, one based on APC2 and called Anaphase-Promoting Complex/Cyclosome (APC/C), and the one based on CUL3.

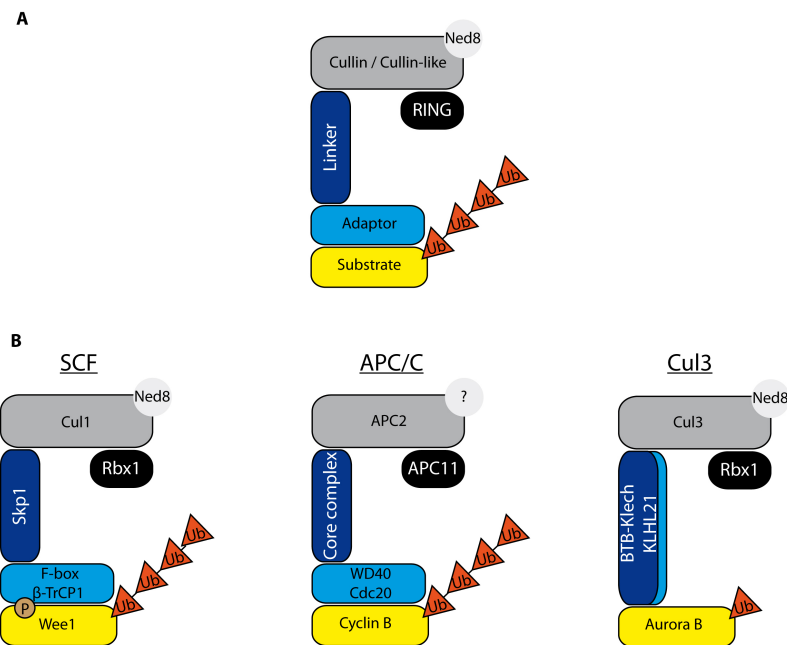


Figure 8. **A.** Schematic representation of the global architecture of Cullin-RING E3-ubiquitin ligase complexes. Cullin (light grey) binds through its carboxy-terminus to the RING-finger protein (black). Its amino-terminus mediates interaction with the substrate recognition module, composed of a linker (dark blue) and an adaptor (light blue) that recognizes the substrate (yellow) to be modified by ubiquitin (orange). Cullin's activity is regulated by neddylation (NED8). **B.** Specificities of CRLs. Only SCF (or CUL1-based E3-ubiquitin ligases) requires previous phosphorylation of substrates to allow interaction with the WD40 domain of its adaptor protein. APC/C (based on APC2) is the most divergent member of the CRL family, composed of at least 13 core-subunits. It binds the RING-finger protein APC11, instead of RBX1 in case of other members, and neddylation does not appear to be required for its activity. In CUL3-based E3-ubiquitin ligases, a single protein acts as the linker and the adaptor. It contacts CUL3 via its BTB-domain, whereas another domain mediates contacts with the substrate, usually a MATH or a Kelch domain. Examples of adaptor proteins and specific substrates for each of the E3 ligase complexes are shown.

4.4.2.1 The SCF complex

Human SCF complex is composed of three subunits: CUL1, RBX1 and SKP1. SKP1 is a linker protein, bridging CUL1 thanks to its F-box domain to the adaptor that will contact the substrate to be ubiquitinated. Several functional complexes of CUL1-RBX1-SKP1 can thereby be formed, based on the adaptor protein used: SCF^{NIPA} mediates Cyclin B1 degradation in interphase, preventing premature mitotic entry (Bassermann et al., 2005). In late G2, CyclinB1/CDK1 actively regulates its own activation by phosphorylating NIPA, which induces its dissociation from SCF and thereby increases CyclinB1/CDK1 concentration (Bassermann et al., 2007). Upon dissociation of NIPA, SCF^{Tome-1} and SCF ^{β -TrCP1} are formed and promote mitotic entry by ubiquitination-dependent degradation of CDK1 inhibitor WEE1 (Ayad et al., 2003; Watanabe et al., 2004). In prophase, SCF ^{β -TrCP1} induces degradation of APC/C inhibitor EMI1, resulting in increased activation of the E3-ubiquitin ligase. Interestingly, the interactions between SCF adaptors and their respective substrates are known to require phosphorylation of the substrates. While this dogma still has to be confirmed for Cyclin B1 recognition by SCF^{NIPA}, both PLK1 and CDK1 phosphorylations of WEE1 and PLK1 phosphorylation of EMI1 are essential for their degradation (Watanabe et al., 2004).

4.4.2.2 The APC/C

Despite following the same global organization like other members of the CRL family, the Anaphase-Promoting Complex/Cyclosome (APC/C) functions quite differently. Firstly, it is a 1.5MDa multiprotein complex, made of at least 13 core subunits (reviewed in (Thornton and Toczyski, 2006)) organized around the Cullin-homology domain of APC2. The latter binds RING-finger protein APC11 (instead of RBX1 in other CRLs) and its activity has not been shown to be dependent on neddylation. It mostly contacts its substrates in a phosphorylation-independent manner, via the WD40 domains of only two distinct adaptors: CDC20 and CDH1.

Upon degradation of Emi1 by SCF ^{β -TrCP1} in prophase (see above), APC/C becomes active and associates with co-activator CDC20 to degrade Cyclin A, allowing progression to the later stages of mitosis (Geley et al., 2001; Kikuchi et al., 2013), and NEK2A initiating centrosomes separation (Hames et al., 2001).

However, the most characterized role of APC/C^{Cdc20} is to drive the metaphase-to-anaphase transition upon SAC inactivation. Indeed, spindle microtubules not correctly attached to kinetochores induce series of phosphorylations leading to SAC activation. In this case, CDC20 catalytic activity is inhibited because of its interaction with the Mitotic Checkpoint Complex (MCC, composed of MAD2, BUB3 and BUBRI) and thereby can not target Cyclin B and SECURIN for degradation, both necessary steps for anaphase onset. When chromosomes become bi-oriented thanks to the action of Aurora B (see part 3.3.3) and its counteracting phosphatase B56-PP2A, SAC is inactivated in a process probably involving phosphatase PP1 recruitment and activity on kinetochore. The MCC releases CDC20, which subsequently becomes active and targets for degradation both Cyclin B and SECURIN. This leads to CDK1 inactivation and activation of separase, resulting in proteolytic cleavage of the Cohesin complex allowing sister chromatids segregation in anaphase (reviewed in (Foley and Kapoor, 2013)). Decrease in Cyclin B concentration leads to inactivation of CDK1, which induces the replacement of CDC20 by CDH1 in anaphase. APC/C^{Cdh1} is responsible for initiating mitotic exit, by degrading major mitotic proteins, including CDC20 itself (Huang, 2001), PLK1 (Lindon and Pines, 2004), Aurora kinases (Littlepage et al., 2002; Stewart and Fang, 2005a) and spindle associated proteins TPX2 and ANILLIN to promote spindle reorganization and contractility of myosin during cytokinesis (Stewart and Fang, 2005b; Zhao and Fang, 2005).

4.4.2.3 CUL3 E3-ubiquitin ligases

The first CUL3-based E3 ubiquitin ligase complex was identified in *C. elegans*, where CUL3 was shown to interact with MEL26 and to be required for degradation of the microtubule-severing protein MEI-1 at the meiosis-to-mitosis transition (Pintard et al., 2003b). The global architecture is quite similar to the one of SCF E3-ubiquitin ligase, except that in case of CUL3 family, a single protein is acting as both the linker and the adaptor. Indeed, CUL3 interacts with adaptors containing a BTB/POZ domain (for Bric-a-brac, Tramtrack and Broad Complex/Pox virus and Zinc finger) associated to a 3-box motif (herein referred as BTB domain) (Canning et al., 2013; Xu et al., 2003; Zhuang et al., 2009). The adaptor contains another protein-protein interaction domain that mediates contacts with the substrate, like a MATH domain in case of CUL3/MEL26 E3-

ubiquitin ligase. Regulation of the activity of CUL3-based E3-ubiquitin ligases is dependent on two distinct mechanisms: like most of the CRLs, CUL3 activity relies on its neddylation state (see above) and secondly, the BTB domain of the adaptor protein provides a platform for complex dimerization (Ahmad et al., 1998; Canning et al., 2013). Interestingly, increasing evidence suggests that this dimeric CUL3/BTB-adaptor binds a single substrate on two distinct sites, like in case of CUL3/KEAP1 complex binding transcription factor NRF2 (McMahon et al., 2006; Tong et al., 2006), or CUL3/SPOP binding to PUC (Zhuang et al., 2009). The functions of CUL3-based E3-ubiquitin ligases are very versatile and are not restricted to mitosis (reviewed in (Genschik et al., 2013)). Interestingly, also during mitosis, depletion of CUL3 by RNAi leads to a whole plethora of phenotypes spanning from chromosome alignment defects to chromosome segregation defects but also to cytokinesis defects (Sumara et al., 2007). During mitosis, CUL3 was shown to interact with BTB-Kelch domain containing proteins via their BTB domains, whereas their Kelch domains act as adaptors to mediate interactions with essential mitotic kinases. Kelch domains adopt a β -propeller domain fold, in which each blade of the propeller is formed from a four-stranded antiparallel β -sheet fold (**Fig. 9A**). All mitotic BTB-Kelch identified to date contain six of these β -sheet modules, which arrange radially around a central axis to form the β -propeller domain (**Fig. 9B**).

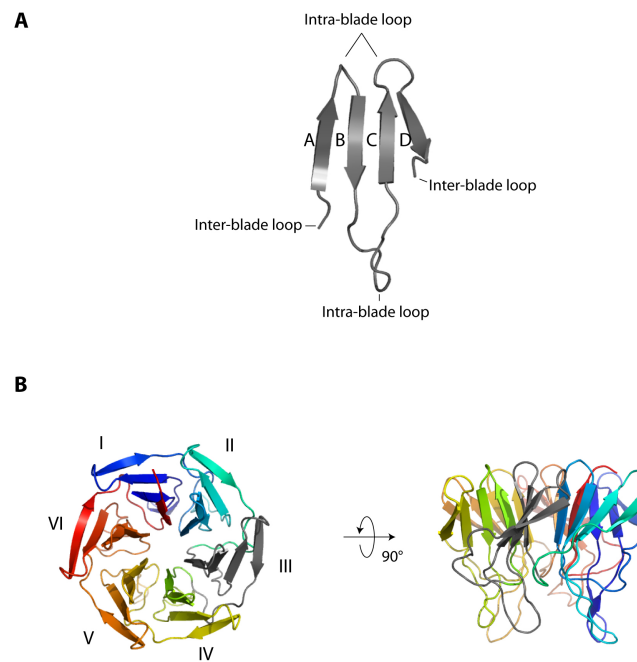


Figure 9. A. Structure of a Kelch-repeat propeller blade. Four β -sheets (named A,B,C and D) constitute one blade. The N- and C-termini loops join the adjacent blades. The depicted blade corresponds to the modelled third blade of KLH22 using Phyre2 software. **B.** Mitotic BTB-Kelch adaptors are composed of six blades connected by inter-blade loops. They adopt a typical β -propeller domain fold. This structure represents the modelled Kelch domain of KLH22 using Phyre2 software.

While structural elements constituting the blades are quite conserved, intra and inter-blade loops show strong divergence in length and amino-acid composition (**Fig. 10A**). This influences the surface properties of individual propeller and thereby contributes to increased specificity of each Kelch domain towards its physiological substrates (**Fig. 10B and 10C**). During mitotic progression, CUL3/KLHL18 is essential for mitotic entry as depletion of KLHL18 delays this process. It ubiquitinates Aurora A at centrosomes, which seems to proceed activation of the kinase (Moghe et al., 2012). During prometaphase, CUL3 association with adaptors KLHL9 and KLHL13 targets Aurora B kinase for ubiquitination, which serves as a signal for its removal from chromosomal arms of condensed chromosomes and correct localization to the spindle midzone (Sumara et al., 2007). At anaphase onset, adaptor KLHL21 localizes to the midzone and interacts with CUL3 to ubiquitinate Aurora B, stabilizing its localization in this location (Maerki et al., 2009), which is required for proper cytokinesis (see part 3.3.3).

A

```

KLHL18-Kelch -289- LITVAVGGGNS--AGDSLNVVEVFDPIANCERCRPMITARS-RVGVAVVNGLIPAGGGYD-----GLRL
KLHL21-Kelch -287- ILVIMGGCDQ--DCDELVTVDYNPQTGQRYLAEPFDHLGGGYSIVALGNDIPVGGSD-----GSRLY
KLHL22-Kelch -299- CUVGGGGHSTFSTVLSQAKYINPLLGGKHFTASLAPRMSNQGLAVLNFPVGGGIN--NVGGRPAE
KLHL09-Kelch -300- -LVTHGGVLR-QQLVVSKELMYDERAQSRSLAPMDAPRY-QHGLAVIGNFLVGGGSNYDTREKTAIV
KLHL13-Kelch -341- HLVTHGGVLR-QQLVVSKELMYDEKAHRSRLAPMDAPRY-QHGLAVIGNFLVGGGSNYDTREKTAIV

KLHL18-Kelch STVEAINPEIDITRFGSMNKRSMGTVVLDGQQLVCGGYDGNSSLSSVGGSPETDMITVVTSMSSNR
KLHL21-Kelch DCVWRINSSVNEPAEVAFMLKAREYHSSSVLDGLIPVVAADS-----TGGPHITDSREALQPMITYM
KLHL22-Kelch SACWRIDPRNPAEQIQSLQZEHADLSVCVVGRYDAVAGRDYHNLNAVGGDFATNSQAYVAFPKREV
KLHL09-Kelch DIVFREDPRINPAEQVASINEKRIFHLSSALKGHDAVGGRSAAAGELATVGGDFPRMNSQYVAMMSEPH
KLHL13-Kelch DIVFREDPRINPAEQVASINEKRIFHLSSALKGHDAVGGRNAAGELPTVGGDFPRMNSQYVAMMSEPH

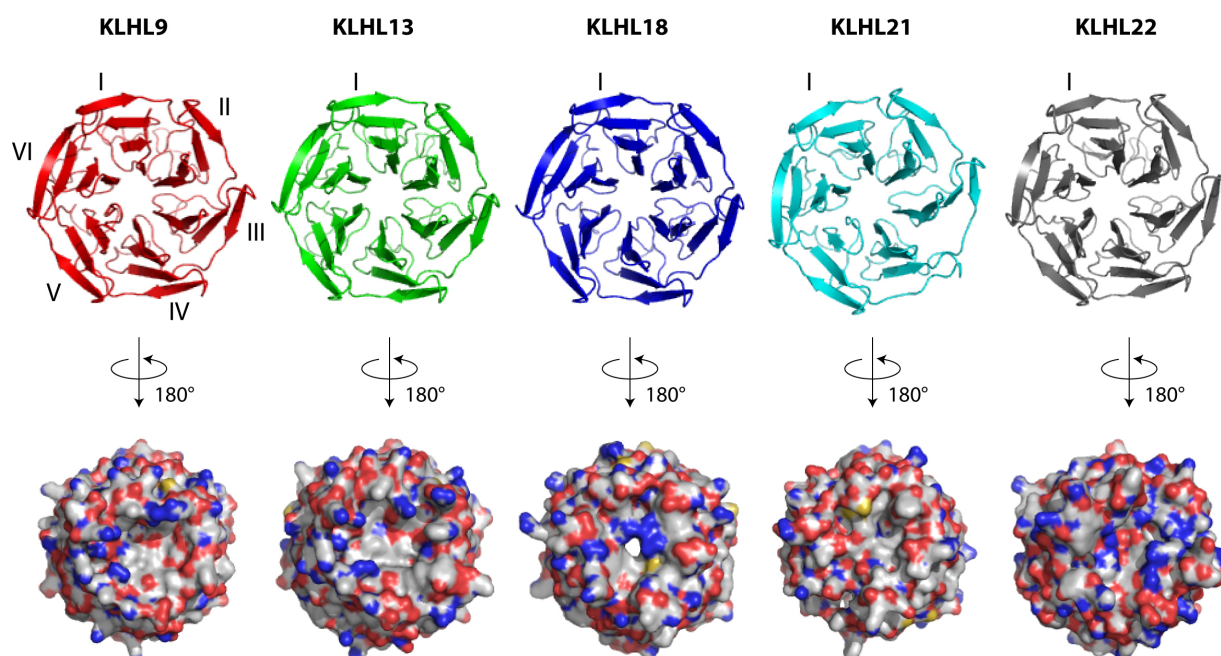
KLHL18-Kelch SAAGVTVFEPEDVSGGHDGLQITSSVEHNNHTATHPAAG--MLNKRGRHGAASLGSKMFVCGG----
KLHL21-Kelch DNCSTTACRGLPAIGSLAG-KEIMVMQCYDPTDMLSLVDCGQLPFWSPFKTATLNGLMYFVRD----
KLHL22-Kelch YAHAGATLGGHPETCGRRGEDYLNKETHCYDPSNTHTLAD--GPFVRAWHGHTLLNKLIVIGGSSND
KLHL09-Kelch YGHAGTVYGGHPLSGGITHDTFQKELMCEPDPTDMHAKAP--MITVRLGHCMCTVGDKLIVIGGNHFR
KLHL13-Kelch YGHAGTVYGGHPLSGGITHDTFQKELMCEPDPTDMHAKAP--MITVRLGHCMCTVGDKLIVIGGNHFR

KLHL18-Kelch -YDGGGFLSIARSSVADGCLIVPHHTARRSVSLVASCGRHINAGG--YDGGSNLSSVGVDETDCH
KLHL21-Kelch ----DSAEVDVGNPTRNEMKIPSMNQVHVGGSLAVLGGHIVYGGYDNTFELSDVGVHDEETRAW
KLHL22-Kelch -AGYRRDVHQVACSTSGGSSVCLFAGHGEPGLAVLDNRHIVGGGSHNRGSRIGVHHYDEKDCW
KLHL09-Kelch GTSDDYDVLSCENSPFLDNTFFAAMLRGQSDVGVAVFENKIVVGGSHNRCVZELGVHDEKDCW
KLHL13-Kelch GTSDDYDVLSCENSPFLDNTFFAAMLRGQSDVGVAVFENKIVVGGSHNRCVZELGVHDEKDCW

KLHL18-Kelch TFMARACHEGGVGVCCFPL--571-
KLHL21-Kelch SVVGRLLPEPTFWHGSVSIFR--560-
KLHL22-Kelch EEGPQLDMSISGLAACVLTLL--593-
KLHL09-Kelch HKVFTLLPESLGGIRACTLTVF--595-
KLHL13-Kelch HKVFTLLPESLGGIRACTLTVF--636-

```

B



C

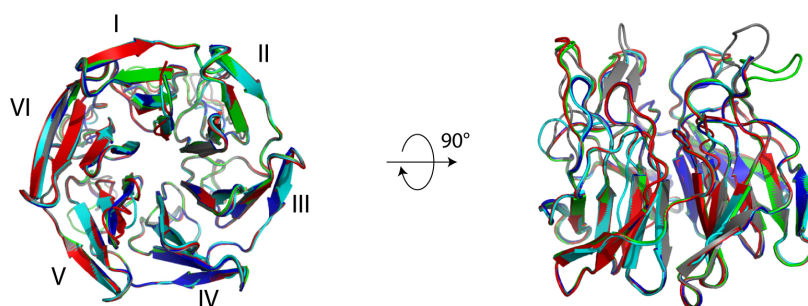


Figure 10. **A.** Multiple sequence alignment of the Kelch domain of BTB-Kelch proteins involved in mitosis (KLHL9, KLHL13, KLHL18, KLHL21 and KLHL22). Black shading indicates identical amino-acids whereas grey shading indicates amino-acids similar in all five Kelch domains. The alignment was obtained using ClustalW. **B.** Cartoon and surface representations of the Kelch domains of KLHL9, KLHL13, KLHL18, KLHL21 and KLHL22. While all five proteins fold into β -propellers, they however exhibit strong divergence in their surface potentials. Carbon and hydrogen atoms are shown in grey, nitrogen in blue, oxygen in red and sulphur in yellow. **C.** Structural superimposition of these Kelch domains. β -sheets display a strong structural conservation but loops appear to be more divergent and might thereby be involved in specificity of substrate recognition. All structures were modelled using Phyre2 and structurally aligned using Coot software.

5 Aim of the thesis

The goal of my thesis is to understand the molecular requirements for substrate recognition by CUL3 E3-ubiquitin ligases. A very significant number of papers shows that protein kinases constitute targets of CUL3/BTB-Kelch E3-ubiquitin ligases (Metzger et al., 2013). Indeed, during mitosis, data already published from our lab as well as from others identified several complexes essential for faithful completion of this process: CUL3/KLHL18 regulating Aurora A, CUL3/KLHL9-KLHL13 and CUL3/KLHL21 acting on Aurora B. Moreover, our work recently identified a novel complex, CUL3/KLHL22 regulating PLK1 during mitosis (Beck et al., 2013). We thereby hypothesized that there must be a common conserved mechanism for kinase recognition by BTB-Kelch proteins. However some molecular determinants must exist in each case to ensure formation of specific complexes *in vivo*.

We used CUL3/KLHL22 complex interacting with PLK1 substrate as an experimental model to gain insights into the detailed molecular mechanisms regulating this interaction. We then planed on extending our knowledge to other complexes, in order to understand what are the common and specific features of kinases binding to BTB-Kelch adaptors.

6 Results

Results are divided in three parts. The first one corresponds to our manuscript published in Nature Cell Biology describing identification of PLK1 as a direct target of the E3-ubiquitin ligase CUL3/KLHL22. The second part focuses on the molecular requirements for PLK1 recognition by adaptor protein KLHL22, and includes one manuscript published in Cell Cycle and several unpublished results. The third and last part shows unpublished results on characterization of novel components of PLK1/KLHL22 pathway.

6.1 Results part 1: Manuscript: Ubiquitylation-dependent localization of PLK1 in mitosis.

Sarah Mäerki *et al.* identified the ubiquitin ligase complex CUL3/KLHL22 as a novel component of the complex regulatory system that ensures faithful progression through mitosis (Maerki et al., 2009). In the study presented here, the regulation of PLK1 by CUL3/KLHL22 was investigated in depth to understand the underlying biochemical and cellular processes. The results were published as an article in Nature Cell Biology (Beck et al., 2013).

Author contributions of experimental data:

Sarah Mäerki and Jochen Beck, under supervision of Izabela Sumara at the ETH Zürich, jointly characterized KLHL22 as an adaptor of CUL3. They observed chromosome alignments defects in KLHL22 depleted cells, quantified the mitotic delay and frequency of apoptosis in these cells and found that these phenotypes are linked to the SAC. They identified and confirmed PLK1 as a CUL3/KLHL22 substrate. They found that KLHL22 depletion leads to PLK1 accumulation at mitotic kinetochores and BubR1 hyperphosphorylation, but does not affect the total protein levels of PLK1. They generated the GFP-PLK1 and His-PLK1 cell lines. They characterized the GFP-PLK1 cell lines and quantified mitotic defects such as mitotic delay, frequency of apoptosis, PLK1 accumulation and BUBRI phosphorylation at kinetochores in cells expressing only the ectopic version of PLK1. They documented the accumulation of endogenous PLK1 at kinetochores at different mitotic stages and confirmed that the PLK1 K492R mutant does not cause centrosome maturation defects, exerts normal kinase activity and is degraded at the same rate as endogenous PLK1. Furthermore, they recorded the localization of GFP-KLHL22, in the stable cell line. In the laboratory of Izabela Sumara at the IGBMC Strasbourg, Thibaud Metzger and Izabela Sumara performed experiments and quantifications showing RANGAP1 localization defects in KLHL22 depleted cells or in cells expressing the non-ubiquitylatable PLK1 mutant. They quantified PLK1 and RANGAP1 signals in the His-PLK1 cell line and showed that PLK1 binding to BUBRI and other phospho-receptors is negatively regulated by CUL3/KLHL22 and that this regulation is depending on the tension between sister chromatids upon attachment of

spindle microtubules to kinetochores of chromosomes. They bacterially expressed and purified recombinant PLK1 and KLHL22 and showed that the two interact with high affinity.

Ubiquitylation-dependent localization of PLK1 in mitosis

Jochen Beck^{1,8}, Sarah Maerki^{1,8,9}, Markus Posch², Thibaud Metzger³, Avinash Persaud⁴, Hartmut Scheel⁵, Kay Hofmann⁶, Daniela Rotin⁴, Patrick Pedrioli⁷, Jason R. Swedlow², Matthias Peter^{1,10} and Izabela Sumara^{1,3,10}

Polo-like kinase 1 (PLK1) critically regulates mitosis through its dynamic localization to kinetochores, centrosomes and the midzone. The polo-box domain (PBD) and activity of PLK1 mediate its recruitment to mitotic structures, but the mechanisms regulating PLK1 dynamics remain poorly understood. Here, we identify PLK1 as a target of the cullin 3 (CUL3)-based E3 ubiquitin ligase, containing the BTB adaptor KLHL22, which regulates chromosome alignment and PLK1 kinetochore localization but not PLK1 stability. In the absence of KLHL22, PLK1 accumulates on kinetochores, resulting in activation of the spindle assembly checkpoint (SAC). CUL3–KLHL22 ubiquitylates Lys 492, located within the PBD, leading to PLK1 dissociation from kinetochore phosphoreceptors. Expression of a non-ubiquitylatable PLK1-K492R mutant phenocopies inactivation of CUL3–KLHL22. KLHL22 associates with the mitotic spindle and its interaction with PLK1 increases on chromosome bi-orientation. Our data suggest that CUL3–KLHL22-mediated ubiquitylation signals degradation-independent removal of PLK1 from kinetochores and SAC satisfaction, which are required for faithful mitosis.

Mitotic division is instrumental for the development of all organisms and defects in its regulatory systems lead to aneuploidy, which is linked to cellular transformation^{1,2}. PLK1 is a critical regulator of mitotic division and an attractive candidate for anticancer drugs³. It controls chromosome alignment, centrosome function and spindle assembly through its dynamic localization to kinetochores, centrosomes and the midzone⁴. Downregulation of PLK1 or pharmacological inhibition of its kinase activity leads to mitotic defects ultimately leading to activation of the SAC and apoptotic death^{5,6}. However, recent data suggest that a fine balance of PLK1 protein levels and its kinase activity is required for chromosome alignment and faithful mitotic progression^{7–9}. First, PLK1 accumulates at the kinetochores during the prometaphase stage to establish kinetochore attachments and subsequently most PLK1 protein has to be removed from kinetochores during metaphase to allow for the maintenance of stable kinetochore–microtubule interactions, SAC silencing and anaphase onset^{7–9}. The PBD and autocatalytic activity of PLK1 have been implicated in its targeting to different mitotic structures, including kinetochores^{10–13}, but the mechanisms regulating PLK1 dynamics remain poorly understood.

Post-translational modifications including phosphorylation and acetylation ensure correct expression and activity of key mitotic factors^{14,15}. Moreover, covalent conjugation of ubiquitin to specific lysine residues of target proteins emerged as a critical regulatory signal in cellular physiology, mediating both proteolysis-dependent and -independent mechanisms^{16,17}. Ubiquitin is attached to a substrate by coordinated cycles of three enzymatic reactions, ubiquitin activation (E1 enzyme), ubiquitin conjugation (E2 enzyme) and ubiquitin ligation (E3 protein ligase). Previous studies in human cells identified critical roles and substrates of cullin–RING E3 ubiquitin ligases (CRL) in cell proliferation and tumour progression^{18,19}. In particular, CUL3 seems to regulate several aspects of mitosis by assembling E3 ubiquitin ligase complexes with specific Bric-a-brac/Tramtrack/Broad complex (BTB) adaptor proteins^{20–22}.

In this study, we identify PLK1 as a target of CUL3, which in complex with the BTB-adaptor protein KLHL22 regulates chromosome alignment and PLK1 kinetochore localization but not PLK1 stability. In the absence of KLHL22, PLK1 accumulates on mitotic kinetochores, resulting in hyperphosphorylation of its target BUBR1, inhibition of stable kinetochore–microtubule interactions and activation of the

¹Institute of Biochemistry, ETH Zurich, Schafmattstrasse 18, 8093 Zurich, Switzerland. ²Wellcome Trust Centre for Gene Regulation and Expression, College of Life Sciences, University of Dundee, Dundee DD1 5EH, UK. ³Institute of Genetics and Molecular and Cellular Biology (IGBMC), 67400 Illkirch, France. ⁴The Hospital for Sick Children, Toronto M5S 1A8, Canada. ⁵Miltenyi Biotec GmbH, 51429 Bergisch Gladbach, Germany. ⁶Institute for Genetics, University of Cologne, 50674 Cologne, Germany. ⁷SCILLS, College of Life Sciences, University of Dundee, Dundee DD1 5EH, UK. ⁸These authors contributed equally to this work. ⁹Present address: Tecan Schweiz AG, 8708 Maennedorf, Switzerland.

¹⁰Correspondence should be addressed to M.P. or I.S. (e-mail: Matthias.Peter@bc.biol.ethz.ch or Izabela.Sumara@igbmc.fr)

Received 17 April 2012; accepted 18 January 2013; published online 3 March 2013; DOI: 10.1038/ncb2695

ARTICLES

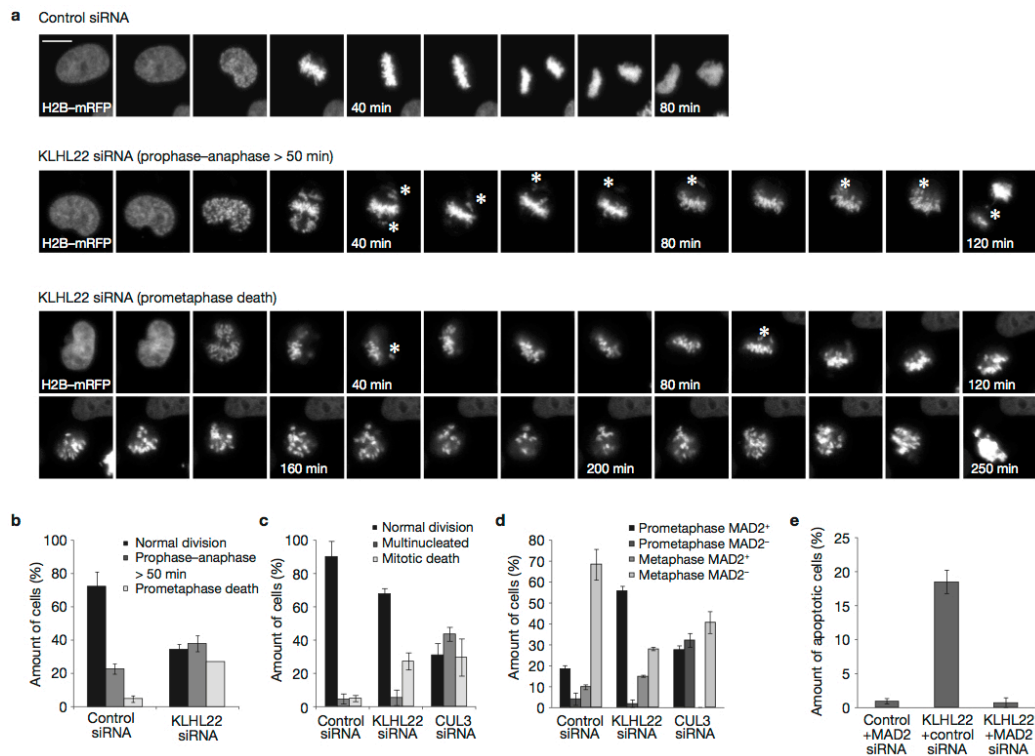


Figure 1 The BTB adaptor protein KLHL22 regulates SAC-dependent chromosome alignment during mitosis. (a) HeLa cells expressing H2B-mRFP were treated with the indicated siRNAs for 48 h and analysed by live-cell microscopy. Asterisks indicate misaligned and lagging chromosomes. Scale bar, 10 μ m. (b) The percentage of cells that complete mitosis normally or with a delay from prophase to anaphase (>50 min) or that undergo apoptosis during prometaphase was quantified ($n=50$). (c) The percentage of cells that undergo normal mitosis, become multinucleated or die during mitosis was quantified ($n=50$). (d) HeLa cells were treated

with the indicated siRNAs for 48 h and analysed by immunofluorescence microscopy for MAD2 and kinetochores. The percentage of prometaphase and metaphase cells that contain one or more MAD2-positive kinetochores was quantified ($n=30$). Example images are shown in Supplementary Fig. S1c. (e) HeLa cells expressing H2B-mRFP were treated with the indicated mixtures of siRNAs for 48 h and analysed by live-cell microscopy. The percentage of cells that die in prometaphase was quantified ($n=50$). Bars represent the mean of three independent experiments. Error bars indicate \pm s.d.

SAC. CUL3–KLHL22 directly binds PLK1 and ubiquitylates Lys 492, located within the PBD, leading to PLK1 dissociation from kinetochore phosphoreceptors. Indeed, expression of a non-ubiquitylatable PLK1-K492R mutant phenocopies inactivation of CUL3–KLHL22. Interestingly, KLHL22 associates with the mitotic spindle and its interaction with PLK1 increases as cells achieve chromosome bi-orientation. Together, our data suggest that CUL3–KLHL22-mediated ubiquitylation signals degradation-independent removal of PLK1 from kinetochores and SAC satisfaction, which are required for faithful progression through mitosis.

RESULTS

The CUL3–KLHL22 E3 ligase regulates SAC-dependent chromosome alignment during mitosis

The BTB–Kelch protein KLHL22 interacts with CUL3 (Supplementary Fig. S1a) and is required for mitotic division²², but its molecular

function and critical ubiquitylation substrates remain unknown. KLHL22 is expressed throughout the cell cycle with levels moderately increasing during mitosis (Supplementary Fig. S1b). Live-cell microscopy of HeLa cells stably expressing the histone marker H2B-mRFP revealed that KLHL22-depleted cells show severe chromosome alignment defects, with 27.9% (\pm 5%) of cells dying after a prolonged prometaphase-like arrest without anaphase initiation (Fig. 1a,b). However, unlike CUL3 depletion, KLHL22 RNA-mediated interference (RNAi) did not lead to an increased occurrence of micronuclei or multinucleated cells (Fig. 1c). To assess whether activation of the SAC causes the observed prometaphase arrest, KLHL22-depleted cells were arrested in mitosis by addition of the proteasome inhibitor MG132, and the protein mitotic arrest deficient 2 (MAD2) was visualized as a marker for unattached kinetochores²³ by immunofluorescence microscopy. In contrast to RNAi controls, MAD2-positive kinetochores could be detected in

96.7% of the mitotically arrested KLHL22-depleted cells (Fig. 1d). The presence of unaligned but MAD2-negative kinetochores in CUL3-depleted cells (Supplementary Fig. S1c) could be explained by pleiotropic effects including SAC slippage²⁴ or incorrect kinetochore attachments, accounting for the fact that CUL3 forms functional complexes with several substrate adaptors²². Importantly, simultaneous inactivation of KLHL22 and MAD2 rescued the KLHL22 mitotic-cell-death phenotype (Fig. 1e and Supplementary Fig. S1d). KLHL22 depletion did not impede bipolar spindle formation, loading of condensin on chromosomes (data not shown) or kinetochore assembly (Supplementary Fig. S1e–h). However, 57.5% of the KLHL22-depleted cells failed to form proper metaphase plates in the presence of MG132, compared with 22.1% of control cells, suggesting that the CUL3–KLHL22 E3 ligase regulates SAC-dependent processes required for efficient chromosome alignment during mitosis.

The CUL3–KLHL22 E3 ligase targets PLK1 and regulates its kinetochore localization during mitosis

The KLHL22 RNAi phenotype suggests that CUL3–KLHL22 targets proteins with essential functions during mitosis. To identify these substrates, we probed protein microarrays containing ~8,300 human proteins for their binding to AlexaFluor647-labelled KLHL22, and for their *in vitro* ubiquitylation by reconstituted CUL3–RBX1–KLHL22 complexes in the presence of FITC-labelled ubiquitin. As expected, MBP–KLHL22 interacted with GST–CUL3–RBX1, but not with GST controls, and reconstituted CUL3–RBX1–KLHL22 complexes promoted autoubiquitylation of GST–CUL3, but not GST- or MBP-tagged negative control substrates (Supplementary Fig. S2). We identified 93 proteins that specifically interacted with MBP–KLHL22 and 30 of these were also ubiquitylated by CUL3–RBX1–KLHL22, suggesting that they may be substrates of this E3 ligase (Supplementary Tables S1 and S2). Interestingly, in our list of candidates we found a ninefold and sixfold over-representation of protein kinases, respectively. Among them was PLK1, which is well known to regulate several processes in mitosis⁵ including chromosome alignment, centrosome function and spindle assembly through its dynamic localization to kinetochores, centrosomes and the midzone region⁴. Consistent with the proteoarray results, endogenous PLK1, but not PLK2, co-immunoprecipitated with FLAG-tagged KLHL22 in extracts prepared from mitotically synchronized cells (Fig. 2a). Likewise, endogenous KLHL22 was efficiently co-immunoprecipitated with endogenous PLK1 from mitotic-stage cells (Fig. 2b). Accordingly, recombinant KLHL22, but not KLHL21, strongly bound purified PLK1 *in vitro* and this interaction was established through the Kelch domain of KLHL22 (Fig. 2c,d). Together, these data suggest that PLK1 is indeed a specific and direct target of CUL3–KLHL22.

To understand the physiological consequences of KLHL22-mediated ubiquitylation of PLK1, we compared its abundance and subcellular localization in control and CUL3–KLHL22-depleted cells using PLK1-specific antibodies. We were unable to detect significant differences in total cellular levels of PLK1 in the presence or absence of KLHL22 (Fig. 3c). Consistent with published results^{4,7,9}, we observed that kinetochore-associated PLK1 levels were markedly reduced as chromosomes become bi-oriented in metaphase (Supplementary Fig. S3a,b). Interestingly, downregulation of KLHL22 or CUL3 led to a striking increase in the level

of PLK1 on kinetochores during prometaphase when compared with control short interfering RNA (siRNA)-treated cells (Fig. 2e,f and Supplementary Fig. S3c), whereas its levels on centrosomes were slightly decreased (Supplementary Fig. S3d,e). In contrast, KLHL22 depletion did not alter the localization of any other kinetochore protein we tested (Fig. 2g and Supplementary Fig. S1e–h). Importantly, PLK1 levels on kinetochores also increased in CUL3- or KLHL22-depleted cells arrested with the microtubule-depolymerizing drug nocodazole (Fig. 2e,f), excluding the possibility that this effect was indirectly caused by the prolonged prometaphase arrest. Consistent with this notion, downregulation of the previously described CUL3 adaptor KLHL21 (ref. 22; Fig. 2e,f) or drug-induced arrest in different mitotic stages (Fig. 2h) did not result in PLK1 accumulation on kinetochores. Taken together, we conclude that the CUL3–KLHL22 E3 ligase may act to remove PLK1 from kinetochores before chromosomes achieve bi-orientation in metaphase, without affecting total PLK1 levels or other subcellular pools of kinetochore proteins.

CUL3–KLHL22 regulates maintenance of stable kinetochore–microtubule interactions

To determine whether CUL3–KLHL22 regulates PLK1 activity, we analysed the phosphorylation state of the kinetochore protein BUBR1. PLK1-mediated phosphorylation of BUBR1 occurs at several sites and has been correlated with stability of kinetochore–microtubule interactions^{7,25}. Whereas total, kinetochore-associated BUBR1 levels were unaffected (Fig. 2g), inactivation of KLHL22, but not KLHL21, in mitotically arrested cells led to a threefold to fourfold augmented phosphorylation of BUBR1 on Ser 676, consistent with the observed increase of PLK1 on kinetochores (Fig. 3a–c). Accordingly, Ser 676 phosphorylation of BUBR1 was abolished on treatment with the PLK1 inhibitor BI 2536 (ref. 6; Fig. 3d). In contrast, PLK1-activity-dependent accumulation of γ -tubulin on centrosomes was normal in mitotic cells (Supplementary Fig. S3e). Together, these results suggest that inactivation of CUL3–KLHL22 leads to increased PLK1 levels and sustained kinase activity specifically at kinetochores, causing an increased level of BUBR1 phosphorylation. As BUBR1 phosphorylation was reported to regulate stable kinetochore–microtubule interactions⁷, we monitored kinetochore localization of RANGAP1, which depends on stable kinetochore–microtubule interactions²⁶. To this end, we arrested control and KLHL22-depleted cells with monastrol, and released them into MG132-containing media to achieve a highly synchronous population of cells with bi-oriented chromosomes. In contrast to control-depleted cells, RANGAP1 failed to efficiently localize to kinetochores and mitotic spindles in the absence of KLHL22 (Supplementary Fig. S3f) and this defect could be reversed by treatment with the PLK1 inhibitor BI 2536 (Fig. 3e). Together these results suggest that in the absence of KLHL22, cells fail to establish stable kinetochore–microtubule interactions because PLK1 accumulates on kinetochores leading to hyperphosphorylation of BUBR1 and, as a consequence, defects in chromosome alignment.

CUL3–KLHL22-mediated ubiquitylation of PLK1 within the PBD regulates faithful chromosome alignment during mitosis

To examine whether PLK1 ubiquitylation is indeed critical for mitotic progression, we next determined the sites ubiquitylated by

ARTICLES

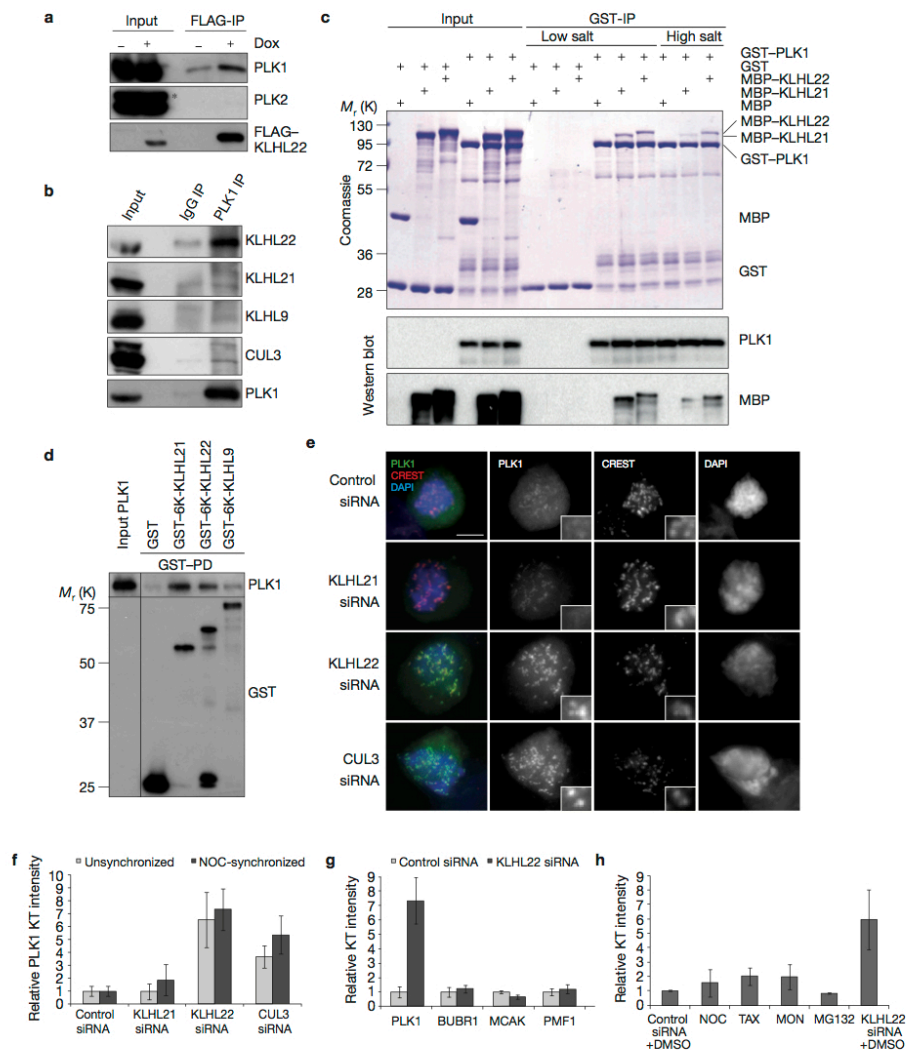


Figure 2 The CUL3-KLHL22 E3 ligase interacts directly with PLK1 and regulates its kinetochore localization during mitosis. (a) HeLa cells inducibly expressing FLAG-KLHL22 were treated with doxycycline (Dox), synchronized by double thymidine block release and collected in mitosis by mitotic shake-off. Cell extracts were immunoprecipitated with anti-FLAG antibodies and analysed by western blotting. The asterisk indicates the band corresponding to PLK2. (b) HeLa cells were synchronized as in **a** and extracts were immunoprecipitated with control (IgG IP) or anti-PLK1 (PLK1 IP) antibodies and analysed by western blotting. (c) Recombinant GST fused to full-length PLK1 (GST-PLK1) was incubated with recombinant MBP, MBP fused to full-length KLHL21 (MBP-KLHL21) or KLHL22 (MBP-KLHL22), and immunoprecipitated using glutathione-Sepharose beads. Immunoprecipitates (GST-IP) were washed in low- and high-salt conditions and analysed by Coomassie blue staining and western blotting. (d) Recombinant GST, GST fused to the Kelch repeats (GST-6K) of KLHL21, KLHL22 or KLHL9 were incubated with recombinant PLK1,

immunoprecipitated using glutathione–Sepharose beads and analysed by western blotting. **(e)** HeLa cells were treated with the indicated siRNAs for 48 h, arrested in mitosis with nocodazole for 14 h and analysed by immunofluorescence microscopy. Scale bar, 5 μ m. Insets show $\times 4$ magnifications of selected kinetochores. **(f)** Quantification of relative intensity ratios of PLK1/CREST staining on individual kinetochores (KTs; from 10 cells) from unsynchronized (as in Supplementary Fig. S3c, light grey) and nocodazole (NOC) synchronized cells (as in e, dark grey). The ratios of control siRNA-treated cells were set to 1. **(g)** Quantification of intensity ratios of different kinetochore markers normalized to the corresponding CREST signals in control (light grey) and KLH22-depleted (dark grey) cells. **(h)** The relative kinetochore intensities of PLK1 were quantified as in f from cells treated with indicated siRNAs and nocodazole (NOC), Taxol (TAX), monastrol (MON), MG132 or dimethylsulphoxide (DMSO). Bars represent the mean of three independent experiments. Error bars indicate \pm s.d. Uncropped images of blots/gels are shown in Supplementary Fig. S6.

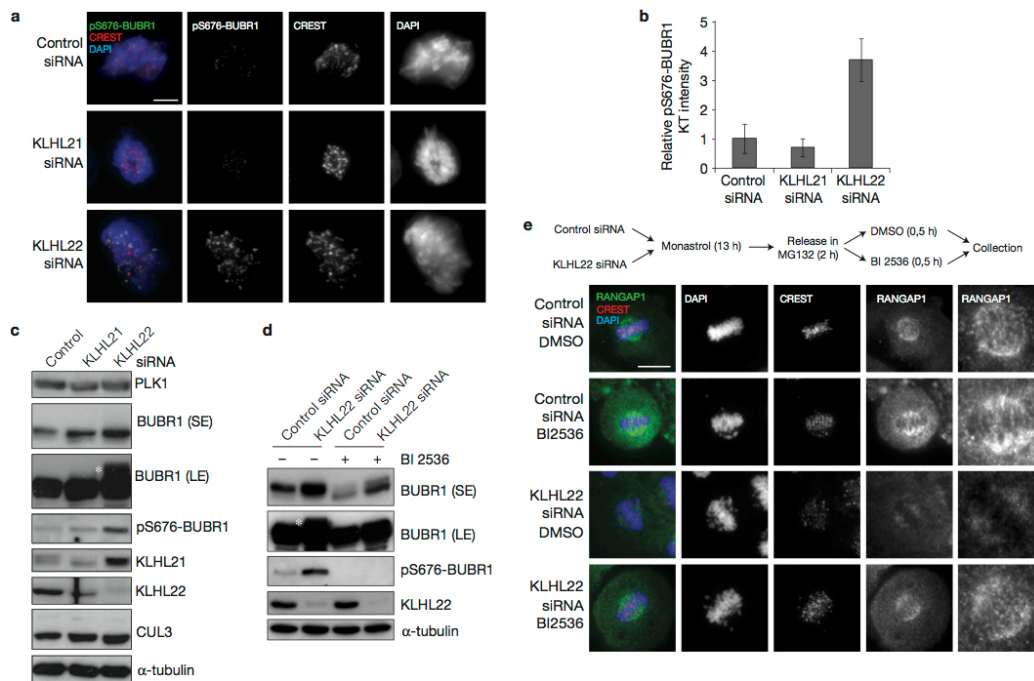


Figure 3 KLHL22 regulates PLK1-mediated phosphorylation of BUBR1 and stable kinetochore-microtubule attachments. (a) HeLa cells were treated with the indicated siRNAs for 48 h, arrested in mitosis with nocodazole for 14 h and analysed by immunofluorescence microscopy. Scale bar, 5 μ m. (b) Quantification of the relative intensity ratios of pS676-BUBR1/CREST on individual kinetochores (KTs; $n = 10$) from a. Bars represent the mean of three independent experiments. Error bars indicate \pm s.d. (c) HeLa cells

were treated as in a, collected by mitotic shake-off and analysed by western blotting. (d) HeLa cells were treated as in c, incubated with BI 2536 as indicated and analysed by western blotting. (e) HeLa cells were treated with the indicated siRNAs for 24 h, synchronized in metaphase and treated with BI 2536 or dimethylsulphoxide (DMSO) as described and analysed by immunofluorescence microscopy. Scale bar, 10 μ m. Uncropped images of blots are shown in Supplementary Fig. S6.

CUL3–KLHL22 complexes *in vitro*. GST–CUL3–RBX1 complexes purified from Sf9 cells reconstituted with MBP-tagged KLHL22 purified from *Escherichia coli* were able to mainly mono-ubiquitylate recombinant PLK1, whereas multiple sites were used with lower efficiency (Fig. 4a). Mass spectrometry analysis identified lysine residues 492 and 19 as ubiquitin acceptor sites. Interestingly, Lys 492 resides in the PBD of PLK1, is conserved from fission yeast to humans (Fig. 4b,c) and was confirmed as a ubiquitin acceptor site *in vivo* in two independent proteomic studies^{27,28}.

As the PBD mediates recruitment to mitotic structures including kinetochores^{11–13} we examined whether ubiquitylation by the CUL3–KLHL22 E3 ligase may regulate PBD-mediated PLK1 function at kinetochores. To this end, we generated HeLa cell lines that allow doxycycline-inducible expression of GFP-fused wild-type (WT) PLK1 or a version of PLK1 with Lys 492 mutated to a non-ubiquitylatable arginine residue (KR). Expression of PLK1^{WT} was able to rescue the mitotic defects induced by 3'UTR-directed siRNA targeting endogenous PLK1, including the delay at the metaphase–anaphase transition and induction of apoptosis (Fig. 4d–f). In contrast, expression of the PLK1^{KR} mutant resulted in severe mitotic

defects leading to prometaphase delay that was often followed by apoptotic death (36%). Moreover, kinetochore localization of the PLK1^{KR} mutant was augmented and these cells showed increased levels of phosphorylated BUBR1 and decreased levels of RANGAP1 on kinetochores (Fig. 4g), thus resembling the KLHL22 RNAi phenotype. These results were confirmed in HeLa cell lines expressing HIS tag-fused PLK1^{WT} or PLK1^{KR} (Fig. 5a,b). As expected, centrosome maturation and bipolar spindle formation were not perturbed under these conditions (data not shown), implying that the PLK1^{KR} mutant is specifically defective for its kinetochore function. Importantly, no significant difference in kinase activity could be detected when comparing PLK1^{WT} and the PLK1^{KR} mutant (Supplementary Fig. S4a). Moreover, the interaction of PLK1 with the APC/C activator CDH1 was not affected by the K492R mutation (Supplementary Fig. S4b). Accordingly, the PLK1^{KR} mutant was efficiently degraded at the end of mitosis with kinetics comparable to PLK1^{WT} or endogenous PLK1 (Supplementary Fig. S4c), implying that the K492R mutation does not influence APC/C^{CDH1}-mediated ubiquitylation and subsequent proteasomal degradation of PLK1. Together, these results suggest that the accumulation of PLK1 at kinetochores and resulting mitotic defects

ARTICLES

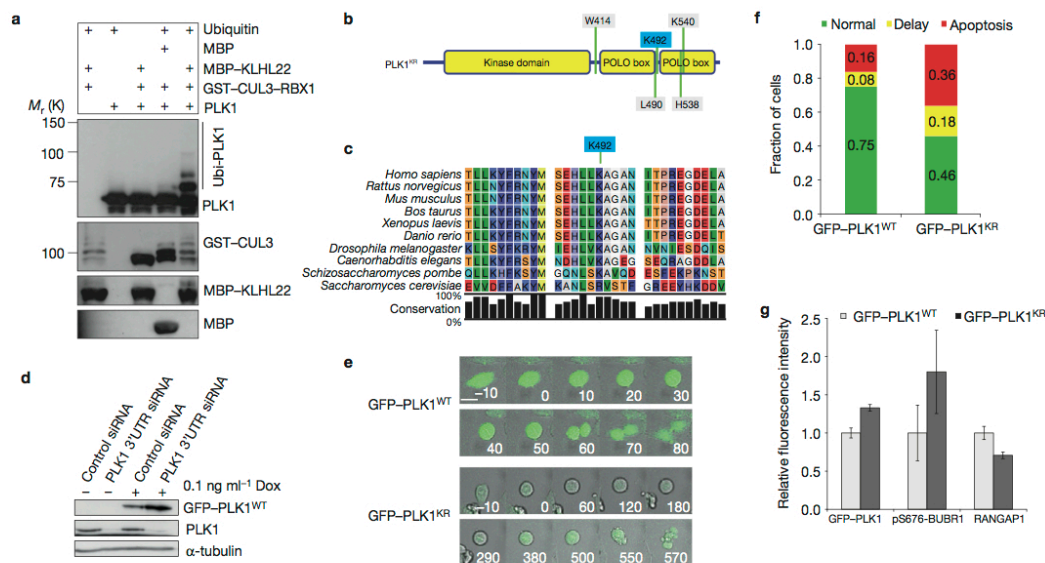


Figure 4 CUL3-KLHL22-mediated ubiquitylation of PLK1 within the PBD domain regulates faithful chromosome alignment during mitosis. (a) Recombinant PLK1 was added to *in vitro* ubiquitylation reactions containing GST-CUL3-RBX1 complexes purified from Sf9 cells. Reactions were incubated for 1 h with MBP or MBP-KLHL22 purified from *E. coli* and analysed by western blotting. Note that PLK1 was mainly mono-ubiquitylated (asterisk) under these conditions, but multiple sites were used with lower efficiency. (b) Schematic representation of PLK1. The ubiquitin acceptor lysine Lys 492 is indicated in blue; residues required for PBD phosphosite targeting are indicated in grey. (c) Alignment of PLK1 regions containing the identified ubiquitin acceptor site Lys 492 from different species. (d) HeLa cells inducibly expressing GFP-PLK1^{WT} were treated with doxycycline (\pm Dox) and transfected with control or PLK1 3'UTR siRNA. Cell extracts were analysed by western blotting. (e) HeLa cell lines inducibly expressing GFP-PLK1^{WT} or the KR mutant were transfected with PLK1 3'UTR siRNA and analysed by live-cell microscopy 24–48 h after transfection. Minutes before and after mitotic entry are indicated. Scale bar, 10 μ m. (f) Quantification of cells from e that complete mitosis (green and yellow) versus cells that undergo apoptosis during prometaphase (red) (total numbers of cells analysed: $n^{\text{WT}} = 312$, $n^{\text{KR}} = 235$). For the cells that complete mitosis,

the duration from prophase to anaphase was quantified and the fraction of cells exhibiting a normal (green) or delayed (yellow) anaphase onset was calculated. Delay is defined as: duration longer than WT average + 1 \times standard deviation. Duration values were quantified from $n^{\text{WT}} = 80$, $n^{\text{KR}} = 78$ cells. (g) Cells expressing GFP-PLK1^{WT} (light grey) or GFP-PLK1^{KR} (dark grey) were transfected with PLK1 3'UTR siRNA, fixed 36 h after transfection and analysed by immunofluorescence microscopy. GFP-PLK1 was visualized by GFP microscopy; pS676-BUBR1, RANGAP1 and CREST were stained using the corresponding antibodies. To quantify kinetochore-associated GFP-PLK1, GFP at individual kinetochores ($n = 322$ kinetochores in total from 3 independent experiments) was normalized both to cytoplasmic GFP and to the corresponding CREST signal at kinetochores using the following equation: $\text{GFP(kinetochore)}/\text{GFP(cytoplasm)}/\text{CREST(kinetochore)}$. pS676-BUBR1 signals of individual kinetochores ($n = 36$ kinetochores from 1 experiment) were normalized both to the corresponding CREST and GFP-PLK1 signal intensities using the following equation: $(\text{pS676-BUBR1}/\text{CREST})/(\text{GFP}/\text{CREST})$; RANGAP1 intensities on individual kinetochores ($n = 322$ kinetochores in total from 3 independent experiments) were normalized to CREST staining. Error bars indicate \pm s.d. Uncropped images of blots are shown in Supplementary Fig. S6.

can be linked to CUL3-KLHL22-mediated ubiquitylation of Lys 492 located in the PBD of PLK1.

The PBD promotes phospho-dependent interactions of PLK1 with its target proteins²⁹. On the basis of structural predictions, Lys 492 is in close proximity to the four key residues involved in phosphosite binding (Trp 414, Leu 490, His 538 and Lys 540; Figs 4b and 5c), raising the possibility that ubiquitylation by the CUL3-KLHL22 E3 ligase may regulate PBD-mediated interactions of PLK1 at kinetochores. Thus, we examined the interaction of PLK1^{WT} and PLK1^{KR} with the phosphoreceptor proteins INCENP and BUBR1 in mitotically synchronized cells. Remarkably, the level of PLK1^{KR} binding to these kinetochore phosphoreceptors was increased as compared with PLK1^{WT} (Fig. 5d,e). Furthermore, KLHL22 overexpression reduced the interaction between BUBR1 and PLK1^{WT} but not PLK1^{KR} (Fig. 5e),

suggesting that ubiquitylation of Lys 492 inhibits PBD-mediated phospho-interactions of PLK1 at kinetochores.

KLHL22 accumulates at the mitotic spindle and its association with PLK1 increases on chromosome bi-orientation

To understand the spatio-temporal regulation of CUL3-KLHL22 E3 ligase, we generated a doxycycline-inducible cell line expressing GFP-KLHL22 and assayed its localization throughout mitosis. GFP-KLHL22 efficiently interacted with endogenous CUL3 (Supplementary Fig. S5a) and PLK1 (Supplementary Fig. S5b), suggesting that the GFP fusion does not affect the function of KLHL22 as a CUL3 adaptor *in vivo*. Whereas GFP-KLHL22 was mostly visible as a diffuse cytoplasmic signal in prophase and prometaphase, it associated with the mitotic spindle as the cells reached chromosome bi-orientation

ARTICLES

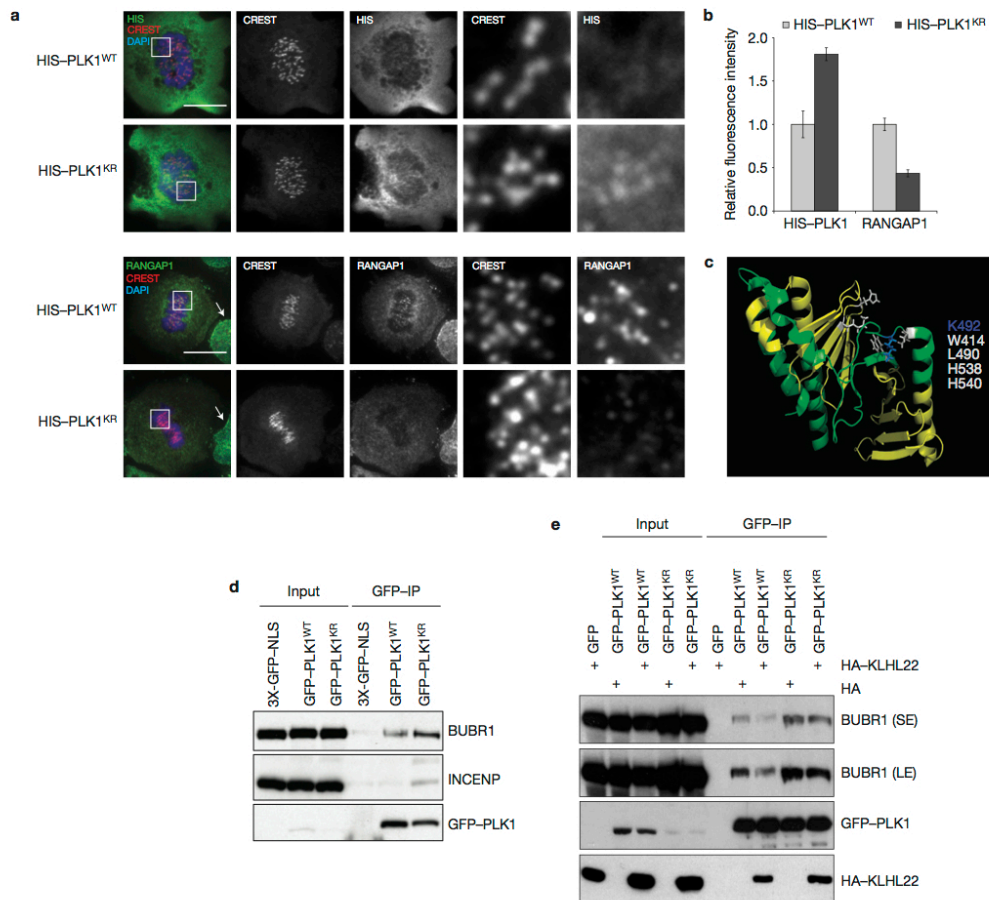


Figure 5 Ubiquitylation of PLK1 by CUL3-KLHL22 regulates PBD-mediated phospho-interactions at kinetochores and stable kinetochore-microtubule attachments. **(a)** HeLa cells inducibly expressing HIS-PLK1^{WT} or the KR mutant were transfected with PLK1 3'UTR siRNA and analysed by immunofluorescence microscopy. The images on the right show 5× magnifications of the area outlined in the left image. Note that expression of the PLK1^{KR} mutant leads to increased kinetochore association of PLK1 and a decrease in RANGAP1 at kinetochores but not at the nuclear envelope (arrows) in interphase cells. Scale bars, 5 μm. **(b)** Cells expressing HIS-PLK1^{WT} (light grey) or HIS-PLK1^{KR} (dark grey) were treated as in Fig. 4g and kinetochore-associated HIS-PLK1 ($n = 150$ kinetochores in total from

3 independent experiments) and RANGAP1 ($n = 170$ kinetochores in total from 3 independent experiments) were quantified. Error bars indicate \pm s.d. **(c)** Model of the PLK1 crystal structure⁴³ highlighting the relevant residues of this study. The ubiquitin acceptor lysine Lys 492 is shown in blue, the residues required for phosphopeptide targeting are shown in grey. **(d)** Cells expressing GFP alone, GFP-PLK1^{WT} or GFP-PLK1^{KR} were synchronized in mitosis, immunoprecipitated using GFP-Trap beads and analysed by western blotting. **(e)** Cells expressing GFP alone, GFP-PLK1^{WT} or GFP-PLK1^{KR} were transfected with either HA alone or HA-KLHL22 and immunoprecipitated using GFP-Trap beads and analysed by western blotting. Uncropped images of blots are shown in Supplementary Fig. S6.

(Fig. 6a), consistent with the reported localization of CUL3 (ref. 30). Interestingly, live-cell video microscopy revealed that GFP-KLHL22 localized to the centrosomes shortly before cells entered anaphase (Fig. 6a and Supplementary Fig. S5c and Videos). After anaphase onset, GFP-KLHL22 was predominantly associated with the polar microtubules connecting the two opposing centrosomes and gradually diffused into the cytoplasm during telophase. Thus, KLHL22 may use the mitotic spindle compartment to remove PLK1 from kinetochores.

To determine whether the interaction of CUL3-KLHL22 with PLK1 is regulated by chromosome bi-orientation, we investigated if KLHL22-PLK1 binding was influenced by the status of kinetochore-microtubule interactions. To this end, PLK1 was immunoprecipitated from cells arrested with monastrol, and released into media containing MG132 to accumulate cells in metaphase. On chromosome bi-orientation, cells were treated with either dimethylsulphoxide, nocodazole or Taxol, to alleviate

ARTICLES

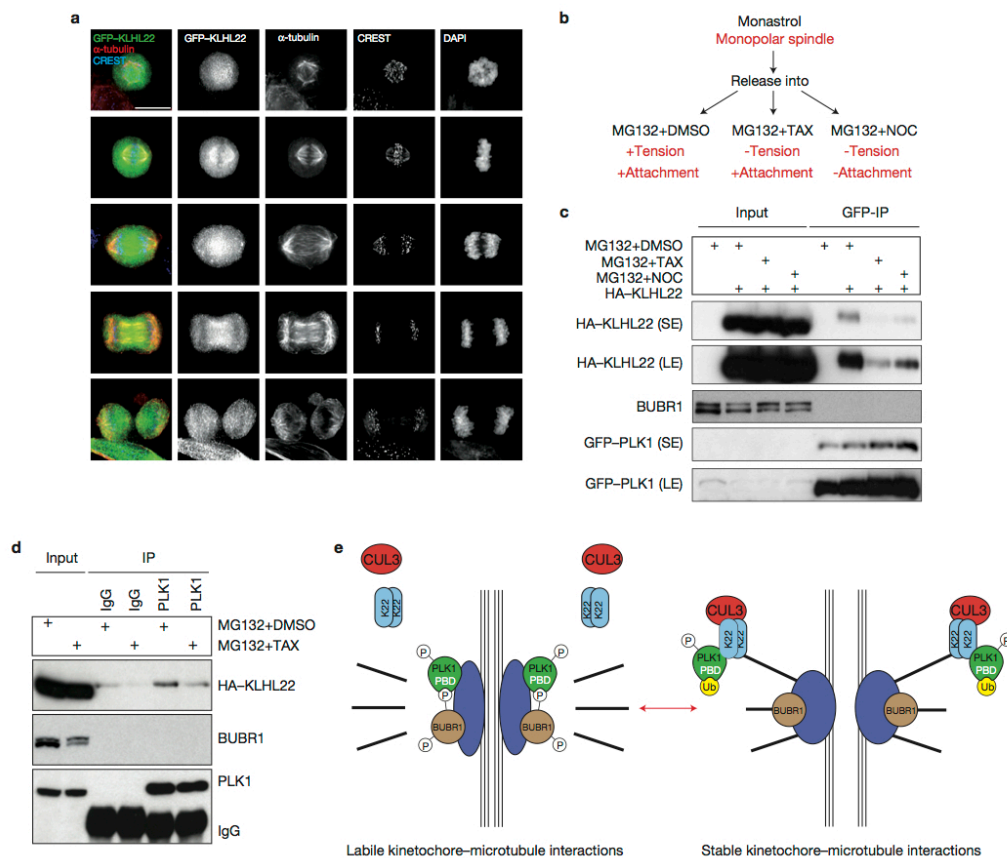


Figure 6 KLHL22 accumulates at the mitotic spindle and its association with PLK1 peaks with chromosome bi-orientation. (a) Immunofluorescence microscopy was performed using a doxycycline-inducible GFP-KLHL22 cell line, which was synchronized in mitosis by RO3306 block and release, fixed and stained with CREST and α -tubulin using specific antibodies. GFP-KLHL22 is visualized only by its GFP fluorescence. Images are maximum-intensity projections through Z-stacks spanning a total depth of 12 μ m in 0.5 μ m increments. Scale bar, 10 μ m. (b) Workflow for synchronizing cells in metaphase and addition of dimethylsulphoxide (DMSO), the microtubule-stabilizing drug Taxol (TAX) or the microtubule-depolymerizing agent nocodazole (NOC). Note that Taxol allows microtubule attachment without tension being exerted on kinetochores, whereas kinetochores in nocodazole-treated cells are not attached to microtubules. (c) HeLa cells expressing HA-KLHL22 and GFP-PLK1 were treated as outlined in b, collected and GFP-PLK1 was immunoprecipitated and analysed by western blotting. (d) HeLa cells expressing HA-KLHL22 were

treated as outlined in b, collected and endogenous PLK1 was immunoprecipitated and analysed by western blotting. (e) Model for ubiquitylation-dependent regulation of PLK1 in mitosis by CUL3-KLHL22. PLK1 (green) localizes to kinetochores (dark blue) and phosphorylates (P) the key SAC component, BUBR1 kinase (beige) to control chromosome alignment during prometaphase and metaphase stages. Following the establishment of stable attachments of kinetochores by microtubules (black bars), CUL3 (red) together with the substrate specific adaptor protein KLHL22 (light blue) binds and ubiquitylates PLK1 (Ub, yellow) within the PBD domain, leading to its dissociation from phosphoreceptor proteins and thereby efficient removal from kinetochores, allowing for silencing of SAC and chromosome segregation. This process may occur dynamically during prometaphase stages to provide a precise correction mechanism sensing stable microtubule-kinetochore interactions and microtubule-exerted tension and satisfaction of the SAC. Uncropped images of blots are shown in Supplementary Fig. S6.

kinetochore attachments and/or tension exerted on kinetochores⁷ (Fig. 6b). As expected, BUBR1 was mostly dephosphorylated in dimethylsulphoxide controls whereas after Taxol or nocodazole treatment BUBR1 was predominantly found in its slow migrating, phosphorylated form. Interestingly, under these conditions

the interaction of GFP-PLK1 with HA-KLHL22 was clearly reduced when compared with dimethylsulphoxide-treated cells, in which the attached microtubules exert tension across the kinetochores (Fig. 6c). Likewise, interaction of the endogenous PLK1 with HA-KLHL22 was reduced on Taxol treatment (Fig. 6d).

ARTICLES

These results suggest that chromosome bi-orientation and the concomitant structural changes in kinetochores may be a prerequisite for efficient binding of CUL3–KLHL22 to PLK1. This mechanism may thus allow for a spatio-temporal control of PLK1 ubiquitylation on Lys 492, which in turn may trigger its dissociation from kinetochores and anaphase onset.

DISCUSSION

In summary, our results strongly suggest that PLK1 is a direct target of the CUL3–KLHL22 E3 ligase complex and that its ubiquitylation within the PBD regulates PLK1 localization at kinetochores, chromosome alignment, SAC satisfaction and ultimately cell survival during metaphase. Defects in PLK1 ubiquitylation result in enhanced interaction with phosphoreceptor proteins and consequently in sustained kinase activity towards its kinetochore substrate BUBR1, which in turn interferes with stable kinetochore–microtubule interactions. PLK1 dissociation from kinetochores has been correlated with bipolar attachment of chromosomes to the mitotic spindle^{7,9}, but the mechanism of its removal was unknown so far. Our data suggest that the CUL3–KLHL22 interaction with PLK1 increases as chromosomes become bi-oriented, leading to PLK1 ubiquitylation and dissociation from kinetochores, thus providing a plausible mechanism of PLK1 removal from kinetochores on bi-orientation and consequently satisfaction of SAC signalling (Fig. 6e).

Versatile functions of CUL3-based ligases

Previous studies established CUL3 as a critical regulator of cellular physiology by assembling E3 ubiquitin ligase complexes with specific BTB adaptor proteins³¹. CUL3 complexes ubiquitylate and target substrates for proteasomal degradation, thereby regulating cellular homeostasis^{32,33} and development of disease^{34,35}. Importantly, several CUL3 complexes were also shown to regulate cell-cycle progression^{20–22,30}.

Our results suggest that the CUL3–KLHL22 E3 ligase ubiquitylates PLK1 at Lys 492 and regulates its localization specifically at kinetochores but does not regulate PLK1 protein stability. Importantly, this site was demonstrated to be ubiquitylated *in vivo* in two recent proteomic studies^{27,28}. Although we were unable to demonstrate the specific type of ubiquitin conjugation to PLK1 catalysed by CUL3–KLHL22 in cells, our *in vitro* ubiquitylation data strongly suggest that PLK1 is modified by attachment of a mono-ubiquitin. It is also possible that only a small fraction of PLK1, associated with kinetochores specifically when chromosomes achieve bi-orientation, gets modified. This modification is likely to be dynamic and rapidly reversed by the activity of an unknown deubiquitylase. Thus, both the temporal and spatial restriction make biochemical detection of such a modification very difficult with conventional methods. However, in light of the available evidence, and because expression of a PLK1 K492R mutant strikingly mimics the mitotic defects observed on downregulation of KLHL22 in cells, and conversely overexpression of KLHL22 reduces the interaction of PLK1 and BUBR1 in a Lys-492-dependent manner, we believe that CUL3–KLHL22 may directly mono-ubiquitylate this site to promote removal of PLK1 from kinetochores on bipolar microtubule attachment. Interestingly, other CUL3-based complexes were recently shown to catalyse mono-ubiquitylation^{36,37}. These findings significantly

expand the versatility and possible functions of CUL3-based ligases, and imply that they not only target substrates for proteasomal degradation, but also regulate reversible processes by regulating subcellular localization and possibly the activity and/or interactions of substrates in space and time.

Spatio-temporal regulation of CUL3/KLHL22

We demonstrate that KLHL22 associates with the mitotic spindle and its interaction with PLK1 increases on chromosome bi-orientation. As CUL3 was previously found to associate with mitotic spindles³⁰, these results may provide insight into how physical attachment of microtubules may convert to a biochemical signal that silences the SAC at kinetochores. Although GFP–KLHL22 did not accumulate at kinetochores, it is known that several dynamic kinetochore components are transported towards the spindle poles following checkpoint inactivation by the dynein/dynactin pathway^{38–40}. Indeed, CUL3 was previously reported to interact with components of the dynein complex^{30,41}, suggesting that CUL3–KLHL22 may use the microtubule-spindle compartment to ubiquitylate and remove PLK1 from kinetochores on chromosome bi-orientation.

CUL3–KLHL22 regulates the kinetochore activity of PLK1 and SAC signalling

We demonstrate that PLK1 ubiquitylation specifically regulates its function at kinetochores. This is achieved by ubiquitylation of a conserved lysine residue (Lys 492) within its PBD. PBD-dependent localization of PLK1 in mitosis is needed for the function of PLK1 only on kinetochores and not on centrosomes¹³, which explains why no defects in bipolar spindle assembly could be observed following the inactivation of CUL3–KLHL22. These findings thus not only provide surprising insights into the temporal and spatial regulation of PLK1, but also suggest that regulated removal of PLK1 from kinetochores is an important process monitoring chromosome alignment. Available evidence suggests that a single pathway may link error correction to SAC activation⁴². Our data support this notion in that the KLHL22-ubiquitylation pathway regulates phosphorylation of BUBR1 (Ser 676) by PLK1 and at the same time is sensed by a MAD2-dependent SAC mechanism. Importantly, both inactivation of KLHL22 and expression of the PLK1-K492R mutant lead to delocalization of the microtubule–kinetochore attachment sensor RANGAP1. Our results thus confirm that the establishment of stable kinetochore–microtubule interactions is tightly regulated^{8,9} and identify a mechanism leading to SAC satisfaction at the metaphase to anaphase transition. Indeed, KLHL22-mediated ubiquitylation of PLK1 prevents the molecular interaction of the PBD with its kinetochore receptor proteins. Thus, the CUL3-ubiquitylation pathway may provide a mode of substrate regulation by affecting the local concentration of essential enzymatic activities. As KLHL22 preferentially interacts with a subset of protein kinases in our protoarrays, it is conceivable that CUL3–KLHL22 complexes may also regulate the activity and/or localization of other protein kinases. Interestingly, previous studies demonstrated the role of a different CUL3-based complex in localization of aurora B kinase^{21,22}. It will therefore be interesting to study whether CUL3 complexes more commonly orchestrate localized kinase activities through non-degradative ubiquitylation. □

ARTICLES

METHODS

Methods and any associated references are available in the online version of the paper.

Note: Supplementary Information is available in the online version of the paper

ACKNOWLEDGEMENTS

We thank W. Piwko, T. Courthoux, P. Meraldi, D. Gerlich, A. Smith, O. Pourquié and M. Labouesse for helpful discussions and editing of the manuscript, E. A. Nigg, J.-M. Peters, P. Meraldi, U. Kutay and F. Barr for antibodies, D. Gerlich and U. Kutay for cell lines and G. Csucs, J. Kusch, O. Biehlmeier and T. Schwarz from the D-BIOL Light Microscopy Center for help with microscopy. J.B. was granted an EMBO Short Term Fellowship, and S.M. was funded by ETHZ and the Boehringer Ingelheim Fonds. I.S. was supported by the ETHZ and the Swiss National Science Foundation (SNF), and research in D.R. and M.P.'s laboratories by the Canadian Institute of Health Research (CIHR), the European Research Council (ERC), the SNF and the ETHZ, respectively. Research in I.S.'s laboratory is supported by the IGBMC, the ATIP-AVENIR program, CNRS, INSERM and Sanofi-Aventis.

AUTHOR CONTRIBUTIONS

J.B., S.M. and T.M. conceived ideas, performed experiments, and analysed and interpreted the data. H.S. and K.H. performed bioinformatic analysis of protein microarray data. A.P. and D.R. collaborated on protein microarray experiments. P.P. conducted the MS analysis of PLK1 ubiquitylation sites. M. Posch and J.R.S. collaborated on live-cell video microscopy techniques. M. Peter and I.S. conceived ideas. J.B., M. Peter and I.S. wrote the manuscript.

COMPETING FINANCIAL INTERESTS

The authors declare no competing financial interests.

Published online at www.nature.com/dofinder/10.1038/ncb2695

Reprints and permissions information is available online at www.nature.com/reprints

1. Williams, B. R. & Amon, A. Aneuploidy: cancer's fatal flaw? *Cancer Res.* **69**, 5289–5291 (2009).
2. Lengauer, C., Kinzler, K. W. & Vogelstein, B. Genetic instabilities in human cancers. *Nature* **396**, 643–649 (1998).
3. Strebhardt, K. Multifaceted polo-like kinases: drug targets and antitargets for cancer therapy. *Nat. Rev. Drug Discov.* **9**, 643–660 (2010).
4. Petronczki, M., Lenart, P. & Peters, J. M. Polo on the rise—from mitotic entry to cytokinesis with Plk1. *Dev. Cell* **14**, 646–659 (2008).
5. Sumara, I. *et al.* Roles of polo-like kinase 1 in the assembly of functional mitotic spindles. *Curr. Biol.* **14**, 1712–1722 (2004).
6. Lenart, P. *et al.* The small-molecule inhibitor BI 2536 reveals novel insights into mitotic roles of polo-like kinase 1. *Curr. Biol.* **17**, 304–315 (2007).
7. Elowe, S., Hummer, S., Uldschmidt, A., Li, X. & Nigg, E. A. Tension-sensitive Plk1 phosphorylation on BubR1 regulates the stability of kinetochore microtubule interactions. *Genes Dev.* **21**, 2205–2219 (2007).
8. Maia, A. R. *et al.* Cdk1 and Plk1 mediate a CLASP2 phospho-switch that stabilizes kinetochore-microtubule attachments. *J. Cell Biol.* **199**, 285–301 (2012).
9. Liu, D., Davydenko, O. & Lampson, M. A. Polo-like kinase-1 regulates kinetochore-microtubule dynamics and spindle checkpoint silencing. *J. Cell Biol.* **198**, 491–499 (2012).
10. Lee, K. S. *et al.* Mechanisms of mammalian polo-like kinase 1 (Plk1) localization: self- versus non-self-priming. *Cell Cycle* **7**, 141–145 (2008).
11. Elia, A. E. *et al.* The molecular basis for phosphodependent substrate targeting and regulation of Plks by the Polo-box domain. *Cell* **115**, 83–95 (2003).
12. Cheng, K. Y., Lowe, E. D., Sinclair, J., Nigg, E. A. & Johnson, L. N. The crystal structure of the human polo-like kinase-1 polo box domain and its phospho-peptide complex. *EMBO J.* **22**, 5757–5768 (2003).
13. Hanisch, A., Wehner, A., Nigg, E. A. & Sillje, H. H. Different Plk1 functions show distinct dependencies on Polo-Box domain-mediated targeting. *Mol. Biol. Cell* **17**, 448–459 (2006).
14. Nigg, E. A. Mitotic kinases as regulators of cell division and its checkpoints. *Nat. Rev. Mol. Cell Biol.* **2**, 21–32 (2001).
15. Mateo, F., Vidal-Laliena, M., Pujol, M. J. & Bachs, O. Acetylation of cyclin A: a new cell cycle regulatory mechanism. *Biochem. Soc. Trans.* **38**, 83–86 (2010).
16. Hershko, A. The ubiquitin system for protein degradation and some of its roles in the control of the cell division cycle. *Cell Death Differ.* **12**, 1191–1197 (2005).
17. Li, W. & Ye, Y. Polyubiquitin chains: functions, structures, and mechanisms. *Cell. Mol. Life Sci.* **65**, 2397–2406 (2008).
18. Deshaies, R. J. SCF and cullin/ring H2-based ubiquitin ligases. *Annu. Rev. Cell Dev. Biol.* **15**, 435–467 (1999).
19. Petroski, M. D. & Deshaies, R. J. Function and regulation of cullin-RING ubiquitin ligases. *Nat. Rev. Mol. Cell Biol.* **6**, 9–20 (2005).
20. Sumara, I., Maerki, S. & Peter, M. E3 ubiquitin ligases and mitosis: embracing the complexity. *Trends Cell Biol.* **18**, 84–94 (2008).
21. Sumara, I. *et al.* A Cul3-based E3 ligase removes Aurora B from mitotic chromosomes, regulating mitotic progression and completion of cytokinesis in human cells. *Dev. Cell* **12**, 887–900 (2007).
22. Maerki, S. *et al.* The Cul3-KLHL21 E3 ubiquitin ligase targets aurora B to midzone microtubules in anaphase and is required for cytokinesis. *J. Cell Biol.* **187**, 791–800 (2009).
23. Li, Y. & Benezra, R. Identification of a human mitotic checkpoint gene: hSMAD2. *Science* **274**, 246–248 (1996).
24. Sumara, I. & Peter, M. A Cul3-based E3 ligase regulates mitosis and is required to maintain the spindle assembly checkpoint in human cells. *Cell Cycle* **6**, 3004–3010 (2007).
25. Matsumura, S., Toyoshima, F. & Nishida, E. Polo-like kinase 1 facilitates chromosome alignment during prometaphase through BubR1. *J. Biol. Chem.* **282**, 15217–15227 (2007).
26. Joseph, J., Liu, S. T., Jablonski, S. A., Yen, T. J. & Dasso, M. The RanGAP1-RanBP2 complex is essential for microtubule-kinetochore interactions *in vivo*. *Curr. Biol.* **14**, 611–617 (2004).
27. Kim, W. *et al.* Systematic and quantitative assessment of the ubiquitin-modified proteome. *Mol. Cell* **44**, 325–340 (2011).
28. Wagner, S. A. *et al.* A proteome-wide, quantitative survey of *in vivo* ubiquitylation sites reveals widespread regulatory roles. *Mol. Cell Proteomics* **10**, 013284 (2011).
29. Park, J. E. *et al.* Polo-box domain: a versatile mediator of polo-like kinase function. *Cell Mol. Life Sci.* **67**, 1957–1970 (2010).
30. Moghe, S. *et al.* The CUL3-KLHL18 ligase regulates mitotic entry and ubiquitylates Aurora-A. *Biol. Open* **1**, 82–91 (2012).
31. Pintard, L., Willems, A. & Peter, M. Cullin-based ubiquitin ligases: Cul3-BTB complexes join the family. *EMBO J.* **23**, 1681–1687 (2004).
32. Villeneuve, N. F., Lau, A. & Zhang, D. D. Regulation of the Nrf2-Keap1 antioxidant response by the ubiquitin proteasome system: an insight into cullin-ring ubiquitin ligases. *Antioxid. Redox. Signal* **13**, 1699–1712 (2010).
33. Huotari, J. *et al.* Cullin-3 regulates late endosome maturation. *Proc. Natl Acad. Sci. USA* **109**, 823–828 (2012).
34. Boyden, L. M. *et al.* Mutations in kelch-like 3 and cullin 3 cause hypertension and electrolyte abnormalities. *Nature* **482**, 98–102 (2012).
35. Yuan, W. C. *et al.* A Cullin3-KLHL20 Ubiquitin ligase-dependent pathway targets PML to potentiate HIF-1 signaling and prostate cancer progression. *Cancer Cell* **20**, 214–228 (2011).
36. Hernandez-Munoz, I. *et al.* Stable X chromosome inactivation involves the PRC1 Polycomb complex and requires histone MACROH2A1 and the CULLIN3/SPOP ubiquitin E3 ligase. *Proc. Natl Acad. Sci. USA* **102**, 7635–7640 (2005).
37. Jin, L. *et al.* Ubiquitin-dependent regulation of COPII coat size and function. *Nature* **482**, 495–500 (2012).
38. Howell, B. J. *et al.* Cytoplasmic dynein/dynactin drives kinetochore protein transport to the spindle poles and has a role in mitotic spindle checkpoint inactivation. *J. Cell Biol.* **155**, 1159–1172 (2001).
39. Varma, D., Monzo, P., Stehman, S. A. & Vallee, R. B. Direct role of dynein motor in stable kinetochore-microtubule attachment, orientation, and alignment. *J. Cell Biol.* **182**, 1045–1054 (2008).
40. Yang, Z., Tulu, U. S., Wadsworth, P. & Rieder, C. L. Kinetochore dynein is required for chromosome motion and congression independent of the spindle checkpoint. *Curr. Biol.* **17**, 973–980 (2007).
41. Bennett, E. J., Rush, J., Gygi, S. P. & Harper, J. W. Dynamics of cullin-RING ubiquitin ligase network revealed by systematic quantitative proteomics. *Cell* **143**, 951–965 (2010).
42. Musacchio, A. & Salmon, E. D. The spindle-assembly checkpoint in space and time. *Nat. Rev. Mol. Cell Biol.* **8**, 379–393 (2007).
43. Yun, S. M. *et al.* Structural and functional analyses of minimal phosphopeptides targeting the polo-box domain of polo-like kinase 1. *Nat. Struct. Mol. Biol.* **16**, 876–882 (2009).

DOI: 10.1038/ncb2695

METHODS

METHODS

Cell lines. The FLAG–KLHL22 and GFP–KLHL22 cell lines were created using the Fip-IN-T-Rex cell line (Invitrogen) and GFP–PLK1 and HIS–PLK1 cell lines using a HeLa FRT/To host cell line kindly provided by U. Kutay (ETH Zurich, Switzerland). The HeLa cell line expressing H2B–RFP (ref. 44) was kindly provided by D. Gerlich (ETH Zurich, Switzerland). The HeLa cell line expressing three GFP tags in tandem, fused to a NLS signal¹⁹ was kindly provided by P. V. Lidsky (Russian Academy of Medical Sciences, Russia). HeLa Kyoto and HEK293T cells were maintained as previously described²¹. Antibiotics for selection were used as follows: hygromycin (Invitrogen) 100 $\mu\text{g ml}^{-1}$, blasticidin (Invitrogen) 15 $\mu\text{g ml}^{-1}$ and puromycin (Sigma Aldrich) 0.5 $\mu\text{g ml}^{-1}$. Doxycycline (Sigma) for induction of protein expression was used at 1 $\mu\text{g ml}^{-1}$ or 0.1 $\mu\text{g ml}^{-1}$.

Chemicals (Sigma) were used as follows: Taxol (paclitaxel) 1 μM (or as indicated), nocodazole 2 μM , hydroxyurea 2 mM, thymidine 2 mM, MG132 50 μM and monastrol 100 μM . The PLK1 inhibitor BI 2536 (Axon Medchem) was used at 100 nM and the deubiquitylase inhibitor PR-619 (TebuBio) at 20 μM .

Complementary DNAs and siRNAs. cDNA (RZPD) transfections were performed using Lipofectamine 2000 (Invitrogen) and siRNA transfections using Oligofectamine (Invitrogen) at a final concentration of 100 nM siRNA. The following siRNA oligonucleotides (Microsynth) were used: non-silencing control: 5'-UUCUCCGAACGUGUCACGU-3'; for KLHL22 3 siRNAs were pooled: 5'-GCAACAAACGAUGCCGGAUA-3'; 5'-CCUAUAUCCUAAAAACUU-3'; 5'-GGACAGCUCUGUGAUAUA-3'; 5'-CAACACUUGGCAAGGAGAC-3'; MAD2: 5'-GAGUCGGGACCAAGUUUA-3'; for PLK1 3'UTR RNAi 3 siRNAs were pooled: 5'-CCAUAUGAAUUGUACAGAA-3'; 5'-GGGUGUCUGUAAAGUUAU-3'; 5'-GGGUGUCUGUGUAAAGUUA-3'.

PLK1 mutagenesis. Point mutants of PLK1 were generated using pfu Turbo DNA Polymerase (Stratagene). Primers used for mutation of K492R were: 5'-GAGCACTGTGCTGAGGGCAGGTGCCAAC-3' and 5'-GTTGGCACTGCCCTC-AGCAAGTGCTC-3'.

Microscopy. Live-cell microscopy was carried out using a LSM510 Screening Confocal Laser Scanning microscope (Zeiss) or a Nikon Eclipse Ti. Immunofluorescence microscopy of fixed cells was performed as previously described^{21,22} using either a Delta Vision personalDV (Applied Precision) or a Leica DM6000B.

Western blotting and immunoprecipitation. Preparation of HeLa cell extracts was described previously²¹. FLAG-tagged KLHL22 was immunoprecipitated using anti-FLAG M2-agarose beads (Sigma). GFP-fused proteins were immunoprecipitated using GFP-Trap agarose beads (Chromotek). Beads were incubated with cell extracts for 2 h at 4 °C under constant rotation. Before elution, beads were washed 5 \times with TBS-T.

For detection of PLK1 interaction with KLHL22 and with the phosphoreceptors, cells were synchronized by Taxol for 13 h and subsequently treated with PR-619 for 1 h. Expression of PLK1^{WT} and PLK1^{KR} was induced for 24 h. To detect the interaction of PLK1 with KLHL22 in response to chromosome bi-orientation, cells were synchronized by treatment with monastrol for 16 h and released into MG132-containing media for 1.5 h to establish metaphase plates. Subsequently, cells were treated with Taxol (10 μM) to abrogate microtubule-exerted tension, nocodazole (10 μM) to depolymerize microtubules or solvent control (dimethylsulphoxide) for a further 1.5 h. For immunoprecipitation of endogenous PLK1, 10 μg of PLK1 rabbit polyclonal antibody (Abcam) or IgG control was coupled to protein A beads (Biorad).

In vitro kinase assay. For *in vitro* kinase assays GFP–PLK1^{WT} or ^{KR} was first immunoprecipitated using GFP-Trap beads as described above but in the presence of 100 nM okadaic acid. After the final wash with immunoprecipitation buffer, the beads were washed 3 \times with kinase buffer (20 mM Tris at pH 7.0, 50 mM KCl, 10 mM MgCl₂ supplemented with 20 mM β -glycerophosphate, 1 mM Na orthovanadate, 2 mM NaF, 1 $\mu\text{g ml}^{-1}$ Pepstatin, 1 $\mu\text{g ml}^{-1}$ leupeptin, 1 mM dithiothreitol, 1 \times Complete Protease Inhibitors and 100 nM okadaic acid). Casein (100 μg) was added and reactions were started by adding 400 μM ATP and 0.5 MBq [γ -³²P]ATP.

Protein microarray experiments. For control protein microarrays, control proteins were spotted at decreasing concentrations onto PATH nitrocellulose slides (Gentel Biosciences) using a Piezoarray platform (Perkin-Elmer). GST–aurora B was purchased from Lucerna-Chem and GST–LAPTM5 and GST–xHect were kindly provided by D. Rotin (The Hospital for Sick Children, Toronto, Canada). Ubiquitylation microarray screens with CUL3–RBX1–KLHL22 were done in duplicates. For ubiquitylation assays, Human ProtoArray PATH V.4 microarray

slides (Invitrogen) were rinsed briefly with 0.5% PBS-T and then blocked at room temperature for 1 h in blocking buffer (50 mM HEPES at pH 7.5, 200 mM NaCl, 0.08% Triton X-100, 25% glycerol, 20 mM glutathione, 1 mM dithiothreitol and 1% BSA). Meanwhile, 10.2 μg of CUL3–RBX1–His–KLHL22 E3 ligase complex was *in vitro*-neddylated with 2.5 μg human Nedd8-activating enzyme E1 (APBP1–Uba3), 2.5 μg human E2 (UbcH12), 10 μg human Nedd8, 1 \times energy regeneration solution (ERS) and 1 \times ubiquitylation buffer (45 mM HEPES, 2 mM NaF, 0.6 mM dithiothreitol) at room temperature for 15 min. The slides were then rinsed gently in 1 \times ubiquitylation buffer for 5 min following incubation with the reaction mixture (270 μl containing the mixture after CUL3-neddylated and in addition 8 μg FITC-ubiquitin, 7.5 μg rabbit E1 (UBE1), 7.5 μg rabbit E2 (UbcH5c), 12.5 mM Mg-ATP and 1 \times ubiquitylation buffer) in the dark for 2 h. Slides were washed 3 \times in 0.5% PBS-T for 10 min and then dried by centrifugation at 1,000g at room temperature for 5 min. Slides were scanned using a 488 nm laser on a ProScan Array HT (Perkin-Elmer).

For binding assays, Human ProtoArray PATH V.4 microarray slides were washed, blocked and rinsed gently in 1 \times ubiquitylation buffer (45 mM HEPES, 2 mM NaF and 0.6 mM dithiothreitol) for 5 min following incubation with binding mixture (300 μl 1 \times ubiquitylation buffer containing 3 μg Alexa647–MBP or Alexa647–MBP–KLHL22; final concentration: 10 ng μl^{-1}) in the dark for 1 h. The slides were washed 2 \times 5 min and 1 \times 10 min in 0.1% PBS-T and then dried by centrifugation at 700g at room temperature for 5 min. Slides were scanned using a 633 nm laser on a ProScan Array HT (Perkin-Elmer). Binding microarray screens with Alexa647–MBP–KLHL22 were done in duplicates whereas a single binding microarray screen was performed with Alexa647–MBP. Spot fluorescence intensities from the microarray screens were quantified using the ProScan Array HT (Perkin-Elmer) software. Protein Prospector Analyser (Invitrogen) was used to compare duplicate screens. Proteins were scored as hits if 50% of the pixels of the corresponding spots of both duplicates on both replica slides showed a signal stronger than 2 \times s.d. values above background.

Ubiquitylation assays and identification of ubiquitylated peptides by mass spectrometry. For *in vitro* ubiquitylation assays, 1 μg S9-purified GST–CUL3–RBX1 (ref. 22) mixed with 2 μg MBP or MBP–KLHL22 purified from *E. coli* was used as E3 ligase. The E3 ligase complexes were mixed with 0.5 μg recombinant PLK1 (Cell Signaling), 15 μg ubiquitin, 550 ng rabbit E1 (UBE1), 850 ng rabbit E2 (UbcH5b), 12.5 mM Mg-ATP and 1 \times ubiquitin reaction buffer, and incubated at 30 °C for 1 h. Reagents were from Boston Biochem. Reactions were terminated by boiling at 95 °C with SDS buffer for 5 min and analysed by western blotting.

For *in vitro* ubiquitylation of PLK1 for mass spectrometry (MS) analysis, the double amount of each reaction component was used in the reaction. After incubation at 30 °C for 1 h, unreacted free ubiquitin was removed by centrifugation in an Amicon Ultra-15 centrifuge filter (cutoff: 30 kDa; Millipore). Dithiothreitol (5 mM) was added and reduction was allowed to proceed at 45 °C for 1 h. After cooling the sample, 15 mM iodoacetamide (Sigma) was added and alkylation was allowed to proceed for 1 h. The sample was digested overnight with sequencing-grade modified trypsin (Promega) in the presence of 0.05% RapiGest (Waters) at 37 °C. Before MS analysis a microspin column packed with C-18 material (The Nest Group) was used for sample clean-up. Briefly, the sample was acidified with 0.1% TFA (Promega), loaded onto the reverse-phase column, washed 3 \times with 0.1% TFA in water, eluted with 0.1% TFA in 80% acetonitrile (Sigma) and dried in a SpeedVac system (Thermo Scientific). Before MS, samples were resuspended in high-performance liquid chromatography (HPLC) buffer A (0.1% formic acid in water) and the peptides were separated on a self-packed 100 \times 0.075 mm C-18 (Michrom Bioresources) micro-capillary fused-silica column (BGB Analytik AG) using a multi-step linear gradient: 2–10% HPLC buffer B (acetonitrile) in 1 min; 10–45% in 120 min; 45–98% in 3 min generated by an Agilent 1100 series HPLC (Agilent). MS and MS/MS data were acquired on a ThermoFinnigan LTQ using a top three data-dependent acquisition method. The raw data were converted to the mzXML format⁴⁶ and analysed using version 4.3.1 of the Trans Proteomics Pipeline. X!Tandem with the comet score plug-in⁴⁷ was used for the MS/MS assignment. The protein database used was ipi.HUMAN.v3.41.fasta. The condition files allowed for a variable modification of 114.1 Da at lysine residues, a static modification of 57 Da at cysteine residues and tryptic peptides with a maximum of 2 missed cleavages.

Antibodies. The following antibodies were used: mouse monoclonal BUBR1 (BD Biosciences 612502, 1:1,000), pSer676 BUBR1 (kind gift from E. A. Nigg, University of Basel, Switzerland, 1:2,000), CREST (Antibodies Incorporated, 15-234, 1:250), rabbit polyclonal CUL3²¹, mouse monoclonal FLAG (Sigma Aldrich F3165, 1:3,000), mouse monoclonal GST (Labforce B-14, 1:4,000), rabbit polyclonal HA (Covance

METHODS

DOI: 10.1038/ncb2695

- HA.11, 1:3,000), rabbit polyclonal KLHL22 and KLHL21 (ref. 22), rabbit polyclonal KLHL9 and 13 (ref. 21), rabbit polyclonal Mad2 (Bethyl Laboratories A300-301A, 1:5,000), mouse monoclonal MBP (Abcam ab49923, 1:1,000), rabbit polyclonal PLK1 (Abcam ab70697, 1:1,000), mouse monoclonal PLK1 (Abcam ab17057, 1:500), rabbit polyclonal PLK2 (kind gift from I. Hoffmann, DKFZ Heidelberg, Germany), mouse monoclonal α tubulin (Sigma T5169, immunofluorescence microscopy 1:5,000, western blotting 1:10,000), rabbit polyclonal γ tubulin (Sigma T3559, 1:1,000), mouse monoclonal cyclin A (Sigma C 4710, 1:2,000), mouse monoclonal cyclin B1 (Santa Cruz GSN1, 1:5,000), rabbit polyclonal phospho histone H3 (Upstate 06-570, 1:500), mouse monoclonal aurora B (BD Biosciences 611082/3, 1:250), mouse monoclonal HEC1 (GeneTex, 1:2,000), rabbit polyclonal pericentrin (Abcam ab4448, 1:2,000), mouse monoclonal GFP (Abcam ab3277, 1:1,000), mouse monoclonal RANGAP1 (Invitrogen 330800, 1:250), mouse monoclonal CDH1 (Abcam ab3242, 1:500) and mouse monoclonal HIS (IGBMC antibody facility, clone IG4, 1:250).
44. Steigemann, P. *et al.* Aurora B-mediated abscission checkpoint protects against tetraploidization. *Cell* **136**, 473–484 (2009).
 45. Belov, G. A. *et al.* Bidirectional increase in permeability of nuclear envelope upon poliovirus infection and accompanying alterations of nuclear pores. *J. Virol.* **78**, 10166–10177 (2004).
 46. Pedrioli, P. G. *et al.* A common open representation of mass spectrometry data and its application to proteomics research. *Nat. Biotechnol.* **22**, 1459–1466 (2004).
 47. MacLean, B., Eng, J. K., Beavis, R. C. & McIntosh, M. General framework for developing and evaluating database scoring algorithms using the TANDEM search engine. *Bioinformatics* **22**, 2830–2832 (2006).

6.2 Results part 2 : How does KLHL22 interact with PLK1 and what about other KELCH/Kinase complexes ?

6.2.1 Manuscript: CUL3 and protein kinases: insights from PLK1/KLHL22 interaction.

Jochen Beck *et al.* identified the mitotic kinase PLK1 as a direct target of the CUL3 E3-ubiquitin ligase complex containing BTB-KELCH adaptor protein KLHL22. In this study, we aimed at analysing the mechanisms of interaction between PLK1 and KLHL22. These results were published as a report in Cell Cycle.

Author contributions of experimental data:

Thibaud Metzger designed, cloned and expressed all constructs. He showed that the catalytic activity of PLK1 is not required for its interaction with KLHL22 and that bacterially expressed KLHL22 interacts with at least two distinct sites of PLK1.

Charlotte Kleiss performed experiments in mammalian cells.

CUL3 and protein kinases

Insights from PLK1/KLHL22 interaction

Thibaud Metzger, Charlotte Kleiss and Izabela Sumara*

Institute of Genetics and Molecular and Cellular Biology (IGBMC), Illkirch, France

Keywords: CUL3, BTB proteins, KLHL22, ubiquitin, kinases, PLK1**Abbreviations:** PLK1, Polo-like kinase 1; DUBs, deubiquitinating enzymes; CRLs, cullin ring ligases; CUL, cullin; APC/C, anaphase promoting complex/cyclosome; PBD, polo box domain

Posttranslational mechanisms drive fidelity of cellular processes. Phosphorylation and ubiquitination of substrates represent very common, covalent, posttranslational modifications and are often co-regulated. Phosphorylation may play a critical role both by directly regulating E3-ubiquitin ligases and/or by ensuring specificity of the ubiquitination substrate. Importantly, many kinases are not only critical regulatory components of these pathways but also represent themselves the direct ubiquitination substrates. Recent data suggest the role of CUL3-based ligases in both proteolytic and non-proteolytic regulation of protein kinases. Our own recent study identified the mitotic kinase PLK1 as a direct target of the CUL3 E3-ligase complex containing BTB-KELCH adaptor protein KLHL22.¹ In this study, we aim at gaining mechanistic insights into CUL3-mediated regulation of the substrates, in particular protein kinases, by analyzing mechanisms of interaction between KLHL22 and PLK1. We find that kinase activity of PLK1 is redundant for its targeting for CUL3-ubiquitination. Moreover, CUL3/KLHL22 may contact two distinct motifs within PLK1 protein, consistent with the bivalent mode of substrate targeting found in other CUL3-based complexes. We discuss these findings in the context of the existing knowledge on other protein kinases and substrates targeted by CUL3-based E3-ligases.

Introduction

Posttranslational mechanisms drive fidelity of cellular processes. Phosphorylation and ubiquitination of substrates represent very common, covalent, and reversible, posttranslational modifications. Human genome encodes for about 600 protein kinases that phosphorylate specific substrates and thereby critically regulate various signaling pathways including cell cycle progression.² Attachment of the small molecule ubiquitin to other proteins is conducted by a coordinated action of different E1, E2, and E3 enzymes.³ There are predicted 600–1000 different E3-ubiquitin ligases in human cells, suggesting huge complexity and specificity of these enzymes. Indeed, unlike most E1 and E2 enzymes, E3 ligases provide substrate specificity, often by association with the adaptor proteins. For different members of the Cullin ring ligases (CRLs), substrate selection is insured by specific protein families, like, for example, F-box protein family members constitute the SCF complexes (Cullin 1 [CUL1]-based), or BTB domain-containing proteins build functional CUL3 E3-ligases.⁴ Given a high number of the substrate-specific adaptor proteins found in humans (i.e., 200 different BTBs⁵), numerous ubiquitination targets of these E3-complexes can be predicted. Indeed, recent mass spectrometry approaches suggest existence of about 5000 different ubiquitination substrates in human cells.⁶ On the

other hand, another important cell cycle E3-ligase, the anaphase-promoting complex/cyclosome (APC/C) utilizes only two distinct adaptor proteins (CDC20 and CDH1) that are each able to bind and target for ubiquitination and subsequent proteolysis many different substrates.⁷

Interestingly, phosphorylation and ubiquitination pathways are often interconnected. Phosphorylation may play a critical role both by directly regulating E3-ligases and/or by ensuring substrate specificity. For example, the APC/C subunits and the substrate adaptors are differentially phosphorylated during mitosis and mitotic exit, regulating activity of these enzymes.^{8,9} On the other hand, the substrates of the SCF E3-ligases need to be phosphorylated, creating a so-called “phosphodegron”, in order to be efficiently targeted for ubiquitination¹⁰ (Fig. 1). Importantly, many kinases are not only critical regulatory components of these pathways but also represent themselves the direct ubiquitination substrates. In many cases, ubiquitination of the kinases may lead to their subsequent proteasomal degradation, ultimately attenuating their enzymatic activity, as has been demonstrated for some mitotic kinases targeted by the APC/C E3-ligase.¹¹ However, ubiquitination may also serve non-proteolytic functions, leading to regulation of subcellular localization, binding affinities, or even enzymatic activities.¹² Recent data suggest the role of CUL3-based ligases in both proteolytic and non-proteolytic regulation of protein kinases (Table 1 and references therein). Our

*Correspondence to: Izabela Sumara; Email: Izabela.Sumara@igbmc.fr
Submitted: 06/05/13; Accepted: 06/11/13
<http://dx.doi.org/10.4161/cc.25369>

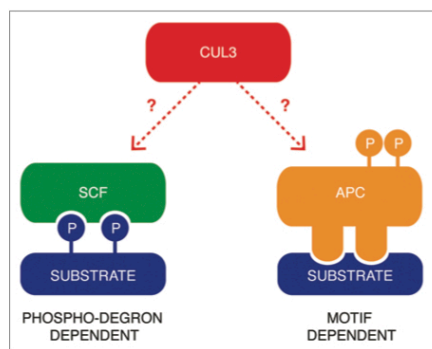


Figure 1. Two common models of substrates recognition by E3-ligase complexes. SCF ligases interact with the phosphorylated residues on the substrates, which create a so-called “phosphodegron”. The APC/C complex recognizes specific short motifs within the amino acid sequence of the targeted proteins, and its activity is regulated by phosphorylation. Little is known about mechanisms of substrate targeting by CUL3-based E3-ligases.

own recent study identified the mitotic kinase PLK1 as a direct target of the CUL3 E3-ligase complex containing BTB-KELCH adaptor protein KLHL22.¹ CUL3/KLHL22-mediated ubiquitination serves a non-proteolytic function and regulates the sub-cellular localization of PLK1 specifically at the kinetochores. Dissociation of the ubiquitinated PLK1 from kinetochores and thereby reduction of its localized kinase activity is an essential event for the anaphase onset in human cells.¹

In this study, we aim at gaining mechanistic insights into CUL3-mediated regulation of the substrates, in particular protein kinases (Fig. 1). By analyzing mechanisms of interaction between KLHL22 and PLK1, we conclude that kinase activity of PLK1 is redundant for its targeting for CUL3-ubiquitination. Moreover, we find that CUL3/KLHL22 may contact at least two distinct motifs within PLK1 protein. We discuss these findings in the context of the existing knowledge on other protein kinases (Table 1) and substrates targeted by CUL3-based complexes.

Results and Discussion

Posttranslational modifications of substrates and recognition by CUL3 E3-ligases. Several substrate-binding mechanisms were identified within the Cullin-RING E3-ligases family. For instance, the SCF E3-ligases require previous phosphorylation of targeted proteins to create a phosphodegron necessary for accurate binding between both components.^{4,10} In contrast, the APC/C binds to short specific motifs (D-Box, A-box, KEN-box)⁷ (Fig. 1). The existing data on the regulation of the CUL3 substrate, transcription factor Nrf2, suggest that Nrf2 may not require prior posttranslational modification for its binding to CUL3/KEAP1^{13,14} and is constitutively targeted for ubiquitination under non-stressed cellular conditions. However, little is known about the recognition mechanisms by CUL3-based

ligases toward other reported substrates (Fig. 1) in particular protein kinases (Table 1). In order to gain insights into molecular basis of the kinases binding by CUL3, we have tested if the kinase activity of the recently reported substrate PLK1¹ is required for its binding to CUL3 adaptor KLHL22. For this purpose, GFP tag-protein alone or GFP-tagged PLK1 were expressed in HeLa cells. Subsequently, cells were synchronized in the mitotic stage by addition of Taxol or specific small-molecule inhibitor of PLK1, BI2536,¹⁵ and GFP proteins were immunoprecipitated (Fig. 2). As expected, the treatment with BI2536 abolished the phosphorylation-dependent mobility shift of the PLK1 substrate, kinetochore protein BubR1¹⁶ (Fig. 2A), and reduced amount of the autophosphorylated form of PLK1 (Fig. 2B). In contrast, the HA-tagged KLHL22 (Fig. 2A) and the endogenous KLHL22 (Fig. 2B) efficiently co-immunoprecipitated with PLK1 under these conditions, suggesting that kinase activity of PLK1 is redundant for its recognition by CUL3/KLHL22 E3-ligase. These data are consistent with the fact that strong, salt-resistant interaction was observed in vitro between PLK1 and KLHL22 expressed in bacterial cells, and that downregulation of CUL3/KLHL22 did not modulate kinase activity of PLK1.¹ Interestingly, a number of studies suggest that unlike for many SCF E3-ligases,^{4,10} there is no evidence that posttranslational modifications are required for substrates interactions with CUL3 E3-ligases. Intriguingly in the case of two BTB adaptor proteins, KEAP1¹⁷ and SPOP,¹⁸ substrate phosphorylation inhibits rather than promotes their recruitment. Also, regulation of IKK β by KEAP1 appears to be independent of IKK β activity,¹⁹ and the kinase-dead mutant of PIPKII β was more efficiently ubiquitinated, and this CUL3/SPOP-mediated ubiquitination was further enhanced by expression of specific phosphatases.²⁰ A similar situation was observed for DAPK, as the kinase-defective and kinase-active mutants bound KLHL20 as effectively as the wild-type DAPK.²¹ During mitotic entry, Aurora A kinase is regulated by the CUL3/KLHL18 E3 ligase,²² and this ubiquitination event seems to proceed the activation of Aurora A, suggesting that KLHL18 interacts with an inactive, unmodified kinase. Taken together, all these findings are in a sharp contrast to SCF-mediated mechanisms, in which substrate modification induced by a stimuli switches on the ubiquitination event. One could speculate that for CUL3-mediated ubiquitination events, some specific extra- or intracellular factors generate an “off” signal for substrate targeting. Indeed, Nrf2 is constitutively recognized and ubiquitinated by CUL3/KEAP1, and oxidative stress conditions interfere with E3-ligase activity.^{13,14} Similarly, DAPK is constitutively targeted to the CUL3-based ligase under basal conditions.²¹ In both cases, regulation of the substrate ubiquitination occurs at the level of the substrate-specific adaptor rather than substrate itself. While KEAP1 is oxidized on the specific cysteine residues,^{13,23} KLHL20 is sequestered away from the substrate into PML nuclear bodies under IFN-stress conditions.²¹ Interestingly, subcellular localization of other mitotic BTB-Kelch proteins involved in CUL3 complexes appears to be regulated in a timely manner during cell cycle progression.^{1,22,24,25}

Insights into molecular architecture of CUL3 ligases. Unlike SCF ligases that interact with the phosphorylated residues on the

Table 1. The list of protein kinases that are direct substrates of CUL3-based E3-ligases in mammalian cells

Substrate specific adaptors	Substrates	Processes	Functions	References
KLHL9/13/21	Aurora B	Mitosis and cytokinesis	Non-proteolytic	24 and 35
KLHL18	Aurora A	Mitotic entry	Non-proteolytic	22
KLHL22	PLK1	Chromosome segregation	Non-proteolytic	1
SPOP	PIPKI β	Phosphoinositide signaling	Non-proteolytic	20
KEAP1/KLHL19	IKK β	NF- κ B signaling	Proteolytic	19 and 34
KLHL20	DAPK	IFN-induced cell death	Proteolytic	21
KLHL3	WNK1, WNK4	Blood pressure	Proteolytic	33 and 36

The table summarizes the current knowledge of the kinases, which were identified as the ubiquitination substrates of CUL3-based E3-ligases in mammalian cells. The identity of the substrate specific adaptor proteins, the roles in the physiological process as well as the function of the ubiquitination events are depicted.

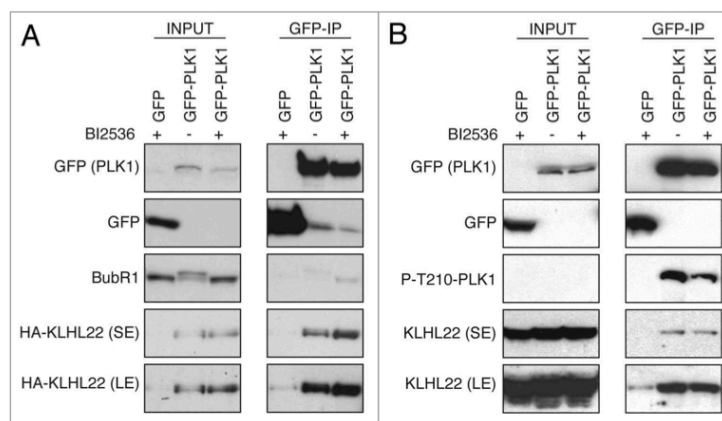


Figure 2. Catalytic activity of PLK1 is not required for its interaction with KLHL22-adaptor protein. **(A)** Cells expressing GFP alone and GFP-PLK1 were transfected with HA-KLHL22 and synchronized in mitosis using Taxol or PLK1 inhibitor BI2536. Extracts were immunoprecipitated using GFP-Trap beads. Inputs and immunoprecipitates were analyzed by western blot. **(B)** Cells expressing GFP alone and GFP-PLK1 only were synchronized and analyzed as in **(A)**. The short (SE) and long (LE) exposures of the representative blots are shown.

substrates, the APC/C complex recognizes specific short motifs within the amino acid sequence of the targeted proteins. Recent studies offer an insight into molecular architecture of the CUL3-based E3-ligase complexes^{18,26} and suggest a quaternary assembly model, where dimers of BTB-adaptor proteins are engaged in a single complex, supporting a bivalent mode of interaction with the substrate proteins. Indeed, it has been demonstrated that two specific acidic motifs within Nrf2 protein are in a direct contact with the β -propeller constituted of the Kelch repeats within KEAP protein,^{17,27} and the SPOP adaptor is also able to engage multiple-binding sites in one substrate, which could be explained by complex structural flexibility and ability to dimerize.¹⁸ However, little is known about the molecular basis of interaction between CUL3-complexes and protein kinases. Interestingly, mutagenesis of the A-box and D-box for APC/C-dependent degradation within Aurora A kinase did not interfere with CUL3-mediated ubiquitination.²²

Therefore, we aimed at understanding if a bivalent mode of substrate-CUL3 interaction is also utilized by PLK1. To this

end, we expressed and purified the GST-tagged fragments corresponding to entire kinase domain and the regulatory domain, the Polo-box domain (PBD) from bacterial cells. Following incubation with the full-length, bacterially derived MBP-tagged KLHL22 protein, we immunoprecipitated the complexes using GSH-Sepharose. As expected, the full-length PLK1 protein efficiently interacted with the MBP-KLHL22 protein (Fig. 3), consistent with a redundancy for prior posttranslational modifications for this interaction and with the previous findings.¹ Interestingly, both PLK1 fragments were able to interact with the full-length KLHL22 protein in vitro (Fig. 3). To corroborate these findings, we expressed the corresponding fragments fused to the GFP-tag in human cells. Following cell synchronization in mitosis by Taxol, we immunoprecipitated the complexes formed. In contrast to the GFP-protein alone, all GFP-fused forms of PLK1 protein were able to efficiently interact with the endogenous KLHL22 protein (Fig. 4). These results suggest that PLK1 utilizes at least two distinct binding interfaces located within two functional domains of the protein (Fig. 5), consistent with

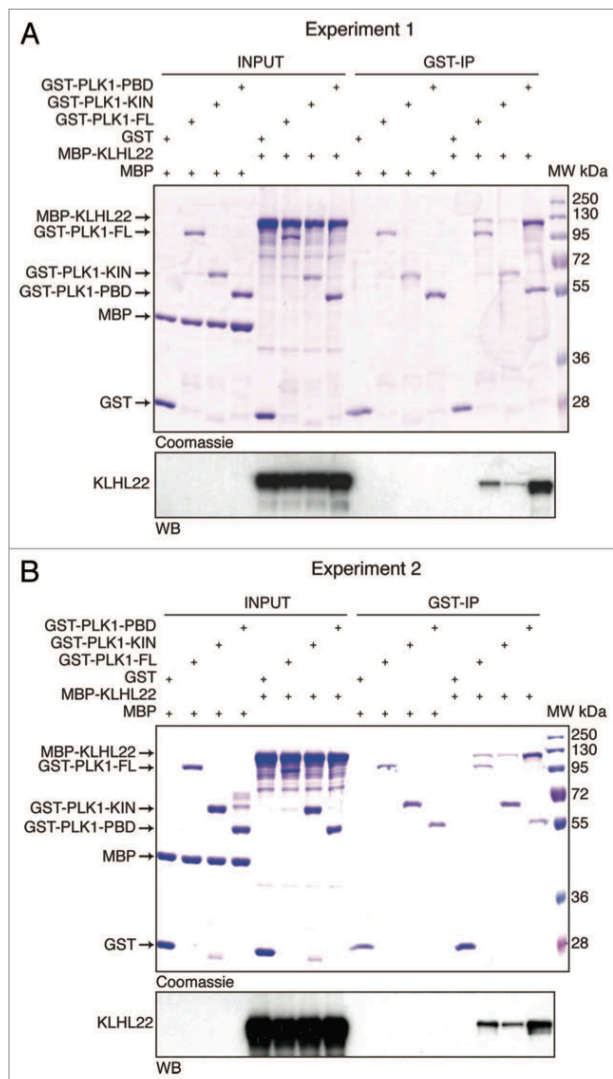


Figure 3. KLHL22 interacts with two domains of PLK1 in vitro. **(A and B)** Recombinant GST or GST fused to full-length PLK1 (GST-PLK1), kinase domain fragment (GST-PLK1-KIN), and PBD fragment (GST-PLK1-PBD) were incubated with recombinant MBP or MBP fused to full-length KLHL22 (MBP-KLHL22), and immunoprecipitated using glutathione-sepharose beads. Immunoprecipitates (GST-IP) were analyzed by coomassie blue staining and western blot. **(A and B)** represent two independent experiments.

the bivalent model of substrate interaction with the KEAP and SPOP substrate adaptors.^{17,18,27} While KLHL22 binding to the kinase domain may, in principle, resemble interactions within

PLK1 N-term (forward): 5'-CGCCTCGAGA TGAGTGCTGC AGTGACTGC-3'; PLK1 C-term (reverse): 5'-CGGGGTACCC CGGAGGCCTT GAGACGG-3'; PLK1-KIN (reverse):

other BTB-KELCH/kinase complexes, interaction with the PBD domain is likely to be more specific to the family of Polo kinases. The PBD can indeed be only found within PLKs from different species and is critically involved in targeting these kinases to specific subcellular localizations, acting as a phosphoreceptor-binding domain.²⁸⁻³² It is interesting that the CUL3/KLHL22-mediated ubiquitination takes place at the specific lysine residue (K492) located within the PBD domain and interferes with the phosphoreceptor-dependent interactions of PLK1 at the kinetochores.¹

While it cannot be rigorously excluded that posttranslational modifications (i.e., phosphorylation), by yet-to-be-identified factors, play a regulatory role for CUL3 complex assembly, our results are consistent with the possibility that specific motifs within substrate proteins exist that mediate their binding to CUL3-complexes (Fig. 5). Indeed, a small acidic region within WNK kinases mediating its interaction with KLHL3 adaptor was recently identified,³³ and, similar to Nrf2,^{17,27} IKK β possess an acidic (D/N)XE(T/S)GE motif within its kinase domain that is required for KEAP1 binding.^{19,34} Before any general rules can be formulated, future studies are needed to identify the sequence motifs involved in the substrate binding to CUL3/KLHL22 and other CUL3-based complexes. As many kinases are found to be targeted by these E3-ligases (Table 1), these studies may also lead to better understanding of the general mode of kinase regulation.

Materials and Methods

cDNAs. The full-length KLHL22 was cloned into pMal-C2X (New England BioLabs) and pcDNA3.1 (Invitrogen) in fusion with the N-terminal HA-tag as described previously.¹ The full-length PLK1 (1–603), the PLK1 kinase domain (PLK1-KIN, 1–320), and the PBD domain (PLK1-PBD, 321–603) were cloned into pGex-6P1 (GE Healthcare) using EcoRI/XhoI restriction sites and into pEGFP-N1 (Clontech) using XhoI/KpnI. The following primers were used for cloning into pGex-6P1: PLK1 N-term (forward): 5'-GCGGAATTCA GTGCTGCAGT GACTGCAGG-3'; PLK1 C-term (reverse): 5'-CGCCTCGAGT TAGGAGGCCT TGAGACGGT-3'; PLK1-KIN (reverse): 5'-CGCCTCGAGA ATGGTCAGGC AGGTGAT-3'; PLK1-PBD (forward): 5'-GCGGAATTCC CACCAAGGTT TTCGATTG-3' and for cloning into pEGFP-N1:

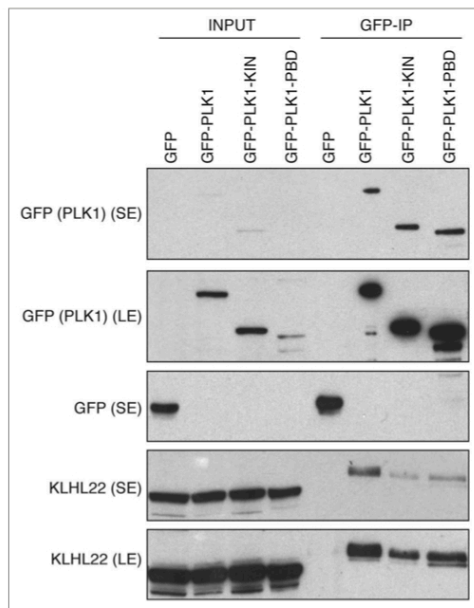


Figure 4. KLHL22 interacts with two domains of PLK1 in cells. Cells expressing GFP alone, GFP fused to full-length PLK1 (GFP-PLK1), kinase domain fragment (GFP-PLK1-KIN), and PBD fragment (GFP-PLK1-PBD) were synchronized in mitosis using Taxol. Extracts were immunoprecipitated using GFP-Trap beads. Inputs and immunoprecipitates were analyzed by western blot. The short (SE) and long (LE) exposures of the representative blots are shown.

5'-CGGGGTACCC CGGTCAGGCA GGTGATGG-3';
PLK1-PBD (forward): 5'-CGCCTCGAGA TGCCACCAAG
GTTTTCG-3'.

Recombinant protein expression. *E. coli* BL21 (DE3) bacteria were transformed with the different pGex-6P1 and pMal-C2X constructs. Once cultures reached $OD_{600} = 0.4-0.6$, they were cooled down at 20 °C for 30 min. Expression was subsequently induced overnight at 20 °C with 1 mM IPTG. Cells were harvested by centrifugation. GST-fusion proteins were resuspended in lysis buffer (50 mM NaCl, 10 mM TRIS-HCl pH 8, 1 mM DTT, Complete Protease Inhibitor Cocktail [Roche]), lysed by sonication, and supernatant was cleared by centrifugation at 40 000 rpm for 1 h using 50.2Ti rotor. The supernatant was incubated for 2 h with 500 μ l of Glutathione Sepharose 4B (GE Healthcare) per 1 liter of culture, previously equilibrated in lysis buffer. Beads were washed with 50 ml of lysis buffer, and elution was done with 20 mM glutathione. The elution fraction was dialyzed overnight into lysis buffer to remove glutathione and concentrated using 10 kDa cut-off centrifugal filter units (Amicon). For expression of the recombinant MBP-KLHL22 the following lysis buffer was used (PBS-EDTA (0.5 mM), 1 mM DTT, Complete Protease Inhibitor Cocktail [Roche]). The cleared lysate was incubated with

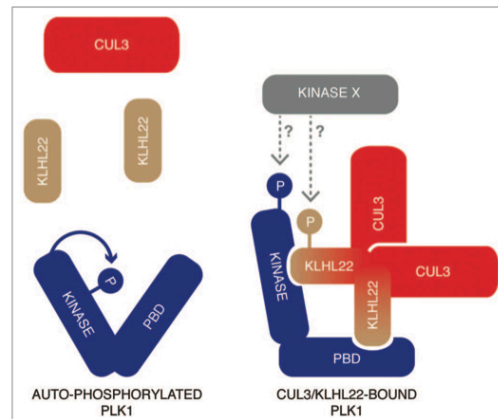


Figure 5. A hypothetical model of the architecture of CUL3/KLHL22 in a complex with PLK1. PLK1 interacts with the substrate specific adaptor protein KLHL22 independent of its kinase activity. It is possible that specific conformational change or modifications by unidentified factors, including upstream kinases (Kinase X), regulate affinity of PLK1 to KLHL22. KLHL22 binds to two distinct domains of PLK1 and may utilize two similar or different motifs within its primary sequence.

2 ml amylose resin (New England Biolabs) per 1 liter of culture. Elution was performed by supplementing lysis buffer with 15 mM maltose. The eluate was dialysed in PBS and concentrated using 50 kDa cut-off centrifugal filter units (Amicon).

Cell culture, transfections, and synchronization. HeLa Kyoto were cultured as previously described³⁵ and transfected using lipofectamine 2000 (Invitrogen), according to the manufacturer's instructions. For mitotic synchronizations, cells were treated with 200 nM Taxol (paclitaxel) (Sigma) or 100 nM PLK1 inhibitor BI2536 (Axon Medchem) for 13 h before harvesting.

Western blotting, immunoprecipitation, and antibodies. Preparation of HeLa cells extracts, immunoprecipitation, and western blotting were described previously.¹ The following antibodies were used in this study: rabbit polyclonal KLHL22,¹ rabbit polyclonal GFP (abcam ab290, 1:2000), mouse monoclonal BubRI (BD Biosciences 612502, 1:1000), rat monoclonal HA (Roche 11867423001, 1:1000), and rabbit polyclonal pThr210PLK1 (Cell Signaling, 1:1000).

Disclosure of Potential Conflicts of Interest

No potential conflicts of interest were disclosed.

Acknowledgments

The authors wish to thank the members of the entire Sumara group for careful reading of the manuscript and for helpful discussions. The research in the laboratory of Izabela Sumara is sponsored by the IGBMC, ATIP-AVENIR program from CNRS, and INSERM, "Programme de Mécénat" from Sanofi-Aventis, University of Strasbourg and Fondation ARC pour la recherche sur le cancer.

References

- Beck J, Maerki S, Posch M, Metzger T, Persaud A, Scheel H, et al. Ubiquitylation-dependent localization of PLK1 in mitosis. *Nat Cell Biol* 2013; 15:430-9; PMID:23455478; <http://dx.doi.org/10.1038/ncb2695>
- Nigg EA. Mitotic kinases as regulators of cell division and its checkpoints. *Nat Rev Mol Cell Biol* 2001; 2:21-32; PMID:11413462; <http://dx.doi.org/10.1038/35048096>
- Komander D, Rape M. The ubiquitin code. *Annu Rev Biochem* 2012; 81:203-29; PMID:22524316; <http://dx.doi.org/10.1146/annurev-biochem-060310-170328>
- Willems AR, Schwab M, Tyers M. A hitchhiker's guide to the cullin ubiquitin ligases: SCF and its kin. *Biochim Biophys Acta* 2004; 1695:133-70; PMID:15571813; <http://dx.doi.org/10.1016/j.bbamer.2004.09.027>
- Stogios PJ, Privé GG. The BACK domain in BTB-kelch proteins. *Trends Biochem Sci* 2004; 29:634-7; PMID:15544948; <http://dx.doi.org/10.1016/j.tibs.2004.10.003>
- Kim W, Bennett EJ, Huttlin EL, Guo A, Li J, Possemato A, et al. Systematic and quantitative assessment of the ubiquitin-modified proteome. *Mol Cell* 2011; 44:325-40; PMID:21906983; <http://dx.doi.org/10.1016/j.molcel.2011.08.025>
- Peters JM. The anaphase promoting complex/cyclosome: a machine designed to destroy. *Nat Rev Mol Cell Biol* 2006; 7:644-56; PMID:16896351; <http://dx.doi.org/10.1038/nrm1988>
- Kraft C, Herzog F, Gieffers C, Mechtler K, Hagting A, Pines J, et al. Mitotic regulation of the human anaphase-promoting complex by phosphorylation. *EMBO J* 2003; 22:6598-609; PMID:14657031; <http://dx.doi.org/10.1093/emboj/cdg627>
- Sumara I, Maerki S, Peter M. E3 ubiquitin ligases and mitosis: embracing the complexity. *Trends Cell Biol* 2008; 18:84-94; PMID:18215523; <http://dx.doi.org/10.1016/j.tcb.2007.12.001>
- Petroski MD, Deshaies RJ. Function and regulation of cullin-RING ubiquitin ligases. *Nat Rev Mol Cell Biol* 2005; 6:9-20; PMID:15688063; <http://dx.doi.org/10.1038/nrm1547>
- Lindon C, Pines J. Ordered proteolysis in anaphase inactivates Plk1 to contribute to proper mitotic exit in human cells. *J Cell Biol* 2004; 164:233-41; PMID:14734534; <http://dx.doi.org/10.1083/jcb.200309035>
- Li W, Ye Y. Polyubiquitin chains: functions, structures, and mechanisms. *Cell Mol Life Sci* 2008; 65:2397-406; PMID:18438605; <http://dx.doi.org/10.1007/s00018-008-8090-6>
- Zhang DD, Hannink M. Distinct cysteine residues in Keap1 are required for Keap1-dependent ubiquitination of Nrf2 and for stabilization of Nrf2 by chemopreventive agents and oxidative stress. *Mol Cell Biol* 2003; 23:8137-51; PMID:14585973; <http://dx.doi.org/10.1128/MCB.23.22.8137-8151.2003>
- Wakabayashi N, Dinkova-Kostova AT, Holtzclaw WD, Kang MI, Kobayashi A, Yamamoto M, et al. Protection against electrophile and oxidant stress by induction of the phase 2 response: fate of cysteines of the Keap1 sensor modified by inducers. *Proc Natl Acad Sci USA* 2004; 101:2040-5; PMID:14764894; <http://dx.doi.org/10.1073/pnas.0307301101>
- Lénárt P, Petronczki M, Steegmaier M, Di Fiore B, Lipp JJ, Hoffmann M, et al. The small-molecule inhibitor BI 2536 reveals novel insights into mitotic roles of Polo-like kinase 1. *Curr Biol* 2007; 17:304-15; PMID:17291761; <http://dx.doi.org/10.1016/j.cub.2006.12.046>
- Elowe S, Hümmer S, Uldschmid A, Li X, Nigg EA. Tension-sensitive Plk1 phosphorylation on BubR1 regulates the stability of kinetochore microtubule interactions. *Genes Dev* 2007; 21:2205-19; PMID:17785528; <http://dx.doi.org/10.1101/gad.436007>
- Lo SC, Li X, Henzl MT, Beamer LJ, Hannink M. Structure of the Keap1:Nrf2 interface provides mechanistic insight into Nrf2 signaling. *EMBO J* 2006; 25:3605-17; PMID:16888629; <http://dx.doi.org/10.1038/sj.emboj.7601243>
- Zhuang M, Calabrese MF, Liu J, Waddell MB, Nourse A, Hammel M, et al. Structures of SPOP-substrate complexes: insights into molecular architectures of BTB-Cul3 ubiquitin ligases. *Mol Cell* 2009; 36:39-50; PMID:19818708; <http://dx.doi.org/10.1016/j.molcel.2009.09.022>
- Lee DE, Kuo HP, Liu M, Chou CK, Xia W, Du Y, et al. KEAP1 E3 ligase-mediated downregulation of NF-kappaB signaling by targeting IKKbeta. *Mol Cell* 2009; 36:131-40; PMID:19818716; <http://dx.doi.org/10.1016/j.molcel.2009.07.025>
- Bunce MW, Boronenkov IV, Anderson RA. Coordinated activation of the nuclear ubiquitin ligase Cul3-SPOP by the generation of phosphatidylinositol 5-phosphate. *J Biol Chem* 2008; 283:8678-86; PMID:18218622; <http://dx.doi.org/10.1074/jbc.M710222000>
- Lee YR, Yuan WC, Ho HC, Chen CH, Shih HM, Chen RH. The Cullin 3 substrate adaptor KLHL20 mediates DAPK ubiquitination to control interferon responses. *EMBO J* 2010; 29:1748-61; PMID:20389280; <http://dx.doi.org/10.1038/emboj.2010.62>
- Moghe S, Jiang F, Miura Y, Cerny RL, Tsai MY, Furukawa M. The Cul3-KLHL18 ligase regulates mitotic entry and ubiquitylates Aurora-A. *Biol Open* 2012; 1:82-91; PMID:23213400; <http://dx.doi.org/10.1242/bio.2011018>
- Zhang DD, Lo SC, Cross JV, Templeton DJ, Hannink M. Keap1 is a redox-regulated substrate adaptor protein for a Cul3-dependent ubiquitin ligase complex. *Mol Cell Biol* 2004; 24:10941-53; PMID:15572695; <http://dx.doi.org/10.1128/MCB.24.24.10941-10953.2004>
- Maerki S, Olma MH, Staubli T, Steigemann P, Gerlich DW, Quadroni M, et al. The Cul3-KLHL21 E3 ubiquitin ligase targets aurora B to midzone microtubules in anaphase and is required for cytokinesis. *J Cell Biol* 2009; 187:791-800; PMID:1995937; <http://dx.doi.org/10.1083/jcb.200906117>
- Maerki S, Beck J, Sumara I, Peter M. Finding the midzone: the role of ubiquitination for CPC localization during anaphase. *Cell Cycle* 2010; 9:2921-2; PMID:20714224; <http://dx.doi.org/10.4161/cc.9.15.12740>
- Canning P, Cooper CD, Krojer T, Murray JW, Pike AC, Chaikud A, et al. Structural basis for Cul3 protein assembly with the BTB-Kelch family of E3 ubiquitin ligases. *J Biol Chem* 2013; 288:7803-14; PMID:23349464; <http://dx.doi.org/10.1074/jbc.M112.437996>
- Kobayashi A, Kang MI, Okawa H, Ohtsujii M, Zenke Y, Chiba T, et al. Oxidative stress sensor Keap1 functions as an adaptor for Cul3-based E3 ligase to regulate proteasomal degradation of Nrf2. *Mol Cell Biol* 2004; 24:7130-9; PMID:15282312; <http://dx.doi.org/10.1128/MCB.24.16.7130-7139.2004>
- Elia AE, Rellos P, Haire LF, Chao JW, Ivins FJ, Hoepker K, et al. The molecular basis for phosphodependent substrate targeting and regulation of Plks by the Polo-box domain. *Cell* 2003; 115:83-95; PMID:14532005; [http://dx.doi.org/10.1016/S0092-8674\(03\)00725-6](http://dx.doi.org/10.1016/S0092-8674(03)00725-6)
- Cheng KY, Lowe ED, Sinclair J, Nigg EA, Johnson LN. The crystal structure of the human Polo-like kinase-1 polo box domain and its phospho-peptide complex. *EMBO J* 2003; 22:5757-68; PMID:14592974; <http://dx.doi.org/10.1093/emboj/cdg558>
- Hanisich A, Wehner A, Nigg EA, Silljé HH. Different Plk1 functions show distinct dependencies on Polo-Box domain-mediated targeting. *Mol Biol Cell* 2006; 17:448-59; PMID:16267267; <http://dx.doi.org/10.1091/mbc.E05-08-0801>
- Lee KS, Park JE, Kang YH, Zimmerman W, Soung NK, Seong YS, et al. Mechanisms of mammalian Polo-like kinase 1 (Plk1) localization: self- versus non-self-priming. *Cell Cycle* 2008; 7:141-5; PMID:18216497; <http://dx.doi.org/10.4161/cc.7.2.5272>
- Park JE, Soung NK, Johmura Y, Kang YH, Liao C, Lee KH, et al. Polo-box domain: a versatile mediator of Polo-like kinase function. *Cell Mol Life Sci* 2010; 67:1957-70; PMID:20148280; <http://dx.doi.org/10.1007/s00018-010-0279-9>
- Ohta A, Schumacher FR, Mehellou Y, Johnson C, Knebel A, Macartney TJ, et al. The Cul3-KLHL3 E3 ligase complex mutated in Gordon's hypertension syndrome interacts with and ubiquitylates WNK isoforms: disease-causing mutations in KLHL3 and WNK4 disrupt interaction. *Biochem J* 2013; 451:111-22; PMID:23387299; <http://dx.doi.org/10.1042/BJ20121903>
- Kim JE, You DJ, Lee C, Ahn C, Seong JY, Hwang JI. Suppression of NF-kappaB signaling by KEAP1 regulation of IKKbeta activity through autophagic degradation and inhibition of phosphorylation. *Cell Signal* 2010; 22:1645-54; PMID:20600852; <http://dx.doi.org/10.1016/j.cellsig.2010.06.004>
- Sumara I, Quadroni M, Frei C, Olma MH, Sumara G, Ricci R, et al. A Cul3-based E3 ligase removes Aurora B from mitotic chromosomes, regulating mitotic progression and completion of cytokinesis in human cells. *Dev Cell* 2007; 12:887-900; PMID:17543862; <http://dx.doi.org/10.1016/j.devcel.2007.03.019>
- Wakabayashi M, Mori T, Isobe K, Sahara E, Sasa K, Anaki Y, et al. Impaired KLHL3-Mediated Ubiquitination of WNK4 Causes Human Hypertension. *Cell Rep* 2013.

6.2.2 Unbiased approaches

6.2.2.1 Peptide array and truncation experiments

The results from our *in vitro* binding assay suggest that there are at least two distinct points of interaction of KLHL22 on PLK1 (Metzger et al., 2013). In order to get more insights into this interaction, we performed peptide array experiments. PLK1 sequence was divided in 15mer peptides with a shift of four amino-acids and synthesized peptides were spotted on a nitrocellulose membrane (Intavis CelluSpots™), and incubated with recombinant KLHL22 proteins and analyzed by western-blot. Whereas no signal could be detected with MBP and GST controls, we could clearly define three different binding interfaces using this approach (**Fig. 11**): one within the kinase domain (peptides C21 to C23), one in the PBD (peptides F1 to F3) and one in the flexible region between these two (peptides D12-D13). In contrast, we were unable to detect any interaction with endogeneous KLHL22 or over-expressed HA-KLHL22 from mitotically synchronized HeLa cell extracts.

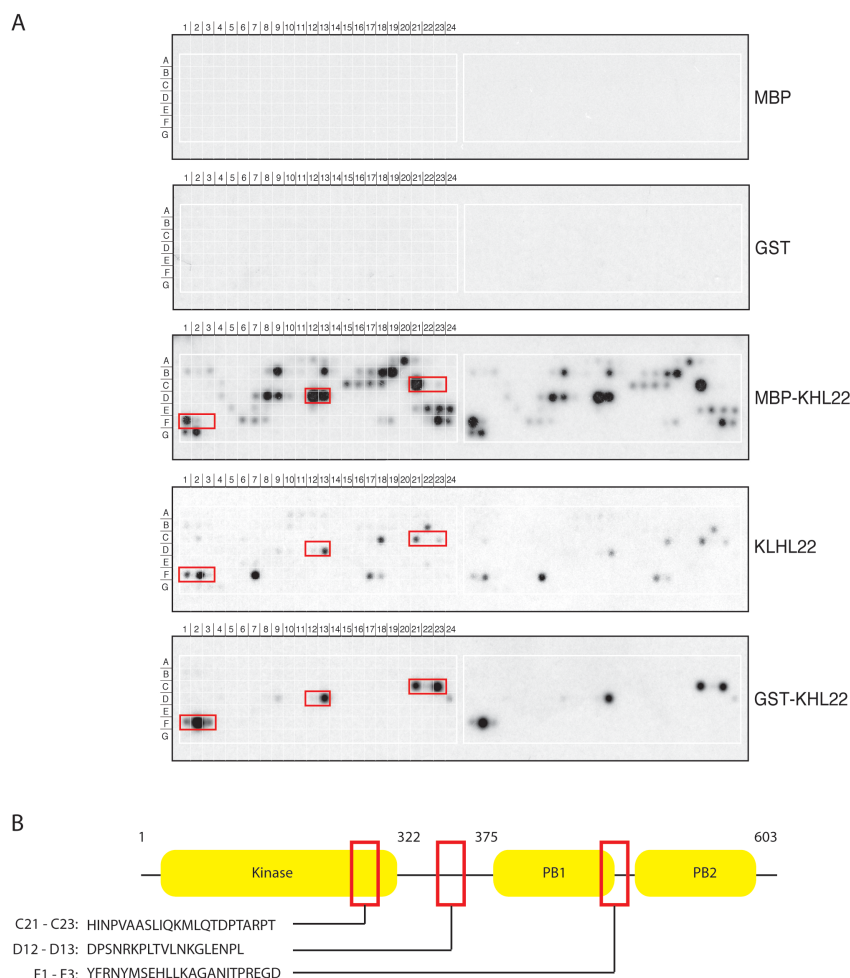


Figure 11. A. *PLK1* was divided in 15mer peptides with a shift of four amino-acids and spotted on nitro-cellulose membrane. After incubation with MBP-, GST-, and untagged-KLHL22, interactions were detected using anti-MBP, anti-GST and anti-KLHL22 antibodies, respectively. Three distinct binding interfaces (red rectangles) could be detected. **B.** Schematic representation of *PLK1* architecture and the potential interaction sites in red.

To confirm the potential sites of interaction lying within the kinase domain (peptides C21 to C23) and the PBD (peptides F1 to F3), we followed the same approach, i.e. generating truncation mutant of *PLK1* lacking the regions identified by the peptide array experiments (**Table 1**). Unfortunately, deletions of these motifs lead to poor expression and increased instability of the constructs and neither using bacteria nor mammalian cells could we get enough material to analyze involvement of these sites (**Table 1**). To solve this issue, and especially considering that the F1-F3 region of *PLK1* has already been shown to be involved in substrate binding (Xu et al., 2013), we are currently

performing site-directed mutagenesis of residues within this motif. As for now, Y481A, F482A and Y485A mutations have been tested (**Fig. 29B and data not shown**), but none of them exhibited different affinity towards KLHL22 than the wild-type GST-PLK1 construct.













Name	Positions	Representation	Bacterial expression	Mammalian expression
Full-length	1 - 603		+	+
Kinase	1 - 321		+	+
Kinase-ΔC21-C23	1 - 272		-	-
Kinase-N-lobe	1 - 134		+	+
Kinase-C-lobe	135 - 321		-	-
PBD	322 - 603		+	+
D12-D13	322 - 374		+	N.D.
PBD-ΔD12-D13	374 - 603		+	N.D.
PB1	322 - 506		+	+
PB1-ΔD12-D13	374 - 506		+	+
PB1-ΔD12-D13-ΔF1-F3	374 - 479		-	-
PB2	507 - 603		-	-

Table 1. Schematic representation of PLK1 and the truncation mutants used, as well as their expression efficiency in both bacterial and mammalian systems.

Interestingly, D12 and D13 peptides contain the so-called Destruction box (D-box) motif of PLK1 (337-RKPL-340). This motif was shown to be essential for recognition and subsequent degradation of PLK1 by the E3-ubiquitin ligase APC/C^{Cdh1} at the end of mitosis (Lindon and Pines, 2004). To study the involvement of the D-box of PLK1 in binding to KLHL22, we performed *in vitro* binding assay with the D12-D13 region fused to GST (**Table 1**). However, this construct was unable to co-purify bacterially expressed KLHL22, suggesting that D12-D13 region is not sufficient to interact with KLHL22 *in vitro* (**Fig. 12A**). Using a shorter construct of our GST-PLK1-PBD, lacking the D12-D13 region (**Table 1**) and using *in vitro* binding assay, we observed that the D-box was also not necessary for the interaction, as KLHL22 co-purified efficiently with both the GST-PLK1-PBD and GST-PLK1-PBD-ΔD12/D13 (**Fig. 12B**).

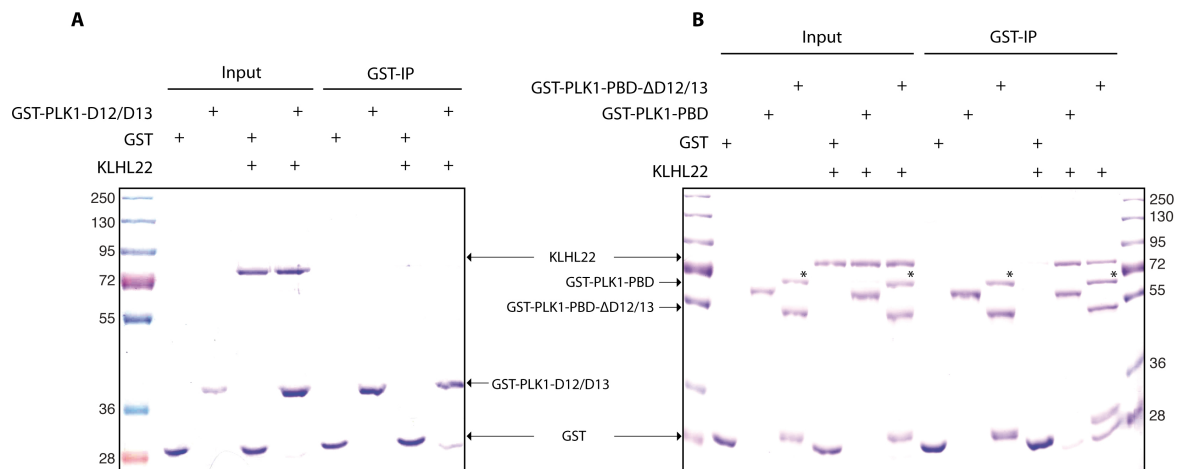


Figure 12. *A and B. In vitro binding assay KLHL22 with GST-PLK1-D12/D13 (A) and with GST-PLK1-PBD and GST-PLK1-PBD-ΔD12/D13 (B). GST was used as a control. The D12/D13 region does not appear to mediate the interaction with KLHL22. (*) indicates chaperone co-purifying with GST-PLK1-PBD-ΔD12/D13.*

We then tested whether a GFP-fused D-box mutant of PLK1, previously shown not to be degraded by APC/C^{Cdh1} anymore (R337A, L340A) (Lindon and Pines, 2004), was able to co-immunoprecipitate KLHL22 in HeLa cells. In contrast to the GFP-protein alone, the interaction between the D-box mutant and KLHL22 was indistinguishable from that of PLK1 wild-type (**Fig. 13**). Taken together, our results show that the D-box region of PLK1 is not involved in its binding to adaptor protein KLHL22. Thus, peptide array experiments and truncation approaches proved to be difficult and may not be appropriate models to study interactions of KLHL22 with PLK1.

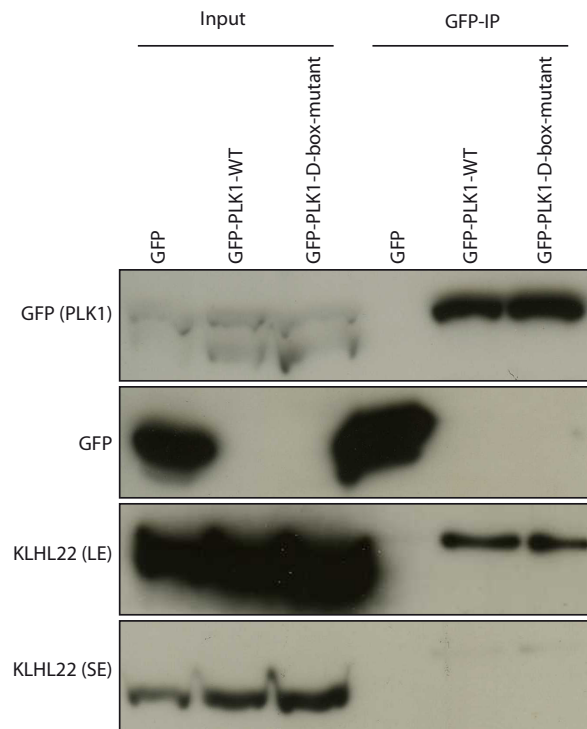


Figure 13. *GFP, GFP-PLK1-WT and GFP-PLK1-D-box mutant (R337A, L340A) plasmids were transfected into HeLa cells. After taxol synchronization, interactions were visualized by IP-WB analysis with GFP and KLHL22 antibodies. Both the WT and mutant form of PLK1 efficiently co-purified KLHL22. (SE) and (LE) indicate short and long exposure times, respectively.*

6.2.2.2 In vitro complex reconstitution of PLK1/KLHL22 and other Kinase/Kelch adaptor complexes

An increasing number of evidence suggests that protein kinases represent targets of CUL3/BTB- Kelch E3-ubiquitin ligases (Metzger et al., 2013). Indeed, CUL3/KLHL22 ubiquitinates PLK1 (Beck et al., 2013), CUL3/KLHL21 ubiquitinates Aurora B kinase (Maerki et al., 2009), CUL3/KLHL20 does so with DAPK (Lee et al., 2010), and CUL3/KLHL18 with Aurora A (Moghe et al., 2012).

Since protein kinases as well as BTB-Kelch proteins are highly conserved (**Fig. 10**), there might be a general mechanism for kinase recognition by CUL3 E3-ubiquitin ligases, which we would like to understand. Slight differences, perhaps only in a few amino-acids, are however expected, in order to ensure substrate specificity.

We decided to first understand how PLK1 contacts specifically adaptor protein KLHL22 , and then extend our knowledge to the other kinase/adaptor complexes.

In order to get insights into the molecular interactions between these two proteins, and because our truncation approaches failed (see part 5.2.2.1), we pursued crystallographic approaches, as they can provide atomic-resolution of multi-protein complexes. Efficient expression of proteins can be done in several hosts, but to date, bacterial E. coli BL21 (DE3) strain represents the most prominent expression system, mostly because of its rapid growth and easy manipulation. Our previous results (Beck et al., 2013; Metzger et al., 2013) indicate that indeed bacterially-derived PLK1 and KLHL22 were able to interact *in vitro*. In order to reconstitute a two-protein complex *in vitro*, two distinct strategies can be used (**Fig. 14**). Firstly, both proteins can be co-expressed in the same bacteria. This technique is widely recognized as a major method for reconstituting protein complexes mostly because of its inherent ability to increase protein solubility. Also, because proteins are already in a complex during the affinity-purification step, this decreases significantly the number of size-exclusion chromatographies, and thereby increases the quantities of recovered proteins after the different purification processes. The second approach consists of expressing and purifying both proteins independently by affinity and size-exclusion chromatography, mixing both proteins and performing another size-exclusion chromatography to recover only the formed, stable complex.

In both cases however, one of the major bottlenecks of structural approaches is to obtain high amounts of homogenous monodisperse samples, otherwise it is very likely that crystals will not grow or show poor X-ray diffraction.

We used both methods in parallel for PLK1/KLHL22 interactions, to be able to choose which one give highest quantity and highest quality of a pure complex.

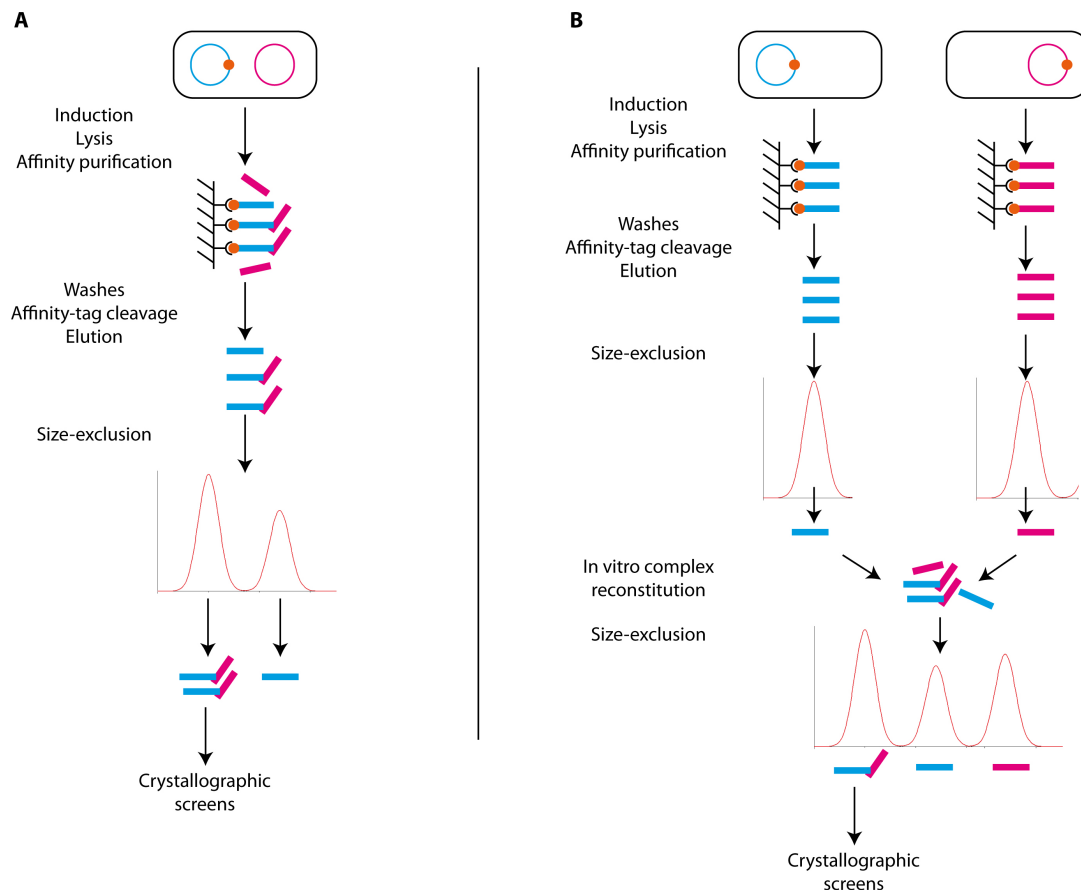


Figure 14. Schematic representation of the two methods used for PLK1/KLHL22 complex purification: the co-expression strategy (A) and the separate expression followed by mixing of individual components (B). Blue and purple rectangles represent both proteins, the orange circle represents the affinity tag.

6.2.2.3 Reconstitution of PLK1/KLHL22 complex by coexpression

The co-expression strategy involves cloning of both proteins into two sets of vectors: one encoding them in fusion with an affinity purification tag (in our case GST-tag), and one allowing expression under their native form, i.e. without any affinity tag. After co-transformation of bacteria, protein expression was induced by addition of IPTG. Cells were subsequently harvested and lysed, and GST-purification was performed. The retained proteins were analyzed by SDS-PAGE followed by Coomassie staining.

We observed that GST-KLHL22 was unable to co-purify untagged PLK1. However, when we pulled on GST-PLK1 with untagged KLHL22, a complex could be reconstituted (**Fig. 15**). Importantly, KLHL22 was not co-purifying with GST alone, meaning that the complex formed was specific to PLK1. This suggests that the complex could be reconstituted using co-expression. However, mostly due to the weak expression of KLHL22, the quantities of recovered complex were too low to fulfill crystallization criteria. We tried to optimize protein expression by changing temperature and time of induction, composition of the lysis buffer, but yields of production remained insufficient (data not shown).

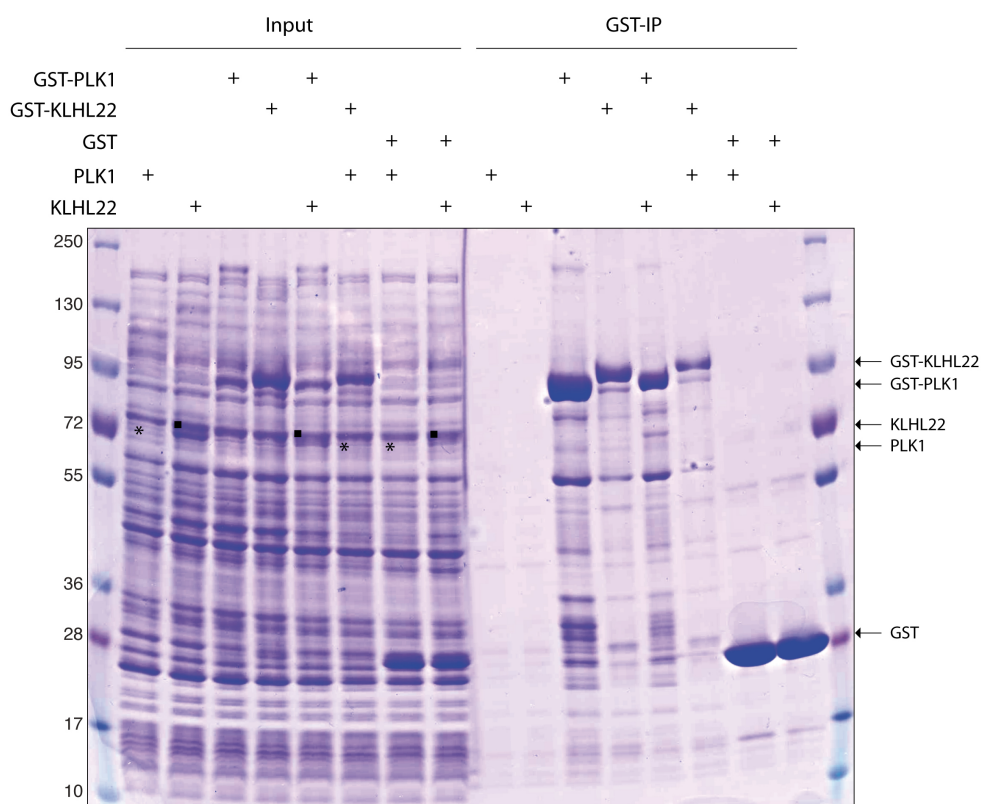


Figure 15. *Small-scale co-expression in E. coli and reconstitution of a stable KLHL22/PLK1 complex. KLHL22 was co-purifying with GST-PLK1 (compare lines 11 and 13), but inverting the position of the purification-tag (GST-KLHL22/PLK1) was not successful for complex purification (compare line 12 and 14). Note: in both cases, levels of expression of PLK1 (*) and KLHL22 (■) in crude lysate were low.*

6.2.2.4 Reconstitution of PLK1/KLHL22 complex by separate expression

Based on our previous data (Beck et al., 2013; Metzger et al., 2013), we know that both proteins PLK1 and KLHL22 can be expressed individually and form a complex *in vitro*. We thereby decided to produce them independently and subsequently mix them to try to recover amounts of complex sufficient for first crystallization screens. As shown in **Fig. 16**, using PBS as a purification buffer, we obtained high quantity of GST-PLK1 (4 mg per litre of culture). However, when loading the sample on size-exclusion chromatography, only few fractions were composed of monomeric or dimeric GST-PLK1. The recombinant protein was indeed mostly found in a high-order multimerized state.

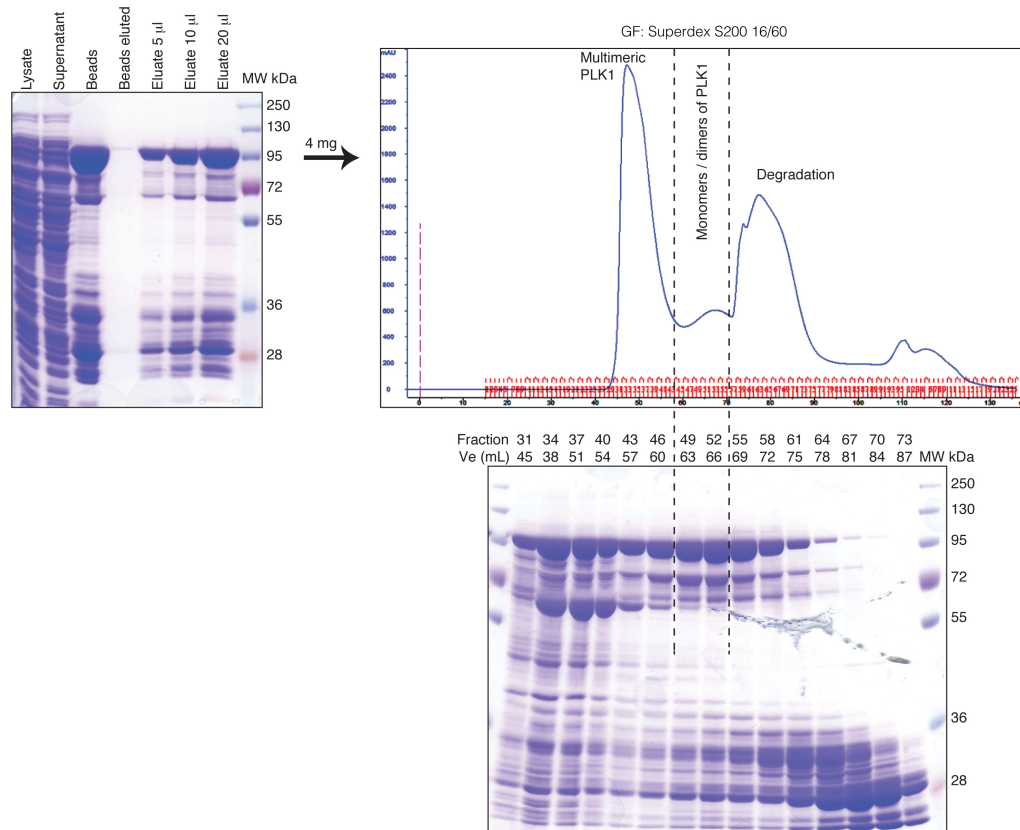


Figure 16. Purification profile of GST-PLK1 in PBS. The upper left part represents the affinity purification step. GST-PLK1 was highly expressed and purified (4 mg/L of culture). The upper right part represents the profile of GST-PLK1 after size-exclusion chromatography on a Superdex S200 16/60 column. Only fractions 47 to 54 contained mono/dimeric form of GST-PLK1. The lower part represents fractions from size-exclusion chromatography loaded on SDS-PAGE and stained by Coomassie.

The heterogeneity of such a state is clearly incompatible with crystallographic studies. To overcome this problem, we performed purification using a high-salt buffer (500mM NaCl/20mM Tris-HCl/pH 8), hoping that this would decrease electrostatic inter-molecular interactions. The quantity of recovered protein was similar (4 mg per liter of culture) (**Fig. 17**) and we indeed changed the equilibrium towards mono- or dimeric GST-PLK1. The fractions 23 to 27 contained highly pure GST-PLK1 suitable, in principle, for interaction studies with KLHL22 and subsequent crystallization assays.

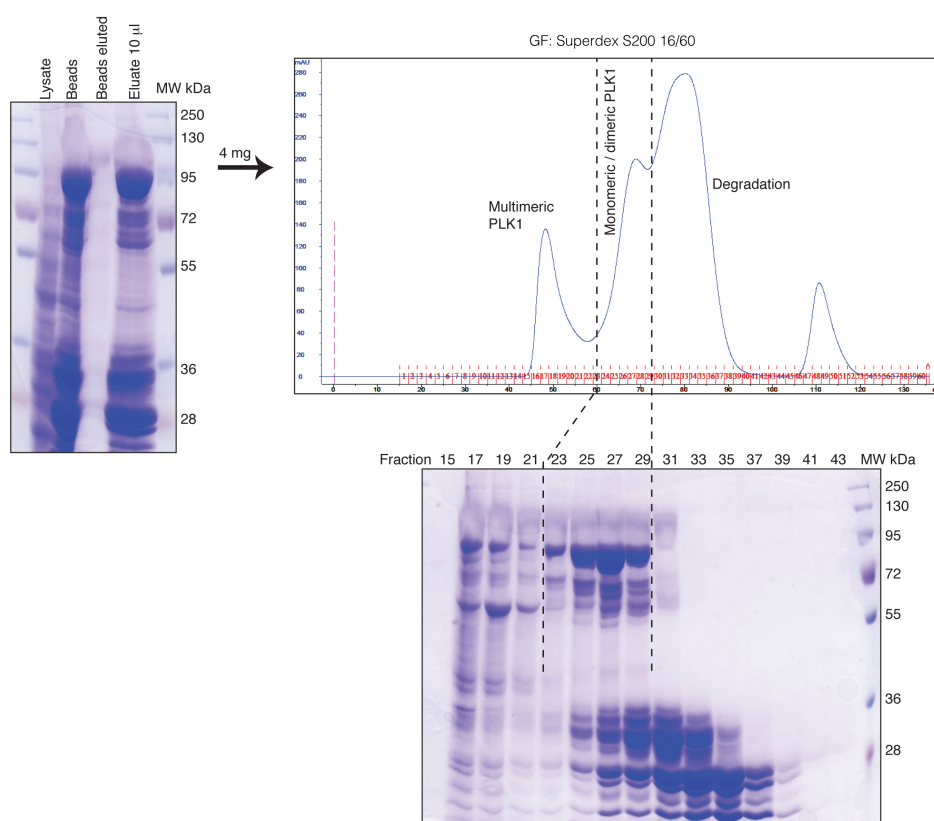


Figure 17. Purification profile of GST-PLK1 in a high-salt buffer. The upper left part represents the affinity purification step. GST-PLK1 was highly expressed and purified (4

mg/L of culture). The upper right part represents the profile of GST-PLK1 after size-exclusion chromatography on a Superdex S200 16/60 column. Fractions 23 to 29 contained mono/dimeric form of GST-PLK1. The lower part represents fractions from size-exclusion chromatography loaded on SDS-PAGE and stained by Coomassie.

The same approach was then used to obtain recombinant purified KLHL22 protein. By expressing GST-KLHL22 and performing affinity purification followed by size-exclusion chromatography, we could observe that the protein was eluted just after the void volume of the column ($V_e = 45$ mL) (**Fig. 18**). This is characteristic of soluble aggregates, as they pass through the column at the same speed as the flow of buffer, without entering the matrix. By comparing with protein markers, we confirmed the aggregated state of GST-KLHL22, as it was eluted 10 mL before the marker protein Ferritin of 440 kDa size (**Fig. 18**)

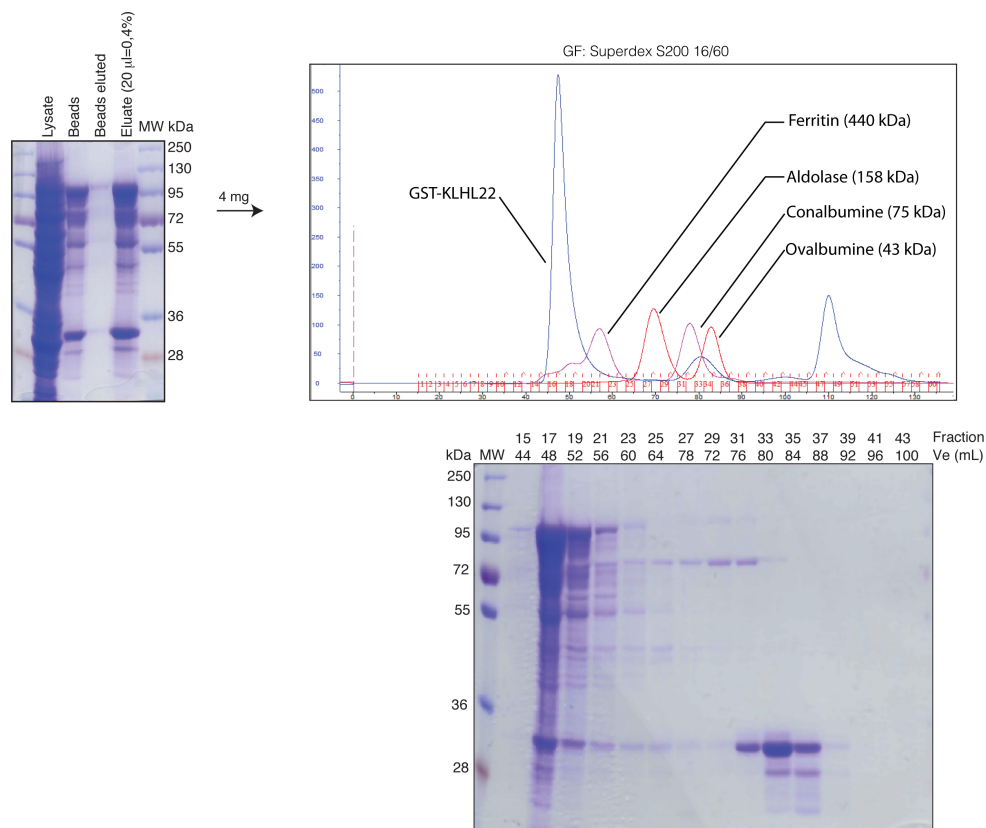


Figure 18. Purification profile of GST-KLHL22 in PBS. The upper left part represents the affinity purification step. GST-KLHL22 was highly expressed and purified (4 mg/L of culture). The upper right part represents the profile of GST-KLHL22 after size-exclusion

chromatography on a Superdex S200 16/60 column. Note: all the protein was present in a soluble aggregated form. The lower part represents fractions from size-exclusion chromatography loaded on SDS-PAGE and stained by Coomassie.

As for purification of PLK1, we subsequently tried to increase the salt concentration of the purification buffer for KLHL22, hoping that this would lead to multimer dissociation. However, this did not influence the solubility of GST-KLHL22, as the chromatogram of size-exclusion is indistinguishable from that of GST-KLHL22 purification in PBS (**Fig. 19**). Due to the ability of GST itself to dimerize, we assumed that removing the GST-tag before size-exclusion chromatography of KLHL22 would decrease its aggregated state. However, after cleavage with PreScission protease, untagged-KLHL22 was still behaving as soluble aggregates (**Fig. 19**).

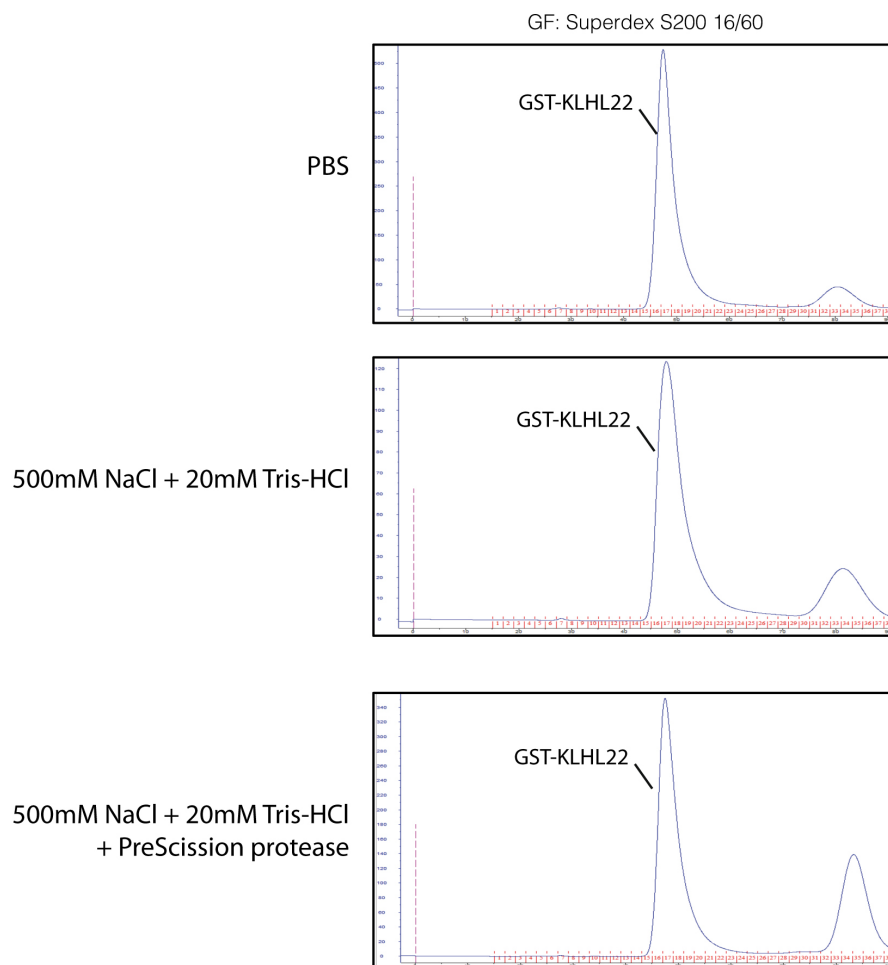


Figure 19. *Purification profile of GST-KLHL22 in different buffers. The protein was only recovered in an aggregated state, independently of both the purification buffer used and the presence of the GST-tag.*

This result is in accordance with a recent paper focusing on structural approaches of BTB-BACK-Kelch proteins (Canning et al., 2013). The authors concluded that soluble expression constructs could only be made of BTB-BACK or Kelch domain only, but not of BACK-Kelch or BTB-BACK-Kelch. Our previous results (Beck et al., 2013) showed that the Kelch domain of KLHL22 was sufficient for interacting with PLK1. We thereby expressed and purified only this domain, but the purified protein remained aggregated after size-exclusion chromatography (data not shown). As a conclusion, due to the aggregated character of KLHL22, we were unable to reconstitute the soluble complex with PLK1 in quantity and quality sufficient to pursue crystallographic studies.

6.2.2.5 Reconstitution of Aurora B/KLHL21 complex by separate expression

Because of the aggregated state of KLHL22, we decided to focus on another kinase/adaptor complex. Thus, we screened expression of several other CUL3-adaptors, including KLHL18 and KLHL21. As shown in **Fig. 20**, after cloning into pGex-6P1 vector, we performed small-scale expression test in which we observed that the yields of production of GST-KLHL21 recombinant protein were higher than for KLHL18. This of course did not insure the quality of the protein, but at least quantities of GST-KLHL21 were sufficient to pursue with further purification processes.

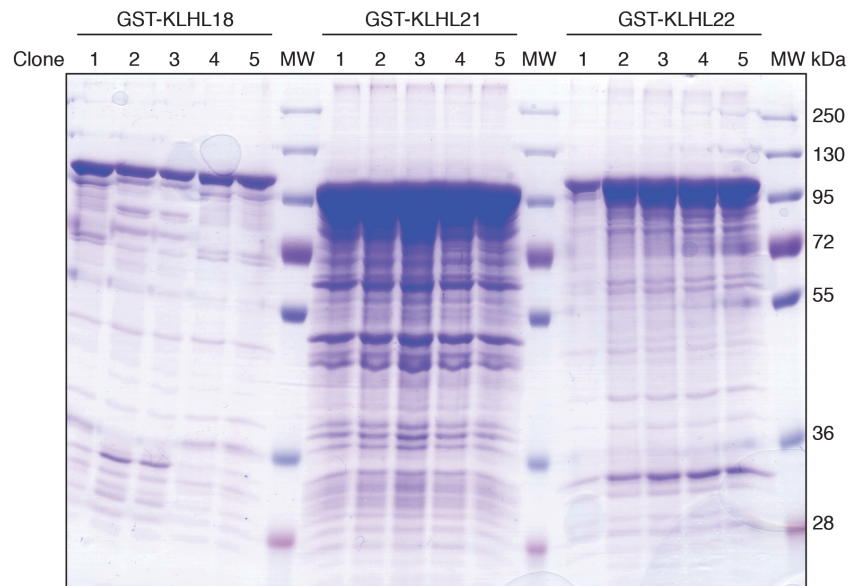


Figure 20. Small-scale purification of several *CUL3* adaptors. In each case, 5 clones of each were tested. The yields of purification of KLHL21 were higher than for KLHL18 or KLHL22.

Thus, we performed ion-exchange followed by gel filtration purifications (**Fig. 21**). The full-length KLHL21 protein was clearly not aggregated but most of it was present in a high-order multimerized state.

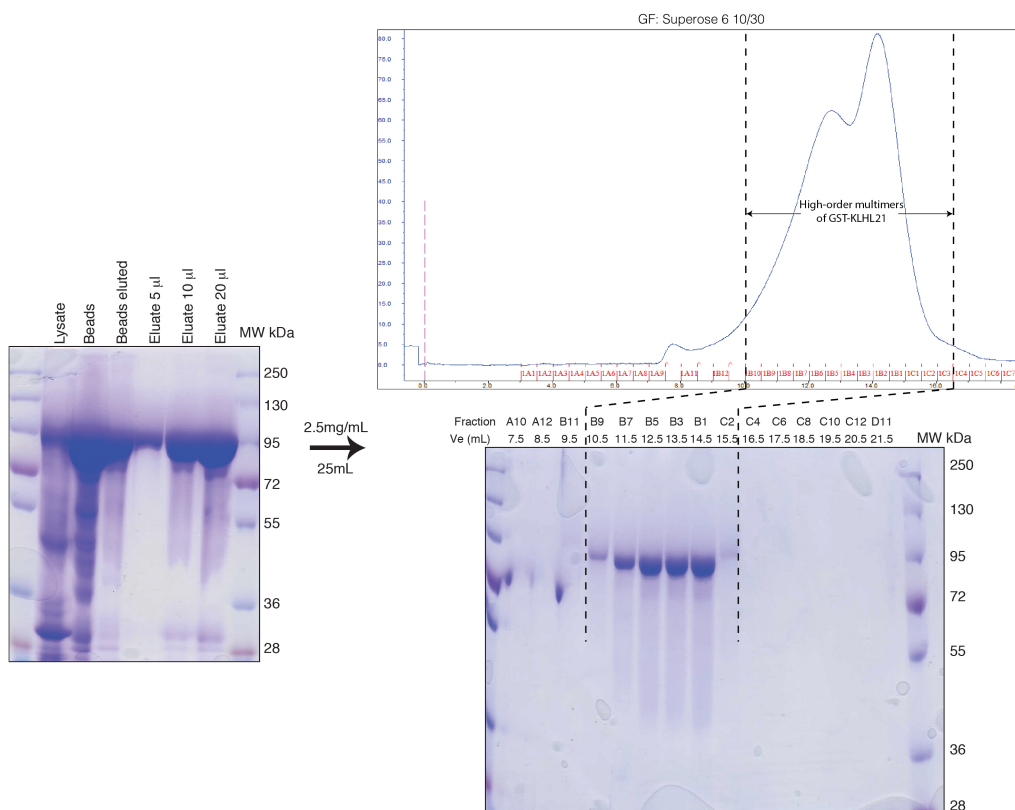


Figure 21. Size exclusion chromatography of purified full-length GST-KLHL21 on a Superose 6 column. The protein is not aggregating but most of it is in highly multimerizing state (V_e 10 to 16 mL).

As for GST-PLK1, we tried several purification buffers, hoping that they would change the equilibrium from multimeric to mono-/dimeric form of GST-KLHL21. Increasing salt concentration indeed decreased oligomerization of GST-KLHL21, but we could still not clearly dissociate the peak corresponding to multimers from the one corresponding to monomers (**Fig. 22**).

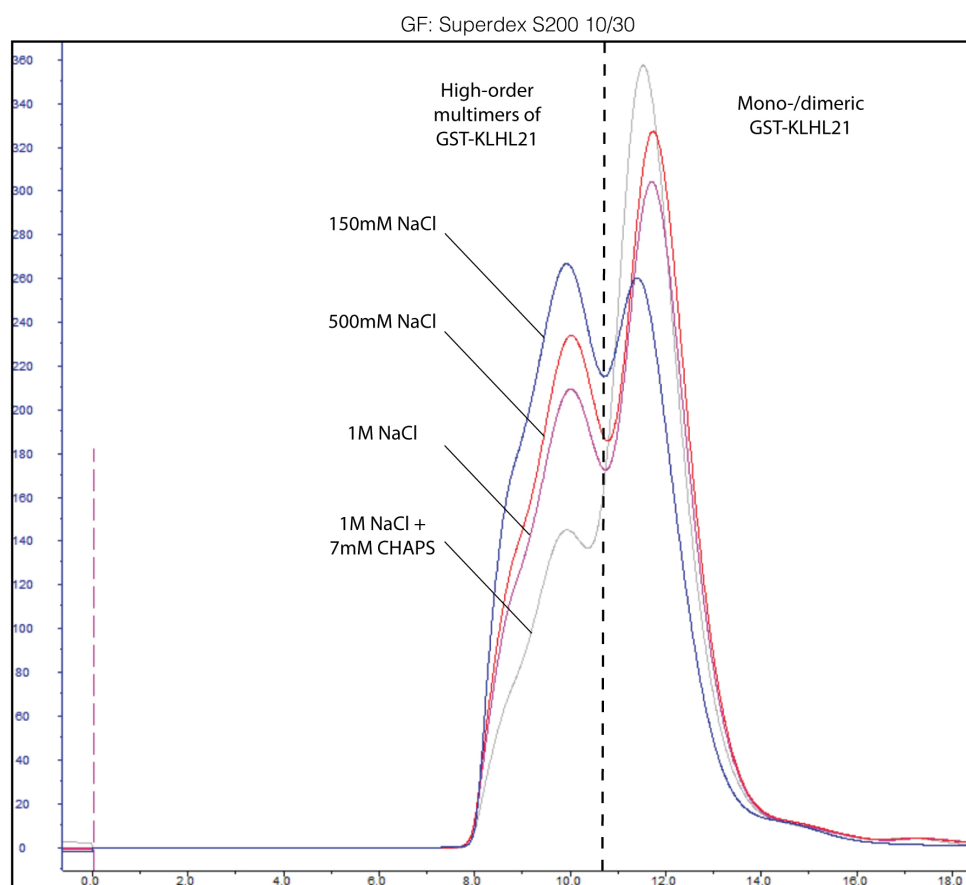


Figure 22. Purification profile of GST-KLHL21 in different buffers. Increasing salt concentration and adding detergents strongly reduces the high-order multimerized state of GST-KLHL21

To solve this problem, and since BTB domains are known to dimerize, we generated recombinant protein expressing only the Kelch domain of KLHL21. This construct was highly expressed in *E. coli* and efficiently purified using GSH-sepharose. The protein was eluted by cleavage of the GST-tag with PreScission protease. Ion-exchange chromatography followed by gel filtration resulted in only one sharp peak (**Fig. 23**). Comparing with molecular weight markers, KLHL21-Kelch appears to be monomeric. We are able to obtain a high quantity of highly pure KLHL21-Kelch protein, presumably suitable with crystallographic studies.

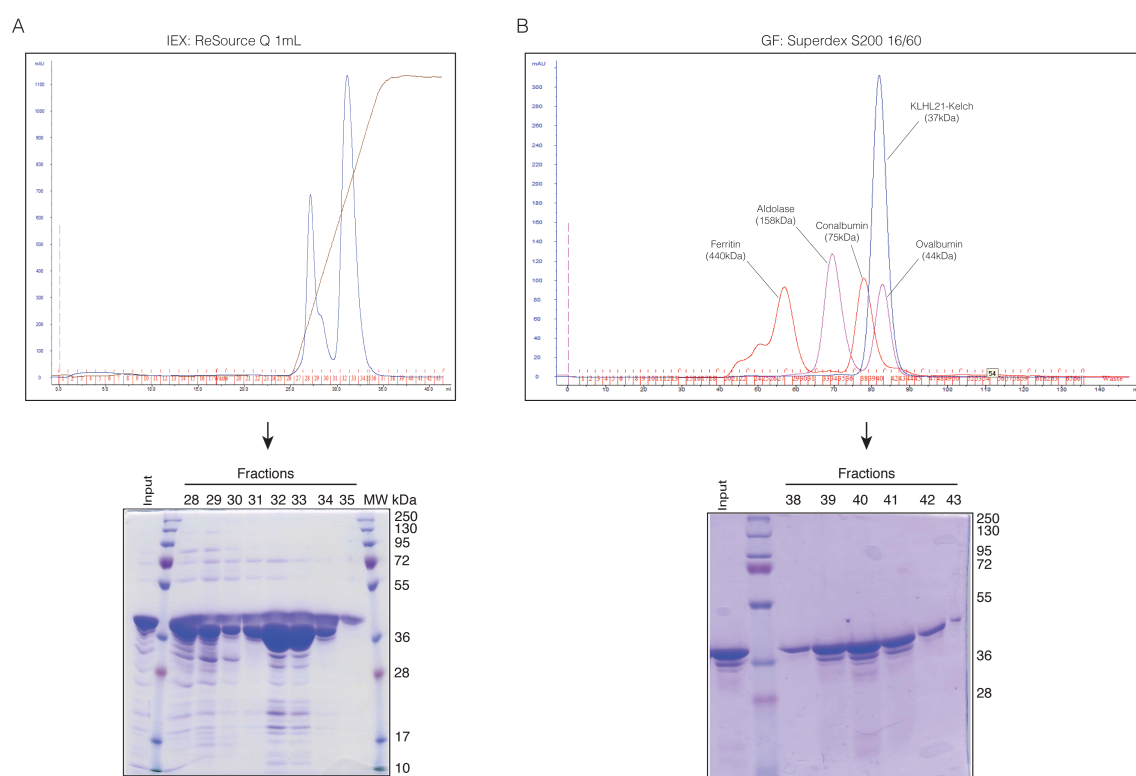


Figure 23. Purification of KLHL21-Kelch on ion-exchange chromatography using ReSource Q column (A) followed by size exclusion chromatography on S200 16/60 (B). The protein appears as one single symmetrical peak, which may correspond to its monomeric form.

Encouraged by these results, we subsequently attempted to prepare recombinant Aurora B protein. Neither the full-length His- nor the GST-constructs were soluble

(Table 2). In accordance with previous data (Elkins et al., 2012), the protein had to be truncated of 55 amino-acids at its N-terminal side for efficient purification. While the GST-Aurora B Δ N55 was soluble, the His-construct as well as Aurora B Δ N55 cleaved-off GST were strongly aggregating **(Table 2)**. Moreover, even if GST-Aurora B Δ N55 was soluble, only a very small fraction was mono/dimeric, most of the protein behaving more like a high-order multimer **(Fig. 24)**. Increasing salt concentration did not change GST-Aurora B oligomerization (data not shown).

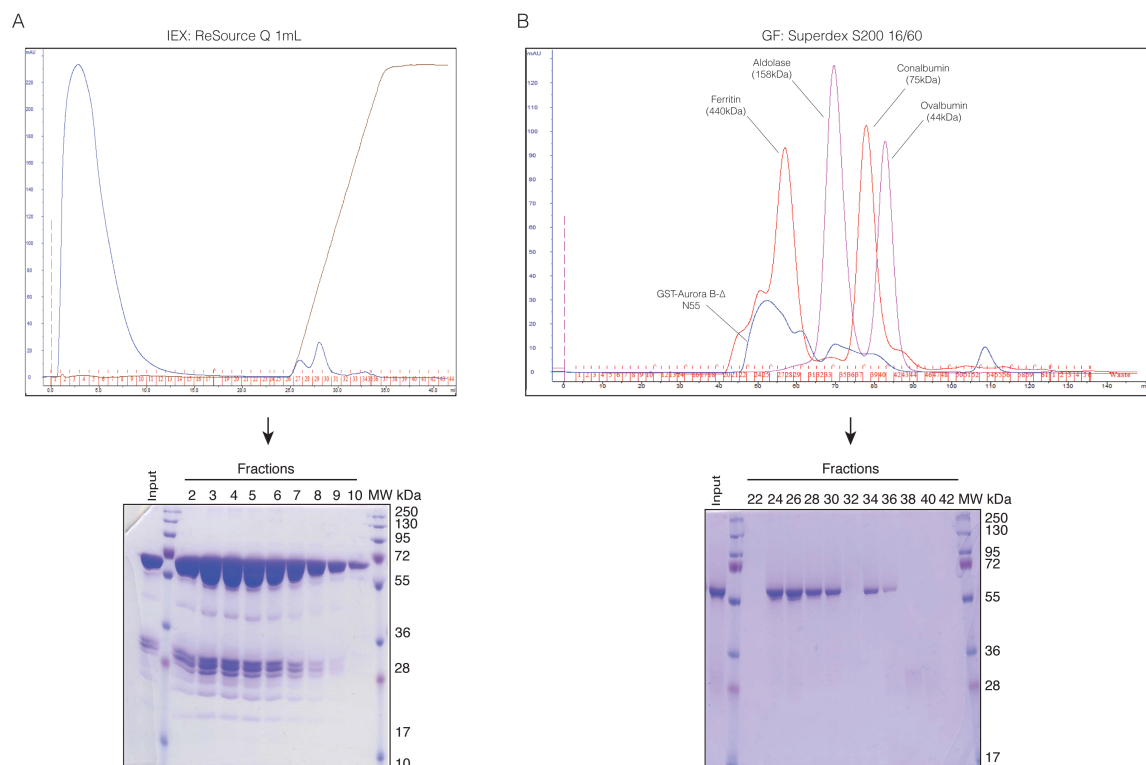


Figure 24. Purification of GST-Aurora-B- Δ N55 on ion-exchange using ReSource Q column (A) followed by size exclusion chromatography on S200 16/60 (B). Only little protein is in a mono/di-meric form.

Nevertheless, we performed an *in vitro* binding assay by mixing the monomeric GST-Aurora B- Δ N55 (fraction 34) with the purified KLHL21-Kelch previously obtained. After incubating both proteins (and corresponding controls) in binding buffer, affinity purifications on glutathione-beads were performed. Using coomassie staining, we could observe that KLHL21-Kelch was retained on beads when GST-Aurora B- Δ N55 was

present, but not when only GST-tag was used (**Fig. 25**). Importantly, the same observation could be made when using the high-order multimerized GST-Aurora B- Δ N55 (fractions 24 to 30) (data not shown). To monitor the complex stability over size-exclusion chromatography, we loaded it on a S200 10/30 column. However, mostly due to the low quantity of GST-Aurora B- Δ N55 available from the start and the dilution factor inherent to the column size, the threshold of detection using OD₂₈₀ was too high for detecting any GST-Aurora B- Δ N55-containing fractions (data not shown).

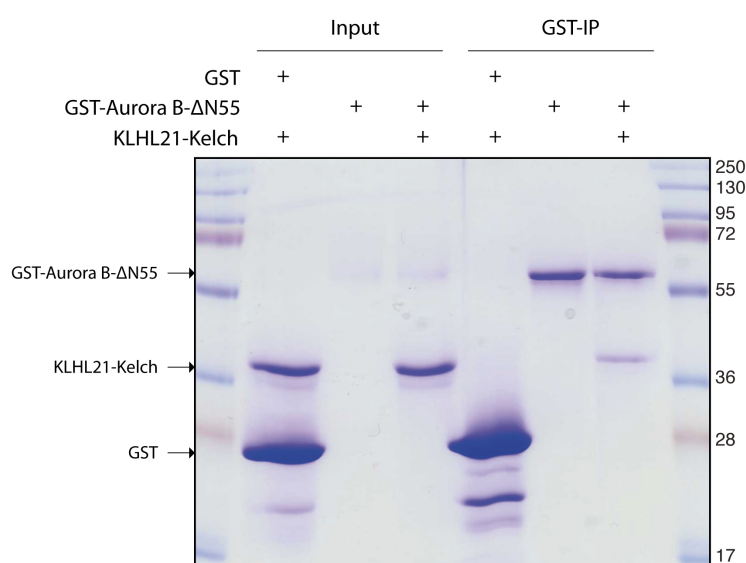


Figure 25. *In vitro* binding assay of GST-Aurora B- Δ N55 with KLHL21-Kelch analyzed by coomassie staining. KLHL21-Kelch is retained on GST-beads only when Aurora-B- Δ N55 is present.

Because of the poor yields of production and solubility of GST-Aurora B- Δ N55 alone, we hypothesized that co-expression or co-lysis with KLHL21-Kelch would help to solubilize the protein. To test this hypothesis, we cloned His-KLHL21-Kelch into pACYC-Duet vector (Novagen), which is compatible with pGex6P1-Aurora B- Δ N55 for co-expression. Unfortunately, co-expression of GST-Aurora B- Δ N55 with His-KLHL21-Kelch did not lead to any complex formation. Instead, we could observe a very strong degradation of Aurora B only when co-expressed with His-KLHL21-Kelch (**Fig. 26**).

Also, when using another construct encoding GST-fusion of *Xenopus laevis* Aurora B in fusion with a fragment of *Xenopus laevis* INCENP known to be essential for the kinase

activation (Sessa et al., 2005), we could not reconstitute a complex with human His-KLHL21- Kelch (**Fig. 26**).

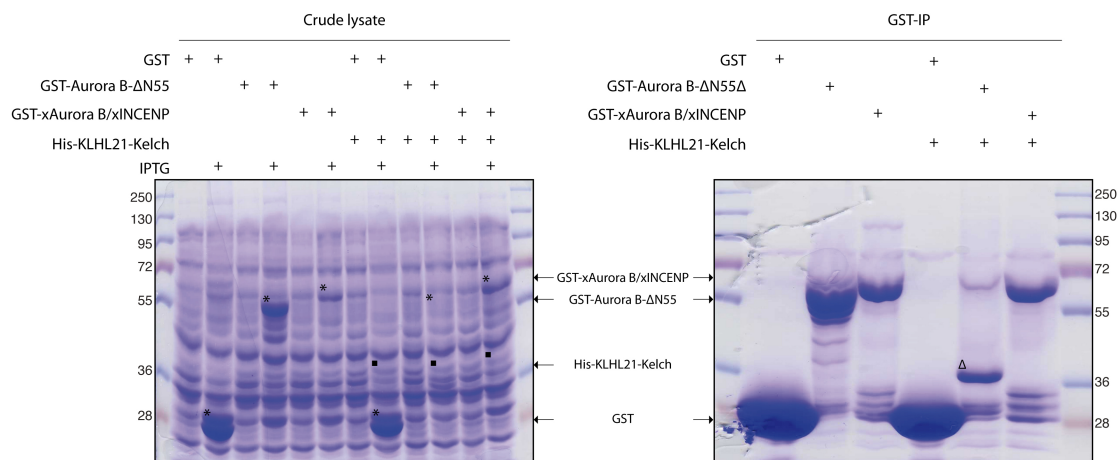


Figure 26. Single and co-expression of GST, GST-Aurora B- Δ N55 or GST-xAurora B/INCENP with HIS-KLHL21-Kelch. Both Aurora B-encoding constructs were insufficient to co-purify with His-KLHL21-Kelch. In crude lysate, all GST-fusions are marked with (*) and His-KLHL21-Kelch (■) to show very low concentrations. (Δ) on the GST-IP panel represents degradation of GST-Aurora B- Δ N55.

Because co-expressing GST-Aurora B- Δ N55 with His-KLHL21-Kelch seemed to actually destabilize both proteins, we performed co-lysis experiments. For this purpose, we expressed proteins separately, mixed and lysed them together. Although protein induction is good, still no complex could be reconstituted with GST-Aurora B- Δ N55 and GST-xAurora B/xINCENP (**Fig. 27**).

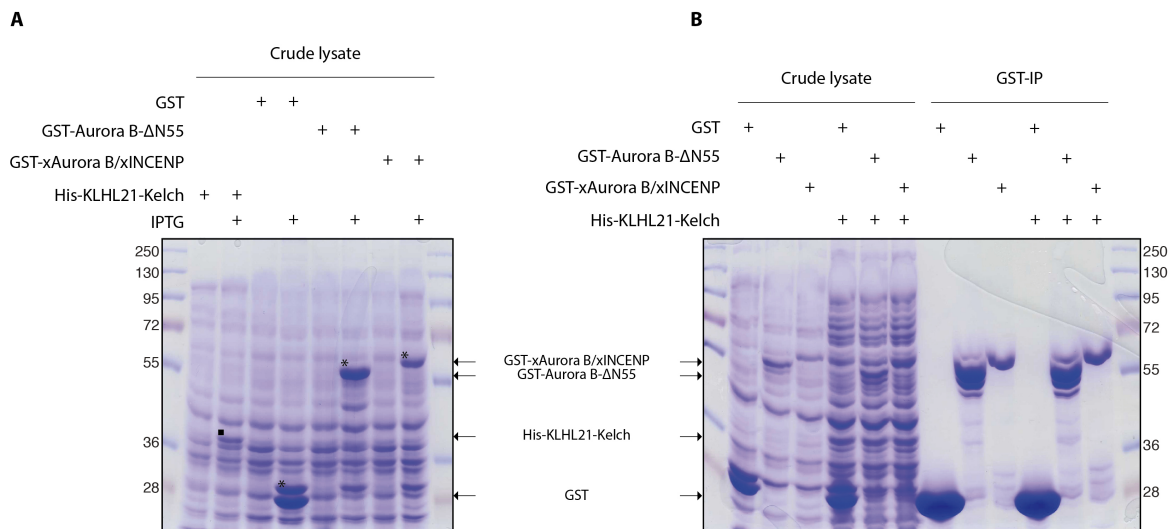


Figure 27. Co-lysis experiments of GST, GST-Aurora B-ΔN55 or GST-xAurora B/INCENP with His-KLHL21-Kelch. Despite the presence of all proteins in crude lysate (A), where all GST-fusions are marked with (*) and His-KLHL21-Kelch (■), no complex could be reconstituted between Aurora B and KLHL21-Kelch (B).

As a conclusion, it seems that the only potential approach that could be followed in order to reconstitute the complex is purifying both proteins separately and mixing them. However, due to the poor quantity and quality of GST-Aurora B-ΔN55 after purification, it will, most likely, not be suitable for the crystallographic studies we are aiming at.

However, it was previously shown that the solubility of Aurora B is increased when co-lysed with the C-terminal part of INCENP (Sessa et al., 2005). It would be interesting to use this Aurora B/INCENP complex to test its ability to interact with KLHL21-Kelch. In line with this idea, we performed pulldown experiments using our GST-KLHL21-Kelch construct, which show that not only endogenous Aurora B, and INCENP co-purified with KLH21 from HeLa cell extract (**Fig. 28**). Interestingly, mass spectrometry analyses confirmed the presence of INCENP, but neither Survivin nor Borealin could be detected using this method. This suggests that KLHL21, Aurora B and INCENP are likely to interact *in vivo* as a complex lacking other canonical members of the Chromosomal Passenger Complex (Survivin and Borealin).

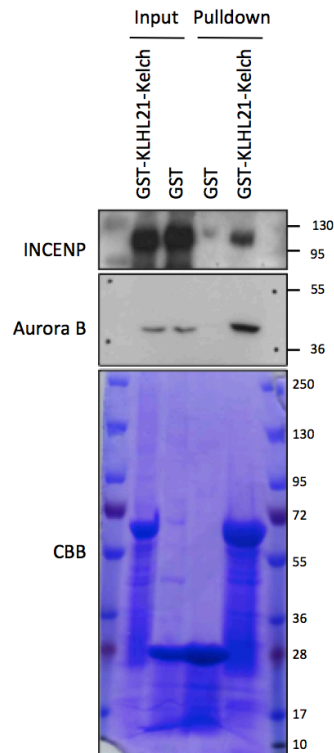


Figure 28. GST-pulldowns of mitotic HeLa cells were performed using GST and GST-KLHL21-Kelch. Samples were visualized by Western-blotting against GST, Aurora B and INCENP. KLHL21-Kelch appears sufficient to pulldown both members of the CPC.

Protein	Construct number	Domain	Tag	Soluble expression	Affinity	Cleavage	Size-exclusion	Co-expression	Mix
PLK1	1	FL (1-603)	GST	OK	OK	OK	OK	Low with (6)	Low with (6)
	2	FL (1-603)	Untagged	Low				No with (3)	No with (3)
KLHL22	3	FL (1-634)	GST	OK	OK	OK	No (aggregates)	No with (2)	No with (2)
	4	BTB-BACK	GST	OK	OK	No	N.D.	N.D.	N.D.
	5	KELCH	GST	OK	OK	No	No (aggregates)	N.D.	N.D.
	6	FL (1-634)	Untagged	Low			No (aggregates)	Low with (1)	Low with (1)
Aurora B	7	FL (1-344)	GST / His	No					
	8	ΔN55 (55-344)	His / Untagged	No					
	9	ΔN55 (55-344)	GST	OK	OK	No	No (mostly multimeric)	No	Low with (12)
KLHL21	10	FL (1-597)	GST	OK	OK	OK	No (mostly multimeric)	N.D.	N.D.
	11	KELCH	GST	OK	OK	OK	N.D.	N.D.	N.D.
	12	KELCH	His/untagged	OK	OK	OK	OK	No	Low with (9)

Table 2. Summary of all the different constructs tested for reconstituting in vitro complexes between PLK1 and KLHL22 and between Aurora B and KLHL21. The high-order

mutimerized states of KLHL22 and Aurora B constituted the major bottleneck of this approach.

Taken together, our aims to reconstitute kinase/adaptor complexes using PLK1/KLHL22 and Aurora B/KLHL21 as models turned out to be very difficult. In both cases, number of tested constructs and experimental settings, summarized in **Table 2**, did not lead to *in vitro* reconstitution of complexes of quality and quantity sufficient for purpose of crystallization.

6.2.3 Hypothesis-driven approaches

6.2.3.1 How does KLHL22 interact with the PBD of PLK1?

We previously showed that PLK1 utilizes at least two distinct binding interfaces to interact with adaptor protein KLHL22: one located within its kinase domain, and the other within its Polo-Box domain (PBD) (Metzger et al., 2013). To understand if this phosphopeptide binding module plays a role in KLHL22 recognition, we used the GST-PLK1-PBD-WT as well as forms mutated within phosphopeptide binding residues (H538A and K540M) and performed GST-pulldown experiments from mitotic HeLa cell extracts over-expressing HA-tagged KLHL22.

As expected, compared to the wild-type PBD, the double mutant H538A/K540M abolished binding to BUBRI phosphoreceptor, but showed similar affinity towards HA-KLHL22. Subsequently, we tested requirement of W414, involved in recognition of non-phosphorylated receptors. W414F mutation in combination with H538A/K540M (**Fig. 29A**) and alone (**Fig. 29B**) dramatically decreased the affinity towards HA-KLHL22. In contrast, mutations of F482 and W514, other residues involved in phosphorylation-independent binding of MAP205 to PLK1-PBD (Xu et al., 2013), did not affect binding to HA-KLHL22. Taken together these results suggest a role for the receptor binding motif of PLK1 in KLHL22 recognition that appears to be dependent on W414 but may not require residues involved in phosphate-coordination (H538 and K540).

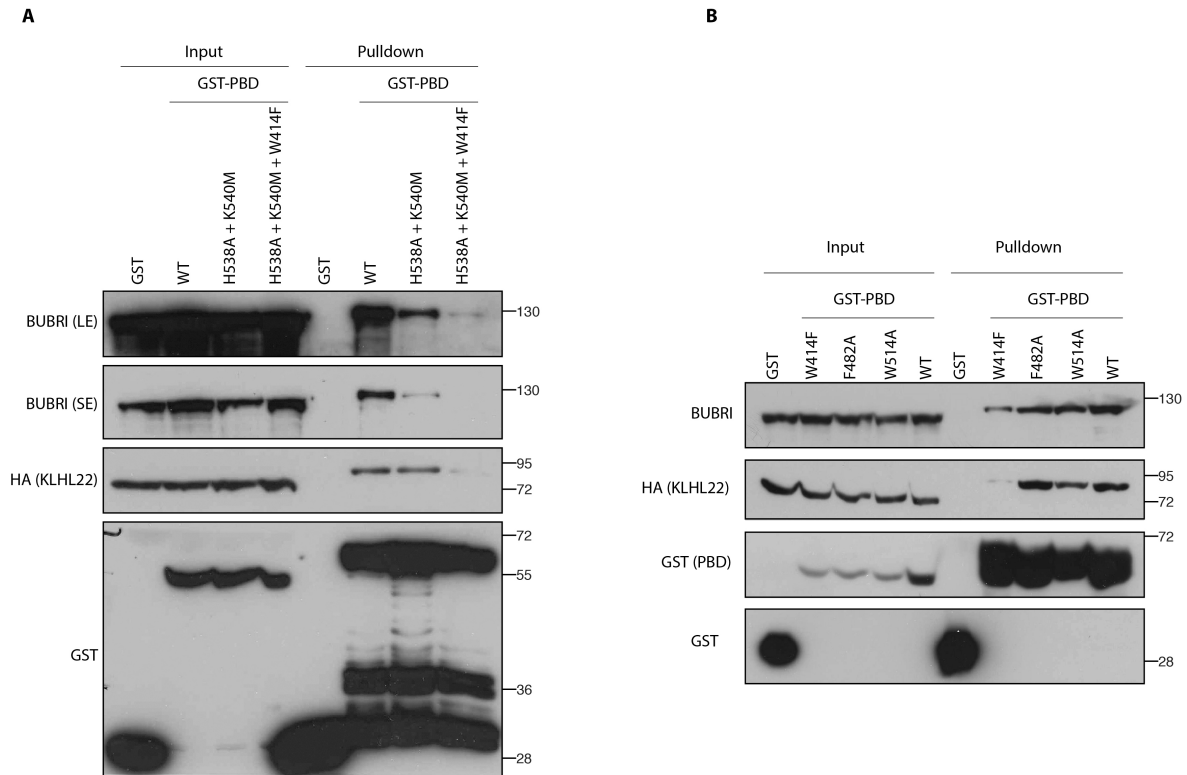


Figure 29. GST-pulldowns of mitotic HeLa cells over-expressing HA-KLHL22 were performed using GST-PLK1-PBD and the indicated mutants. Samples were analyzed by Western-blotting with GST, HA and BUBRI antibodies. Whereas mutations of H538 and K540 did not influence the binding, combination with W414F (**A**), or this mutation alone (**B**), significantly decreased the affinity of KLHL22 towards GST-PLK1-PBD. (SE) and (LE) indicate short and long exposure times, respectively.

In search for PLK1-interacting motifs within KLHL22, we used software prediction analyses (Liu et al., 2013). KLHL22 contains only two potential phosphopincer interacting sites: one high-scoring motif, centered around T309 and one lower-scoring, around T605 (**Fig. 30A**).

Interestingly, the T309-motif is indeed very similar to the consensus previously described (Yun et al., 2009). Therefore, we first performed series of mutations of KLHL22 T-309-motif that could disrupt interaction with PLK1. The Serine in position -1 of the phosphorylated residue was previously shown to be important for the interaction between PLK1 and its binding substrates (Elia et al., 2003a). However, mutation of S308 to Alanine (S308A) did not disrupt the interaction with PLK1 (**Fig. 30B**). We also

mutated the presumably phosphorylated residue to Alanine or Aspartate (T309A and T309D, respectively). In both cases however, mutated HA-KLHL22 were pulled-down to the similar extent as wild-type HA-KLHL22 (**Fig. 30B**). Thus, we performed mass spectrometry analysis of GST-PLK1-PBD interacting proteins and their modifications. These experiments confirmed the absence of phosphorylation of KLHL22 on T309. Interestingly, the only phosphorylated residue of KLHL22 detected in this analysis was T605 (**Fig. 30C**), i.e. the second potential PBD-interacting site highlighted in our *in silico* test (**Fig. 30A**). We are currently performing site-directed mutagenesis of T605 to Alanine and Aspartate (T605A and T605D, respectively) to confirm the importance of this residue for KLHL22 interaction with PLK1.

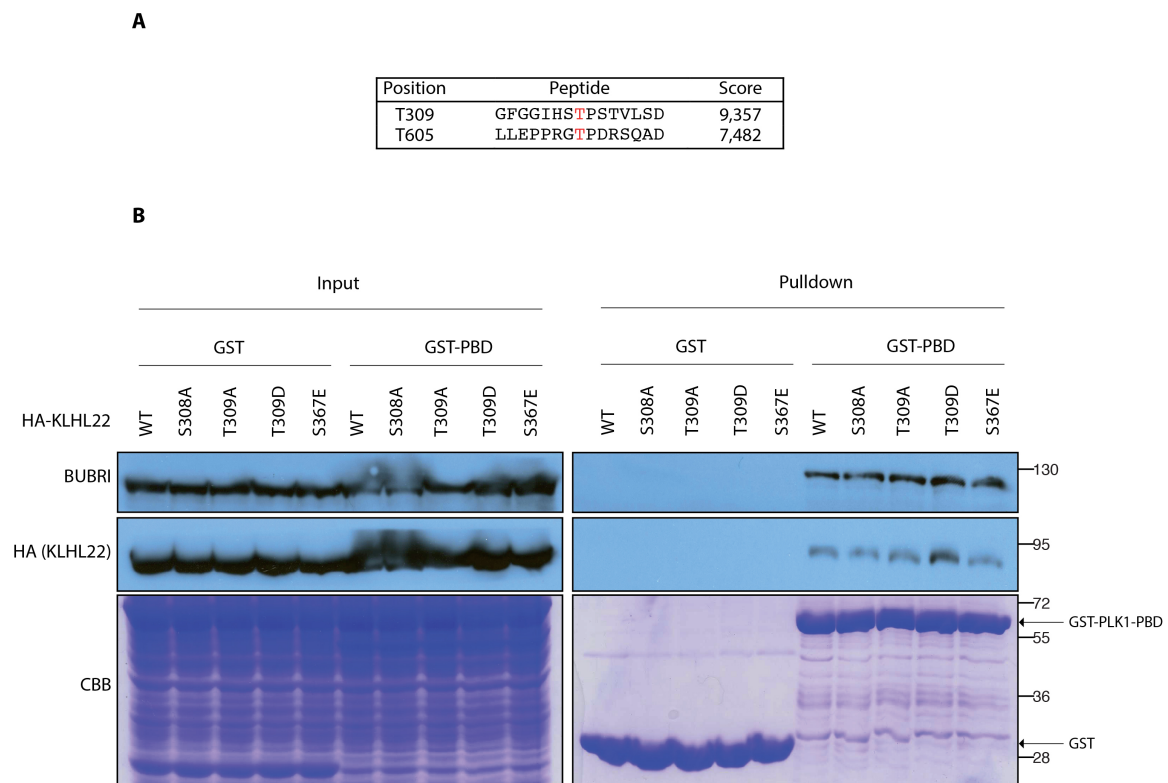


Figure 30. **A.** *In silico* prediction of the putative PBD-binding sites on KLHL22. **B.** GST-pulldowns of mitotic HeLa cells over-expressing HA-KLHL22 and the indicated mutants were performed using GST-PLK1-PBD. Samples were analyzed by Western-blotting with GST, HA and BUBRI antibodies. None of the mutations of KLHL22 could significantly affect its affinity towards GST-PLK1-PBD. **C.** GST-PLK1-PBD pulldowns samples were analyzed by mass spectrometry. After phospho-peptide enrichment, only the T605 of KLHL22 was identified as phosphorylated.

6.2.3.2 How does KLHL22 interact with the kinase domain of PLK1?

PLK1 is not the only known substrate of CUL3 to use at least two distinct interfaces for interacting with its adaptor protein. Indeed, the prevalent model of interaction between transcription factor NRF2 and BTB-Kelch protein KEAP1 involves its dimerization via the BTB domain. Two sites (the ETGE and the DLG motifs) within the same molecule of NRF2 mediate interaction with both Kelch domains (McMahon et al., 2006; Tong et al., 2006). Therefore we analysed PLK1 by bioinformatics and could identify an exact ETGE motif, located within its PBD (amino-acids 365 to 368). However, mutagenesis of 365-ETGE-368 to AAGA did not affect KLHL22 binding. Interestingly, despite absence of a DLG motif within PLK1, the kinase domain contains DFG residues located at the beginning of the activation loop (amino-acids 194 to 196). DFG motif is very conserved throughout evolution and present in almost every kinase (**Fig. 31**) as it is an essential regulator of their activities. Indeed the aspartate residue coordinates the magnesium ion (Mg^{2+}) essential for transferring the phosphate from ATP to the substrate. In the DFG-in conformation, the magnesium ion can be coordinated and the kinase is in its active state, whereas in DFG-out conformation, the motif is in a position incompatible with proper catalysis and thereby the kinase is in an inactive state (Bayliss et al., 2012). Because leucine to phenylalanine substitution is quite neutral, we hypothesized that this motif could be very similar to the DLG found in NRF2 (McMahon et al., 2006; Tong et al., 2006). Indeed, several kinases, including mitotic NEK6, NEK7, BUB1, contain DLG motif instead of DFG found in PLK1 (**Fig. 31A**). To test our hypothesis, we mutated PLK1 DFG-motif into 194-AGE-196 to neutralize charges. After co-transfecting HeLa cells with HA-KLHL22, cells were synchronized in the mitotic stage by addition of Taxol, and GFP proteins were immunoprecipitated (**Fig. 31B**). Surprisingly, in contrast to ETGE-motif

mutants, both DFG-mutant containing constructs exhibited increased binding of KLHL22 (**Fig. 31B**), which denotes the potential importance of this site for the interaction. Interestingly, mutating the DFG-glycine residue to glutamate within B-Raf protein increased the kinase activity (Moretti et al., 2009), presumably by forcing a DFG-in conformation. In this sense, our DFG to AGE mutant of PLK1 could act similarly, i.e. over-activating the kinase, which could explain the increased interaction with KLHL22. To corroborate these preliminary observations, we are currently analysing mutations predicted to induce a DFG-out conformation of PLK1, and monitoring whether forced inactivation of the kinase also influences KLHL22 interaction.

A

```

PLK1  —EDLEVKIGDEGLATKVEYD
Aurora A —SAGEIKIADEGNSVHAP--
Aurora B —LKGELKIADEGNSVHAP--
DAPK  —PKPRIKIIDEFLAHKID-F
IKKb  —QRLIHKIIDLGYAKELD-Q
WNK1  —PTGSVKIGDLGLATLKR--
WNK4  —PTGSVKIGDLGLATLKR--
B-Raf —EDLTVKIGDEGLATVKSrw
Bub1  —LSAGLALIDLQSIDMKLF
Nek6  —ATGVVKLGDLGLGRFFSSE
Nek7  —ATGVVKLGDLGLGRFFSSK
Nrf2  —EDLWRQDIDLGVsREVF--

```

B

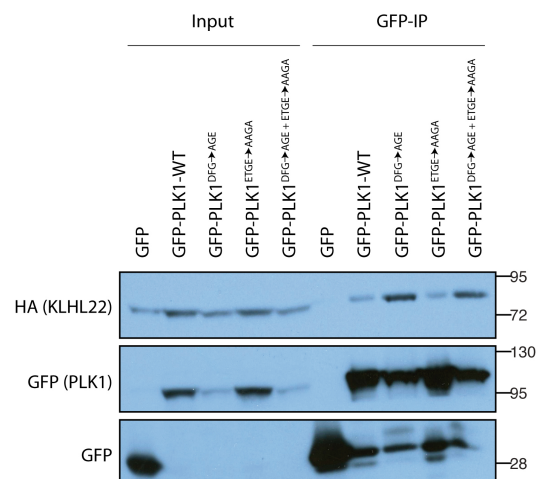


Figure 31. A. Multiple sequence alignment of protein kinase domains and the NRF2-DLG motif. DFG/DLG motifs are very conserved among protein kinases as they function as

essential magnesium coordinators. Black shading indicates identical amino-acids whereas grey shading indicates amino-acids similarity with a 70% shading-threshold. The alignment was obtained using ClustalW. B. HeLa cells were co-transfected with HA-KLHL22 and GFP, GFP-PLK1-WT or the indicated mutants and subsequently synchronized in mitosis using Taxol. Extracts were immunoprecipitated using GFP-trap beads. Inputs and immunoprecipitates were analyzed by western-blotting with indicated antibodies. While no significant different was observed with the ETGE-mutant of PLK1, the DFG-mutants showed increased affinity towards HA-KLHL22 compared to wild-type PLK1.

6.3 Results part 3: Identification and characterization of novel components of PLK1/KLHL22 pathway

In parallel to our studies on the regulation of complex formation between PLK1 and KLHL22, we were also interested in understanding the complexity of PLK1/KLHL22 pathway. For this purpose, we aimed at identification of novel interacting components. Having established GST-pulldown strategies between PLK1 and KLHL22 (see part 2.2), we used these samples to identify novel interactors of PLK1. We expressed and purified either GST as a control or GST-PLK1-PBD from bacteria, and incubated them with HeLa cell extracts over-expressing HA-tagged KLHL22 and synchronized in the mitotic stage by addition of Taxol. We confirmed the pulldown efficiency by monitoring the binding of two known substrates of PLK1-PBD, BUBRI and KLHL22 by western-blot (see 6.2.3). Samples were subsequently trypsin digested and analysed on an Orbitrap mass spectrometer. As depicted in **Figure 32**, 441 proteins were identified in the GST sample, compared to 1321 in GST-PLK1-PBD. Among these, 320 proteins were present in both samples, and 1001 proteins were specific of GST-PBD.

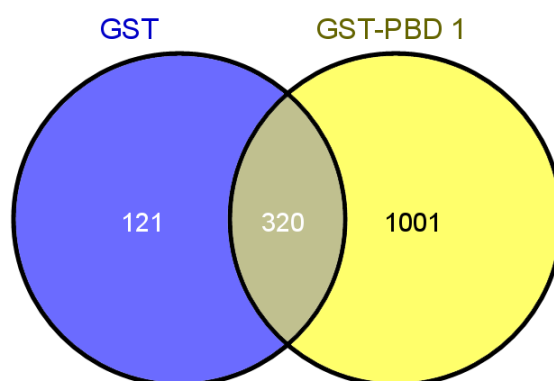


Figure 32. Venn diagram representing specific hits of either GST or GST-PLK1-PBD and their overlap. More than one thousand hits specific of GST-PLK1-PBD were identified.

Performing independent replicates of this experiment gave a high number of confident hits: more than 600 proteins specific of GST-PLK1-PBD were common to all four samples (**Fig. 33 and Appendix 1**). Among them, 108 were identified as cell cycle regulators by DAVID annotation clustering tool, including major known interactors of

PLK1 were present, such as CDC25, WEE1, ROCK2, BUB1, BUBR1, and importantly KLHL22. The complete list is shown in **Annexe I**.

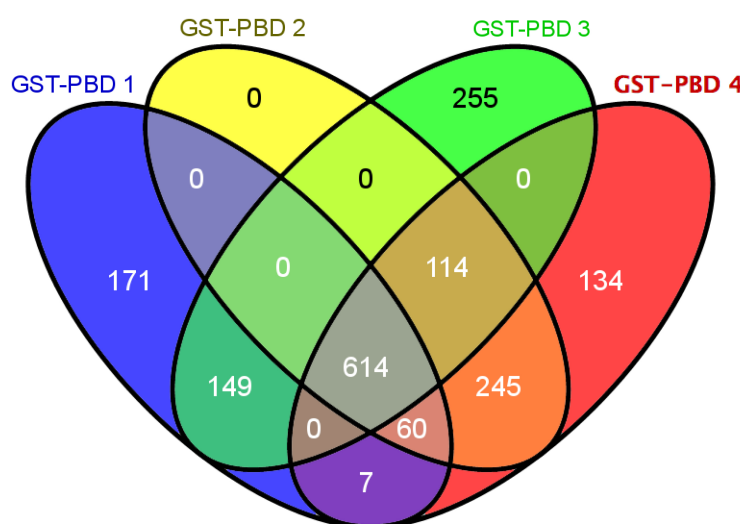


Figure 33. Venn diagram representing the hits found in each of four GST-PLK1-PBD pulldowns. 614 hits were common to all experiments.

Interestingly, comparing our results with already published PLK1-PBD proteome using HeLa cells synchronized in microtubule-depolymerizing drug Nocodazol (Lowery et al., 2007) revealed 140 hits common to both lists, 35% of which were classified as cell cycle regulators by DAVID annotation clustering tool.

In this sense, several proteins that never have been correlated with PLK1 or even mitotic functions were identified in our pulldowns. The protein UBAP2L, also called NICE-4, focused our attention for several reasons. Firstly, its high-scoring position on our mass spectrometry data set (between positions 14 and 16 among >1000 proteins) and its absence in any of our GST control samples (**Appendix I**). Secondly, a UBA domain has been identified on the amino-terminal side of NICE-4, which makes it a good candidate for interacting with PLK1 ubiquitinated by CUL3/KLHL22. Finally, analysing potential new regulators of mitosis by high-throughput siRNA screening in our laboratory, NICE-4 was identified as a potential hit. Indeed, analysis of the end-point phenotype of HeLa cells transfected with Dharmarcon On-Target Plus (OTP) siRNA for NICE-4 showed an increased number of nuclear-shape defects, as well as an increased number of mitotic cells (**Fig. 34**).

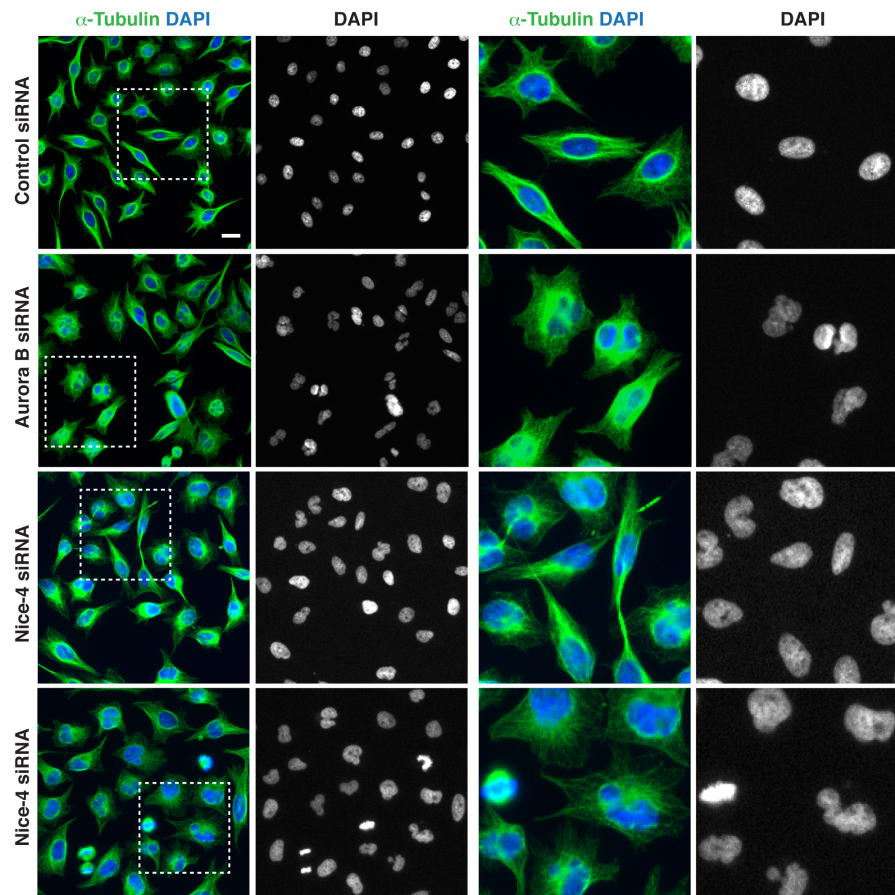


Figure 34. *HeLa cells were transfected with either non-silencing siRNA (control siRNA) or OTP pool of siRNA directed against UBAP2L/NICE-4. NICE-4 depletion leads to an increased number of abnormal nuclei.*

In collaboration with S. Schmucker from our laboratory, we deconvoluted the effect observed with the OTP siRNA pool by transfecting independently the four siRNAs. RT-qPCR confirmed that indeed transfection with all four siRNAs leads to approximately 95% decreased expression of NICE-4 mRNA (**Fig. 35A**) and this down-regulation correlated nicely with the protein levels (**Fig. 35B**).

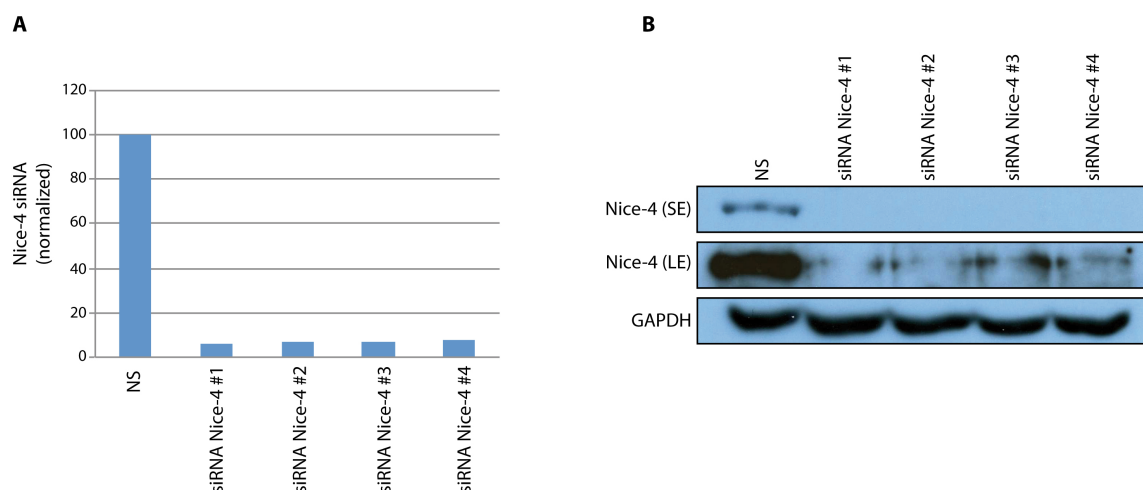


Figure 35. *HeLa cells were transfected with control or individual NICE-4 siRNAs for 48h. cDNAs and protein extracts were prepared and knock-down was analyzed by qPCR (A) and western-blotting (B). All four individual siRNAs induce a 95% decrease of Nice-4 expression. (SE) and (LE) indicate short and long exposure times, respectively.*

We next confirmed the phenotype observed by immune-fluorescence with the OTP siRNA pool by synchronizing cells in mitosis using the double thymidine block and release protocol and simultaneously transfecting them with individual siRNAs. All four siRNAs confirmed a 35 to 40% increase of abnormal nuclei and an increase of number of mitotic cells, compared to the non-silencing control (**Fig. 36**). These results suggest that NICE-4 might be an important factor for faithful completion of mitosis as its depletion lead to strong mitotic defects.

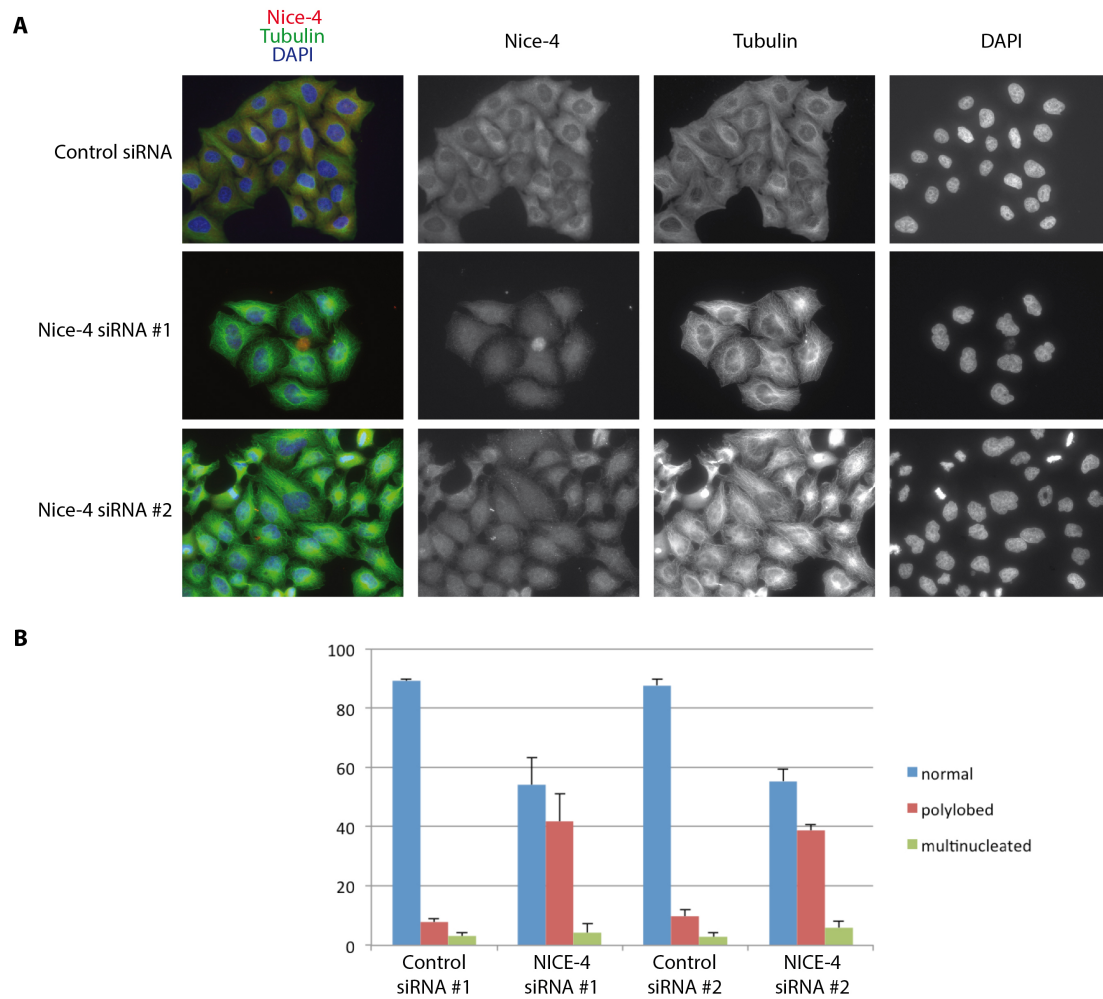


Figure 36. *Nice-4* depletion causes mitotic defects. **A.** *HeLa* cells were synchronized by double-thymidine block and release, and transfected with non-silencing (control siRNA) or individual *NICE-4* siRNA for 48h. Note: *NICE-4* down-regulation leads to an increased number of polylobed nuclei. **B.** The percentage of cells that undergo normal mitosis, become polylobed or multinucleated was quantified ($n=100$). Bars represent the mean of three independent experiments. Error bars indicate \pm s.d.

Because *NICE-4* has only been identified as interacting with *PLK1* by mass spectrometry, we wanted to be able to detect this interaction on the protein level, by western-blotting. To this end, we performed a GST-*PLK1*-PBD pulldown of mitotic *HeLa* cells extract, and immunoblotted with antibodies to *NICE-4*. In contrast to the GST-control sample, we observed a significant enrichment of the protein when pulled-down with GST-*PLK1*-PBD (**Fig. 37**), confirming the results obtained by mass spectrometry.

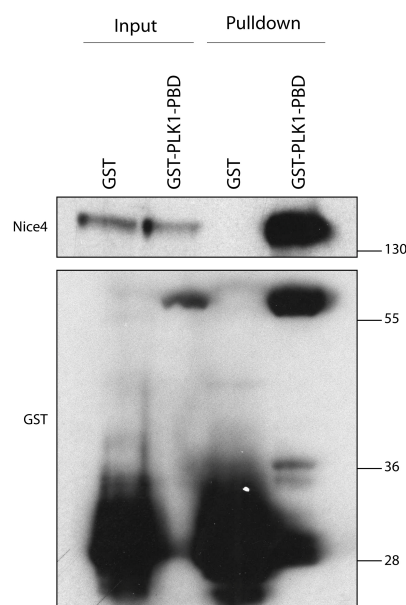


Figure 37. *GST-pulldowns of mitotic HeLa cells were performed using GST and GST-PLK1-PBD. Samples were visualized by Western-blotting against GST and NICE-4. The PBD of PLK1 interacts strongly with NICE-4.*

We are currently trying to reproduce this interaction in mammalian cells, by performing GFP-immuno-precipitation of the full-length GFP-PLK1. Since NICE-4 down-regulation displays a strong phenotype, characterizing its relationship with PLK1 will undoubtedly help us deciphering the molecular mechanisms underlying these defects.

As a second line of investigation of PLK1/KLHL22 pathway, we were also interested in understanding what happens downstream of PLK1 ubiquitination by the E3 ubiquitin-ligase CUL3/KLHL22. Since this phenomenon is very transient, we actually never detected biochemically PLK1 ubiquitinated *in vivo*. We have tried several approaches to enrich for ubiquitinated PLK1, like preventing its deubiquitination by treatment with DUB inhibitor PR-619, or overexpressing the component of the ligase CUL3/KLHL22, but this remained unsuccessful (data not shown). We thereby never could identify the downstream targets of this modified form of the kinase. Is it deubiquitinated by a DUB for subsequent recycling, or is it interacting with a UBP to regulate its function after chromosome congression?

To answer this question we generated a chimeric construct of PLK1, in which the lysine previously identified as ubiquitinated by CUL3/KLHL22 (K492) (Beck et al., 2013) is replaced by the sequence of ubiquitin itself (**Fig. 38A**).

To identify potential interactors of this “ubiquitination mimic” mutant, we cloned the PBD of PLK1 in fusion with ubiquitin sequence in a pGex6P1 for bacterial expression, and used this construct to perform GST-pulldowns from mitotically synchronized HeLa cells, as described previously (see part 6.2.3.1). By comparison with the GST-PLK1-PBD wild-type, we observed that the presence of the ubiquitination mimic does not disturb binding of KLHL22, but the binding of BUBRI is greatly reduced in that case, as expected from our previous findings (Beck et al., 2013) (**Fig. 38B**).

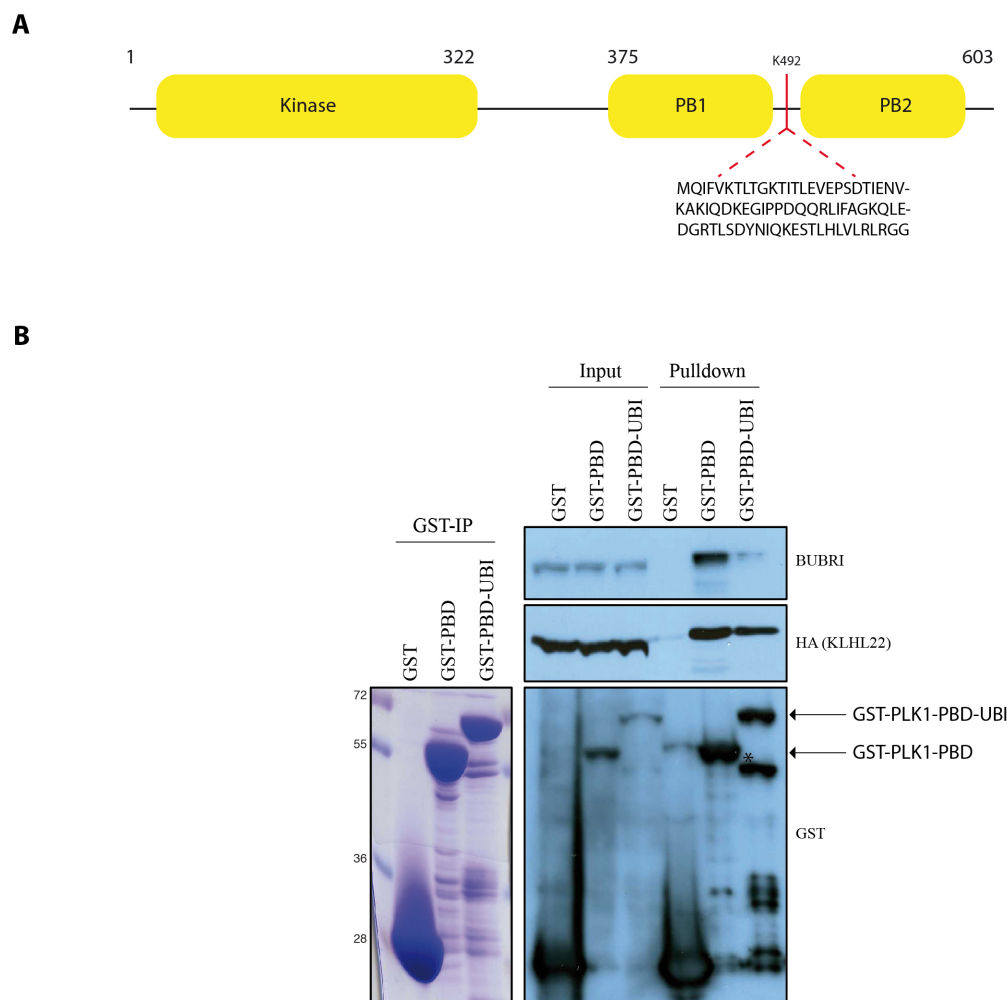


Figure 38. A. Schematic representation of the chimeric construct of PLK1 in which K492 has been substituted by the sequence of Ubiquitin itself. **B.** GST-pulldowns of mitotic HeLa cells were performed using GST and GST-PLK1-PBD and GST-PLK1-PBD-UBI. Samples were

visualized by Coomassie staining (CBB) and Western-blotting against GST, HA and BubR1. No significant difference in KLHL22 binding was observed. In contrast, binding of BubR1 was strikingly reduced with the ubiquitinated mutant of PLK1. (*) indicates the presumable degradation product of GST-PLK1-PBD-UBI.

We subsequently performed mass spectrometry analysis of these samples, to identify proteins interacting differentially between GST-PLK1-PBD wild-type and the ubiquitination mutant. The GST-PLK1-PBD-WT sample contained 1174 interacting proteins (**Fig. 33, red ellipse**), the GST-PLK1-PBD-UBI sample was composed of 601 proteins (**Fig. 39**). When comparing them with the 614 proteins common to all our GST-PLK1-PBD pulldown experiments, 342 were specific to GST-PLK1-PBD-UBI, whereas 116 were common to both GST-PLK1-PBD wild-type and ubiquitinated mutant (**Fig. 39 and Appendix II**).

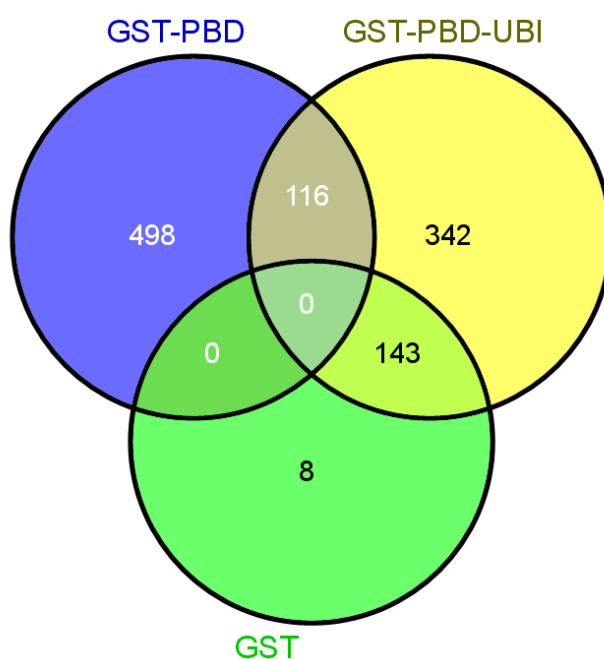


Figure 39. Venn diagram representing the hits found in GST-PLK1-PBD-WT, GST-PLK1-PBD-UBI and in GST as a control. 16 hits were specific of the ubiquitinated form, whereas 115 were shared by both the wild-type PBD and the ubiquitination mimick.

We assume that, to ensure some specificity, the potential DUB and UBP of PLK1-ubiquitinated should to some extent also be able to bind the non-ubiquitinated form of PLK1-PBD domain. We are thereby currently focusing on finding which proteins among

the 115 common hits (**Appendix III**) display a specific binding pattern that would correspond to low binding of GST-PLK1-PBD-WT but very strong binding GST-PLK1-PBD-UBI. Interestingly, NICE-4 interaction with PLK1 appeared greatly reduced in case of the ubiquitination mimic (**Appendix III**), which suggests that NICE-4 might act with PLK1 independently of its ubiquitination by CUL3/KLHL22 or protect PLK1 from ubiquitination by CUL3.

Taken together, these results will allow identification of novel components acting in a PLK1-dependent manner downstream of the CUL3/KLHL22 pathway. It will create a basis for future studies aiming at understanding the molecular mechanisms involved in faithful mitotic progression.

7 Discussion

7.1 A general mechanism for kinase recognition by BTB-Kelch adaptors?

Together with both manuscripts (Beck et al., 2013; Metzger et al., 2013), the results presented here aim at gaining mechanistic insights into CUL3-mediated regulation of protein kinases involved in mitosis. Indeed, previous papers from our lab and others (reviewed in (Metzger et al., 2013) and (Genschik et al., 2013)) identified several protein kinases as targets of CUL3/BTB-Kelch E3-ubiquitin ligases. We thereby hypothesized that there must be a global mechanism of interaction between CUL3-based E3-ubiquitin ligases and their substrates, but that some determinants must exist in order to ensure specificity *in vivo*. We decided to use PLK1 interaction with adaptor protein KLHL22 as a model complex to gain insights into the detailed molecular mechanisms regulating its formation and to subsequently extend our knowledge to other complexes like Aurora A/KLHL18 or Aurora B/KLHL21. This will ultimately help us to decipher if any common mechanism of interaction between kinases and BTB-Kelch adaptors exist.

This idea is however reinforced by the fact that *in vitro* interaction tests between mitotic adaptors KLHL9, KLHL13, KLHL21 and KLHL22 and PLK1 showed that all four BTB-Kelch proteins could reconstitute a complex with the kinase (Beck et al., 2013) (data not shown). However, *in vivo*, KLHL21 depletion did not influence PLK1 functions, in contrast to KLHL22 (Beck et al., 2013), showing that at least a certain degree of specificity must exist.

7.2 Post-translational modifications may not be required for PLK1/KLHL22 interaction

Two major mechanisms have been characterized for substrate recognition by Cullin-RING E3-ubiquitin ligases. The SCF E3-ubiquitin ligase requires previous phosphorylation of the substrate for accurate binding between the two components, but post-translational modifications of substrate do not appear to be involved in case of APC/C recognition, which targets specific motifs within its substrates (A-box, D-box,

KEN-box). In the case of Cullin-3, we first showed that inhibiting the kinase activity of PLK1 does not influence its ability to co-immunoprecipitate KLHL22 (Metzger et al., 2013). We also demonstrated that bacterially expressed PLK1 and KLHL22 were able to interact *in vitro* (Beck et al., 2013; Metzger et al., 2013), which excludes the requirement of the kinase activity of PLK1 as bacterially expressed PLK1 is inactive and the requirement of many other post-translational modifications, which do not occur in bacteria. This however does not exclude that post-translational modification(s) might act *in vivo* to regulate the interaction but only pinpoints to the fact that, in contrast to SCF E3-ubiquitin ligase, they are not absolutely required for both proteins to interact. In this sense, KLHL22 might act similarly to APC/C, by recognizing specific motif(s) within PLK1 to subsequently target the protein for ubiquitination.

7.3 The DLG/DFG-motif could constitute a common recognition site between kinases and BTB-Kelch adaptors

To identify these motifs, we performed series of truncations of PLK1, to map the minimal requirements for its recognition by KLHL22. Interestingly, expression of only the kinase domain or only the PBD of PLK1 was sufficient to mediate interaction with KLHL22 (Metzger et al., 2013). This is consistent with previous data showing a bivalent mode of interaction for CUL3-based E3-ubiquitin ligases. Indeed, in case of CUL3/KEAP1 which regulates transcription factor NRF2, two molecules of CUL3/KEAP1 are brought together via the dimerization interface of the BTB-domain of KEAP1 and subsequently contact only one molecule of NRF2 via their Kelch domains, but on two distinct sites: the ETGE and the DLG motifs. Interestingly, the PBD of PLK1 contains an exact ETGE motif, but site-directed mutagenesis excluded its requirement for KLHL22 recognition. Also, although PLK1 does not contain any DLG motif, it harbours a very similar DFG sequence in its kinase domain. Site-directed mutagenesis showed that DFG to AGE mutations increased affinity of PLK1 towards KLHL22, in contrast to DLG to AGE mutations within NRF2 that abrogates its binding to KEAP1 adaptor protein. This indicates that even if in both cases the DFG/DLG motif is playing a role in the interaction of PLK1/NRF2 with their respective adaptors, the mechanism by which it is acting must be different. Importantly, residues of KEAP1 identified as interacting with NRF2 DLG-

motif (the arginine triad R380, R415 and R483) are not conserved in KLHL22, but another electropositive patch is present at the surface of KLHL22. Indeed, according to our structural model of KLHL22 (**Fig. 10B**), lateral chains of R407, R454, R508 and R556 point towards the surface of the β -propeller and could potentially mediate interactions with the DFG-motif of PLK1.

Interestingly, DFG (or often DLG) motifs are highly conserved among protein kinases, as they are essential regulator of their activities by coordinating the magnesium ion required for transferring the γ -phosphate from ATP to the substrate. In the absence of magnesium, DFG motif adopts an *out* inactive conformation. Mg^{2+} binding induces structural changes where DFG flips-in (DFG-*in* conformation), allowing proper ion coordination and thereby kinase activation. In this sense, altering the DFG motif results in changes in the activation state of the kinase. It was previously shown that mutating the glycine residue of B-RAF to glutamate increased its kinase activity, probably by mimicking the DFG-*in* conformation. It is likely that our DFG to AGE mutant of PLK1 acts in a similar way, over-activating the kinase on kinetochores. The increased binding of KLHL22 to the mutated form of PLK1 is consistent with this notion, as cells could use this mechanism to remove the excess of active PLK1 from kinetochores to allow onset of anaphase. However, changing DFG to oppositely-charged AGE enhances KLHL22 binding, hence it is likely that KLHL22 does not interact specifically with these amino-acids, otherwise mutating them should lead to a decreased interaction. It is more probable that KLHL22 recognizes the active DFG-*in* conformation induced by these changes. To test this hypothesis, we are currently mutating the DFG-motif of PLK1 to VFG. This mutation was previously characterized in B-RAF kinase as forcing an inactive DFG-*out* conformation. We thereby expect a decreased affinity of KLHL22 towards this inactive PLK1. Moreover, we are also monitoring the localization of these mutated forms by immunofluorescence, to confirm that DFG-*in* conformation leads to decrease in PLK1 localization on kinetochore, most probably because of its strong interaction with KLHL22. In addition, we are also using a novel, type II PLK1 inhibitor called SBE13, that selectively blocks the kinase activity by freezing it in a DFG-*out* conformation (Keppner et al., 2010, 2011), allowing us to monitor its effect on endogenous localization and interaction with KLHL22. In summary, the DFG/DLG-motif present within every kinase could be part of the common mechanism of interaction between protein and CUL3/BTB-Kelch E3-ubiquitin ligases.

7.4 The PBD-mediated interaction of PLK1 with KLHL22 might ensure specificity of this complex

In addition to the kinase domain, PLK1-PBD appeared sufficient for mediating interaction with KLHL22 (Metzger et al., 2013). The PBD being only present in the PLK-family of protein kinases, it may provide essential determinants for ensuring specificity of PLK1 towards KLHL22. Mutations in its phosphopeptide binding module (H538A and K540M) did not influence KLHL22 affinity (**Fig. 29A**), reinforcing the hypothesis that phosphorylation of the adaptor protein may not be involved in the interaction. Interestingly, mutating W414 to phenylalanine (W414F) within PLK1-PBD was sufficient to almost completely abolish KLHL22 binding (**Fig. 29B**). However, this mutation was also decreasing BUBRI affinity, and has previously been characterized to disrupt the ability of PLK1-PBD to bind its target proteins (García-Alvarez et al., 2007; Lee et al., 1998), probably by increasing internal flexibility and thereby by changing structural orientation of PLK1-PBD (Kamaraj et al., 2013). Thus, the W414F mutant of PLK1-PBD constitutes an interesting non-binding control for *in vitro* interaction studies, but the physiological relevance of this mutation has to be considered with caution.

7.5 The D-box of PLK1 does not appear to be involved in KLHL22 binding

Following our strategy to narrow down the potential interaction interfaces observed in both the kinase domain and the PBD we generated shorter constructs (the N-lobe or the C-lobe of the kinase domain, the first or the second polo-box). Unfortunately, due to the poor solubility of these truncated forms, we never could test their affinities towards KLHL22 (summarized in **Table 1**). Protein solubility was also an issue for confirming two of the three regions identified by peptide array experiments. Indeed, both the kinase domain depleted of the C21-C23 peptides and the PBD lacking the F1-F3 region were insoluble, preventing us from testing their respective interaction with KLHL22. We are currently performing site-directed mutagenesis of residues located within these motifs, but so far none of the mutations tested (**Fig. 29B**) exhibit any significant difference in

KLHL22-binding compared to the wild type form. The third region identified in peptide array (peptides D12-D13) contains PLK1 D-box. D-boxes correspond to RxxL motifs (where x represents any amino-acid) essential for protein recognition by APC/C^{Cdh1} E3-ubiquitin ligase and subsequent degradation. Interestingly, the involvement of this site for KLHL22 recognition could explain why so many substrates of APC/C are also substrates of CUL3. However, following combination of truncation mutants and site-directed mutagenesis, we concluded that this site was not a putative recognition motif involved in PLK1 interaction with KLHL22. Indeed, a truncated form of the PBD lacking the D-box region was still able to bind KLHL22 *in vitro* (**Fig. 12B**). Even if this binding could be explained by the presence of the F1-F3 region in this construct, we however expected at least a decreased affinity compared to wild-type PBD. Moreover, a GST-fusion of this D12-D13 peptide was not able to co-purify KLHL22 *in vitro* (**Fig. 12A**) and mutations of the D-box known to prevent PLK1 degradation by APC/C^{Cdh1} did not show any differential affinity towards KLHL22 compared to the wild type (**Fig. 13**), suggesting that PLK1 D-box is probably not involved in KLHL22 binding. The same observations were previously made in the lab, where mutations of Aurora B in its APC/C recognition sites (D-box, A-Box, Ken-Box) did not influence KLHL21 binding (Beck J., personal communication)

It is important to mention that in our hands PLK1-D-box mutations also did not influence the binding of Cdh1 (data not shown). It is thereby likely that the D-box motif, even if essential for degradation of the kinase, is not the main recognition site for APC/C^{Cdh1}, which might use another, yet unidentified motif to contact PLK1.

In summary, our peptide array strategy identified three potential binding sites of KLHL22 within PLK1, but so far none of them could be confirmed as a putative interacting motif, putting into questions the reliability of such an array. Indeed, if KLHL22 recognition were to depend on the tertiary structure of PLK1, peptide array technology would not provide any answer, as only 15-mer peptides of PLK1, probably lacking structural organization, are spotted on the membrane. Also, peptide arrays only provide limited semi-quantitative results, allowing to distinguish between weak, medium and strong binding efficiencies. Indeed, the quantity of spotted peptides is highly dependent on their overall purity, which is a reflection of successful synthesis based on their amino-acid sequences. A probably good indication is that the quantity of peptide per spot is approximately 5pmol, and the overall purity of 15-mer peptide

synthesis is averaging 75%. Last but not least, we could not confirm the positive hits obtained using recombinant KLHL22 with a preparation obtained from mammalian cells. We tried to monitor the binding of both endogenous and over-expressed HA-KLHL22 produced in HeLa cells, but no signal could be detected, which could be due to two major limitations: firstly, KLHL22 affinity towards 5pmol 15-mer peptides of PLK1 could be below threshold of detection by immuno-blot, which is quite unlikely as our antibodies gave strong signals in immuno-precipitation experiments. Secondly, the behaviour of KLHL22 itself could be highly dependent on the expression system used. In this case two options are to consider: either KLHL22 solubility is highly decreased in mammalian system, hence no interaction with PLK1 peptides using HeLa extracts, or KLHL22 purification from bacteria is of poor quality, and the results obtained in our peptide array experiments are actually false-positives. This last option appears to be the most likely one as none of the hits identified using bacterially expressed KLHL22 could be confirmed by other methods. Also, when subsequently loading bacterial KLHL22 on size-exclusion chromatography, we observed that it was behaving as a soluble aggregate (**Fig. 18-19**). This constituted a major bottleneck for interaction studies, as aggregated proteins do not display physiological biochemical properties, and thereby may question not only the results obtained from peptide array experiments, but also the rest of our data using bacterially-expressed KLHL22.

7.6 Poor protein stability prevented structural studies

Undoubtedly, the aggregated state of KLHL22 also prevented us from pursuing our *in vitro* complex reconstitution for crystallographic studies. So far structures of the kinase and the PBD of PLK1 have only been obtained independently, probably because of the high flexibility between these two domains. We were hoping that the bivalent mode of interaction of KLHL22, that can contact both domains, would decrease intra-molecular movements of PLK1, allowing efficient complex purification and subsequent crystallization assays. Ultimately, this would have allowed us not only to study the molecular mechanisms of PLK1/KLHL22 interaction but also to obtain the first full-length structure of PLK1. Even when we could reconstitute a complex between PLK1 and KLHL22 using co-expression strategy (**Fig. 15**), the quantities obtained were too low to fulfil crystallization requirements. We thereby opted for independent production

and purification of PLK1 and KLHL22, followed by *in vitro* complex reconstitution and its subsequent isolation. However, despite promising PLK1 purification, we observed a strong aggregated state of KLHL22. Buffer optimization by changing salt or detergent concentrations, as well as pH variations had no influence on KLHL22 solubility. As a consequence, we decided to abort our cristallisation studies on PLK1/KLHL22 complex. Thus, we obtained our current model of PLK1 recognition by adaptor protein KLHL22 (**Fig. 40**) using hypothesis-driven approaches (see part 6.2.3).

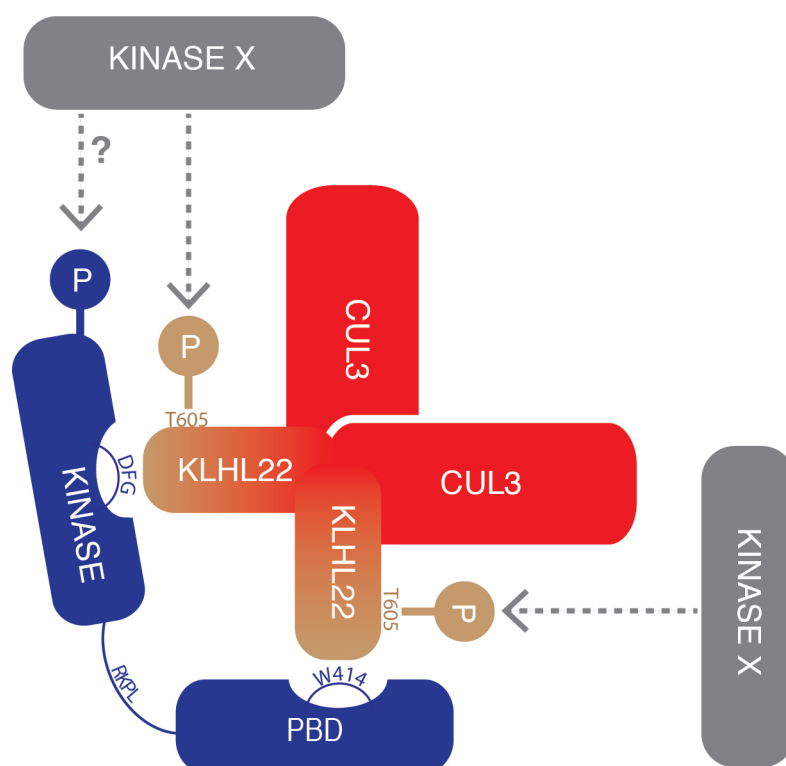


Figure 40. Hypothetical model of the architecture of CUL3/KLHL22 in a complex with PLK1. A CUL3/KLHL22 dimer contacts one molecule of PLK1 on two distinct sites. The DFG motif within its kinase domain and the tryptophan W414 within its PBD appears to be involved in the interaction. PLK1 kinase activity and PLK1-D-box motif (RKLP) do not appear to be essential for its recognition by CUL3/KLHL22. Phosphorylation of KLHL22 on its threonine T605 by an upstream kinase might be important for its interaction with PLK1. Future studies are needed to validate this model.

We subsequently focused on Aurora B/KLHL21 complex. Indeed, if a common mechanism of regulation of kinases by BTB-Kelch adaptors exists, Aurora B association with KLHL21 could help us identifying it. The purification of GST-KLHL21 appeared more promising. The protein was highly expressed in *E. coli* and not aggregating as shown on the size-exclusion chromatogram (**Fig. 20-21**). However, a certain degree of oligomerization was still present, which could be due to the combined ability of GST and BTB-domains to dimerize. We thereby expressed and purified only the Kelch domain of KLHL21, and this construct appeared stable and monomeric (**Fig. 23**). The purification of Aurora B was more challenging, as only a small fraction of a shortened construct of the kinase was soluble and monomeric (**Fig. 24**). Even if a complex could be reconstituted *in vitro* by mixing this monomeric Aurora B with our KLHL21-Kelch preparation (**Fig. 25**), this result has to be considered with caution given the poor state of Aurora B purification. More compelling are the results obtained when using Aurora B in fusion with a fragment of INCENP. This construct was indeed previously shown as well-behaved, soluble and active (Elkins et al., 2012; Sessa et al., 2005). Unfortunately, by co-expressing or co-lysing it with our KLHL21-Kelch construct, no complex could be recovered (**Fig. 26-27**). Several hypothesis can be made: perhaps Aurora B/INCENP construct, since arising from *Xenopus laevis*, lacks essential amino-acids that mediate interactions with human KLHL21 despite the 80% identity between their kinase domains. In this sense also the *Xenopus laevis* Aurora B/INCENP construct lacks the first 60 amino-acids of the kinase. This removal is essential to make the protein soluble, but could be deleterious for the interaction with KLHL21. Indeed, this region contains both the A-box and the D-box of Aurora B, which was previously shown in human cells to mediate its faithful ubiquitination and subsequent degradation by APC/C^{Cdh1}. Another hypothesis could be that INCENP inhibits binding of KLHL21 to Aurora B, either by inducing conformational changes within the kinase that would prevent its recognition by KLHL21, or by competing for the same residues as KLHL21 for binding to Aurora B. However, we could observe that GST-KLHL21-Kelch was sufficient to pulldown both Aurora B and INCENP from HeLa cell extracts (**Fig. 28**), which suggests that a heterotrimeric complex made of KLHL21, Aurora B and INCENP could co-exist *in vitro*. It is also possible that we are missing a co-adjuvant to the reaction that would be essential for KLHL21 binding. This could be a post-translational modification of any of the components of the complex, or simply another, yet unidentified protein that would be

required for mediating proper interactions. Interestingly, previous unpublished data obtained in the lab shows that phosphorylation of Aurora B is not involved in KLH21 binding (Beck J., personal communication), and mass spectrometry experiments revealed that neither Survivin, nor Borealin, both components of the CPC, were pulled-down from HeLa cells using our GST-KLHL21-Kelch construct (data not shown).

In summary, our work on Aurora B/KLHL21 interaction did not lead to any significant conclusion, as no convincing complex could be so far reconstituted between the two proteins. Given that Aurora B acts in a complex with other members of the CPC *in vivo*, this increases complexity of the interaction, as we currently do not know to which extend each subunit of the CPC contributes to KLHL21 binding. The fact that Aurora B/INCENP does not interact *in vitro* with KLHL21 and that Aurora B alone displays very poor solubility brings huge limitations to our studies. For future studies, it would be perhaps interesting to focus on another pair of kinase/BTB-Kelch, especially Aurora A/KLHL18, as the kinase has already been shown to be soluble on its own when produced in insect cells (Cheetham et al., 2002). In this sense also, expression of all the previously tested complexes could be monitored in other systems, including insect and mammalian cells, as they contain specific chaperones and allow post-translational modifications, both of which can highly influence protein solubility and complex formation.

7.7 The PLK1-PBD shows mitosis-specific interactions with proteins involved in cell cycle regulation

In parallel to our studies on the regulation of complex formation between protein kinases and BTB-Kelch adaptor proteins, we were interested in understanding what are the other components of the PLK1/KLHL22 pathway, and how its regulation occurs *in vivo*. For this purpose we performed GST-pulldowns from our GST-PLK1-PBD construct using HeLa cell over-expressing HA-KLHL22 and synchronized in mitosis using Taxol. GST-PLK1-PBD enriched for 1321 proteins and 1001 of them were specific to this construct since 320 were overlapping with our GST-alone control (**Fig. 32**). Performing independent replicates narrowed down 614 proteins specific to GST-PLK1-PBD, among which 108 were classified as cell cycle regulators by DAVID annotation clustering

algorithm (**Fig. 33 and Appendix 1**). This included proteins previously demonstrated to associate with PLK1, such as CDC20, CDC25, WEE1, BUB1, BUBR1, ROCK2, KLHL22, members of the Mini-Chromosome Maintenance complex, Septins,... Some expected proteins (like Anillin or PRC1) were however absent from our list, which could be explained in several ways: firstly, all proteins present in both the GST-alone control and GST-PLK1-PBD sample were excluded, with no regards towards the number of peptides identified in each condition. This is for instance the case of Anillin, a well-established substrate of PLK1 (D'Avino, 2009; Straight et al., 2005). Even if 27 peptides were scored in the GST-PLK1-PBD sample, 2 peptides identified in the GST-control were sufficient to exclude it from our list. Secondly, the lack of the kinase domain in our GST-PLK1-PBD construct might prevent the binding of certain substrates, and lastly, the Taxol synchronization blocks cells in metaphase-like state without functional spindle, thereby several late interactors of PLK1 might be missing, like for instance PRC1, which is essential for translocation of PLK1 from kinetochores to the spindle midzone after anaphase onset (Hu et al., 2012).

To understand what happens downstream of PLK1 ubiquitination, we generated a PLK1-PBD-K492-ubiquitination mimic mutant, by replacing this specific lysine by the sequence of ubiquitin itself and performed pulldown experiments. Mass spectrometry analyses allowed identification of 601 proteins in the GST-PLK1-PBD-UBI sample, among which 143 were also present in the GST sample. 342 were specific of this construct and 116 were found in both the GST-PLK1-PBD-WT and the ubiquitinated mutant (**Fig. 39 and Appendix 2-3**). We could observe that the affinity of KLHL22 towards this ubiquitinated form of PLK1-PBD was not significantly affected, whereas BUBR1 binding was greatly reduced (**Fig. 38B**), consistent with our previous data suggesting that K492-ubiquitination inhibits PBD-mediated phospho-interactions of PLK1 at kinetochores (Beck et al., 2013).

7.8 NICE-4 interacts with PLK1-PBD and is involved in faithful mitotic regulation

Our hits from GST-PLK1-PBD pulldowns allowed identification of several proteins that were never linked to PLK1 pathway or even with mitotic functions. Among them, NICE-4

(also called UBAP2L), is a UBA-domain containing protein and was detected with high confidence. Interestingly, we previously identified this protein as a potential mitotic regulator using high-throughput siRNA screening since its down-regulation in HeLa cells caused very severe mitotic defects. We indeed observed an increased number of abnormal nuclear-shape cells, which could be consistent with chromosome segregation defects downstream of PLK1/KLHL22 pathway (**Fig. 34**). We confirmed this phenotype using different siRNAs (**Fig. 35-36**) and subsequently monitored the presence of NICE-4 in PLK1-PBD pulldowns by western-blot. Surprisingly for a UBA-domain containing protein, pulldown performed using our chimeric construct of GST-PLK1-PBD-UBI indicates a significant decrease of NICE-4 affinity towards the ubiquitinated PLK1 compared to GST-PLK1-PBD sample, with a PSM differential of -41 (**Appendix 3**). This could indicate that ubiquitination of PLK1 actually inhibits binding of NICE-4, which in this sense is likely to interact with the kinase independently of its UBA-domain. On the other hand, we do not know how our chimeric GST-PLK1-PBD-UBI mutant is behaving compared to endogenously ubiquitinated full-length PLK1 and the fact that our mutant binds less to NICE-4 actually emphasizes the importance of the region surrounding K492 of PLK1 for the interaction with NICE-4. We are currently trying to understand what causes the end-point phenotypes observed upon NICE-4 depletion and preliminary data obtained by S. Schmucker showed an increased number of lagging chromosomes in anaphase in these down-regulated cells (**Fig. 41**). Also, we are trying to confirm the interaction between PLK1-PBD or full-length and NICE-4 using mammalian cells and analyse the localization of PLK1 upon depletion of NICE-4. Indeed, if there is no doubt that NICE-4 down-regulation displays strong phenotype, characterizing its relationship with PLK1 will undoubtedly help us deciphering the molecular mechanisms underlying these defects.

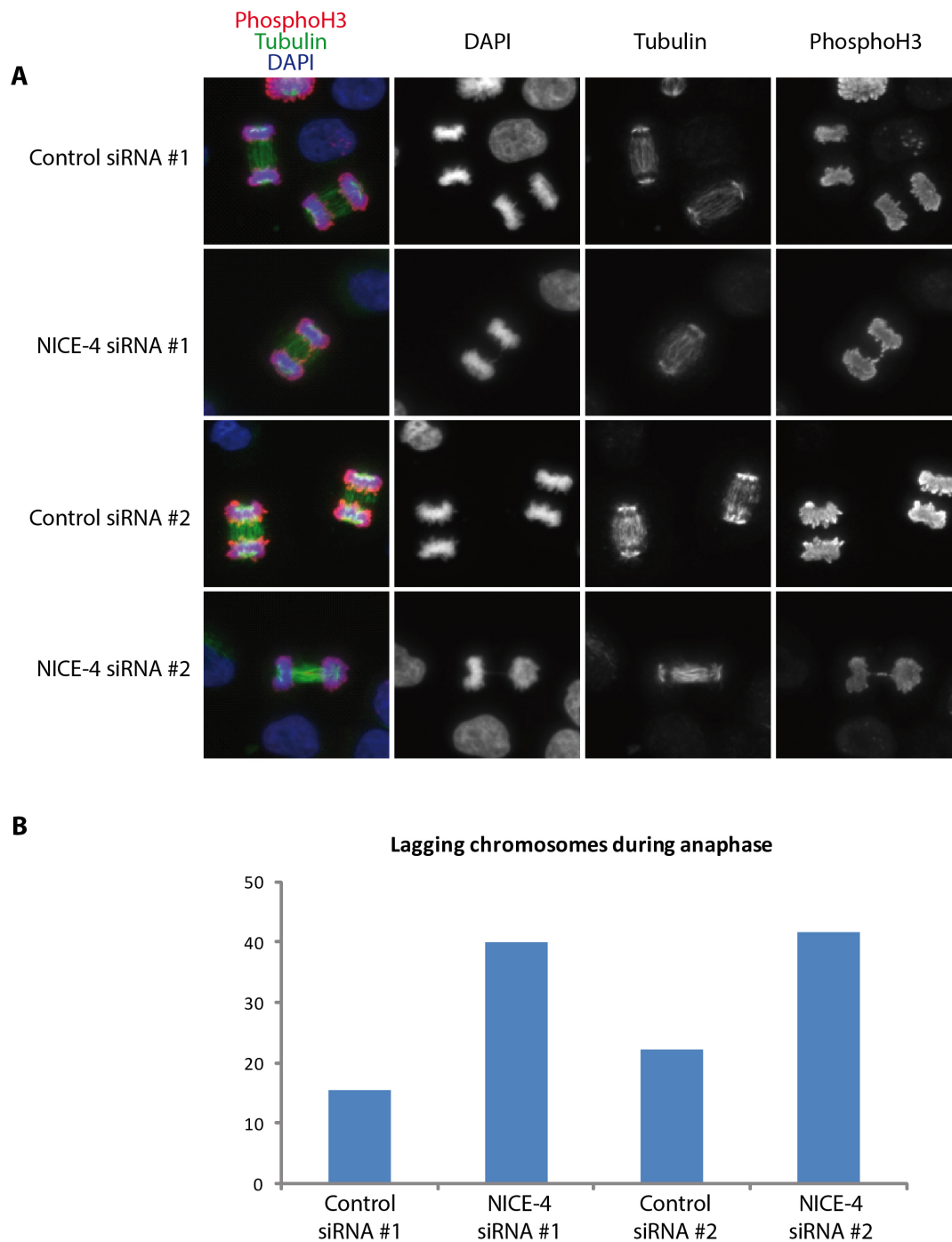


Figure 41. *Nice-4* depletion causes lagging chromosomes during anaphase. **A.** HeLa cells were synchronized by double-thymidine block and release, and transfected with non-silencing (control siRNA) or individual *NICE-4* siRNA for 48h. Note: *NICE-4* down-regulation leads to an increased number of lagging chromosomes in anaphase. **B.** The percentage of cells displaying lagging chromosomes in anaphase was quantified ($n=24$). So far, the experiment was only performed once, hence the lack of standard deviation.

8 Materials and methods

Expression vectors

The full-length KLHL22 was cloned into pMal-C2X (New England Biolabs) as described previously (Metzger et al., 2013). The GST-fusions were all cloned in pGex-6P1 (GE Healthcare) using EcoRI/XhoI restriction sites except the GST-PLK1-PBD-UBI construct that required EcoRI/NotI. Untagged proteins were expressed in pncS vector (kind gift from C. Romier, IGBMC, Strasbourg, France) and in pACYC-Duet (Novagen). KLHL18 cDNA was obtained from DNASU plasmid repository (HsCD00082252). peYFP-PLK1-WT and D-box mutant were kindly provided by Jonathon Pines (Gurdon Institute, Cambridge, United Kingdom) and pGex-Aurora B⁶⁰⁻³⁶¹-K122R-INCENP⁷⁹⁰⁻⁸⁵⁶ by A. Musacchio (MPI Dortmund, Germany). The 5'-3' sequence of all primers used for cloning is presented at the end of this section.

Mutagenesis

Point mutations were generated using the QuickChange site-directed mutagenesis protocol (Stratagene) with Phusion DNA polymerase (New England Biolabs). The list of all primers used is presented at the end of this section.

siRNA and qPCR primers

The following siRNAs were used: Control siRNA #1: siGENOME (Dharmacon) non-targeting pool #1; Control siRNA #2: siGENOME (Dharmacon) individual #2: 5'-UAAGGCUAUGAAGAGAUAC-3'; NICE-4 #1: 5'-CAACACAGCAGCACGUUAU-3'; NICE-4 #2: 5'-GUGUGGAGAGUGAGGCGAA-3'; NICE-4 #3: 5'-CAACAGAACCAGACGCAGA-3'; NICE-4 #4: 5'-CCUGGGAGAUGGUCGGGAA-3'. For NICE-4 OTP pool, all four individual siRNA were equimolarly mixed. Transfections were performed using Oligofectamine (Invitrogen) at a final concentration of 100nM siRNA. qPCR was performed using two distinct pairs of primers: 5'-GATTGGATGGCACCAAGAGT-3' with 5'-AAAGTGGCCAGTGTGTTCC-3' and 5'-TGTGTCTTCAGTGCCTCTGC-3' with 5'-TGATATGGCAGTCTGCTTCG-3'.

Recombinant protein expression

Protein expression were performed as previously described (Metzger et al., 2013). Cleavage of the GST purification tag was performed on beads using PreScission protease (GE Healthcare) over-night at 4°C. The flow-through was recovered and concentrated as previously described (Metzger et al., 2013).

Peptide array

The 15-mer peptides of PLK1 (Intavis) were first blocked in 5% milk-TBS-T for 2 h, and subsequently incubated for 3 h with recombinant protein diluted in milk-TBS-T at 1µg/mL in a final volume of 2mL. After extensive washing, primary antibodies diluted in milk-TBS-T were incubated over-night at 4°C. Following washing steps, secondary antibodies were incubated for 2h and standard Enhanced ChemiLuminescence (ECL) protocol was used for detecting interactions.

GST-pulldown and mass spectrometry analyses

Protein expression was performed as previously described (Metzger et al., 2013). When several GST-fusions were used, equal amounts of recombinant protein were determined empirically by normalizing expression to the OD₆₀₀. Bacterial lysis was performed by sonication in purification buffer (300mM NaCl / 10mM Tris pH 8 / 5% glycerol). After incubation with 50µL GSH-beads (GE-Healthcare), the excess was removed by extensive washing, and beads were subsequently washed two times in extraction buffer (100mM NaCl / 20mM Tris pH 7.5 / 20mM β-glycerophosphate / 5mM MgCl₂ / 1mM NaF / 1mM DTT / 0,2% NP-40 / 10% glycerol) supplemented with 3% BSA. During BSA-block, HeLa cell lysates were prepared by sonicating cultures previously resuspended in extraction buffer. Lysates were then incubated with GSH-beads for 2 hours at 4°, extensively washed, and the GST-fusion were eluted in 150µL of purification buffer supplemented with 20mM glutathione. Samples were either supplemented with 75µL of 2x sample-buffer for western-blot analysis, or shock-frozen in liquid nitrogen for mass spectrometry analysis. IGBMC's proteomic platform subsequently digested samples using LysC and Trypsin, and after desalting, proteins were analysed using Orbitrap Elite mass spectrometer.

Cell culture, transfections and synchronization

HeLa Kyoto were cultured as previously described (Sumara et al., 2007) and transfected using Lipofectamine 2000 (Invitrogen). For a 80% confluent 10cm culture plate 7500ng of DNA and 15 μ L of Lipofectamine 2000 were each incubated in 500 μ L Opti-MEM. After 5 minutes, both were mixed and incubated for 20 minutes. The 1mL DNA-Lipofectamine complex was added to cells in a final volume of 9 mL fresh media. For mitotic synchronization, cells were treated with 200nM Taxol (Paclitaxel) (Sigma) for 13 h before harvesting.

Western blotting, immunoprecipitation and antibodies

Preparation of HeLa cells extracts, immunoprecipitation and western blotting were described previously (Beck et al., 2013). The following antibodies were used in this study: rabbit polyclonal KLHL22 (Beck et al., 2013), rabbit polyclonal GFP (Abcam ab290, 1:2000), mouse monoclonal BUBRI (BD Bioscience 612501, 1:1000), rat monoclonal HA (Roche 11867423001, 1:1000), mouse monoclonal Aurora B (BD Bioscience 611083, 1:1000), rabbit polyclonal INCENP (Sigma I5283, 1:1000), rabbit polyclonal NICE-4 (Bethyl Laboratories A300-534A 1:2000), mouse monoclonal MBP-HRP-conjugated (New England Biolabs E8038, 1:1000), mouse monoclonal CDH1 (Abcam ab3242, 1:1000), mouse monoclonal PLK1 (Santa Cruz sc-17783, 1:250), rabbit polyclonal H3-pSer10 (Millipore 06-570, 1:500) and mouse monoclonal GST was generated in house (15TF2-1D10, 1:2000).

Primers for cloning

Listed here are the primers used for generating all the constructs used in this study. All primers were synthesized by Sigma at 0,025 μ mol scale, purification desalted, with no additional modification. ID indicates internal Sumara group identifier.

Gene	ID	Name	Extra base	Restriction site	Restriction Seq	Frame	Annealing	Destination vector	Name Sigma	FL sequence
PLK1	1	N53	GCG	EcoRI	GAATTC		ATGTATGTGCGGGGC C	pGEX	(B) PLK1 N53 EcoRI	GCGGAATTCATGTATGTGCGGGGCC
	2	C305	CGC	XhoI	CTCGAG		TTAAAAGAACTCGTCA TTAAGCAGC	pGex	(B) PLK1 C305 XhoI	CGCCTCGAGTTAAAAGAACTCGTCATTAAGCAGC
	3	C479	CGC	XhoI	CTCGAG		TTAAAGGAGGGTGAT CTTCTTCAT	pGex	(B) PLK1 C479 XhoI	CGCCTCGAGTTAAAGGAGGGTGATCTTCTTCAT
	4	N-term	GGAT ATC	NdeI	CATATG		AGTGCTGCAGTGA CTGC	pnEA-TH	PLK1 N-term	GGATATCCATATGAGTGCTGCAGTGA CTGC
	5	C-term	CGC	BamHI	GGATCC		TTAGGAGGCCTTGAG ACGGTT	pnEA-TH	PLK1 C-term	CGCGGATCCTTAGGAGGCCTTGAGACGGTT
	6	Kin C-ter	CGC	BamHI	GGATCC		TTAAGCAATCGAAAAC CTTGGTGG	pnEA-TH	PLK1 NM1C	CGCGGATCCTTAAGCAATCGAAAACCTTGGTGG
	7	PBD N-ter	GGAT ATC	NdeI	CATATG		CCACCAAGGTTTTTCA TTGCT	pnEA-TH	PLK1 M1NC	GGATATCCATATGCCACCAAGGTTTTTCGATTGCT
	8	N-term	CCG	XhoI	CTCGAG		ATGAGTGCTGCAGTG ACTGC	peGFP	(M) PLK1 N-term	CCGCTCGAGATGAGTGCTGCAGTGACTGC
	9	C-term	CGG	KpnI	GGTACC		GGAGGCCTTGAGACG GTTG	pEGFP	(M) PLK1 -term	CGGGGTACCGGAGGCCTTGAGACGGTTG
	10	Kin 3'	CGC	KpnI	GGTACC		CCAGCAATCGAAAACC TTGGTG	peGFP	(M) PLK1 Kin 3' KpnI	CCGCGGTACCCAGCAATCGAAAACCTTGGTG
	11	N24	GCG	EcoRI	GAATTC		GGAGTTGCAGCTCCC G	pGEX	(B) PLK1 5' aa24 EcoRI	GCGGAATTCGGAGTTGCAGCTCCCG
	12	C374	CGC	XhoI	CTCGAG		GAGGTGGCAGTCGAC C	pGEX	(B) PLK1 Flex 3' XhoI C374	CGCCTCGAGGAGGTGGCAGTCGACC
	13	Kin1 C-ter	CGC	XhoI	CTCGAG		GCGGCAGAGCTCCA	pGEX	(B) PLK1 Kinase 1 3' XhoI	CGCCTCGAGGCGGCAGAGCTCCA
	14	Kin 2 Nter	GCG	EcoRI	GAATTC		CGGAGGTCTCTCTGG	pGEX	(B) PLK1 Kinase 2 5' EcoRI	GCGGAATTCGGAGGTCTCTCTGG

	15	Kin2 Cter	CGC	XhoI	CTCGAG		AATGGTCAGGCAGGT GAT	pGEX	(B)PLK1 Kinase 2 3' XhoI	CGCCTCGAGAATGGTCAGGCAGGTGAT
	16	Polo1 Nter	GCG	EcoRI	GAATTC		CCACCAAGGTTTTCGA TTG	pGEX	(B) PLK1 Polo 1 5' EcoRI	GCGGAATTCACCAAGGTTTTCGATTG
	17	Polo1 Cter	CGC	XhoI	CTCGAG		GGCGAGCTCATCACCT	pGEX	(B) PLK1 Polo 1 3' XhoI	CGCCTCGAGGGCGAGCTCATCACCT
	18	Polo 2 Nter	GCG	EcoRI	GAATTC		CGGCTGCCCTACCTAC	pGEX	(B) PLK1 Polo 2 5' EcoRI	GCGGAATTCGGCTGCCCTACCTAC
	19	C272	CGC	XhoI	CTCGAG		TACTTGGGAATACTG TATTCATTCTTC	pGEX	(B) PLK1 Kinase C- 272 XhoI 3'	CGCCTCGAGTTACTTGGGAATACTGTATTCATTCTTC
	20	N375	GCG	EcoRI	GAATTC		AGTGACATGCTGCAG CAG	pGEX	(B) PLK1 PBD N- 375 EcoRI 5'	GCGGAATTCAGTGACATGCTGCAGCAG
	21	N-term	GCG	EcoRI	GAATTC		AGTGCTGCAGTGACT GCAGG	pGEX	(B) PLK1 5' EcoRI pGex6P	GCGGAATTCAGTGCTGCAGTGACTGCAGG
	22	C-term	CGC	XhoI	CTCGAG		TTAGGAGGCCTTGAG ACGG	pGEX	(B) PLK1 3' XhoI pGex6P	CGCCTCGAGTTAGGAGGCCTTGAGACGGT
KLHL 22	1	N50	GCG	EcoRI	GAATTC		ATGTTTCGATGTTGTG TGGT	pGex	(B) KLHL22 N50 EcoRI	GCGGAATTTTCATGTTTCGATGTTGTGCTGGT
	2	C150	CGC	XhoI	CTCGAG		TACTCTTCGTCCACCC AGG	pGex	(B) KLHL22 C150 XhoI	CGCCTCGAGTTACTCTTCGTCCACCCAGG
	3	N151	GCG	EcoRI	GAATTC		ATGAACATTCTCGATG TCTACCG	pGex	(B) KLHL22 N151 EcoRI	GCGGAATTCATGAACATTCTCGATGTCTACCG
	4	C297	CGC	XhoI	CTCGAG		TTAGAAGTCCGACCGC AG	pGex	(B) KLHL22 C297	CGCCTCGAGTTAGAAGTCCGACCGCAG
	5	N298	GCG	EcoRI	GAATTC		ATGCAGTGC GTTG GGC	pGex	(B) KLHL22 N298 EcoRI	GCGGAATTCATGCAGTGC GTTG TGGGC
	6	C591	CGC	XhoI	CTCGAG		TTAGAGCACACAGGC CGC	pGex	(B) KLHL22 C591 XhoI	CGCCTCGAGTTAGAGCACACAGGCCGC
	7	Nterm	GGAT ATC	NdeI	CATATG		GCAGAGGAGCAGGAG TTC	pnEA-tH	KLHL22 N-term	GGATATCCATATGGCAGAGGAGCAGGAGTTC
	8	Cterm	CGC	BamHI	GGATCC		CTAGTCCTCACTGGAG TTGTC	pnEA-tH	KLHL22 C-term	CGCGGATCCCTAGTCCTCACTGGAGTTGTC
	9	NM1C	CGC	BamHI	GGATCC		TTATGGCCACTGTGTC CCTCAAA	pnEA-tH	(B) KLHL22 NM1C	CGCGGATCCTTATGGCCACTGTGTCCCTCAAA
	10	M1NC	GGAT	NdeI	CATATG		TTGAGGGACACAGTG	pnEA-tH	(B)KLHL22 M1NC	GGATATCCATATGTTGAGGGACACAGTGGCCA

			ATC				GCCA			
	11	N-ter	GCG	EcoRI	GAATTC		GCAGAGGAGCAGGAG TTC	pGex	(B) KLHL22 pGex6P EcoRI 5'	GCGGAATTCGCAGAGGAGCAGGAGTTC
	12	C-term	CGC	XhoI	CTCGAG		CTAGTCCTCACTGGAG TTGTC	pGex	(B) KLHL22 pGex6P XhoI 3'	CGCCTCGAGCTAGTCCTCACTGGAGTTGTC
	13	N283	GCG	EcoRI	GAATTC		CTGCGGTCGGACTTCC	pGex	(B) KLHL22 Kelch N-283 EcoRI 5'	GCGGAATTCCTGCGGTCGGACTTCC
	14	C599	CGC	XhoI	CTCGAG		TTAAAGGAGCAGGGA GCG	pGex	(B) KLHL22 Kelch C-599 XhoI 3'	CGCCTCGAGTTAAAGGAGCAGGGAGCG
	15	N1 (HA- Tag)	GCG	EcoRI	GAATTC		GCAGAGGAGCAGGAG TTCACCCAG	pcDNA3.1 Zeo +	(M) KLHL22 N1 EcoRI HA 5'	GCGGAATTCATGTACCCATACGATGTTCCAGATT ACGCTGCAGAGGAGCAGGAGTTCACCCAG
	16	N298	GCG	EcoRI	GAATTC		CAGTGCGTTGTGGGCT TCGG	pcDNA3.1 Zeo +	(M) KLHL22 N298 EcoRI HA 5'	GCGGGAATTCATGTACCCATACGATGTTCCAGAT TACGCTCAGTGCGTTGTGGGCTTCGG
	17	N1(with ATG)	GCG	EcoRI	GAATTC		ATGGCAGAGGAGCAG G	pcDNA3.1 Zeo +	(M) KLHL22 N1 EcoRI	GCGGAATTCATGGCAGAGGAGCAGG
	18	C633(HA- Tag + Stop)	GCG	XhoI	CTCGAG		GTCCTCACTGGAGTTG TCAAAC	pcDNA3.1 Zeo +	(M) KLHL22 C633- HA XhoI	GCGCTCGAGTTAAGCGTAATCTGGAACATCGTAT GGGTAGTCCTCACTGGAGTTGTCAAAC
Auro ra B	1	N77	GCG	EcoRI	GAATTC		ATGTTTGAGATTGGGC GTCC	pGex	(B) AurKB N77 EcoRI	GCGGAATTCATGTTTGAGATTGGGCGTCC
	2	C327	CGC	XhoI	CTCGAG		TTAGACCCAAGGGTG GG	pGex	(B) AurKB C327 XhoI	CGCCTCGAGTTAGACCCAAGGGTG
	3	N55	GCG	EcoRI	GAATTC		CAGAAGGTGATGGAG AATAGC	pGex	(B) AurKB N55C EcoRI 5' pGex	GCGGAATTCAGAAGGTGATGGAGAATAGC
	4	Nter	GCG	EcoRI	GAATTC	T	ATGGCCCAGAAGGAG AAC	pACYC/pC DF MCS1	(B) AurKB Nter EcoRI 5' MCS1	GCGGAATTCATGGCCCAGAAGGAGAAC
	5	Nter	GCG	NdeI	CATATG		ATGGCCCAGAAGGAG AAC	pACYC/pC DF MCS2	(B) AurKB Nter NdeI 5' MCS2	GCGCATATGATGGCCCAGAAGGAGAAC
	6	Cter	CGC	HindIII	AAGCTT		TCAGGCGACAGATTG AAGG	pACYC/pC DF MCS1	(B) AurKB Cter Hind3 3' MCS1	CGCAAGCTTTCAGGCGACAGATTGAAGG
	7	Cter	CGC	XhoI	CTCGAG		TCAGGCGACAGATTG AAGG	pACYC/pC DF MCS2	(B) AurKB Cter XhoI 3' MCS2	CGCCTCGAGTCAGGCGACAGATTGAAGG
	8	N55	CGC	EcoRI	GAATTC	T	CAGAAGGTGATGGAG AATAGC	pACYC/pC DF MCS1	(B) AurKB N55 EcoRI 5' MCS1	CGCGAATTCCTAGAAGGTGATGGAGAATAGC
	9	N-term	GGAT	NdeI	CATATG		GCCCAGAAGGAGAAC	pnEA-tH	(B) hAurKB N-	GGATATCCATATGGCCCAGAAGGAGAACTC

			ATC				TC		term	
	10	C-term	CGC	BamHI	GGATCC		TCAGGCGACAGATTG AAGGG	pnEA-tH	(B) hAurKA C- term	CGCGGATCCTCAGGCGACAGATTGAAGGG
	11	C-term	CGC	XhoI	CTCGAG		TTATCAGGCGACAGAT TGATTGAAGGGC	pGex	...rKB XhoI 3' for pGex	CTCGAGTTATCAGGCGACAGATTGATTGAAGGG C
KLHL 21	1	N273	GCG	EcoRI	GAATTC	T	TGTCCCCGAATGCG	pACYC/pC DF MCS1	(B) K21 N273C 5' EcoRI pACYC	GCGGAATTCTTGTCCCCGAATGCG
	2	N-ter MCS2	GCG	NdeI	CATATG		GAGGCGACCGGCGC	pACYC/pC DF MCS2	(B) K21 Nter NdeI 5' MCS2	GCGCATATGGAGCGACCGGCGC
	3	C-ter MCS1	CGC	HindIII	AAGCTT		CTAGTGCAGCTCATCG GG	pACYC/pC DF MCS1	(B) K21 Cter Hind3 3' MCS1	CGCAAGCTTCTAGTGCAGCTCATCGGG
	4	N1	GCG	EcoRI	GAATTC		ATGGAGCGACCGGC	pGex	(B) KLHL21 N1 EcoRI	GCGGAATTCATGGAGCGACCGGC
	5	C597	CGC	XhoI	CTCGAG		CTAGTGCAGCTCATCG GG	pGex	(B) KLHL21 C597 XhoI	CGCCTCGAGCTAGTGCAGCTCATCGGG
	6	N273	GCG	EcoRI	GAATTC		TGTCCCCGAATGCG	pGex	(B) K21 N273C 5' EcoRI	GCGGAATTCTGTCCCCGAATGCG
	7	Nter	GCG	EcoRI	GAATTC	T	ATGGAGCGACCGGCG CC	pACYC/pC DF MCS1	(B) K21 Nter EcoRI 5' MCS1	GCGGAATTCTATGGAGCGACCGGCGCC
	8	N-term	GGAT ATC	NdeI	CATATG		GAGCGACCGGCGCCC	pnEA-tH	(B) KLHL21 N- term	GGATATCCATATGGAGCGACCGGCGCCC
	9	C-term	CGC	BamHI	GGATCC		CTAGTGCAGCTCATCG GGG	pnEA-tH	(B) KLHL21 C- term	CGCGGATCCCTAGTGCAGCTCATCGGG

Primer for mutagenesis

Listed here are the primers used for performing all mutagenesis described in this study. All primers were synthesized by Sigma at 0,025 μ mol scale, purification desalted, with no additional modification. ID indicates internal Sumara group identifier.

Gene	ID	Mutation	Sens	Sequence
PLK1	1	W414F	5'	CATCTTCTGGGTGAGCAAGTTTGCGGACTATTCGGACAAGTACG
	2		3'	CGTACTTGTCGAATAGTCCGCAAAGTCTGCTGACCCAGAAGATG
	3	L472A	5'	GCCTTGGGTATCAGGCCTGTGATAACAGCG
	4		3'	CGCTGTTATCACAGGCCTGATACCCAAGGC
	5	DFG to AGE	5'	GAAAATAGGGGCTGGTGAAGTGGCAACCAAAGTCGAATATGAC
	6		3'	GGTTGCCAGTTCACAGCCCTATTTTCACCTCCAGATCTTC
	7	T1206C	5'	GGCTTGAGGACCCTGCCTGC
	8		3'	GCAGGCAGGGTCCTCAGCC
	9	T210A	5'	GAGGAAGAAGGCCCTGTGTG
	10		3'	CACACAGGGCCTTCTTCCTC
	11	K492R	5'	CTTGCTGAGGGCAGGTG
	12		3'	CACCTGCCCTCAGCAAG
	13	K492R	5'	GCGAGCACTTGCTGAAGGCAGGTGCCAACATC
	14		3'	GATGTTGGCACCTGCCTTCAGCAAGTGCTCGC
	15	H538A/K540M	5'	CAGGATGCCACCATGCTCATC
	16		3'	GATGAGCATGGTGGCATCCTG
	17	H538A/K540M	5'	CAGATCAACTTCTCCAGGATGCCACCATGCTCATCTTGCGCCACTGATG
	18		3'	CATCAGTGGGCACAAGATGAGCATGGTGGCATCCTGGAAGAAGTTGATCTG
	19	V415A (if W414F)	5'	GTCAGCAAGTTCGCGGACTATTCGGAC
	20		3'	GTCCGAATAGTCCGCGAACTTGCTGAC
	21	W414F	5'	CTGGGTGAGCAAGTTCGTGGACTATTCGGAC
	22		3'	GTCCGAATAGTCCACGAACTTGCTGACCCAG
	23	Y481A	5'	GAAGATCACCTCCTTAAAGCTTCCGCAATTACATGAG

	24		3'	CTCATGTAATTGCGGAAAGCTTTAAGGAGGGTGATCTTC
	25	F482A	5'	CACCCTCCTTAAATATGCCCCGAATTACATGAGCG
	26		3'	CGCTCATGTAATTGCGGGCATATTTAAGGAGGGTG
	27	W514A	5'	CTACCTACGGACCGCATTCCGCACCCGAG
	28		3'	CTGCGGGTGCGGAATGCGGTCCGTAGGTAG
	030S_plk1_NotI_rev	PLK1 Not1 C-ter		ATTATTGCGGCCGCTTAGGAGGCCTTGAGACGGTTGCTG
	019S_PLK1491ubi1_rev	PLK1-PBD-UBI N-ter rev	3'	GTCAGAGTCTTCACGAAGATCTGCA TCAGCAAGTGCTCGCTCATGTAATTGC
	020S_ubi76PLK1493_for	PLK1-PBD-UBi C-ter Fw	5'	CCTGGTACTCCGTCTCAGAGGTGGG GCAGGTGCCAACATCACGCCGCGCG
	021S_ubi_for	UBI N-ter Fw	5'	ATGCAGATCTTCGTGAAGACTCTGAC
	022S_ubi_rev	UBI C-ter Rev	3'	CCCACCTCTGAGACGGAGTACCAGG
	164S_PLK1 ETGE to AAGA rev	ETGE to AAGA rev	3'	CAGTCGACCACCGCACCTGCCGCTCGAACCCTGGTTCTTC
	165S_PLK1 ETGE to AAGA fwd	ETGE to AAGA Fw	5'	CAGTGGTTCGAGCGGCAGGTGCGGTGGTCTGACTGCCACCTCAG
	166S_PLK1 DFG to AGE rev	DFG to AGE rev	3'	GGTTGCCAGTTCACCAGCCCCTATTTTCACCTCCAGATC
	167S_PLK1 DFG to AGE fwd	DFG to AGE Fw	5'	GAAAATAGGGGCTGGTGAAGTGGCAACCAAAGTCGAATATG
KLHL22	1	C572T	5'	ACCGCCAGCTTCCATTGGAGA
	2		3'	TCTCCAATGGAAGCTGGCGGT
	3	S308A	5'	CTTCGGGGGCATTACGCAACGCCGTCCACTGTC
	4		3'	GACAGTGGACGGCGTTGCGTGAATGCCCCGAAG
	5	S367E	5'	GGATTCGAGCAGAGGAGCGATGCTGGAGGTATG
	6		3'	CATACCTCCAGCATCGCTCCTCTGCTCGAAATCC
	7	T309A	5'	GGCATTCACTCCGCGCCGTCCACTG
	8		3'	CAGTGGACGGCGCGGAGTGAATGCC
	9	T309D	5'	GGGCATTCACTCCGACCCGTCCACTGTCC
	10		3'	GGACAGTGGACGGGTCTGGAGTGAATGCCC

Plasmid list

Listed here are all the plasmids used in this study. All were sequenced and validated. ID indicates internal Sumara group identifier.

Gene	Name	ID	Backbone	Resistance	Restriction site 5'	Restriction site 3'	Tag
Controls	GFP	1	peGFP-N1	Kan			GFP
	GST	2	pGex-6P1	Amp			GST
	MBP	3	pMal-C2X	Amp			MBP
PLK1	GST-PLK1-FL	4	pGex-6P1	Amp	EcoRI	XhoI	N-t GST
	GST-PLK1-KIN	5	pGex-6P1	Amp	EcoRI	XhoI	N-t GST
	GST-PLK1-PBD Texte	6	pGex-6P1	Amp	EcoRI	XhoI	N-t GST
	GST-PLK1-KIN-N-lobe	7	pGex-6P1	Amp	EcoRI	XhoI	N-t GST
	GST-PLK1-KIN-C-lobe	8	pGex-6P1	Amp	EcoRI	XhoI	N-t GST
	GST-PLK1-PBD-PB1	9	pGex-6P1	Amp	EcoRI	XhoI	N-t GST
	GST-PLK1-PBD-PB2	10	pGex-6P1	Amp	EcoRI	XhoI	N-t GST
	GST-PLK1-KIN-C272	11	pGex-6P1	Amp	EcoRI	XhoI	N-t GST
	GST-PLK1-Flex	12	pGex-6P1	Amp	EcoRI	XhoI	N-t GST
	GST-PLK1-PBD-Δflex	13	pGex-6P1	Amp	EcoRI	XhoI	N-t GST
	GST-PLK1-PBD-PB1-Δflex	14	pGex-6P1	Amp	EcoRI	XhoI	N-t GST
	GST-PLK1-PBD-PB1-Δflex-ΔF1F3	15	pGex-6P1	Amp	EcoRI	XhoI	N-t GST
	GST-PLK1-PBD-W414F	16	pGex-6P1	Amp	EcoRI	XhoI	N-t GST
	GST-PLK1-PBD-F482A	17	pGex-6P1	Amp	EcoRI	XhoI	N-t GST
	GST-PLK1-PBD-W514A	18	pGex-6P1	Amp	EcoRI	XhoI	N-t GST
	GST-PLK1-PBD-H538A-K540M	19	pGex-6P1	Amp	EcoRI	XhoI	N-t GST
	GST-PLK1-PBD-W414F-H538A-K540M	20	pGex-6P1	Amp	EcoRI	XhoI	N-t GST
	GST-PLK1-FL-DFG to AGE	21	pGex-6P1	Amp	EcoRI	XhoI	N-t GST
	GST-PLK1-FL-ETGE to AAGA	22	pGex-6P1	Amp	EcoRI	XhoI	N-t GST
	GST-PLK1-FL-DFG to AGE - ETGE to	23	pGex-6P1	Amp	EcoRI	XhoI	N-t GST

	AAGA						
	GST-PLK1-PBD-UBI	24	pGex-6P1	Amp	EcoRI	XhoI	N-t GST
	GFP-PLK1-FL	25	peGFP-N1	Kan	XhoI	KpnI	C-t GFP
	GFP-PLK1-KIN	26	peGFP-N1	Kan	XhoI	KpnI	C-t GFP
	GFP-PLK1-PBD	27	peGFP-N1	Kan	XhoI	KpnI	C-t GFP
	GFP-PLK1-KIN-N-lobe	28	peGFP-N1	Kan	XhoI	KpnI	C-t GFP
	GFP-PLK1-KIN-C-lobe	29	peGFP-N1	Kan	XhoI	KpnI	C-t GFP
	GFP-PLK1-PBD-PB1	30	peGFP-N1	Kan	XhoI	KpnI	C-t GFP
	GFP-PLK1-PBD-PB2	31	peGFP-N1	Kan	XhoI	KpnI	C-t GFP
	YFP-PLK1-FL	32	peYFP-C3	Kan	NheI	SalI	N-t GFP
	YFP-PLK1-Dbox-mutant	33	peYFP-C3	Kan	NheI	SalI	N-t GFP
	PLK1-FL	34	pnCS	Spec	NdeI	BamHI	
KLHL22	GST-KLHL22-FL	35	pGex-6P1	Amp	EcoRI	XhoI	N-t GST
	GST-KLHL22-BTB	36	pGex-6P1	Amp	EcoRI	XhoI	N-t GST
	GST-KLHL22-BACK	37	pGex-6P1	Amp	EcoRI	XhoI	N-t GST
	GST-KLHL22-KELCH	38	pGex-6P1	Amp	EcoRI	XhoI	N-t GST
	GST-KLHL22-BTB-BACK	39	pGex-6P1	Amp	EcoRI	XhoI	N-t GST
	GST-KLHL22-BACK-KELCH	40	pGex-6P1	Amp	EcoRI	XhoI	N-t GST
	HA-KLHL22-FL	41	pcDNA 3.1	Amp			N-t HA
	HA-KLHL22-FL (my)	42	pcDNA 3.1	Amp	EcoRI	XhoI	N-t HA
	HA-KLHL22-FL	43	pcDNA 3.1	Amp	EcoRI	XhoI	C-t HA
	HA-KLHL22-BTB-BACK	44	pcDNA 3.1	Amp	EcoRI	XhoI	N-t HA
	HA-KLHL22-KELCH	45	pcDNA 3.1	Amp	EcoRI	XhoI	N-t HA
	HA-KLHL22-FL-S308A	46	pcDNA 3.1	Amp			N-t HA
	HA-KLHL22-FL-T309A	47	pcDNA 3.1	Amp			N-t HA
	HA-KLHL22-FL-T309D	48	pcDNA 3.1	Amp			N-t HA
	HA-KLHL22-FL-S367E	49	pcDNA 3.1	Amp			N-t HA
	MBP-KLHL22	50	pMal-C2X	Amp	EcoRI	BamHI	N-t MBP

	pnCS-KLHL22	51	pnCS	Spec	NdeI	BamHI	
Aurora B	GST-AurKB-FL	52	pGex-6P1	Amp	EcoRI	XhoI	N-t GST
	GST-AurKB-N55	53	pGex-6P1	Amp	EcoRI	XhoI	N-t GST
	GST-xAurKB(60-361)- K122R/xINCENP(790-856)	54	pGex-2RBS	Amp			N-t GST
	His-AurKB	55	pACYC-Duet	Cm	EcoRI	HindIII	N-t HIS
	His-AurKB-N55	56	pACYC-Duet	Cm	EcoRI	HindIII	N-t HIS
KLHL21	MBP-KLHL21	57	pMal-C2X	Amp	EcoRI	BamHI	N-t MBP
	GST-KLHL21-FL	58	pGex-6P1	Amp	EcoRI	XhoI	N-t GST
	GST-KLHL21-KELCH	59	pGex-6P1	Amp	EcoRI	XhoI	N-t GST
	His-KLHL21-KELCH	60	pACYC-Duet	Cm	EcoRI	HindIII	N-t HIS

9 Abbreviations

APC/C: Anaphase-Promoting complex / Cyclosome

ATP: Adenosine triphosphate

BTB: Bric-a-brac, tramtrack and broad complex

CDK: Cyclin-dependent kinase

CPC: Chromosomal Passenger complex

CRL: Cullin-RING E3-ubiquitin ligase

CUL3: Cullin-3

D-box: Death-box

Da: Dalton

DNA: Deoxyribonucleic acid

DUB: Deubiquitinase

GF: Gel filtration

GFP: Green fluorescent protein

GST: Glutathione S-transferase

HA: Hemagglutinin

HECT: Homologous to the E6-AP carboxy terminus

IGBMC: Institute of genetics and molecular and cellular biology

IP: Immuno-precipitation

IPTG: Isopropyl β -D-1-thiogalactopyranoside

KT-MT: Kinetochore-microtubule

MATH: Meprin and TRAF homology

MBP: Maltose-binding protein

MCC: Mitotic Checkpoint complex

OTP: On-target plus

PBD: Polo-box domain

PBS: Phosphate-buffered saline

PLK: Polo-like kinase

RING: Really interesting new gene

RNA: Ribonucleic acid

SAC: Spindle-Assembly Checkpoint

SCF: Skp1-Cullin 1-F-box

siRNA: Small-interfering ribonucleic acid

TBS-T: Tris-buffered saline - tween

TBS: Tris-buffered saline

Ub: Ubiquitin

UBP: Ubiquitin binding protein

WB: Western-blot

WT: Wild-type

10 References

- Abe, S., Nagasaka, K., Hirayama, Y., Kozuka-Hata, H., Oyama, M., Aoyagi, Y., Obuse, C., and Hirota, T. (2011). The initial phase of chromosome condensation requires Cdk1-mediated phosphorylation of the CAP-D3 subunit of condensin II. *Genes Dev.* 25, 863–874.
- Ahmad, K.F., Engel, C.K., and Privé, G.G. (1998). Crystal structure of the BTB domain from PLZF. *Proc. Natl. Acad. Sci. U. S. A.* 95, 12123–12128.
- Alexandru, G., Uhlmann, F., Mechtler, K., Poupart, M. a, and Nasmyth, K. (2001). Phosphorylation of the cohesin subunit Scc1 by Polo/Cdc5 kinase regulates sister chromatid separation in yeast. *Cell* 105, 459–472.
- Anand, S., Penrhyn-low, S., and Venkitaraman, A.R. (2003). AURORA-A amplification overrides the mitotic spindle assembly checkpoint , inducing resistance to Taxol. 3, 51–62.
- Archambault, V., D’Avino, P.P., Deery, M.J., Lilley, K.S., and Glover, D.M. (2008). Sequestration of Polo kinase to microtubules by phosphoprimer-independent binding to Map205 is relieved by phosphorylation at a CDK site in mitosis. *Genes Dev.* 22, 2707–2720.
- Ayad, N.G., Rankin, S., Murakami, M., Jebanathirajah, J., Gygi, S., and Kirschner, M.W. (2003). Tome-1, a trigger of mitotic entry, is degraded during G1 via the APC. *Cell* 113, 101–113.
- Bassermann, F., von Klitzing, C., Münch, S., Bai, R.-Y., Kawaguchi, H., Morris, S.W., Peschel, C., and Duyster, J. (2005). NIPA defines an SCF-type mammalian E3 ligase that regulates mitotic entry. *Cell* 122, 45–57.
- Bassermann, F., von Klitzing, C., Illert, A.L., Münch, S., Morris, S.W., Pagano, M., Peschel, C., and Duyster, J. (2007). Multisite phosphorylation of nuclear interaction partner of ALK (NIPA) at G2/M involves cyclin B1/Cdk1. *J. Biol. Chem.* 282, 15965–15972.

- Bayliss, R., Fry, A., Haq, T., and Yeoh, S. (2012). On the molecular mechanisms of mitotic kinase activation On the molecular mechanisms of mitotic kinase activation Author for correspondence :
- Beck, J., Maerki, S., Posch, M., Metzger, T., Persaud, A., Scheel, H., Hofmann, K., Rotin, D., Pedrioli, P., Swedlow, J.R., et al. (2013). Ubiquitylation-dependent localization of PLK1 in mitosis. *Nat. Cell Biol.* *15*, 430–439.
- Berdnik, D., and Knoblich, J. a (2002). Drosophila Aurora-A is required for centrosome maturation and actin-dependent asymmetric protein localization during mitosis. *Curr. Biol.* *12*, 640–647.
- Bishop, J.D., and Schumacher, J.M. (2002). Phosphorylation of the carboxyl terminus of inner centromere protein (INCENP) by the Aurora B Kinase stimulates Aurora B kinase activity. *J. Biol. Chem.* *277*, 27577–27580.
- Blangy, a, Lane, H. a, d'Hérin, P., Harper, M., Kress, M., and Nigg, E. a (1995). Phosphorylation by p34cdc2 regulates spindle association of human Eg5, a kinesin-related motor essential for bipolar spindle formation in vivo. *Cell* *83*, 1159–1169.
- Canning, P., Cooper, C.D.O., Krojer, T., Murray, J.W., Pike, A.C.W., Chaikuad, A., Keates, T., Thangaratnarajah, C., Hojzan, V., Ayinampudi, V., et al. (2013). Structural basis for Cul3 protein assembly with the BTB-Kelch family of E3 ubiquitin ligases. *J. Biol. Chem.* *288*, 7803–7814.
- Carmena, M., and Earnshaw, W.C. (2003). The cellular geography of aurora kinases. *Nat. Rev. Mol. Cell Biol.* *4*, 842–854.
- Do Carmo Avides, M., Tavares, a, and Glover, D.M. (2001). Polo kinase and Asp are needed to promote the mitotic organizing activity of centrosomes. *Nat. Cell Biol.* *3*, 421–424.
- Casenghi, M., Barr, F. a, and Nigg, E. a (2005). Phosphorylation of Nlp by Plk1 negatively regulates its dynein-dynactin-dependent targeting to the centrosome. *J. Cell Sci.* *118*, 5101–5108.

- Chan, E.H.Y., Santamaria, A., Silljé, H.H.W., and Nigg, E. a (2008). Plk1 regulates mitotic Aurora A function through betaTrCP-dependent degradation of hBora. *Chromosoma* 117, 457–469.
- Chau, V., Tobias, J.W., Bachmair, A., Marriotr, D., Ecker, D.J., Gonda, D.K., and Varshavsky, A. (1989). Targeted to Specific Protein UX-E. 714.
- Cheeseman, I.M., Chappie, J.S., Wilson-Kubalek, E.M., and Desai, A. (2006). The conserved KMN network constitutes the core microtubule-binding site of the kinetochore. *Cell* 127, 983–997.
- Cheetham, G.M.T., Knegt, R.M. a, Coll, J.T., Renwick, S.B., Swenson, L., Weber, P., Lippke, J. a, and Austen, D. a (2002). Crystal structure of aurora-2, an oncogenic serine/threonine kinase. *J. Biol. Chem.* 277, 42419–42422.
- Cheng, K.-Y., Lowe, E.D., Sinclair, J., Nigg, E. a, and Johnson, L.N. (2003). The crystal structure of the human polo-like kinase-1 polo box domain and its phospho-peptide complex. *EMBO J.* 22, 5757–5768.
- Cope, G. a, Suh, G.S.B., Aravind, L., Schwarz, S.E., Zipursky, S.L., Koonin, E. V, and Deshaies, R.J. (2002). Role of predicted metalloprotease motif of Jab1/Csn5 in cleavage of Nedd8 from Cul1. *Science* 298, 608–611.
- D’Avino, P.P. (2009). How to scaffold the contractile ring for a safe cytokinesis - lessons from Anillin-related proteins. *J. Cell Sci.* 122, 1071–1079.
- Douglas, M.E., Davies, T., Joseph, N., and Mishima, M. (2010). Aurora B and 14-3-3 coordinately regulate clustering of centralspindlin during cytokinesis. *Curr. Biol.* 20, 927–933.
- Duda, D.M., Borg, L. a, Scott, D.C., Hunt, H.W., Hammel, M., and Schulman, B. a (2008). Structural insights into NEDD8 activation of cullin-RING ligases: conformational control of conjugation. *Cell* 134, 995–1006.
- Dutertre, S., Cazales, M., Quaranta, M., Froment, C., Trabut, V., Dozier, C., Mirey, G., Bouché, J.-P., Theis-Febvre, N., Schmitt, E., et al. (2004). Phosphorylation of CDC25B by

Aurora-A at the centrosome contributes to the G2-M transition. *J. Cell Sci.* **117**, 2523–2531.

Elia, A.E.H., Rellos, P., Haire, L.F., Chao, J.W., Ivins, F.J., Hoepker, K., Mohammad, D., Cantley, L.C., Smerdon, S.J., and Yaffe, M.B. (2003a). The molecular basis for phosphodependent substrate targeting and regulation of Plks by the Polo-box domain. *Cell* **115**, 83–95.

Elia, A.E.H., Cantley, L.C., and Yaffe, M.B. (2003b). Proteomic screen finds pSer/pThr-binding domain localizing Plk1 to mitotic substrates. *Science* **299**, 1228–1231.

Elkins, J.M., Santaguida, S., Musacchio, A., and Knapp, S. (2012). Crystal structure of human aurora B in complex with INCENP and VX-680. *J. Med. Chem.* **55**, 7841–7848.

Elowe, S., Hümmer, S., Uldschmid, A., Li, X., and Nigg, E. a (2007). Tension-sensitive Plk1 phosphorylation on BubR1 regulates the stability of kinetochore microtubule interactions. *Genes Dev.* **21**, 2205–2219.

Eyers, P. a, and Maller, J.L. (2004). Regulation of *Xenopus* Aurora A activation by TPX2. *J. Biol. Chem.* **279**, 9008–9015.

Floyd, S., Pines, J., and Lindon, C. (2008). Targets Aurora Kinase APC / C to Control Reorganization of the Mitotic Spindle at Anaphase. *Curr. Biol.* **18**, 1649–1658.

Foley, E. a, and Kapoor, T.M. (2013). Microtubule attachment and spindle assembly checkpoint signalling at the kinetochore. *Nat. Rev. Mol. Cell Biol.* **14**, 25–37.

Fournane, S., Krupina, K., Kleiss, C., and Sumara, I. (2012). Decoding ubiquitin for mitosis. *Genes Cancer* **3**, 697–711.

García-Alvarez, B., de Cárcer, G., Ibañez, S., Bragado-Nilsson, E., and Montoya, G. (2007). Molecular and structural basis of polo-like kinase 1 substrate recognition: Implications in centrosomal localization. *Proc. Natl. Acad. Sci. U. S. A.* **104**, 3107–3112.

Geley, S., Kramer, E., Gieffers, C., Gannon, J., Peters, J.M., and Hunt, T. (2001). Anaphase-promoting complex/cyclosome-dependent proteolysis of human cyclin A starts at the

beginning of mitosis and is not subject to the spindle assembly checkpoint. *J. Cell Biol.* **153**, 137–148.

Genschik, P., Sumara, I., and Lechner, E. (2013). The emerging family of CULLIN3-RING ubiquitin ligases (CRL3s): cellular functions and disease implications. *EMBO J.* **32**, 2307–2320.

Goldstein, G., Scheid, M., Hammerling, U., Schlesinger, D.H., Niall, H.D., and Boyse, E. a (1975). Isolation of a polypeptide that has lymphocyte-differentiating properties and is probably represented universally in living cells. *Proc. Natl. Acad. Sci. U. S. A.* **72**, 11–15.

Golsteyn, R.M., Mundt, K.E., Fry, a M., and Nigg, E. a (1995). Cell cycle regulation of the activity and subcellular localization of Plk1, a human protein kinase implicated in mitotic spindle function. *J. Cell Biol.* **129**, 1617–1628.

Goto, H., Kiyono, T., Tomono, Y., Kawajiri, A., Urano, T., Furukawa, K., Nigg, E. a, and Inagaki, M. (2006). Complex formation of Plk1 and INCENP required for metaphase-anaphase transition. *Nat. Cell Biol.* **8**, 180–187.

Guse, A., Mishima, M., and Glotzer, M. (2005). Phosphorylation of ZEN-4/MKLP1 by aurora B regulates completion of cytokinesis. *Curr. Biol.* **15**, 778–786.

Habedanck, R., Stierhof, Y.-D., Wilkinson, C.J., and Nigg, E. a (2005). The Polo kinase Plk4 functions in centriole duplication. *Nat. Cell Biol.* **7**, 1140–1146.

Hames, R.S., Wattam, S.L., Yamano, H., Bacchieri, R., and Fry, a M. (2001). APC/C-mediated destruction of the centrosomal kinase Nek2A occurs in early mitosis and depends upon a cyclin A-type D-box. *EMBO J.* **20**, 7117–7127.

Hannak, E., Kirkham, M., Hyman, a a, and Oegema, K. (2001). Aurora-A kinase is required for centrosome maturation in *Caenorhabditis elegans*. *J. Cell Biol.* **155**, 1109–1116.

Hauf, S., Cole, R.W., LaTerra, S., Zimmer, C., Schnapp, G., Walter, R., Heckel, A., van Meel, J., Rieder, C.L., and Peters, J.-M. (2003). The small molecule Hesperadin reveals a role for Aurora B in correcting kinetochore-microtubule attachment and in maintaining the spindle assembly checkpoint. *J. Cell Biol.* **161**, 281–294.

- Hu, C.-K., Ozl , N., Coughlin, M., Steen, J.J., and Mitchison, T.J. (2012). Plk1 negatively regulates PRC1 to prevent premature midzone formation before cytokinesis. *Mol. Biol. Cell* 23, 2702–2711.
- Huang, J.N. (2001). Activity of the APC^{Cdh1} form of the anaphase-promoting complex persists until S phase and prevents the premature expression of Cdc20p. *J. Cell Biol.* 154, 85–94.
- Induced, A., Overexpression, A., Dutertre, S., Hamard-p ron, E., and Cremet, J. (2005). The Absence of p53 Aggravates Polyploidy and Centrosome Number Report ND ES SC ACKNOWLEDGEMENTS RIB. 1783–1787.
- Jackman, M., Lindon, C., Nigg, E. a, and Pines, J. (2003). Active cyclin B1-Cdk1 first appears on centrosomes in prophase. *Nat. Cell Biol.* 5, 143–148.
- Jin, L., Williamson, A., Banerjee, S., Philipp, I., and Rape, M. (2008). Mechanism of ubiquitin-chain formation by the human anaphase-promoting complex. *Cell* 133, 653–665.
- Joo, H.-Y., Zhai, L., Yang, C., Nie, S., Erdjument-Bromage, H., Tempst, P., Chang, C., and Wang, H. (2007). Regulation of cell cycle progression and gene expression by H2A deubiquitination. *Nature* 449, 1068–1072.
- Kamaraj, B., Rajendran, V., Sethumadhavan, R., and Purohit, R. (2013). In-silico screening of cancer associated mutation on PLK1 protein and its structural consequences. *J. Mol. Model.* 19, 5587–5599.
- Kang, Y.H., Park, J.-E., Yu, L.-R., Soung, N.-K., Yun, S.-M., Bang, J.K., Seong, Y.-S., Yu, H., Garfield, S., Veenstra, T.D., et al. (2006). Self-regulated Plk1 recruitment to kinetochores by the Plk1-PBIP1 interaction is critical for proper chromosome segregation. *Mol. Cell* 24, 409–422.
- Keppner, S., Proschak, E., Kaufmann, M., Strebhardt, K., Schneider, G., and Sp nkuch, B. (2010). Biological impact of freezing Plk1 in its inactive conformation in cancer cells. *Cell Cycle* 9, 761–773.

- Keppner, S., Proschak, E., Schneider, G., and Spänkuch, B. (2011). Fate of primary cells at the G 1 /S boundary after polo-like kinase 1 inhibition by SBE13. *Cell Cycle* 10, 708–720.
- Kikuchi, R., Ohata, H., Ohoka, N., Kawabata, A., and Naito, M. (2013). Apollon Promotes Early Mitotic Cyclin A Degradation Independent of the Spindle Assembly Checkpoint. *J. Biol. Chem.*
- Kimura, M. (1999). Cell Cycle-dependent Expression and Centrosome Localization of a Third Human Aurora/Ipl1-related Protein Kinase, AIK3. *J. Biol. Chem.* 274, 7334–7340.
- Kraft, C., Herzog, F., Gieffers, C., Mechtler, K., Hagting, A., Pines, J., and Peters, J.-M. (2003). Mitotic regulation of the human anaphase-promoting complex by phosphorylation. *EMBO J.* 22, 6598–6609.
- Lan, W., Zhang, X., Kline-Smith, S.L., Rosasco, S.E., Barrett-Wilt, G. a, Shabanowitz, J., Hunt, D.F., Walczak, C.E., and Stukenberg, P.T. (2004). Aurora B phosphorylates centromeric MCAK and regulates its localization and microtubule depolymerization activity. *Curr. Biol.* 14, 273–286.
- Lane, H. a, and Nigg, E. a (1996). Antibody microinjection reveals an essential role for human polo-like kinase 1 (Plk1) in the functional maturation of mitotic centrosomes. *J. Cell Biol.* 135, 1701–1713.
- Lee, K., and Rhee, K. (2011). PLK1 phosphorylation of pericentrin initiates centrosome maturation at the onset of mitosis. *J. Cell Biol.* 195, 1093–1101.
- Lee, K.S., Grenfell, T.Z., Yarm, F.R., and Erikson, R.L. (1998). Mutation of the polo-box disrupts localization and mitotic functions of the mammalian polo kinase Plk. *Proc. Natl. Acad. Sci. U. S. A.* 95, 9301–9306.
- Lee, Y.-R., Yuan, W.-C., Ho, H.-C., Chen, C.-H., Shih, H.-M., and Chen, R.-H. (2010). The Cullin 3 substrate adaptor KLHL20 mediates DAPK ubiquitination to control interferon responses. *EMBO J.* 29, 1748–1761.
- Li, W., and Ye, Y. (2008). Polyubiquitin chains: functions, structures, and mechanisms. *Cell. Mol. Life Sci.* 65, 2397–2406.

- Li, X., Sakashita, G., Matsuzaki, H., Sugimoto, K., Kimura, K., Hanaoka, F., Taniguchi, H., Furukawa, K., and Urano, T. (2004). Direct association with inner centromere protein (INCENP) activates the novel chromosomal passenger protein, Aurora-C. *J. Biol. Chem.* 279, 47201–47211.
- Lindon, C., and Pines, J. (2004). Ordered proteolysis in anaphase inactivates Plk1 to contribute to proper mitotic exit in human cells. *J. Cell Biol.* 164, 233–241.
- Lioutas, A., and Vernos, I. (2013). Aurora A kinase and its substrate TACC3 are required for central spindle assembly. *EMBO Rep.* 14, 829–836.
- Littlepage, L.E., Wu, H., Andresson, T., Deanehan, J.K., Amundadottir, L.T., and Ruderman, J. V (2002). Identification of phosphorylated residues that affect the activity of the mitotic kinase Aurora-A. *Proc. Natl. Acad. Sci. U. S. A.* 99, 15440–15445.
- Liu, Z., Ren, J., Cao, J., He, J., Yao, X., Jin, C., and Xue, Y. (2013). Systematic analysis of the Plk-mediated phosphoregulation in eukaryotes. *Brief. Bioinform.* 14, 344–360.
- Lowery, D.M., Clauser, K.R., Hjerrild, M., Lim, D., Alexander, J., Kishi, K., Ong, S.-E., Gammeltoft, S., Carr, S. a, and Yaffe, M.B. (2007). Proteomic screen defines the Polo-box domain interactome and identifies Rock2 as a Plk1 substrate. *EMBO J.* 26, 2262–2273.
- Lüscher, B., Brizuela, L., Beach, D., and Eisenman, R.N. (1991). A role for the p34cdc2 kinase and phosphatases in the regulation of phosphorylation and disassembly of lamin B2 during the cell cycle. *EMBO J.* 10, 865–875.
- Lyapina, S., Cope, G., Shevchenko, a, Serino, G., Tsuge, T., Zhou, C., Wolf, D. a, Wei, N., and Deshaies, R.J. (2001). Promotion of NEDD-CUL1 conjugate cleavage by COP9 signalosome. *Science* 292, 1382–1385.
- Ma, S., Charron, J., and Erikson, R.L. (2003). Role of Plk2 (Snk) in Mouse Development and Cell Proliferation Role of Plk2 (Snk) in Mouse Development and Cell Proliferation. 2.

- Maerki, S., Olma, M.H., Staubli, T., Steigemann, P., Gerlich, D.W., Quadroni, M., Sumara, I., and Peter, M. (2009). The Cul3-KLHL21 E3 ubiquitin ligase targets aurora B to midzone microtubules in anaphase and is required for cytokinesis. *J. Cell Biol.* *187*, 791–800.
- Matthew, E.M., Yen, T.J., Dicker, D.T., and Dorsey, J.F. (2007). Replication Stress, Defective S-phase Checkpoint and Increased Death in Plk2-Deficient Human Cancer Cells. *Cell Cycle* 2571–2578.
- McMahon, M., Thomas, N., Itoh, K., Yamamoto, M., and Hayes, J.D. (2006). Dimerization of substrate adaptors can facilitate cullin-mediated ubiquitylation of proteins by a “tethering” mechanism: a two-site interaction model for the Nrf2-Keap1 complex. *J. Biol. Chem.* *281*, 24756–24768.
- Metzger, T., Kleiss, C., and Sumara, I. (2013). Insights from PLK1 / KLHL22 interaction CUL3 and protein kinases. *Cell Cycle* *12:14*, 2291–2296.
- Moghe, S., Jiang, F., Miura, Y., Cerny, R.L., Tsai, M.-Y., and Furukawa, M. (2012). The CUL3-KLHL18 ligase regulates mitotic entry and ubiquitylates Aurora-A. *Biol. Open* *1*, 82–91.
- Moretti, S., De Falco, V., Tamburrino, A., Barbi, F., Tavano, M., Avenia, N., Santeusano, F., Santoro, M., Macchiarulo, A., and Puxeddu, E. (2009). Insights into the molecular function of the inactivating mutations of B-Raf involving the DFG motif. *Biochim. Biophys. Acta* *1793*, 1634–1645.
- Morgan, D.O. (1997). Cyclin-dependent kinases: engines, clocks, and microprocessors. *Annu. Rev. Cell Dev. Biol.* *13*, 261–291.
- Nigg, E. a (2001). Mitotic kinases as regulators of cell division and its checkpoints. *Nat. Rev. Mol. Cell Biol.* *2*, 21–32.
- Nishino, M., Kurasawa, Y., Evans, R., Lin, S.-H., Brinkley, B.R., and Yu-Lee, L.-Y. (2006). NudC is required for Plk1 targeting to the kinetochore and chromosome congression. *Curr. Biol.* *16*, 1414–1421.
- Oshimori, N., Ohsugi, M., and Yamamoto, T. (2006). The Plk1 target Kizuna stabilizes mitotic centrosomes to ensure spindle bipolarity. *Nat. Cell Biol.* *8*, 1095–1101.

- Ouyang, B. (1997). Human Prk Is a Conserved Protein Serine/Threonine Kinase Involved in Regulating M Phase Functions. *J. Biol. Chem.* 272, 28646–28651.
- Peter, M., Nakagawa, J., Dorée, M., Labbé, J.C., and Nigg, E. a (1990). In vitro disassembly of the nuclear lamina and M phase-specific phosphorylation of lamins by cdc2 kinase. *Cell* 61, 591–602.
- Pintard, L., Kurz, T., Glaser, S., Willis, J.H., Peter, M., and Bowerman, B. (2003a). Neddylation and Deneddylation of CUL-3 Is Required to Target MEI-1 / Katanin for Degradation at the Meiosis-to-Mitosis Transition in *C. elegans*. 13, 911–921.
- Pintard, L., Willis, J.H., Willems, A., Johnson, J.F., Srayko, M., Kurz, T., and Glaser, S. (2003b). The BTB protein MEL-26 is a substrate-specific adaptor of the CUL-3 ubiquitin-ligase. 425, 311–316.
- Qi, W., Tang, Z., and Yu, H. (2006). Phosphorylation- and Polo-Box – dependent Binding of Plk1 to Bub1 Is Required for the Kinetochore Localization of Plk1 □. 17, 3705–3716.
- Rumpf, S., and Jentsch, S. (2006). Functional division of substrate processing cofactors of the ubiquitin-selective Cdc48 chaperone. *Mol. Cell* 21, 261–269.
- Sakata, E., Yamaguchi, Y., Miyauchi, Y., Iwai, K., Chiba, T., Saeki, Y., Matsuda, N., Tanaka, K., and Kato, K. (2007). Direct interactions between NEDD8 and ubiquitin E2 conjugating enzymes upregulate cullin-based E3 ligase activity. *Nat. Struct. Mol. Biol.* 14, 167–168.
- Sasai, K., Katayama, H., Stenoién, D.L., Fujii, S., Honda, R., Kimura, M., Okano, Y., Tatsuka, M., Suzuki, F., Nigg, E. a, et al. (2004). Aurora-C kinase is a novel chromosomal passenger protein that can complement Aurora-B kinase function in mitotic cells. *Cell Motil. Cytoskeleton* 59, 249–263.
- Seki, A., Coppinger, J. a, Jang, C.-Y., Yates, J.R., and Fang, G. (2008). Bora and the kinase Aurora a cooperatively activate the kinase Plk1 and control mitotic entry. *Science* 320, 1655–1658.

- Sessa, F., Mapelli, M., Ciferri, C., Tarricone, C., Areces, L.B., Schneider, T.R., Stukenberg, P.T., and Musacchio, A. (2005). Mechanism of Aurora B activation by INCENP and inhibition by hesperadin. *Mol. Cell* 18, 379–391.
- Slattery, S.D., Mancini, M. a, Brinkley, B.R., and Hall, R.M. (2009). Aurora-C kinase supports mitotic progression in the absence of Aurora-B. *Cell Cycle* 8, 2984–2994.
- Spence, J., Sadis, S., Haas, A.L., Finley, D., Spence, J., Sadis, S., and Haas, A.L. (1995). A ubiquitin mutant with specific defects in DNA repair and multiubiquitination . These include: A Ubiquitin Mutant with Specific Defects in DNA Repair and Multiubiquitination. 15.
- Stewart, S., and Fang, G. (2005a). Destruction box-dependent degradation of aurora B is mediated by the anaphase-promoting complex/cyclosome and Cdh1. *Cancer Res.* 65, 8730–8735.
- Stewart, S., and Fang, G. (2005b). Anaphase-Promoting Complex / Cyclosome Controls the Stability of TPX2 during Mitotic Exit Anaphase-Promoting Complex / Cyclosome Controls the Stability of TPX2 during Mitotic Exit. 25.
- Straight, A.F., Field, C.M., and Mitchison, T.J. (2005). Anillin Binds Nonmuscle Myosin II and Regulates the Contractile Ring □. 16, 193–201.
- Sugimoto, K., Urano, T., Zushi, H., Inoue, K., Tasaka, H., and Tachibana, M. (2002). Molecular Dynamics of Aurora-A Kinase in Living Mitotic Cells Simultaneously Visualized with Histone H3 and Nuclear Membrane Protein Importin α . 467, 457–467.
- Sumara, I., and Peter, M. (2007). A Cul3-based E3 ligase regulates mitosis and is required to maintain the spindle assembly checkpoint in human cells. *Cell Cycle* 6, 3004–3010.
- Sumara, I., Vorlaufer, E., Gieffers, C., Peters, B.H., and Peters, J.M. (2000). Characterization of vertebrate cohesin complexes and their regulation in prophase. *J. Cell Biol.* 151, 749–762.

- Sumara, I., Vorlaufer, E., Stukenberg, P.T., Kelm, O., Redemann, N., Nigg, E. a, and Peters, J.-M. (2002). The dissociation of cohesin from chromosomes in prophase is regulated by Polo-like kinase. *Mol. Cell* 9, 515–525.
- Sumara, I., Gime, J.F., Gerlich, D., Hirota, T., Kraft, C., Torre, C. De, Ellenberg, J., and Peters, J. (2004). Roles of Polo-like Kinase 1 in the Assembly of Functional Mitotic Spindles. *14*, 1712–1722.
- Sumara, I., Quadroni, M., Frei, C., Olma, M.H., Sumara, G., Ricci, R., and Peter, M. (2007). A Cul3-based E3 ligase removes Aurora B from mitotic chromosomes, regulating mitotic progression and completion of cytokinesis in human cells. *Dev. Cell* 12, 887–900.
- Sumara, I., Maerki, S., and Peter, M. (2008). E3 ubiquitin ligases and mitosis: embracing the complexity. *Trends Cell Biol.* 18, 84–94.
- Thornton, B.R., and Toczyski, D.P. (2006). Precise destruction: an emerging picture of the APC. *Genes Dev.* 20, 3069–3078.
- Tong, K.I., Katoh, Y., Kusunoki, H., Itoh, K., Tanaka, T., and Yamamoto, M. (2006). Keap1 recruits Neh2 through binding to ETGE and DLG motifs: characterization of the two-site molecular recognition model. *Mol. Cell. Biol.* 26, 2887–2900.
- Toyoshima-morimoto, F., Taniguchi, E., and Shinya, N. (2001). Polo-like kinase 1 phosphorylates cyclin B1 and targets it to the nucleus during prophase. *Nature* 410, 215–220.
- Toyoshima-Morimoto, F., Taniguchi, E., and Nishida, E. (2002). Plk1 promotes nuclear translocation of human Cdc25C during prophase. *EMBO Rep.* 3, 341–348.
- Vigneron, S., Prieto, S., Bernis, C., Labbe, J., Castro, A., and Lorca, T. (2004). Kinetochores: Localization of Spindle Checkpoint Proteins : Who Controls Whom ? □. *15*, 4584–4596.
- Waizenegger, I.C., Hauf, S., Meinke, A., and Peters, J. (2000). Cohesin from Chromosome Arms in Prophase and from Centromeres in Anaphase. *103*, 399–410.

- Wang, C., Deng, L., Hong, M., Akkaraju, G.R., Inoue, J., and Chen, Z.J. (2001). TAK1 is a ubiquitin-dependent kinase of MKK and IKK. *Nature* **412**, 346–351.
- Wang, F., Dai, J., Daum, J.R., Niedzialkowska, E., Banerjee, B., Stukenberg, P.T., Gorbsky, G.J., and Higgins, J.M.G. (2010). Histone H3 Thr-3 phosphorylation by Haspin positions Aurora B at centromeres in mitosis. *Science* **330**, 231–235.
- Wang, Q., Xie, S., Chen, J., Fukasawa, K., Naik, U., Traganos, F., Darzynkiewicz, Z., Jhanwar-uniyal, M., and Dai, W. (2002). Cell Cycle Arrest and Apoptosis Induced by Human Polo-Like Kinase 3 Is Mediated through Perturbation of Microtubule Integrity Cell Cycle Arrest and Apoptosis Induced by Human Polo-Like Kinase 3 Is Mediated through Perturbation of Microtubule Integrity.
- Watanabe, N., Arai, H., Nishihara, Y., Taniguchi, M., Watanabe, N., Hunter, T., and Osada, H. (2004). M-phase kinases induce phospho-dependent ubiquitination of somatic Wee1 by SCFbeta-TrCP. *Proc. Natl. Acad. Sci. U. S. A.* **101**, 4419–4424.
- Welburn, J.P.I., Vleugel, M., Liu, D., Yates, J.R., Lampson, M. a, Fukagawa, T., and Cheeseman, I.M. (2010). Aurora B phosphorylates spatially distinct targets to differentially regulate the kinetochore-microtubule interface. *Mol. Cell* **38**, 383–392.
- Welchman, R.L., Gordon, C., and Mayer, R.J. (2005). Ubiquitin and ubiquitin-like proteins as multifunctional signals. *Nat. Rev. Mol. Cell Biol.* **6**, 599–609.
- Wolfe, B. a, Takaki, T., Petronczki, M., and Glotzer, M. (2009). Polo-like kinase 1 directs assembly of the HsCyk-4 RhoGAP/Ect2 RhoGEF complex to initiate cleavage furrow formation. *PLoS Biol.* **7**, e1000110.
- Wu, K., Chen, a, and Pan, Z.Q. (2000). Conjugation of Nedd8 to CUL1 enhances the ability of the ROC1-CUL1 complex to promote ubiquitin polymerization. *J. Biol. Chem.* **275**, 32317–32324.
- Xie, S., Wu, H., Wang, Q., Cogswell, J.P., Husain, I., Conn, C., Stambrook, P., Jhanwar-Uniyal, M., and Dai, W. (2001). Plk3 functionally links DNA damage to cell cycle arrest and apoptosis at least in part via the p53 pathway. *J. Biol. Chem.* **276**, 43305–43312.

- Xie, S., Wang, Q., Ruan, Q., Liu, T., Jhanwar-Uniyal, M., Guan, K., and Dai, W. (2004). MEK1-induced Golgi dynamics during cell cycle progression is partly mediated by Polo-like kinase-3. *Oncogene* 23, 3822–3829.
- Xu, J., Shen, C., Wang, T., and Quan, J. (2013). Structural basis for the inhibition of Polo-like kinase 1. *Nat. Struct. Mol. Biol.* 20, 1047–1053.
- Xu, L., Wei, Y., Reboul, J., Vaglio, P., Shin, T.-H., Vidal, M., Elledge, S.J., and Harper, J.W. (2003). BTB proteins are substrate-specific adaptors in an SCF-like modular ubiquitin ligase containing CUL-3. *Nature* 425, 316–321.
- Yamagishi, Y., Honda, T., Tanno, Y., and Watanabe, Y. (2010). Two histone marks establish the inner centromere and chromosome bi-orientation. *Science* 330, 239–243.
- Yan, X., Cao, L., Li, Q., Wu, Y., Zhang, H., Saiyin, H., Liu, X., Zhang, X., Shi, Q., and Yu, L. (2005). Aurora C is directly associated with Survivin and required for cytokinesis. *Genes Cells* 10, 617–626.
- Yao, T., and Cohen, R.E. (2002). A cryptic protease couples deubiquitination and degradation by the proteasome. *419*, 403–407.
- Yasui, Y., Urano, T., Kawajiri, A., Nagata, K., Tatsuka, M., Saya, H., Furukawa, K., Takahashi, T., Izawa, I., and Inagaki, M. (2004). Autophosphorylation of a newly identified site of Aurora-B is indispensable for cytokinesis. *J. Biol. Chem.* 279, 12997–13003.
- Yüce, O., Piekny, A., and Glotzer, M. (2005). An ECT2-centralspindlin complex regulates the localization and function of RhoA. *J. Cell Biol.* 170, 571–582.
- Yun, S.-M., Moulaei, T., Lim, D., Bang, J.K., Park, J.-E., Shenoy, S.R., Liu, F., Kang, Y.H., Liao, C., Soung, N.-K., et al. (2009). Structural and functional analyses of minimal phosphopeptides targeting the polo-box domain of polo-like kinase 1. *Nat. Struct. Mol. Biol.* 16, 876–882.

Zhang, X., Lan, W., Ems-mcclung, S.C., Stukenberg, P.T., and Walczak, C.E. (2007). Aurora B Phosphorylates Multiple Sites on Mitotic Centromere-associated Kinesin to Spatially and Temporally Regulate Its Function □. *18*, 3264–3276.

Zhang, X.-Y., Varthi, M., Sykes, S.M., Phillips, C., Warzecha, C., Zhu, W., Wyce, A., Thorne, A.W., Berger, S.L., and McMahon, S.B. (2008). The putative cancer stem cell marker USP22 is a subunit of the human SAGA complex required for activated transcription and cell-cycle progression. *Mol. Cell* 29, 102–111.

Zhao, W.-M., and Fang, G. (2005). Anillin is a substrate of anaphase-promoting complex/cyclosome (APC/C) that controls spatial contractility of myosin during late cytokinesis. *J. Biol. Chem.* 280, 33516–33524.

Zhuang, M., Calabrese, M.F., Liu, J., Waddell, M.B., Nourse, A., Hammel, M., Miller, D.J., Walden, H., Duda, D.M., Seyedin, S.N., et al. (2009). Structures of SPOP-substrate complexes: insights into molecular architectures of BTB-Cul3 ubiquitin ligases. *Mol. Cell* 36, 39–50.

11 Appendix

11.1 Appendix I. List of the 614 hits found in each of four GST-PLK1-PBD pulldowns.

Hits were sorted by decreasing number of peptide spectrum mass (PSM). Coverage, number of peptides identified and number of PSM are shown for each protein identified. In blue are depicted the 108 proteins classified as cell cycle regulators by Functional Annotation Clustering using DAVID Bioinformatics Resources 6.7 from NIAID, NIH.

Uniprot ID	Protein names	Gene names	Length	Score	Coverage (%)	# Peptides	# PSM
Q15365	Poly(rC)-binding protein 1 (Alpha-CP1) (Heterogeneous nuclear ribonucleoprotein E1) (hnRNP E1) (Nucleic acid-binding protein SUB2.3)	PCBP1	356	402,88	68,26	14	100
P49736	DNA replication licensing factor MCM2 (EC 3.6.4.12) (Minichromosome maintenance protein 2 homolog) (Nuclear protein BM28)	MCM2 BM28 CCNL1 CDCL1 KIAA0030	904	387,65	49,45	32	90
P33991	DNA replication licensing factor MCM4 (EC 3.6.4.12) (CDC21 homolog) (P1-CDC21)	MCM4 CDC21	863	362,73	46,58	29	81
Q14566	DNA replication licensing factor MCM6 (EC 3.6.4.12) (p105MCM)	MCM6	821	335,62	44,70	32	78
Q8WX93	Palladin (SIH002) (Sarcoma antigen NY-SAR-77)	PALLD KIAA0992 CGI-151	1383	274,22	32,10	30	65
Q7Z6Z7	E3 ubiquitin-protein ligase HUWE1 (EC 6.3.2.-)	HUWE1 KIAA0312 KIAA1578 URB1	4374	265,69	18,50	50	63
P33993	DNA replication licensing factor MCM7 (EC 3.6.4.12) (CDC47 homolog) (P1.1-MCM3)	MCM7 CDC47 MCM2	719	254,39	59,81	29	61
Q8WUM4	Programmed cell death 6-interacting protein (PDCD6-interacting protein) (ALG-2-interacting protein 1) (ALG-2-interacting protein X) (Hp95)	PDCD6IP AIP1 ALIX KIAA1375	868	240,76	36,75	23	56
Q13509	Tubulin beta-3 chain (Tubulin beta-4 chain) (Tubulin beta-III)	TUBB3 TUBB4	450	209,48	45,56	16	49
P09913	Interferon-induced protein with tetratricopeptide repeats 2 (IFIT-2) (ISG-54 K) (Interferon-induced 54 kDa protein) (IFI-54K) (P54)	IFIT2 CIG-42 G10P2 IFI54 ISG54	472	200,03	46,40	19	45
P23588	Eukaryotic translation initiation factor 4B (eIF-4B)	EIF4B	611	171,31	31,75	15	43
Q14157	Ubiquitin-associated protein 2-like (Protein NICE-4)	UBAP2L KIAA0144 NICE4	1087	176,04	35,23	21	41

Q93052	Lipoma-preferred partner (LIM domain-containing preferred translocation partner in lipoma)	LPP	612	167,54	47,22	14	38
Q9C0C9	Ubiquitin-conjugating enzyme E2 O (EC 6.3.2.19) (Ubiquitin carrier protein O)	UBE2O KIAA1734	1292	152,41	28,48	23	38
P68366	Tubulin alpha-4A chain (Alpha-tubulin 1)	TUBA4A TUBA1	448	160,53	45,31	14	37
Q14C86	GTPase-activating protein and VPS9 domain-containing protein 1 (GAPex-5) (Rab5-activating protein 6)	GAPVD1 GAPEX5 KIAA1521 RAP6	1478	151,31	26,86	25	37
Q9BQE3	Tubulin alpha-1C chain (Alpha-tubulin 6) (Tubulin alpha-6 chain)	TUBA1C TUBA6	449	166,53	54,57	15	37
Q9H3Q1	Cdc42 effector protein 4 (Binder of Rho GTPases 4)	CDC42EP4 BORG4 CEP4	356	166,08	58,71	14	37
O94979	Protein transport protein Sec31A (ABP125) (ABP130) (SEC31-like protein 1) (SEC31-related protein A) (Web1-like protein)	SEC31A KIAA0905 SEC31L1 HSPC275 HSPC334	1220	150,23	30,90	23	36
P51858	Hepatoma-derived growth factor (HDGF) (High mobility group protein 1-like 2) (HMG-1L2)	HDGF HMG1L2	240	162,37	55,00	11	36
O00267	Transcription elongation factor SPT5 (hSPT5) (DRB sensitivity-inducing factor 160 kDa subunit)	SUPT5H SPT5 SPT5H	1087	151,40	33,76	23	35
Q8IWS0	PHD finger protein 6 (PHD-like zinc finger protein)	PHF6 KIAA1823	365	152,64	48,77	14	35
Q96HC4	PDZ and LIM domain protein 5 (Enigma homolog) (Enigma-like PDZ and LIM domains protein)	PDLIM5 ENH L9	596	142,27	43,79	19	35
P25205	DNA replication licensing factor MCM3 (EC 3.6.4.12)	MCM3	808	144,73	43,07	24	34
P49023	Paxillin	PXN	591	136,84	41,46	15	33
O95218	Zinc finger Ran-binding domain-containing protein 2 (Zinc finger protein 265) (Zinc finger, splicing)	ZRANB2 ZIS ZNF265	330	142,18	37,88	17	32
Q6XZF7	Dynamin-binding protein (Scaffold protein Tuba)	DNMBP KIAA1010	1577	139,43	27,52	27	32
Q9UBC2	Epidermal growth factor receptor substrate 15-like 1 (Eps15-related protein) (Eps15R)	EPS15L1 EPS15R	864	130,81	36,57	21	32
P09884	DNA polymerase alpha catalytic subunit (EC 2.7.7.7) (DNA polymerase alpha catalytic subunit p180)	POLA1 POLA	1462	134,18	26,61	26	31
Q16513	Serine/threonine-protein kinase N2 (EC 2.7.11.13) (PKN gamma) (Protein kinase C-like 2) (Protein-kinase C-related kinase 2)	PKN2 PRK2 PRKCL2	984	127,26	34,55	24	31
O60271	C-Jun-amino-terminal kinase-interacting protein 4 (JIP-4) (JNK-interacting protein 4) (Cancer/testis antigen 89) (CT89)	SPAG9 HSS KIAA0516 MAPK8IP4 SYD1 HLC6	1321	121,14	28,39	27	30
Q96KB5	Lymphokine-activated killer T-cell-originated protein kinase (EC 2.7.12.2) (Cancer/testis antigen 84) (CT84)	PBK TOPK	322	123,54	60,25	12	30

Appendix

O75116	Rho-associated protein kinase 2 (EC 2.7.11.1) (Rho kinase 2)	ROCK2 KIAA0619	1388	126,06	22,77	22	29
Q96G74	OTU domain-containing protein 5 (EC 3.4.19.12) (Deubiquitinating enzyme A) (DUBA)	OTUD5	571	131,83	33,10	13	29
O43719	HIV Tat-specific factor 1 (Tat-SF1)	HTATSF1	755	127,74	30,99	16	28
Q9Y383	Putative RNA-binding protein Luc7-like 2	LUC7L2 CGI-59 CGI-74	392	118,46	33,16	13	28
O60566	Mitotic checkpoint serine/threonine-protein kinase BUB1 beta (EC 2.7.11.1) (MAD3/BUB1-related protein kinase) (hBUBR1) (Mitotic checkpoint kinase MAD3L)	BUB1B BUBR1 MAD3L SSK1	1050	115,87	30,10	21	27
O60716	Catenin delta-1 (Cadherin-associated Src substrate) (CAS) (p120 catenin) (p120(ctn)) (p120(cas))	CTNND1 KIAA0384	968	111,35	29,34	19	27
O95819	Mitogen-activated protein kinase kinase kinase kinase 4 (EC 2.7.11.1)	MAP4K4 HGK KIAA0687 NIK	1239	108,24	24,54	18	27
Q68CZ2	Tensin-3 (Tensin-like SH2 domain-containing protein 1) (Tumor endothelial marker 6)	TNS3 TEM6 TENS1 TPP	1445	121,33	30,17	22	27
Q7LBC6	Lysine-specific demethylase 3B (EC 1.14.11.-) (JmjC domain-containing histone demethylation protein 2B) (Jumonji domain-containing protein 1B)	KDM3B C5orf7 JHDM2B JMJD1B KIAA1082	1761	111,68	22,71	21	27
Q9UK59	Lariat debranching enzyme (EC 3.1.-.-)	DBR1	544	105,17	43,75	15	27
Q9ULT8	E3 ubiquitin-protein ligase HECTD1 (EC 6.3.2.-) (E3 ligase for inhibin receptor) (EULIR) (HECT domain-containing protein 1)	HECTD1 KIAA1131	2610	112,90	15,33	23	27
Q7Z5K2	Wings apart-like protein homolog (Friend of EBNA2 protein)	WAPAL FOE KIAA0261 WAPL	1190	105,50	26,13	22	26
Q8N122	Regulatory-associated protein of mTOR (Raptor) (p150 target of rapamycin (TOR)-scaffold protein)	RPTOR KIAA1303 RAPTOR	1335	106,73	21,87	19	26
Q93008	Probable ubiquitin carboxyl-terminal hydrolase FAF-X (EC 3.4.19.12) (Deubiquitinating enzyme FAF-X) (Fat facets in mammals) (hFAM) (USP9X DFFRX FAM USP9	2570	109,28	14,86	23	26
P33992	DNA replication licensing factor MCM5 (EC 3.6.4.12) (CDC46 homolog) (P1-CDC46)	MCM5 CDC46	734	95,87	38,15	19	25
P46937	Yorkie homolog (65 kDa Yes-associated protein) (YAP65)	YAP1 YAP65	504	107,64	46,03	11	25
Q53GT1	Kelch-like protein 22	KLHL22	634	97,27	35,02	14	25
P33176	Kinesin-1 heavy chain (Conventional kinesin heavy chain) (Ubiquitous kinesin heavy chain) (UKHC)	KIF5B KNS KNS1	963	106,95	31,15	22	24
O00148	ATP-dependent RNA helicase DDX39A (EC 3.6.4.13) (DEAD box protein 39) (Nuclear RNA helicase URH49)	DDX39A DDX39	427	103,08	42,39	12	23

Q14974	Importin subunit beta-1 (Importin-90) (Karyopherin subunit beta-1) (Nuclear factor p97) (Pore targeting complex 97 kDa subunit) (PTAC97)	KPNB1 NTF97	876	99,08	28,88	16	23
Q15942	Zyxin (Zyxin-2)	ZYX	572	90,27	26,92	8	23
Q5TDH0	Protein DDI1 homolog 2	DDI2	399	105,13	47,87	11	23
Q8WVG6	MAP kinase-activating death domain protein (Differentially expressed in normal and neoplastic cells)	MADD DENN IG20 KIAA0358	1647	101,48	20,52	17	23
P00533	Epidermal growth factor receptor (EC 2.7.10.1) (Proto-oncogene c-ErbB-1) (Receptor tyrosine- protein kinase erbB-1)	EGFR ERBB ERBB1 HER1	1210	94,96	23,88	17	22
P98082	Disabled homolog 2 (DOC-2) (Differentially- expressed protein 2)	DAB2 DOC2	770	100,53	28,70	14	22
O14617	AP-3 complex subunit delta-1 (AP-3 complex subunit delta) (Adapter-related protein complex 3 subunit delta-1) (Delta-adaptin)	AP3D1 PRO0039	1153	90,20	17,95	16	21
O96006	Zinc finger BED domain-containing protein 1 (Putative Ac-like transposable element) (dREF homolog)	ZBED1 ALTE DREF KIAA0785 TRAMP	694	89,73	30,55	12	21
Q04637	Eukaryotic translation initiation factor 4 gamma 1 (eIF-4-gamma 1) (eIF-4G 1) (eIF-4G1) (p220)	EIF4G1 EIF4F EIF4G EIF4GI	1599	82,96	16,39	16	21
Q86WB0	Nuclear-interacting partner of ALK (Nuclear- interacting partner of anaplastic lymphoma kinase) (hNIPA) (Zinc finger C3HC-type protein 1)	ZC3HC1 NIPA HSPC216	502	87,74	46,22	14	21
Q9BUF5	Tubulin beta-6 chain (Tubulin beta class V)	TUBB6	446	79,24	33,63	9	21
Q9UGP4	LIM domain-containing protein 1	LIMD1	676	97,64	46,01	14	21
O95155	Ubiquitin conjugation factor E4 B (Homozygously deleted in neuroblastoma 1) (Ubiquitin fusion degradation protein 2)	UBE4B HDNB1 KIAA0684 UFD2	1302	87,02	18,97	15	20
P49790	Nuclear pore complex protein Nup153 (153 kDa nucleoporin) (Nucleoporin Nup153)	NUP153	1475	87,42	19,46	15	20
Q12888	Tumor suppressor p53-binding protein 1 (53BP1) (p53-binding protein 1) (p53BP1)	TP53BP1	1972	91,08	18,00	19	20
Q5JSZ5	Protein PRRC2B (HLA-B-associated transcript 2-like 1) (Proline-rich coiled-coil protein 2B)	PRRC2B BAT2L BAT2L1 KIAA0515	2229	89,81	11,26	17	20
Q86TC9	Myopalladin (145 kDa sarcomeric protein)	MYPN MYOP	1320	88,08	21,14	15	20
Q8NCE2	Myotubularin-related protein 14 (EC 3.1.3.-) (HCV NS5A-transactivated protein 4 splice variant A- binding protein 1) (NS5ATP4ABP1) (hJumpy)	MTMR14 C3orf29	650	85,98	28,92	12	20
Q9H0B6	Kinesin light chain 2 (KLC 2)	KLC2	622	78,73	30,39	14	20

Appendix

Q9Y2Z0	Suppressor of G2 allele of SKP1 homolog (Protein 40-6-3) (Sgt1)	SUGT1	365	97,65	42,74	11	20
P45974	Ubiquitin carboxyl-terminal hydrolase 5 (EC 3.4.19.12) (Deubiquitinating enzyme 5) (Isopeptidase T) (Ubiquitin thioesterase 5)	USP5 ISOT	858	75,90	27,62	14	19
Q15742	NGFI-A-binding protein 2 (EGR-1-binding protein 2) (Melanoma-associated delayed early response protein) (Protein MADER)	NAB2 MADER	525	74,94	31,24	12	19
Q2NWX8	DNA excision repair protein ERCC-6-like (EC 3.6.4.12) (ATP-dependent helicase ERCC6-like) (PLK1-interacting checkpoint helicase)	ERCC6L PICH	1250	79,35	18,88	15	19
Q96GX5	Serine/threonine-protein kinase greatwall (GW) (GWL) (hGWL) (EC 2.7.11.1) (Microtubule-associated serine/threonine-protein kinase-like) (MAST-L)	MASTL GW GWL THC2	879	79,09	21,73	12	19
P35658	Nuclear pore complex protein Nup214 (214 kDa nucleoporin) (Nucleoporin Nup214) (Protein CAN)	NUP214 CAIN CAN KIAA0023	2090	74,44	14,16	15	18
P52701	DNA mismatch repair protein Msh6 (hMSH6) (G/T mismatch-binding protein) (GTBP) (GTMBP) (MutS-alpha 160 kDa subunit) (p160)	MSH6 GTBP	1360	72,78	17,06	14	18
Q16204	Coiled-coil domain-containing protein 6 (Papillary thyroid carcinoma-encoded protein) (Protein H4)	CCDC6 D10S170 TST1	474	81,34	20,04	7	18
Q7KZ85	Transcription elongation factor SPT6 (hSPT6) (Histone chaperone suppressor of Ty6) (Tat-cotransactivator 2 protein) (Tat-CT2 protein)	SUPT6H KIAA0162 SPT6H	1726	81,89	14,83	15	18
Q96F86	Enhancer of mRNA-decapping protein 3 (LSM16 homolog) (YjeF N-terminal domain-containing protein 2) (YjeF_N2) (hYjeF_N2)	EDC3 LSM16 YJDC YJEFN2 PP844	508	72,08	37,40	12	18
Q96SU4	Oxysterol-binding protein-related protein 9 (ORP-9) (OSBP-related protein 9)	OSBPL9 ORP9 OSBP4	736	76,84	25,95	12	18
Q99590	Protein SCAF11 (CTD-associated SR protein 11) (Renal carcinoma antigen NY-REN-40) (SC35-interacting protein 1) (SR-related and CTD-associated factor 11)	SCAF11 CASP11 SFRS2IP SIP1 SRSF2IP	1463	79,23	14,42	12	18
Q9H6Z4	Ran-binding protein 3 (RanBP3)	RANBP3	567	81,25	25,04	10	18
Q9H773	dCTP pyrophosphatase 1 (EC 3.6.1.12) (Deoxycytidine-triphosphatase 1) (dCTPase 1) (RS21C6) (XTP3-transactivated gene A protein)	DCTPP1 XTP3TPA CDA03	170	68,51	71,76	9	18
Q9UDY2	Tight junction protein ZO-2 (Tight junction protein 2) (Zona occludens protein 2) (Zonula occludens protein 2)	TJP2 X104 ZO2	1190	76,69	16,64	14	18
O43865	Putative adenosylhomocysteinase 2 (AdoHcyase 2) (EC 3.3.1.1) (DC-expressed AHCY-like molecule) (S-adenosyl-L-homocysteine hydrolase 2)	AHCYL1 DCAL XPVKONA	530	69,80	27,36	9	17

P49454	Centromere protein F (CENP-F) (AH antigen) (Kinetochore protein CENPF) (Mitotin)	CENPF	3210	70,14	6,20	14	17
P53621	Coatamer subunit alpha (Alpha-coat protein) (Alpha-COP) (HEP-COP) (HEPCOP) [Cleaved into: Xenin (Xenopsin-related peptide); Proxenin]	COPA	1224	69,66	20,83	17	17
Q08499	cAMP-specific 3',5'-cyclic phosphodiesterase 4D (EC 3.1.4.53) (DPDE3) (PDE43)	PDE4D DPDE3	809	74,44	17,55	10	17
Q8TEU7	Rap guanine nucleotide exchange factor 6 (PDZ domain-containing guanine nucleotide exchange factor 2) (PDZ-GEF2) (RA-GEF-2)	RAPGEF6 PDZGEF2	1601	71,87	19,18	17	17
Q8TEW0	Partitioning defective 3 homolog (PAR-3) (PARD-3) (Atypical PKC isotype-specific-interacting protein) (ASIP) (CTCL tumor antigen se2-5) (PAR3-alpha)	PARD3 PAR3 PAR3A	1356	69,99	12,24	11	17
O95235	Kinesin-like protein KIF20A (GG10_2) (Mitotic kinesin-like protein 2) (MKlp2) (Rab6-interacting kinesin-like protein) (Rabkinesin-6)	KIF20A MKLP2 RAB6KIFL	890	69,52	29,55	16	16
P15170	Eukaryotic peptide chain release factor GTP-binding subunit ERF3A (Eukaryotic peptide chain release factor subunit 3a) (eRF3a) (G1 to S phase transition protein 1 homolog)	GSPT1 ERF3A	499	67,84	34,67	11	16
P15923	Transcription factor E2-alpha (Class B basic helix-loop-helix protein 21) (bHLHb21) (Immunoglobulin enhancer-binding factor E12/E47)	TCF3 BHLHB21 E2A ITF1	654	61,97	26,61	9	16
P49643	DNA primase large subunit (EC 2.7.7.-) (DNA primase 58 kDa subunit) (p58)	PRIM2 PRIM2A	509	65,29	33,01	11	16
P50542	Peroxisomal targeting signal 1 receptor (PTS1 receptor) (PTS1R) (PTS1-BP) (Peroxin-5) (Peroxisomal C-terminal targeting signal import receptor)	PEX5 PXR1	639	79,28	35,05	12	16
Q15398	Disks large-associated protein 5 (DAP-5) (Discs large homolog 7) (Disks large-associated protein DLG7) (Hepatoma up-regulated protein) (HURP)	DLGAP5 DLG7 KIAA0008	846	64,91	22,93	12	16
Q69YN2	CWF19-like protein 1	CWF19L1	538	70,35	39,78	13	16
Q9BSJ8	Extended synaptotagmin-1 (E-Syt1) (Membrane-bound C2 domain-containing protein)	ESYT1 FAM62A KIAA0747 MBC2	1104	60,81	17,39	13	16
Q9BTE3	Mini-chromosome maintenance complex-binding protein (MCM-BP) (MCM-binding protein)	MCMBP C10orf119	642	72,64	28,66	12	16
Q9Y2U5	Mitogen-activated protein kinase kinase kinase 2 (EC 2.7.11.25) (MAPK/ERK kinase kinase 2) (MEK kinase 2) (MEKK 2)	MAP3K2 MAPKKK2 MEKK2	619	64,53	34,73	13	16
Q9Y4H2	Insulin receptor substrate 2 (IRS-2)	IRS2	1338	68,24	15,77	13	16
O60333	Kinesin-like protein KIF1B (Klp)	KIF1B KIAA0591 KIAA1448	1816	63,42	13,16	14	15

Appendix

O60749	Sorting nexin-2 (Transformation-related gene 9 protein) (TRG-9)	SNX2 TRG9	519	61,90	32,56	13	15
O75694	Nuclear pore complex protein Nup155 (155 kDa nucleoporin) (Nucleoporin Nup155)	NUP155 KIAA0791	1391	69,78	12,80	11	15
O95251	Histone acetyltransferase KAT7 (EC 2.3.1.48) (Histone acetyltransferase binding to ORC1) (Lysine acetyltransferase 7)	KAT7 HBO1 HBOa MYST2	611	61,46	24,22	10	15
P29966	Myristoylated alanine-rich C-kinase substrate (MARCKS) (Protein kinase C substrate, 80 kDa protein, light chain) (80K-L protein) (PKCSL)	MARCKS MACS PRKCSL	332	68,51	34,64	8	15
P35606	Coatomer subunit beta' (Beta'-coat protein) (Beta'-COP) (p102)	COPB2	906	59,68	25,17	15	15
P51003	Poly(A) polymerase alpha (PAP-alpha) (EC 2.7.7.19) (Polynucleotide adenyltransferase alpha)	PAPOLA PAP	745	59,15	25,10	11	15
P52564	Dual specificity mitogen-activated protein kinase kinase 6 (MAP kinase kinase 6) (MAPKK 6) (EC 2.7.12.2) (MAPK/ERK kinase 6) (MEK 6)	MAP2K6 MEK6 MKK6 PRKMK6 SKK3	334	66,18	34,73	8	15
Q14674	Separin (EC 3.4.22.49) (Caspase-like protein ESPL1) (Extra spindle poles-like 1 protein) (Separase)	ESPL1 ESP1 KIAA0165	2120	62,82	10,24	13	15
Q15393	Splicing factor 3B subunit 3 (Pre-mRNA-splicing factor SF3b 130 kDa subunit) (SF3b130) (STAF130) (Spliceosome-associated protein 130) (SAP 130)	SF3B3 KIAA0017 SAP130	1217	69,04	14,79	11	15
Q32MZ4	Leucine-rich repeat flightless-interacting protein 1 (LRR FLII-interacting protein 1) (GC-binding factor 2) (TAR RNA-interacting protein)	LRRFIP1 GCF2 TRIP	808	68,16	25,99	13	15
Q5H9R7	Serine/threonine-protein phosphatase 6 regulatory subunit 3 (SAPS domain family member 3) (Sporulation-induced transcript 4-associated protein SAPL)	PPP6R3 C11orf23 KIAA1558 PP6R3 SAPL SAPS3	873	61,38	21,42	13	15
Q96EB6	NAD-dependent protein deacetylase sirtuin-1 (hSIRT1) (EC 3.5.1.-) (Regulatory protein SIR2 homolog 1) (SIR2-like protein 1) (hSIR2)	SIRT1 SIR2L1	747	68,19	28,65	12	15
Q96I24	Far upstream element-binding protein 3 (FUSE-binding protein 3)	FUBP3 FBP3	572	59,01	33,39	12	15
Q9UNZ2	NSFL1 cofactor p47 (UBX domain-containing protein 2C) (p97 cofactor p47)	NSFL1C UBXN2C	370	60,41	34,59	9	15
Q9Y2W1	Thyroid hormone receptor-associated protein 3 (Thyroid hormone receptor-associated protein complex 150 kDa component) (Trap150)	THRAP3 TRAP150	955	57,40	18,95	13	15
A0JNW5	UHRF1-binding protein 1-like	UHRF1BP1L KIAA0701	1464	64,06	14,75	12	14
O00750	Phosphatidylinositol 4-phosphate 3-kinase C2 domain-containing subunit beta (PI3K-C2-beta) (PtdIns-3-kinase C2 subunit beta)	PIK3C2B	1634	65,42	14,44	14	14

O75122	CLIP-associating protein 2 (Cytoplasmic linker-associated protein 2) (Protein Orbit homolog 2) (hOrbit2)	CLASP2 KIAA0627	1294	64,02	13,45	12	14
O95487	Protein transport protein Sec24B (SEC24-related protein B)	SEC24B	1268	63,72	16,80	12	14
O95628	CCR4-NOT transcription complex subunit 4 (EC 6.3.2.-) (CCR4-associated factor 4) (E3 ubiquitin-protein ligase CNOT4) (Potential transcriptional repressor NOT4Hp)	CNOT4 NOT4	575	63,96	36,35	12	14
Q14671	Pumilio homolog 1 (HsPUM) (Pumilio-1)	PUM1 KIAA0099 PUMH1	1186	61,99	13,66	10	14
Q15437	Protein transport protein Sec23B (SEC23-related protein B)	SEC23B	767	60,53	22,43	11	14
Q5T4S7	E3 ubiquitin-protein ligase UBR4 (EC 6.3.2.-) (600 kDa retinoblastoma protein-associated factor) (N-recognin-4)	UBR4 KIAA0462 KIAA1307 RBAF600 ZUBR1	5183	58,32	4,92	12	14
Q5VZ89	DENN domain-containing protein 4C	DENND4C C9orf55 C9orf55B	1673	56,72	13,39	13	14
Q8WWM7	Ataxin-2-like protein (Ataxin-2 domain protein) (Ataxin-2-related protein)	ATXN2L A2D A2LG A2LP A2RP	1075	55,77	13,77	11	14
Q9NRR5	Ubiquitin-4 (Ataxin-1 interacting ubiquitin-like protein) (A1Up) (Ataxin-1 ubiquitin-like-interacting protein A1U)	UBQLN4 C1orf6 CIP75 UBIN	601	70,38	21,30	8	14
Q9NRY4	Rho GTPase-activating protein 35 (Glucocorticoid receptor DNA-binding factor 1) (Glucocorticoid receptor repression factor 1) (GRF-1)	ARHGAP35 GRF1 GRLF1 KIAA1722	1499	60,21	15,61	13	14
O14545	TRAF-type zinc finger domain-containing protein 1 (Protein FLN29)	TRAFD1 FLN29	582	51,94	25,43	10	13
O60504	Vinexin (SH3-containing adapter molecule 1) (SCAM-1) (Sorbin and SH3 domain-containing protein 3)	SORBS3 SCAM1	671	53,15	26,83	12	13
O94782	Ubiquitin carboxyl-terminal hydrolase 1 (EC 3.4.19.12) (Deubiquitinating enzyme 1) (hUBP) (Ubiquitin thioesterase 1)	USP1	785	57,13	20,89	12	13
P26639	Threonine--tRNA ligase, cytoplasmic (EC 6.1.1.3) (Threonyl-tRNA synthetase) (ThrRS)	TARS	723	52,95	22,96	10	13
P42566	Epidermal growth factor receptor substrate 15 (Protein Eps15) (Protein AF-1p)	EPS15 AF1P	896	58,69	21,54	11	13
Q5T6F2	Ubiquitin-associated protein 2 (UBAP-2)	UBAP2 KIAA1491	1119	54,89	16,62	11	13
Q5VT52	Regulation of nuclear pre-mRNA domain-containing protein 2	RPRD2 KIAA0460 HSPC099	1461	55,59	14,37	11	13
Q7Z309	Protein FAM122B	FAM122B	247	52,04	46,15	7	13

Appendix

Q8NFA0	Ubiquitin carboxyl-terminal hydrolase 32 (EC 3.4.19.12) (Deubiquitinating enzyme 32) (Renal carcinoma antigen NY-REN-60)	USP32 USP10	1604	56,35	12,72	11	13
Q8WUF5	RelA-associated inhibitor (Inhibitor of ASPP protein) (Protein iASPP) (NFkB-interacting protein 1) (PPP1R13B-like protein)	PPP1R13L IASPP NKIP1 PPP1R13BL RAI	828	49,32	21,01	10	13
Q92625	Ankyrin repeat and SAM domain-containing protein 1A (Odin)	ANKS1A ANKS1 KIAA0229 ODIN	1134	61,81	14,81	9	13
Q96K76	Ubiquitin carboxyl-terminal hydrolase 47 (EC 3.4.19.12) (Deubiquitinating enzyme 47) (Ubiquitin thioesterase 47)	USP47	1375	60,27	14,25	13	13
Q96RE7	Nucleus accumbens-associated protein 1 (NAC-1) (BTB/POZ domain-containing protein 14B)	NAC1 BTBD14B NAC1	527	53,79	31,31	12	13
Q96S55	ATPase WRNIP1 (EC 3.6.1.3) (Werner helicase-interacting protein 1)	WRNIP1 WHIP	665	52,22	32,33	12	13
Q9C0B0	RING finger protein unkempt homolog (Zinc finger CCH domain-containing protein 5)	UNK KIAA1753 ZC3H5 ZC3HDC5	810	56,46	21,98	10	13
Q9Y485	DmX-like protein 1 (X-like 1 protein)	DMXL1 XL1	3027	57,05	7,00	11	13
Q9Y4B4	Helicase ARIP4 (EC 3.6.4.12) (Androgen receptor-interacting protein 4) (RAD54-like protein 2)	RAD54L2 ARIP4 KIAA0809	1467	64,08	13,70	11	13
O00410	Importin-5 (Imp5) (Importin subunit beta-3) (Karyopherin beta-3) (Ran-binding protein 5) (RanBP5)	IPO5 KPNB3 RANBP5	1097	56,06	15,22	9	12
O43684	Mitotic checkpoint protein BUB3	BUB3	328	54,70	46,95	7	12
P23497	Nuclear autoantigen Sp-100 (Nuclear dot-associated Sp100 protein) (Speckled 100 kDa)	SP100	879	53,91	13,08	8	12
P28702	Retinoic acid receptor RXR-beta (Nuclear receptor subfamily 2 group B member 2) (Retinoid X receptor beta)	RXRBB NR2B2	533	49,51	31,71	10	12
P31350	Ribonucleoside-diphosphate reductase subunit M2 (EC 1.17.4.1) (Ribonucleotide reductase small chain) (Ribonucleotide reductase small subunit)	RRM2 RR2	389	46,05	25,96	7	12
Q00653	Nuclear factor NF-kappa-B p100 subunit (DNA-binding factor KBF2) (H2TF1) (Lymphocyte translocation chromosome 10 protein)	NFKB2 LYT10	900	49,61	18,67	11	12
Q07866	Kinesin light chain 1 (KLC 1)	KLC1 KLC KNS2	573	48,96	20,59	8	12
Q13131	5'-AMP-activated protein kinase catalytic subunit alpha-1 (AMPK subunit alpha-1) (EC 2.7.11.1) (Acetyl-CoA carboxylase kinase) (ACACA kinase)	PRKAA1 AMPK1	559	52,13	25,94	9	12
Q13506	NGFI-A-binding protein 1 (EGR-1-binding protein 1) (Transcriptional regulatory protein p54)	NAB1	487	54,79	29,77	9	12

Q14192	Four and a half LIM domains protein 2 (FHL-2) (LIM domain protein DRAL) (Skeletal muscle LIM-protein 3) (SLIM-3)	FHL2 DRAL SLIM3	279	51,79	48,03	8	12
Q14498	RNA-binding protein 39 (Hepatocellular carcinoma protein 1) (RNA-binding motif protein 39) (RNA-binding region-containing protein 2)	RBM39 HCC1 RNPC2	530	50,83	29,43	10	12
Q14839	Chromodomain-helicase-DNA-binding protein 4 (CHD-4) (EC 3.6.4.12) (ATP-dependent helicase CHD4) (Mi-2 autoantigen 218 kDa protein) (Mi2-beta)	CHD4	1912	46,51	9,57	10	12
Q86VP6	Cullin-associated NEDD8-dissociated protein 1 (Cullin-associated and neddylation-dissociated protein 1) (TBP-interacting protein of 120 kDa A)	CAND1 KIAA0829 TIP120 TIP120A	1230	44,81	14,39	12	12
Q8NI08	Nuclear receptor coactivator 7 (140 kDa estrogen receptor-associated protein) (Estrogen nuclear receptor coactivator 1)	NCOA7 ERAP140 ESNA1 Nbla00052 Nbla10993	942	49,22	22,19	12	12
Q92783	Signal transducing adapter molecule 1 (STAM-1)	STAM STAM1	540	51,90	24,07	8	12
Q99700	Ataxin-2 (Spinocerebellar ataxia type 2 protein) (Trinucleotide repeat-containing gene 13 protein)	ATXN2 ATX2 SCA2 TNRC13	1313	45,86	7,84	7	12
Q9H0G5	Nuclear speckle splicing regulatory protein 1 (Coiled-coil domain-containing protein 55) (Nuclear speckle-related protein 70) (NSrp70)	NSRP1 CCDC55 NSRP70	558	50,18	17,92	8	12
Q9Y5X1	Sorting nexin-9 (SH3 and PX domain-containing protein 1) (Protein SDP1) (SH3 and PX domain-containing protein 3A)	SNX9 SH3PX1 SH3PXD3A	595	47,77	35,63	11	12
Q43823	A-kinase anchor protein 8 (AKAP-8) (A-kinase anchor protein 95 kDa) (AKAP 95)	AKAP8 AKAP95	692	53,80	21,24	8	11
O75717	WD repeat and HMG-box DNA-binding protein 1 (Acidic nucleoplasmic DNA-binding protein 1) (And-1)	WDHD1 AND1	1129	49,88	14,17	10	11
P38432	Coilin (p80)	COIL CLN80	576	48,72	12,15	6	11
P49840	Glycogen synthase kinase-3 alpha (GSK-3 alpha) (EC 2.7.11.26) (Serine/threonine-protein kinase GSK3A) (EC 2.7.11.1)	GSK3A	483	43,64	19,25	6	11
Q00613	Heat shock factor protein 1 (HSF 1) (Heat shock transcription factor 1) (HSTF 1)	HSF1 HSTF1	529	43,43	19,28	7	11
Q04726	Transducin-like enhancer protein 3 (Enhancer of split groucho-like protein 3) (ESG3)	TLE3 KIAA1547	772	42,64	20,21	9	11
Q05397	Focal adhesion kinase 1 (FADK 1) (EC 2.7.10.2) (Focal adhesion kinase-related nonkinase) (FRNK) (Protein phosphatase 1 regulatory subunit 71) (PPP1R71)	PTK2 FAK FAK1	1052	39,76	14,83	9	11

Appendix

Q13409	Cytoplasmic dynein 1 intermediate chain 2 (Cytoplasmic dynein intermediate chain 2) (Dynein intermediate chain 2, cytosolic) (DH IC-2)	DYNC112 DNCI2 DNCIC2	638	45,89	29,94	9	11
Q14697	Neutral alpha-glucosidase AB (EC 3.2.1.84) (Alpha-glucosidase 2) (Glucosidase II subunit alpha)	GANAB G2AN KIAA0088	944	46,92	14,94	9	11
Q8IWR0	Zinc finger CCCH domain-containing protein 7A	ZC3H7A ZC3H7 ZC3HDC7 HSPC055	971	44,39	16,48	10	11
Q8TAF3	WD repeat-containing protein 48 (USP1-associated factor 1) (WD repeat endosomal protein) (p80)	WDR48 KIAA1449 UAF1	677	43,87	18,32	9	11
Q92995	Ubiquitin carboxyl-terminal hydrolase 13 (EC 3.4.19.12) (Deubiquitinating enzyme 13) (Isopeptidase T-3) (ISOT-3) (Ubiquitin thioesterase 13)	USP13 ISOT3	863	50,54	19,58	9	11
Q99081	Transcription factor 12 (TCF-12) (Class B basic helix-loop-helix protein 20) (bHLHb20) (DNA-binding protein HTF4) (E-box-binding protein)	TCF12 BHLHB20 HEB HTF4	682	45,87	30,79	9	11
Q99570	Phosphoinositide 3-kinase regulatory subunit 4 (PI3-kinase regulatory subunit 4) (EC 2.7.11.1) (PI3-kinase p150 subunit)	PIK3R4	1358	44,18	12,67	10	11
Q9BX66	Sorbin and SH3 domain-containing protein 1 (Ponsin) (SH3 domain protein 5) (SH3P12) (c-Cbl-associated protein) (CAP)	SORBS1 KIAA0894 KIAA1296 SH3D5	1292	44,77	11,22	10	11
Q9H8V3	Protein ECT2 (Epithelial cell-transforming sequence 2 oncogene)	ECT2	914	46,19	13,24	8	11
Q9P0K7	Ankyrin repeat and coiled-coil structure-containing protein (Novel retinal pigment epithelial cell protein) (Retinoic acid-induced protein 14)	RAI14 KIAA1334 NORPEG	980	45,50	13,78	10	11
Q9UHD8	Septin-9 (MLL septin-like fusion protein MSF-A) (MLL septin-like fusion protein) (Ovarian/Breast septin) (Ov/Br septin) (Septin D1)	SEPT9 KIAA0991 MSF	586	43,11	27,30	9	11
Q9UKG1	DCC-interacting protein 13-alpha (Dip13-alpha) (Adapter protein containing PH domain, PTB domain and leucine zipper motif 1)	APPL1 APPL DIP13A KIAA1428	709	47,69	21,58	10	11
Q9Y6Q9	Nuclear receptor coactivator 3 (NCoA-3) (EC 2.3.1.48) (ACTR) (Amplified in breast cancer 1 protein) (AIB-1) (CBP-interacting protein) (pCIP)	NCOA3 AIB1 BHLHE42 RAC3 TRAM1	1424	48,32	12,78	11	11
O14641	Segment polarity protein dishevelled homolog DVL-2 (Dishevelled-2) (DSH homolog 2)	DVL2	736	40,93	19,29	8	10
O14964	Hepatocyte growth factor-regulated tyrosine kinase substrate (Hrs) (Protein pp110)	HGS HRS	777	37,18	13,00	9	10
O43314	Inositol hexakisphosphate and diphosphoinositol-pentakisphosphate kinase 2 (EC 2.7.4.21)	PIIP5K2 HISPPD1 KIAA0433 VIP2	1243	43,00	12,23	10	10
O75113	NEDD4-binding protein 1 (N4BP1)	N4BP1 KIAA0615	896	42,83	13,06	7	10

O75179	Ankyrin repeat domain-containing protein 17 (Gene trap ankyrin repeat protein) (Serologically defined breast cancer antigen NY-BR-16)	ANKRD17 GTAR KIAA0697	2603	39,51	6,88	9	10
P11532	Dystrophin	DMD	3685	38,91	3,93	10	10
P68400	Casein kinase II subunit alpha (CK II alpha) (EC 2.7.11.1)	CSNK2A1 CK2A1	391	47,46	29,67	7	10
P78347	General transcription factor II-I (GTFII-I) (TFII-I) (Bruton tyrosine kinase-associated protein 135) (BAP-135) (BTK-associated protein 135)	GTF2I BAP135 WBSCR6	998	43,48	12,32	8	10
P82094	TATA element modulatory factor (TMF) (Androgen receptor coactivator 160 kDa protein) (Androgen receptor-associated protein of 160 kDa)	TMF1 ARA160	1093	39,65	12,08	10	10
Q03252	Lamin-B2	LMNB2 LMN2	600	38,39	17,50	9	10
Q13428	Treacle protein (Treacher Collins syndrome protein)	TCOF1	1488	35,77	6,99	8	10
Q13439	Golgin subfamily A member 4 (256 kDa golgin) (Golgin-245) (Protein 72.1) (Trans-Golgi p230)	GOLGA4	2230	39,51	6,73	10	10
Q5W0B1	RING finger protein 219	RNF219 C13orf7	726	43,55	18,73	9	10
Q7L2J0	7SK snRNA methylphosphate capping enzyme (MePCE) (EC 2.1.1.-) (Bicoid-interacting protein 3 homolog) (Bin3 homolog)	MEPCE BCDIN3	689	39,00	21,77	9	10
Q7L576	Cytoplasmic FMR1-interacting protein 1 (Specifically Rac1-associated protein 1) (Sra-1) (p140sra-1)	CYFIP1 KIAA0068	1253	39,86	9,74	9	10
Q86W92	Liprin-beta-1 (Protein tyrosine phosphatase receptor type f polypeptide-interacting protein-binding protein 1) (PTPRF-interacting protein-binding protein 1)	PPFIBP1 KIAA1230	1011	39,19	14,54	10	10
Q8IWX8	Calcium homeostasis endoplasmic reticulum protein (ERPROT 213-21) (SR-related CTD-associated factor 6)	CHERP DAN26 SCAF6	916	38,80	19,65	9	10
Q8IX03	Protein KIBRA (HBeAg-binding protein 3) (Kidney and brain protein) (KIBRA) (WW domain-containing protein 1)	WWC1 KIAA0869	1113	39,97	12,40	8	10
Q8N3F8	MICAL-like protein 1 (Molecule interacting with Rab13) (MIRab13)	MICALL1 KIAA1668 MIRAB13	863	44,36	15,87	8	10
Q8NEY1	Neuron navigator 1 (Pore membrane and/or filament-interacting-like protein 3) (Steerin-1) (Unc-53 homolog 1) (unc53H1)	NAV1 KIAA1151 KIAA1213 POMFIL3 STEERIN1	1877	46,06	6,77	8	10
Q8WUM0	Nuclear pore complex protein Nup133 (133 kDa nucleoporin) (Nucleoporin Nup133)	NUP133	1156	44,98	13,84	9	10
Q99575	Ribonucleases P/MRP protein subunit POP1 (hPOP1) (EC 3.1.26.5)	POP1 KIAA0061	1024	42,53	16,60	10	10

Appendix

Q9BXB4	Oxysterol-binding protein-related protein 11 (ORP-11) (OSBP-related protein 11)	OSBPL11 ORP11 OSBP12	747	39,88	19,81	10	10
Q9HC35	Echinoderm microtubule-associated protein-like 4 (EMAP-4) (Restrictedly overexpressed proliferation-associated protein) (Ropp 120)	EML4 C2orf2 EMAPL4	981	40,23	10,70	8	10
Q9NRA8	Eukaryotic translation initiation factor 4E transporter (4E-T) (eIF4E transporter) (Eukaryotic translation initiation factor 4E nuclear import factor 1)	EIF4ENIF1	985	40,39	13,20	8	10
Q9P270	SLAIN motif-containing protein 2	SLAIN2 KIAA1458	581	43,46	32,19	9	10
Q9UQR0	Sex comb on midleg-like protein 2	SCML2	700	42,00	25,00	10	10
Q9UQR1	Zinc finger protein 148 (Transcription factor ZBP-89) (Zinc finger DNA-binding protein 89)	ZNF148 ZBP89	794	47,56	17,38	8	10
Q9Y613	FH1/FH2 domain-containing protein 1 (Formin homolog overexpressed in spleen 1) (FHOS) (Formin homology 2 domain-containing protein 1)	FHOD1 FHOS FHOS1	1164	46,05	10,22	7	10
Q9Y678	Coatomer subunit gamma-1 (Gamma-1-coat protein) (Gamma-1-COP)	COPG1 COPG	874	47,42	21,40	10	10
O15027	Protein transport protein Sec16A (SEC16 homolog A)	SEC16A KIAA0310 SEC16 SEC16L	2179	40,09	8,26	6	9
O60216	Double-strand-break repair protein rad21 homolog (hHR21) (Nuclear matrix protein 1) (NXP-1) (SCC1 homolog)	RAD21 HR21 KIAA0078 NXP1	631	36,55	23,61	8	9
O95359	Transforming acidic coiled-coil-containing protein 2 (Anti-Zuai-1) (AZU-1)	TACC2	2948	37,91	4,10	7	9
P19793	Retinoic acid receptor RXR-alpha (Nuclear receptor subfamily 2 group B member 1) (Retinoid X receptor alpha)	RXRA NR2B1	462	34,80	20,35	8	9
P20810	Calpastatin (Calpain inhibitor) (Sperm BS-17 component)	CAST	708	43,89	17,51	7	9
P27540	Aryl hydrocarbon receptor nuclear translocator (ARNT protein) (Class E basic helix-loop-helix protein 2) (bHLHe2) (Dioxin receptor, nuclear translocator)	ARNT BHLHE2	789	40,97	18,12	7	9
P38398	Breast cancer type 1 susceptibility protein (EC 6.3.2.-) (RING finger protein 53)	BRCA1 RNF53	1863	36,25	8,80	9	9
P49642	DNA primase small subunit (EC 2.7.7.-) (DNA primase 49 kDa subunit) (p49)	PRIM1	420	38,11	23,10	8	9
Q08AD1	Calmodulin-regulated spectrin-associated protein 2 (Calmodulin-regulated spectrin-associated protein 1-like protein 1)	CAMSAP2 CAMSAP1L1 KIAA1078	1489	32,73	10,01	8	9

Q09028	Histone-binding protein RBBP4 (Chromatin assembly factor 1 subunit C) (CAF-1 subunit C) (Chromatin assembly factor I p48 subunit) (CAF-I 48 kDa subunit)	RBBP4 RBAP48	425	34,01	45,88	8	9
Q12800	Alpha-globin transcription factor CP2 (SAA3 enhancer factor) (Transcription factor LSF)	TFCP2 LSF SEF	502	41,79	22,11	7	9
Q12857	Nuclear factor 1 A-type (NF1-A) (Nuclear factor 1/A) (CCAAT-box-binding transcription factor) (CTF) (Nuclear factor I/A) (NF-I/A) (NFI-A)	NFIA KIAA1439	509	35,92	26,13	7	9
Q13620	Cullin-4B (CUL-4B)	CUL4B KIAA0695	913	39,53	10,51	7	9
Q14181	DNA polymerase alpha subunit B (DNA polymerase alpha 70 kDa subunit)	POLA2	598	38,00	20,74	7	9
Q5TKA1	Protein lin-9 homolog (HuLin-9) (hLin-9) (Beta subunit-associated regulator of apoptosis) (TUDOR gene similar protein)	LIN9 BARA TGS	542	39,19	27,49	9	9
Q66K14	TBC1 domain family member 9B	TBC1D9B KIAA0676	1250	34,46	9,76	8	9
Q7Z4S6	Kinesin-like protein KIF21A (Kinesin-like protein KIF2) (Renal carcinoma antigen NY-REN-62)	KIF21A KIAA1708 KIF2	1674	38,22	7,65	7	9
Q7Z5J4	Retinoic acid-induced protein 1	RAI1 KIAA1820	1906	40,58	6,51	7	9
Q86SQ0	Pleckstrin homology-like domain family B member 2 (Protein LL5-beta)	PHLDB2 LL5B	1253	32,44	11,17	9	9
Q8N163	Cell cycle and apoptosis regulator protein 2 (Cell division cycle and apoptosis regulator protein 2)	CCAR2 DBC1 KIAA1967	923	44,74	14,08	6	9
Q8TEM1	Nuclear pore membrane glycoprotein 210 (Nuclear pore protein gp210) (Nuclear envelope pore membrane protein POM 210) (POM210)	NUP210 KIAA0906 PSEC0245	1887	38,70	7,21	9	9
Q96TA1	Niban-like protein 1 (Meg-3) (Melanoma invasion by ERK) (MINERVA) (Protein FAM129B)	FAM129B C9orf88	746	35,81	16,22	9	9
Q9BSV6	tRNA-splicing endonuclease subunit Sen34 (EC 3.1.27.9) (Leukocyte receptor cluster member 5) (tRNA-intron endonuclease Sen34) (HsSen34)	TSEN34 LENG5 SEN34	310	39,67	38,71	6	9
Q9H089	Large subunit GTPase 1 homolog (hLsg1) (EC 3.6.1.-)	LSG1	658	36,49	20,52	8	9
Q9NYL2	Mitogen-activated protein kinase kinase kinase MLT (EC 2.7.11.25) (Human cervical cancer suppressor gene 4 protein) (HCCS-4)	MLTK ZAK HCCS4	800	41,73	16,00	8	9
Q9UQE7	Structural maintenance of chromosomes protein 3 (SMC protein 3) (SMC-3) (Basement membrane-associated chondroitin proteoglycan)	SMC3 BAM BMH CSPG6 SMC3L1	1217	39,99	10,27	8	9
A3KN83	Protein strawberry notch homolog 1 (Monocyte protein 3) (MOP-3)	SBNO1 MOP3	1393	35,02	7,82	8	8

Appendix

O00203	AP-3 complex subunit beta-1 (Adapter-related protein complex 3 subunit beta-1) (Adaptor protein complex AP-3 subunit beta-1) (Beta-3A-adaptin)	AP3B1 ADTB3A	1094	34,18	9,87	7	8
O14776	Transcription elongation regulator 1 (TATA box-binding protein-associated factor 2S) (Transcription factor CA150)	TCERG1 CA150 TAF2S	1098	32,71	10,66	8	8
O43175	D-3-phosphoglycerate dehydrogenase (3-PGDH) (EC 1.1.1.95)	PHGDH PGDH3	533	31,57	15,95	6	8
O60343	TBC1 domain family member 4 (Akt substrate of 160 kDa) (AS160)	TBC1D4 AS160 KIAA0603	1298	32,71	8,63	8	8
O75376	Nuclear receptor corepressor 1 (N-CoR) (N-CoR1)	NCOR1 KIAA1047	2440	29,45	5,90	8	8
O75496	Geminin	GMNN	209	38,74	27,27	4	8
P11274	Breakpoint cluster region protein (EC 2.7.11.1) (Renal carcinoma antigen NY-REN-26)	BCR BCR1 D22S11	1271	38,46	9,36	6	8
P30260	Cell division cycle protein 27 homolog (Anaphase-promoting complex subunit 3) (APC3) (CDC27 homolog) (CDC27Hs) (H-NUC)	CDC27 ANAPC3 D0S1430E D17S978E	824	33,10	17,11	8	8
P36776	Lon protease homolog, mitochondrial (EC 3.4.21.-) (LONHs) (Lon protease-like protein) (LONP) (Mitochondrial ATP-dependent protease Lon)	LONP1 PRSS15	959	31,76	11,68	8	8
P40425	Pre-B-cell leukemia transcription factor 2 (Homeobox protein PBX2) (Protein G17)	PBX2 G17	430	35,87	34,19	7	8
P42167	Lamina-associated polypeptide 2, isoforms beta/gamma (Thymopoietin, isoforms beta/gamma) (TP beta/gamma)	TMPO LAP2	454	38,21	26,65	7	8
Q00587	Cdc42 effector protein 1 (Binder of Rho GTPases 5) (Serum protein MSE55)	CDC42EP1 BORG5 CEP1 MSE55	391	31,81	26,60	6	8
Q14680	Maternal embryonic leucine zipper kinase (hMELK) (EC 2.7.11.1) (Protein kinase Eg3) (pEg3 kinase) (Protein kinase PK38) (hPK38)	MELK KIAA0175	651	31,07	14,44	6	8
Q14683	Structural maintenance of chromosomes protein 1A (SMC protein 1A) (SMC-1-alpha) (SMC-1A) (Sb1.8)	SMC1A DXS423E KIAA0178 SB1.8 SMC1 SMC1L1	1233	37,67	6,65	6	8
Q15019	Septin-2 (Neural precursor cell expressed developmentally down-regulated protein 5) (NEDD-5)	SEPT2 DIFF6 KIAA0158 NEDD5	361	32,54	36,57	8	8
Q16181	Septin-7 (CDC10 protein homolog)	SEPT7 CDC10	437	30,38	17,85	6	8
Q6VY07	Phosphofurin acidic cluster sorting protein 1 (PACS-1)	PACS1 KIAA1175	963	33,13	13,71	8	8
Q7L7X3	Serine/threonine-protein kinase TAO1 (EC 2.7.11.1) (Kinase from chicken homolog B) (hKFC-B) (MARK Kinase) (MARKK)	TAOK1 KIAA1361 MAP3K16 MARKK	1001	36,63	9,49	6	8

Q7Z6J9	tRNA-splicing endonuclease subunit Sen54 (SEN54 homolog) (HsSEN54) (tRNA-intron endonuclease Sen54)	TSEN54 SEN54	526	39,37	18,06	6	8
Q8IWW6	Rho GTPase-activating protein 12 (Rho-type GTPase-activating protein 12)	ARHGAP12	846	35,01	14,30	7	8
Q8N1F7	Nuclear pore complex protein Nup93 (93 kDa nucleoporin) (Nucleoporin Nup93)	NUP93 KIAA0095	819	38,49	10,99	5	8
Q8NCE0	tRNA-splicing endonuclease subunit Sen2 (EC 3.1.27.9) (tRNA-intron endonuclease Sen2) (HsSen2)	TSEN2 SEN2	465	28,15	25,38	8	8
Q8ND04	Protein SMG8 (Amplified in breast cancer gene 2 protein) (Protein smg-8 homolog)	SMG8 ABC2 C17orf71	991	34,20	14,33	7	8
Q8TD19	Serine/threonine-protein kinase Nek9 (EC 2.7.11.1) (Nercc1 kinase) (Never in mitosis A-related kinase 9) (NimA-related protein kinase 9)	NEK9 KIAA1995 NEK8 NERCC	979	35,32	13,69	7	8
Q92997	Segment polarity protein dishevelled homolog DVL-3 (Dishevelled-3) (DSH homolog 3)	DVL3 KIAA0208	716	31,68	15,22	5	8
Q96B97	SH3 domain-containing kinase-binding protein 1 (CD2-binding protein 3) (CD2BP3) (Cbl-interacting protein of 85 kDa)	SH3KBP1 CIN85	665	36,62	17,29	6	8
Q96C12	Armadillo repeat-containing protein 5	ARMC5	935	32,76	10,27	6	8
Q96I18	Leucine-rich repeat and calponin homology domain-containing protein 3	LRCH3	777	34,92	17,25	7	8
Q96JM3	Chromosome alignment-maintaining phosphoprotein 1 (Zinc finger protein 828)	CHAMP1 C13orf8 CAMP KIAA1802 ZNF828	812	34,26	12,32	7	8
Q96KG9	N-terminal kinase-like protein (Coated vesicle-associated kinase of 90 kDa) (SCY1-like protein 1) (Telomerase regulation-associated protein)	SCYL1 CVAK90 GKLP NTKL TAPK TEIF TRAP HT019	808	32,89	14,85	8	8
Q9BTC0	Death-inducer obliterator 1 (DIO-1) (hDido1) (Death-associated transcription factor 1) (DATF-1)	DIDO1 C20orf158 DATF1 KIAA0333	2240	44,53	5,58	6	8
Q9BWU0	Kanadaplin (Human lung cancer oncogene 3 protein) (HLC-3) (Kidney anion exchanger adapter protein)	SLC4A1AP HLC3	796	39,84	10,55	5	8
Q9BYX2	TBC1 domain family member 2A (Armus) (Prostate antigen recognized and identified by SEREX 1)	TBC1D2 PARIS1 PP8997 TBC1D2A	928	35,24	12,61	8	8
Q9C0H5	Rho GTPase-activating protein 39	ARHGAP39 KIAA1688	1083	34,98	11,36	7	8
Q9H0D6	5'-3' exoribonuclease 2 (EC 3.1.13.-) (DHM1-like protein) (DHP protein)	XRN2	950	31,35	13,58	8	8
Q9H0W8	Protein SMG9 (Protein smg-9 homolog)	SMG9 C19orf61	520	31,56	20,77	7	8
Q9H6U6	Breast carcinoma-amplified sequence 3 (GAOB1)	BCAS3	928	34,11	15,95	8	8

Appendix

Q9NQC3	Reticulon-4 (Foocen) (Neurite outgrowth inhibitor) (Nogo protein) (Neuroendocrine-specific protein) (NSP) (Neuroendocrine-specific protein C homolog) (RTN4 KIAA0886 NOMO My043 SP1507	1192	36,90	6,80	4	8
Q9NTI5	Sister chromatid cohesion protein PDS5 homolog B (Androgen-induced proliferation inhibitor)	PDS5B APRIN AS3 KIAA0979	1447	31,81	6,84	7	8
Q9NYZ3	G2 and S phase-expressed protein 1 (GTSE-1) (Protein B99 homolog)	GTSE1	720	35,76	9,17	4	8
Q9UJX3	Anaphase-promoting complex subunit 7 (APC7) (Cyclosome subunit 7)	ANAPC7 APC7	599	33,61	15,19	6	8
Q9UKV3	Apoptotic chromatin condensation inducer in the nucleus (Acinus)	ACIN1 ACINUS KIAA0670	1341	33,78	11,48	8	8
Q9UNH7	Sorting nexin-6 (TRAF4-associated factor 2) [Cleaved into: Sorting nexin-6, N-terminally processed]	SNX6	406	30,98	23,15	7	8
Q9UPT8	Zinc finger CCCH domain-containing protein 4	ZC3H4 C19orf7 KIAA1064	1303	36,84	9,98	7	8
Q9Y5K6	CD2-associated protein (Adapter protein CMS) (Cas ligand with multiple SH3 domains)	CD2AP	639	30,23	17,53	8	8
Q9Y6Y0	Influenza virus NS1A-binding protein (NS1-BP) (NS1-binding protein) (Aryl hydrocarbon receptor-associated protein 3)	IVNS1ABP ARA3 FLARA3 KIAA0850 NS1 NS1BP HSPC068	642	34,89	20,72	7	8
O00629	Importin subunit alpha-3 (Importin alpha Q1) (Qip1) (Karyopherin subunit alpha-4)	KPNA4 QIP1	521	31,99	24,57	6	7
O00712	Nuclear factor 1 B-type (NF1-B) (Nuclear factor 1/B) (CCAAT-box-binding transcription factor) (CTF) (Nuclear factor I/B) (NF-I/B) (NFI-B)	NFIB	420	27,06	20,00	5	7
O43399	Tumor protein D54 (hD54) (Tumor protein D52-like 2)	TPD52L2	206	29,62	49,51	7	7
O43482	Protein Mis18-beta (Cancer/testis antigen 86) (CT86) (Opa-interacting protein 5) (OIP-5)	OIP5 MIS18B	229	30,12	40,17	5	7
O95071	E3 ubiquitin-protein ligase UBR5 (EC 6.3.2.-) (E3 ubiquitin-protein ligase, HECT domain-containing 1) (Hyperplastic discs protein homolog) (hHYD)	UBR5 EDD EDD1 HYD KIAA0896	2799	26,83	3,97	6	7
P29372	DNA-3-methyladenine glycosylase (EC 3.2.2.21) (3-alkyladenine DNA glycosylase) (3-methyladenine DNA glycosidase) (ADPG)	MPG AAG ANPG MID1	298	29,68	33,89	6	7
P47755	F-actin-capping protein subunit alpha-2 (CapZ alpha-2)	CAPZA2	286	28,98	33,57	5	7
P49354	Protein farnesyltransferase/geranylgeranyltransferase type-1 subunit alpha (EC 2.5.1.58) (EC 2.5.1.59) (CAAX farnesyltransferase subunit alpha) (FTase-alpha)	FNTA	379	28,67	27,70	7	7
P53992	Protein transport protein Sec24C (SEC24-related protein C)	SEC24C KIAA0079	1094	30,85	9,69	7	7

P54132	Bloom syndrome protein (EC 3.6.4.12) (DNA helicase, RecQ-like type 2) (RecQ2) (RecQ protein-like 3)	BLM RECQ2 RECQL3	1417	35,56	7,41	6	7
P54619	5'-AMP-activated protein kinase subunit gamma-1 (AMPK gamma1) (AMPK subunit gamma-1) (AMPKg)	PRKAG1	331	23,58	25,38	7	7
P62820	Ras-related protein Rab-1A (YPT1-related protein)	RAB1A RAB1	205	32,68	41,95	6	7
Q07889	Son of sevenless homolog 1 (SOS-1)	SOS1	1333	29,94	6,00	6	7
Q13200	26S proteasome non-ATPase regulatory subunit 2 (26S proteasome regulatory subunit RPN1) (26S proteasome regulatory subunit S2)	PSMD2 TRAP2	908	27,86	11,45	7	7
Q13492	Phosphatidylinositol-binding clathrin assembly protein (Clathrin assembly lymphoid myeloid leukemia protein)	PICALM CALM	652	32,33	16,56	5	7
Q14432	cGMP-inhibited 3',5'-cyclic phosphodiesterase A (EC 3.1.4.17) (Cyclic GMP-inhibited phosphodiesterase A) (CGI-PDE A)	PDE3A	1141	31,52	8,24	5	7
Q14493	Histone RNA hairpin-binding protein (Histone stem-loop-binding protein)	SLBP HBP	270	29,55	16,67	3	7
Q14694	Ubiquitin carboxyl-terminal hydrolase 10 (EC 3.4.19.12) (Deubiquitinating enzyme 10) (Ubiquitin thioesterase 10)	USP10 KIAA0190	798	29,33	12,41	6	7
Q14966	Zinc finger protein 638 (Cutaneous T-cell lymphoma-associated antigen se33-1) (CTCL-associated antigen se33-1) (Nuclear protein 220)	ZNF638 NP220 ZFML	1978	26,10	5,36	6	7
Q15436	Protein transport protein Sec23A (SEC23-related protein A)	SEC23A	765	26,25	12,55	7	7
Q15796	Mothers against decapentaplegic homolog 2 (MAD homolog 2) (Mothers against DPP homolog 2) (JV18-1) (Mad-related protein 2) (hMAD-2)	SMAD2 MADH2 MADR2	467	28,35	19,91	7	7
Q6FI81	Anamorsin (Cytokine-induced apoptosis inhibitor 1) (Fe-S cluster assembly protein DRE2 homolog)	CIAPIN1 CUA001 PRO0915	312	28,10	22,44	5	7
Q6NZY4	Zinc finger CCHC domain-containing protein 8	ZCCHC8	707	31,78	15,28	6	7
Q86YV5	Tyrosine-protein kinase Sgk223 (EC 2.7.10.2) (Sugen kinase 223)	SGK223	1402	30,82	8,27	6	7
Q8IYB3	Serine/arginine repetitive matrix protein 1 (SR-related nuclear matrix protein of 160 kDa) (SRm160) (Ser/Arg-related nuclear matrix protein)	SRRM1 SRM160	904	30,81	5,97	6	7
Q8N6T3	ADP-ribosylation factor GTPase-activating protein 1 (ARF GAP 1) (ADP-ribosylation factor 1 GTPase-activating protein) (ARF1 GAP)	ARFGAP1 ARF1GAP	406	31,39	18,47	4	7
Q8N8S7	Protein enabled homolog	ENAH MENA	591	32,47	13,03	6	7

Appendix

Q8WVV9	Heterogeneous nuclear ribonucleoprotein L-like (hnRNPLL) (Stromal RNA-regulating factor)	HNRNPLL HNRPLL SRRF BLOCK24	542	29,00	20,66	7	7
Q92613	Protein Jade-3 (PHD finger protein 16)	PHF16 JADE3 KIAA0215	823	30,43	14,09	6	7
Q969G3	SWI/SNF-related matrix-associated actin-dependent regulator of chromatin subfamily E member 1 (BRG1-associated factor 57) (BAF57)	SMARCE1 BAF57	411	29,14	25,55	6	7
Q96EP5	DAZ-associated protein 1 (Deleted in azoospermia-associated protein 1)	DAZAP1	407	31,64	20,15	5	7
Q96RT1	Protein LAP2 (Densin-180-like protein) (Erbp2-interacting protein) (Erbin)	ERBB2IP ERBIN KIAA1225 LAP2	1412	28,92	7,86	6	7
Q96S82	Ubiquitin-like protein 7 (Bone marrow stromal cell ubiquitin-like protein) (BMSC-UbP) (Ubiquitin-like protein SB132)	UBL7 BMSCUBP SB132	380	29,44	24,47	5	7
Q99496	E3 ubiquitin-protein ligase RING2 (EC 6.3.2.-) (Huntingtin-interacting protein 2-interacting protein 3) (HIP2-interacting protein 3) (Protein DinG)	RNF2 BAP1 DING HIP13 RING1B	336	28,40	28,87	7	7
Q99961	Endophilin-A2 (EEN fusion partner of MLL) (Endophilin-2) (Extra eleven-nineteen leukemia fusion gene protein) (EEN) (SH3 domain protein 2B)	SH3GL1 CNSA1 SH3D2B	368	29,02	20,11	5	7
Q9BXB5	Oxysterol-binding protein-related protein 10 (ORP-10) (OSBP-related protein 10)	OSBPL10 ORP10 OSBP9	764	26,54	13,48	7	7
Q9NP74	Palmdelphin (Paralemmelin-like protein)	PALMD C1orf11 PALML	551	26,44	22,69	6	7
Q9NXV6	CDKN2A-interacting protein (Collaborator of ARF)	CDKN2AIP CARF	580	31,66	17,76	6	7
Q9NZJ0	Denticleless protein homolog (DDB1- and CUL4-associated factor 2) (Lethal(2) denticleless protein homolog)	DTL CDT2 CDW1 DCAF2 L2DTL RAMP	730	30,82	14,66	6	7
Q9ULR3	Protein phosphatase 1H (EC 3.1.3.16)	PPM1H ARHCL1 KIAA1157 URCC2	514	30,85	21,40	6	7
Q9ULW0	Targeting protein for Xklp2 (Differentially expressed in cancerous and non-cancerous lung cells 2) (DIL-2) (Hepatocellular carcinoma-associated antigen 519) (TPX2 C20orf1 C20orf2 DIL2 HCA519	747	29,20	14,06	6	7
Q9UMX0	Ubiquilin-1 (Protein linking IAP with cytoskeleton 1) (PLIC-1) (hPLIC-1)	UBQLN1 DA41 PLIC1	589	35,46	11,54	4	7
Q9Y2T2	AP-3 complex subunit mu-1 (AP-3 adapter complex mu3A subunit) (Adapter-related protein complex 3 subunit mu-1) (Mu-adaptin 3A) (Mu3A-adaptin)	AP3M1	418	32,20	26,56	6	7
Q9Y5P4	Collagen type IV alpha-3-binding protein (Ceramide transfer protein) (hCERT) (Goodpasture antigen-binding protein) (GPBP)	COL4A3BP CERT STARD11	624	28,44	14,58	6	7

O00743	Serine/threonine-protein phosphatase 6 catalytic subunit (PPP6C) (EC 3.1.3.16)	PPP6C PPP6	305	28,60	26,23	5	6
O15042	U2 snRNP-associated SURP motif-containing protein (140 kDa Ser/Arg-rich domain protein)	U2SURP KIAA0332 SR140	1029	33,23	8,94	5	6
O60573	Eukaryotic translation initiation factor 4E type 2 (eIF-4E type 2) (eIF4E type 2) (Eukaryotic translation initiation factor 4E homologous protein)	EIF4E2 EIF4EL3	245	21,29	13,88	3	6
P04150	Glucocorticoid receptor (GR) (Nuclear receptor subfamily 3 group C member 1)	NR3C1 GRL	777	24,04	11,45	6	6
P05556	Integrin beta-1 (Fibronectin receptor subunit beta) (Glycoprotein IIa) (GPIIA) (VLA-4 subunit beta) (CD antigen CD29)	ITGB1 FNRB MDF2 MSK12	798	24,57	8,90	4	6
P14618	Pyruvate kinase PKM (EC 2.7.1.40) (Cytosolic thyroid hormone-binding protein) (CTHBP) (Opa-interacting protein 3) (OIP-3)	PKM OIP3 PK2 PK3 PKM2	531	29,16	18,46	6	6
P25054	Adenomatous polyposis coli protein (Protein APC) (Deleted in polyposis 2.5)	APC DP2.5	2843	28,49	4,05	6	6
P29590	Protein PML (Promyelocytic leukemia protein) (RING finger protein 71) (Tripartite motif-containing protein 19)	PML MYL PP8675 RNF71 TRIM19	882	24,68	9,75	6	6
P30307	M-phase inducer phosphatase 3 (EC 3.1.3.48) (Dual specificity phosphatase Cdc25C)	CDC25C	473	28,07	10,36	3	6
P41743	Protein kinase C iota type (EC 2.7.11.13) (Atypical protein kinase C-lambda/iota) (PRKC-lambda/iota) (PRKCI DXS1179E	596	26,24	11,41	4	6
P49750	YLP motif-containing protein 1 (Nuclear protein ZAP3) (ZAP113)	YLPM1 C14orf170 ZAP3	1951	22,67	3,95	6	6
P52948	Nuclear pore complex protein Nup98-Nup96 [Cleaved into: Nuclear pore complex protein Nup98 (98 kDa nucleoporin) (Nucleoporin Nup98) (Nup98)]	NUP98 ADAR2	1817	26,73	4,79	6	6
Q04917	14-3-3 protein eta (Protein AS1)	YWHAH YWHA1	246	22,97	20,73	4	6
Q06265	Exosome complex component RRP45 (Autoantigen PM/Sc1 1) (Exosome component 9)	EXOSC9 PMSCL1	439	26,60	18,45	6	6
Q06587	E3 ubiquitin-protein ligase RING1 (EC 6.3.2.-) (Polycomb complex protein RING1) (RING finger protein 1) (Really interesting new gene 1 protein)	RING1 RNF1	406	29,34	22,91	5	6
Q12968	Nuclear factor of activated T-cells, cytoplasmic 3 (NF-ATc3) (NFATc3) (NFATx) (T-cell transcription factor NFAT4) (NF-AT4)	NFATC3 NFAT4	1075	28,04	10,33	5	6
Q15596	Nuclear receptor coactivator 2 (NCoA-2) (Class E basic helix-loop-helix protein 75) (bHLHe75) (Transcriptional intermediary factor 2) (hTIF2)	NCOA2 BHLHE75 TIF2	1464	24,00	5,60	5	6

Appendix

Q6P2E9	Enhancer of mRNA-decapping protein 4 (Autoantigen Ge-1) (Autoantigen RCD-8) (Human enhancer of decapping large subunit) (Hedls)	EDC4 HEDLS	1401	25,10	5,85	4	6
Q71RC2	La-related protein 4 (La ribonucleoprotein domain family member 4)	LARP4 PP13296	724	25,06	13,95	6	6
Q8N3D4	EH domain-binding protein 1-like protein 1	EHBP1L1	1523	28,52	5,06	4	6
Q8NFH5	Nucleoporin NUP53 (35 kDa nucleoporin) (Mitotic phosphoprotein 44) (MP-44) (Nuclear pore complex protein Nup53) (Nucleoporin Nup35)	NUP35 MP44 NUP53	326	30,08	24,23	4	6
Q8WUA2	Peptidyl-prolyl cis-trans isomerase-like 4 (PPIase) (EC 5.2.1.8) (Cyclophilin-like protein PPIL4) (Rotamase PPIL4)	PPIL4	492	29,09	14,84	5	6
Q92609	TBC1 domain family member 5	TBC1D5 KIAA0210	795	29,85	13,46	5	6
Q92900	Regulator of nonsense transcripts 1 (EC 3.6.4.-) (ATP-dependent helicase RENT1) (Nonsense mRNA reducing factor 1) (NORF1)	UPF1 KIAA0221 RENT1	1129	24,02	8,24	6	6
Q93009	Ubiquitin carboxyl-terminal hydrolase 7 (EC 3.4.19.12) (Deubiquitinating enzyme 7) (Herpesvirus-associated ubiquitin-specific protease)	USP7 HAUSP	1102	21,48	9,17	6	6
Q96G46	tRNA-dihydrouridine(47) synthase [NAD(P)(+)]-like (EC 1.3.1.-) (tRNA-dihydrouridine synthase 3-like)	DUS3L	650	25,92	12,46	5	6
Q96RL1	BRCA1-A complex subunit RAP80 (Receptor-associated protein 80) (Retinoid X receptor-interacting protein 110)	UIMC1 RAP80 RXRIP110	719	25,86	11,27	5	6
Q9H4G0	Band 4.1-like protein 1 (Neuronal protein 4.1) (4.1N)	EPB41L1 KIAA0338	881	26,33	10,90	6	6
Q9H4L5	Oxysterol-binding protein-related protein 3 (ORP-3) (OSBP-related protein 3)	OSBPL3 KIAA0704 ORP3 OSBP3	887	28,13	8,12	5	6
Q9NYP9	Protein Mis18-alpha (FAPP1-associated protein 1)	MIS18A C21orf45 C21orf46 FASP1	233	27,57	33,91	4	6
Q9NZI7	Upstream-binding protein 1 (Transcription factor LBP-1)	UBP1 LBP1	540	31,83	16,85	5	6
Q9Y4E6	WD repeat-containing protein 7 (Rabconnectin-3 beta) (TGF-beta resistance-associated protein TRAG)	WDR7 KIAA0541 TRAG	1490	27,08	6,51	6	6
Q9Y6A5	Transforming acidic coiled-coil-containing protein 3 (ERIC-1)	TACC3 ERIC1	838	21,69	10,62	6	6
Q9Y6X3	MAU2 chromatid cohesion factor homolog (MAU-2) (Cohesin loading complex subunit SCC4 homolog)	MAU2 KIAA0892 SCC4	613	25,09	15,99	5	6
Q9Y6Y8	SEC23-interacting protein (p125)	SEC23IP MSTP053	1000	24,88	8,30	6	6

O00512	B-cell CLL/lymphoma 9 protein (B-cell lymphoma 9 protein) (Bcl-9) (Protein legless homolog)	BCL9	1426	18,56	6,10	4	5
O14936	Peripheral plasma membrane protein CASK (hCASK) (EC 2.7.11.1) (Calcium/calmodulin-dependent serine protein kinase) (Protein lin-2 homolog)	CASK LIN2	926	21,40	8,10	5	5
O43852	Calumenin (Crocalbin) (IEF SSP 9302)	CALU	315	23,21	24,44	5	5
O95219	Sorting nexin-4	SNX4	450	19,61	12,44	5	5
O95429	BAG family molecular chaperone regulator 4 (BAG-4) (Bcl-2-associated athanogene 4) (Silencer of death domains)	BAG4 SODD	457	21,64	14,00	4	5
P08621	U1 small nuclear ribonucleoprotein 70 kDa (U1 snRNP 70 kDa) (U1-70K) (snRNP70)	SNRNP70 RNP1Z RPU1 SNRP70 U1AP1	437	23,38	19,22	4	5
P08651	Nuclear factor 1 C-type (NF1-C) (Nuclear factor 1/C) (CCAAT-box-binding transcription factor) (CTF) (Nuclear factor I/C) (NF-I/C) (NFI-C)	NFIC NFI	508	21,18	13,78	4	5
P30291	Wee1-like protein kinase (WEE1hu) (EC 2.7.10.2) (Wee1A kinase)	WEE1	646	24,00	8,98	3	5
P31327	Carbamoyl-phosphate synthase [ammonia], mitochondrial (EC 6.3.4.16) (Carbamoyl-phosphate synthetase I) (CPSase I)	CPS1	1500	21,19	5,93	5	5
P32519	ETS-related transcription factor Elf-1 (E74-like factor 1)	ELF1	619	25,97	14,86	4	5
P35226	Polycomb complex protein BMI-1 (Polycomb group RING finger protein 4) (RING finger protein 51)	BMI1 PCGF4 RNF51	326	24,92	16,87	3	5
P60842	Eukaryotic initiation factor 4A-I (eIF-4A-I) (eIF4A-I) (EC 3.6.4.13) (ATP-dependent RNA helicase eIF4A-1)	EIF4A1 DDX2A EIF4A	406	23,14	16,01	4	5
P61289	Proteasome activator complex subunit 3 (11S regulator complex subunit gamma) (REG-gamma) (Activator of multicatalytic protease subunit 3)	PSME3	254	23,19	20,87	4	5
P63010	AP-2 complex subunit beta (AP105B) (Adapter-related protein complex 2 subunit beta) (Adaptor protein complex AP-2 subunit beta) (Beta-2-adaptin)	AP2B1 ADTB2 CLAPB1	937	21,61	9,61	5	5
Q00341	Vigilin (High density lipoprotein-binding protein) (HDL-binding protein)	HDLBP HBP VGL	1268	19,95	5,84	5	5
Q13017	Rho GTPase-activating protein 5 (Rho-type GTPase-activating protein 5) (p190-B)	ARHGAP5 RHOGAP5	1502	21,71	4,59	4	5
Q13045	Protein flightless-1 homolog	FLII FLIL	1269	22,22	4,65	3	5
Q13164	Mitogen-activated protein kinase 7 (MAP kinase 7) (MAPK 7) (EC 2.7.11.24) (Big MAP kinase 1) (BMK-1) (Extracellular signal-regulated kinase 5) (ERK-5)	MAPK7 BMK1 ERK5 PRKM7	816	18,63	6,86	3	5

Appendix

Q13425	Beta-2-syntrophin (59 kDa dystrophin-associated protein A1 basic component 2) (Syntrophin-3) (SNT3) (Syntrophin-like) (SNTL)	SNTB2 D16S2531E SNT2B2 SNTL	540	20,09	14,81	5	5
Q14677	Clathrin interactor 1 (Clathrin-interacting protein localized in the trans-Golgi region) (Clint) (Enthoprotin) (Epsin-4) (Epsin-related protein) (EpsinR)	CLINT1 ENTH EPN4 EPNR KIAA0171	625	19,87	11,68	5	5
Q15020	Squamous cell carcinoma antigen recognized by T-cells 3 (SART-3) (hSART-3) (Tat-interacting protein of 110 kDa) (Tip110)	SART3 KIAA0156 TIP110	963	17,85	6,33	4	5
Q15424	Scaffold attachment factor B1 (SAF-B) (SAF-B1) (HSP27 estrogen response element-TATA box-binding protein) (HSP27 ERE-TATA-binding protein)	SAFB HAP HET SAFB1	915	21,91	5,57	4	5
Q4V328	GRIP1-associated protein 1 (GRASP-1)	GRIPAP1 KIAA1167	841	22,51	9,63	5	5
Q5T5U3	Rho GTPase-activating protein 21 (Rho GTPase-activating protein 10) (Rho-type GTPase-activating protein 21)	ARHGAP21 ARHGAP10 KIAA1424	1957	21,99	4,34	5	5
Q68DK7	Male-specific lethal 1 homolog (MSL-1) (Male-specific lethal 1-like 1) (MSL1-like 1) (Male-specific lethal-1 homolog 1)	MSL1 MSL1L1	614	23,20	7,33	3	5
Q6PKG0	La-related protein 1 (La ribonucleoprotein domain family member 1)	LARP1 KIAA0731 LARP	1096	20,39	5,75	4	5
Q6ULP2	Aftiphilin	AFTPH AFTH	937	19,77	6,51	5	5
Q6Y7W6	PERQ amino acid-rich with GYF domain-containing protein 2 (GRB10-interacting GYF protein 2) (Trinucleotide repeat-containing gene 15 protein)	GIGYF2 KIAA0642 PERQ2 TNRC15	1299	21,77	6,24	4	5
Q7Z401	C-myc promoter-binding protein (DENN domain-containing protein 4A)	DENND4A IRLB MYCPBP	1863	26,05	5,15	5	5
Q7Z460	CLIP-associating protein 1 (Cytoplasmic linker-associated protein 1) (Multiple asters homolog 1) (Protein Orbit homolog 1) (hOrbit1)	CLASP1 KIAA0622 MAST1	1538	22,25	4,16	4	5
Q7Z569	BRCA1-associated protein (EC 6.3.2.-) (BRAP2) (Impedes mitogenic signal propagation) (IMP) (RING finger protein 52) (Renal carcinoma antigen NY-REN-63)	BRAP RNF52	592	21,98	11,66	5	5
Q86UE8	Serine/threonine-protein kinase tousled-like 2 (EC 2.7.11.1) (HsHPK) (PKU-alpha) (Tousled-like kinase 2)	TLK2	772	20,33	11,53	5	5
Q86WP2	Vasculin (GC-rich promoter-binding protein 1) (Vascular wall-linked protein)	GPBP1 GPBP SSH6	473	21,87	20,08	5	5
Q86XL3	Ankyrin repeat and LEM domain-containing protein 2 (LEM domain-containing protein 4)	ANKLE2 KIAA0692 LEM4	938	21,94	9,17	5	5

Q86YS7	C2 domain-containing protein 5 (C2 domain-containing phosphoprotein of 138 kDa)	C2CD5 CDP138 KIAA0528	1000	22,47	8,30	4	5
Q8IW35	Centrosomal protein of 97 kDa (Cep97) (Leucine-rich repeat and IQ domain-containing protein 2)	CEP97 LRRIQ2	865	19,86	12,37	5	5
Q8N573	Oxidation resistance protein 1	OXR1 Nbla00307	874	22,84	9,38	5	5
Q8NB46	Serine/threonine-protein phosphatase 6 regulatory ankyrin repeat subunit C (PP6-ARS-C)	ANKRD52	1076	23,54	6,88	3	5
Q8NB90	Spermatogenesis-associated protein 5 (ATPase family protein 2 homolog) (Spermatogenesis-associated factor protein)	SPATA5 AFG2 SPAF	893	22,22	7,95	4	5
Q8NDI1	EH domain-binding protein 1	EHBP1 KIAA0903 NACSIN	1231	22,28	6,01	4	5
Q8WUA4	General transcription factor 3C polypeptide 2 (TF3C-beta) (Transcription factor IIIC 110 kDa subunit) (TFIIIC 110 kDa subunit) (TFIIIC110)	GTF3C2 KIAA0011	911	21,24	8,34	4	5
Q92834	X-linked retinitis pigmentosa GTPase regulator	RPGR RP3 XLRP3	1020	24,75	8,14	4	5
Q96D71	RalBP1-associated Eps domain-containing protein 1 (RalBP1-interacting protein 1)	REPS1	796	19,56	11,56	5	5
Q96JP5	E3 ubiquitin-protein ligase ZFP91 (EC 6.3.2.-) (Zinc finger protein 757) (Zinc finger protein 91 homolog) (Zfp-91)	ZFP91 ZNF757 FKSG11	570	18,50	5,96	2	5
Q96N21	AP-4 complex accessory subunit tepsin (ENTH domain-containing protein 2) (Epsin for AP-4) (Tetra-epsin)	ENTHD2 C17orf56	525	19,91	16,00	5	5
Q99567	Nuclear pore complex protein Nup88 (88 kDa nucleoporin) (Nucleoporin Nup88)	NUP88	741	20,80	6,61	3	5
Q9BRD0	BUD13 homolog	BUD13	619	19,69	11,95	5	5
Q9BSU1	UPF0183 protein C16orf70	C16orf70 C16orf6	422	20,02	14,45	3	5
Q9BUT9	Protein FAM195A	FAM195A C16orf14	160	25,88	42,50	3	5
Q9BZL6	Serine/threonine-protein kinase D2 (EC 2.7.11.13) (nPKC-D2)	PRKD2 PKD2 HSPC187	878	19,58	7,06	4	5
Q9H9A7	RecQ-mediated genome instability protein 1 (BLM-associated protein of 75 kDa) (BLAP75) (FAAP75)	RMI1 C9orf76	625	26,01	12,64	5	5
Q9UBQ5	Eukaryotic translation initiation factor 3 subunit K (eIF3k) (Eukaryotic translation initiation factor 3 subunit 12) (Muscle-specific gene M9 protein)	EIF3K EIF3S12 ARG134 HSPC029 MSTP001 PTD001	218	21,45	33,03	4	5
Q9UHB7	AF4/FMR2 family member 4 (ALL1-fused gene from chromosome 5q31 protein) (Protein AF-5q31) (Major CDK9 elongation factor-associated protein)	AFF4 AF5Q31 MCEF HSPC092	1163	19,95	6,19	5	5

Appendix

Q9UHI6	Probable ATP-dependent RNA helicase DDX20 (EC 3.6.4.13) (Component of gems 3) (DEAD box protein 20) (DEAD box protein DP 103) (Gemin-3)	DDX20 DP103 GEMIN3	824	18,45	5,70	3	5
Q9UKI8	Serine/threonine-protein kinase tousled-like 1 (EC 2.7.11.1) (PKU-beta) (Tousled-like kinase 1)	TLK1 KIAA0137	766	20,58	7,70	4	5
Q9UPN9	E3 ubiquitin-protein ligase TRIM33 (EC 6.3.2.-) (Ectodermin homolog) (RET-fused gene 7 protein) (TRIM33 KIAA1113 RFG7 TIF1G	1127	22,68	7,63	5	5
Q9Y2A7	Nck-associated protein 1 (NAP 1) (Membrane-associated protein HEM-2) (p125Nap1)	NCKAP1 HEM2 KIAA0587 NAP1	1128	20,63	5,14	4	5
Q9Y4G8	Rap guanine nucleotide exchange factor 2 (Cyclic nucleotide ras GEF) (CNrasGEF) (Neural RAP guanine nucleotide exchange protein) (nRap GEP)	RAPGEF2 KIAA0313 NRAPGEP PDZGEF1	1499	19,82	5,00	5	5
O14497	AT-rich interactive domain-containing protein 1A (ARID domain-containing protein 1A) (B120) (BRG1-associated factor 250) (BAF250)	ARID1A BAF250 BAF250A C1orf4 OSA1 SMARCF1	2285	21,22	2,45	3	4
O15226	NF-kappa-B-repressing factor (NFkB-repressing factor) (Protein ITBA4) (Transcription factor NRF)	NKRF ITBA4 NRF	690	17,28	9,42	4	4
O43683	Mitotic checkpoint serine/threonine-protein kinase BUB1 (hBUB1) (EC 2.7.11.1) (BUB1A)	BUB1 BUB1L	1085	15,77	6,27	4	4
O75175	CCR4-NOT transcription complex subunit 3 (CCR4-associated factor 3) (Leukocyte receptor cluster member 2)	CNOT3 KIAA0691 LENG2 NOT3	753	18,22	7,70	4	4
O75420	PERQ amino acid-rich with GYF domain-containing protein 1 (GRB10-interacting GYF protein 1)	GIGYF1 CDS2 PERQ1 PP3360	1035	18,29	3,86	2	4
O94868	FCH and double SH3 domains protein 2 (Carom) (SH3 multiple domains protein 3)	FCHSD2 KIAA0769 SH3MD3	740	17,26	8,38	4	4
O94916	Nuclear factor of activated T-cells 5 (NF-AT5) (T-cell transcription factor NFAT5)	NFAT5 KIAA0827 TONEBP	1531	18,08	4,83	4	4
O95232	Luc7-like protein 3 (Cisplatin resistance-associated-overexpressed protein) (Luc7A) (Okadaic acid-inducible phosphoprotein OA48-18)	LUC7L3 CREAP1 CROP O48	432	19,76	14,81	4	4
P12268	Inosine-5'-monophosphate dehydrogenase 2 (IMP dehydrogenase 2) (IMPD 2) (IMPDH 2) (EC 1.1.1.205) (IMPDH-II)	IMPDH2 IMPD2	514	14,58	12,84	4	4
P14678	Small nuclear ribonucleoprotein-associated proteins B and B' (snRNP-B) (Sm protein B/B') (Sm-B/B') (Smb/B')	SNRPB COD SNRPB1	240	17,66	12,08	2	4
P17980	26S protease regulatory subunit 6A (26S proteasome AAA-ATPase subunit RPT5) (Proteasome 26S subunit ATPase 3) (Proteasome subunit P50)	PSMC3 TBP1	439	15,50	13,44	4	4
P27694	Replication protein A 70 kDa DNA-binding subunit (RP-A p70) (Replication factor A protein 1) (RF-A protein 1)	RPA1 REPA1 RPA70	616	14,75	8,77	4	4

P30419	Glycylpeptide N-tetradecanoyltransferase 1 (EC 2.3.1.97) (Myristoyl-CoA:protein N-myristoyltransferase 1) (NMT 1)	NMT1 NMT	496	16,71	10,89	4	4
P40938	Replication factor C subunit 3 (Activator 1 38 kDa subunit) (A1 38 kDa subunit) (Activator 1 subunit 3) (Replication factor C 38 kDa subunit)	RFC3	356	17,18	19,10	4	4
P50402	Emerin	EMD EDMD STA	254	15,69	18,11	4	4
P50548	ETS domain-containing transcription factor ERF (Ets2 repressor factor) (PE-2)	ERF	548	17,54	16,24	4	4
P52294	Importin subunit alpha-5 (Karyopherin subunit alpha-1) (Nucleoprotein interactor 1) (NPI-1) (RAG cohort protein 2) (SRP1-beta)	KPNA1 RCH2	538	15,95	10,22	4	4
P61163	Alpha-centractin (Centractin) (ARP1) (Actin-RPV) (Centrosome-associated actin homolog)	ACTR1A CTRN1	376	15,61	17,29	4	4
P62805	Histone H4	HIST1H4A H4/A H4FA; HIST1H4B H4/I H4FI; HIST1H4C	103	13,58	27,18	3	4
P78332	RNA-binding protein 6 (Lung cancer antigen NY-LU-12) (Protein G16) (RNA-binding motif protein 6) (RNA-binding protein DEF-3)	RBM6 DEF3	1123	13,62	6,23	4	4
Q05209	Tyrosine-protein phosphatase non-receptor type 12 (EC 3.1.3.48) (PTP-PEST) (Protein-tyrosine phosphatase G1) (PTPG1)	PTPN12	780	18,19	8,72	4	4
Q14186	Transcription factor Dp-1 (DRTF1-polypeptide 1) (DRTF1) (E2F dimerization partner 1)	TFDP1 DP1	410	17,56	15,37	3	4
Q14203	Dynactin subunit 1 (150 kDa dynein-associated polypeptide) (DAP-150) (DP-150) (p135) (p150-glued)	DCTN1	1278	15,53	5,40	4	4
Q15003	Condensin complex subunit 2 (Barren homolog protein 1) (Chromosome-associated protein H) (hCAP-H)	NCAPH BRRN BRRN1 CAPH KIAA0074	741	13,92	8,77	3	4
Q15007	Pre-mRNA-splicing regulator WTAP (Female-lethal(2)D homolog) (hFL(2)D) (WT1-associated protein) (Wilms tumor 1-associating protein)	WTAP KIAA0105	396	18,11	15,66	4	4
Q15021	Condensin complex subunit 1 (Chromosome condensation-related SMC-associated protein 1)	NCAPD2 CAPD2 CNAP1 KIAA0159	1401	16,16	5,21	3	4
Q3ZCQ8	Mitochondrial import inner membrane translocase subunit TIM50	TIMM50 TIM50 PRO1512	353	14,60	15,30	4	4
Q4G0J3	La-related protein 7 (La ribonucleoprotein domain family member 7) (P-TEFb-interaction protein for 7SK stability) (PIP7S)	LARP7 HDCMA18P	582	17,59	10,31	4	4
Q53ET0	CREB-regulated transcription coactivator 2 (Transducer of regulated cAMP response element-binding protein 2) (TORC-2)	CRTC2 TORC2	693	17,68	15,87	4	4

Appendix

Q58WW2	DDB1- and CUL4-associated factor 6 (Androgen receptor complex-associated protein) (ARCAP) (IQ motif and WD repeat-containing protein 1)	DCAF6 IQWD1 MSTP055	860	17,50	10,35	4	4
Q55W79	Centrosomal protein of 170 kDa (Cep170) (KARP-1-binding protein) (KARP1-binding protein)	CEP170 FAM68A KAB KIAA0470	1584	16,76	4,04	4	4
Q5T200	Zinc finger CCCH domain-containing protein 13	ZC3H13 KIAA0853	1668	13,59	2,70	4	4
Q5UIP0	Telomere-associated protein RIF1 (Rap1-interacting factor 1 homolog)	RIF1	2472	18,09	2,35	4	4
Q5VTR2	E3 ubiquitin-protein ligase BRE1A (BRE1-A) (hBRE1) (EC 6.3.2.-) (RING finger protein 20)	RNF20 BRE1A	975	17,66	6,15	4	4
Q5VZK9	Leucine-rich repeat-containing protein 16A (CARMIL homolog)	LRRC16A CARMIL CARMIL1a LRRC16	1371	18,12	4,16	4	4
Q6KC79	Nipped-B-like protein (Delangin) (SCC2 homolog)	NIPBL IDN3	2804	15,83	2,78	4	4
Q6UN15	Pre-mRNA 3'-end-processing factor FIP1 (hFip1) (FIP1-like 1 protein) (Factor interacting with PAP) (Rearranged in hypereosinophilia)	FIP1L1 FIP1 RHE	594	16,52	13,47	4	4
Q6UXN9	WD repeat-containing protein 82 (Protein TMEM113) (Swd2)	WDR82 TMEM113 WDR82A UNQ9342/PRO34047	313	17,04	25,56	4	4
Q6W2J9	BCL-6 corepressor (BCoR)	BCOR KIAA1575	1755	17,73	3,36	4	4
Q70E73	Ras-associated and pleckstrin homology domains-containing protein 1 (RAPH1) (Amyotrophic lateral sclerosis 2 chromosomal region candidate gene 18 protein)	RAPH1 ALS2CR18 ALS2CR9 KIAA1681 LPD PREL2 RMO1	1250	16,40	4,00	3	4
Q7L2E3	Putative ATP-dependent RNA helicase DHX30 (EC 3.6.4.13) (DEAH box protein 30)	DHX30 DDX30 KIAA0890	1194	15,84	5,36	4	4
Q7Z417	Nuclear fragile X mental retardation-interacting protein 2 (82 kDa FMRP-interacting protein) (82-FIP) (Cell proliferation-inducing gene 1 protein)	NUFIP2 KIAA1321 PIG1	695	16,22	7,48	4	4
Q86VQ1	Glucocorticoid-induced transcript 1 protein	GLCC1	547	19,27	13,16	4	4
Q8IX01	SURP and G-patch domain-containing protein 2 (Arginine/serine-rich-splicing factor 14) (Splicing factor, arginine/serine-rich 14)	SUGP2 KIAA0365 SFRS14	1082	16,14	7,86	3	4
Q8IY57	YY1-associated factor 2	YAF2	180	22,07	25,00	2	4
Q8N3U4	Cohesin subunit SA-2 (SCC3 homolog 2) (Stromal antigen 2)	STAG2 SA2	1231	17,60	4,87	4	4
Q8N3V7	Synaptopodin	SYNPO KIAA1029	929	15,03	6,78	3	4
Q8ND56	Protein LSM14 homolog A (Protein FAM61A) (Protein SCD6 homolog) (Putative alpha-synuclein-binding protein) (AlphaSNBP) (RNA-associated protein 55A)	LSM14A C19orf13 FAM61A RAP55 RAP55A	463	17,25	20,30	4	4

Q8NHV4	Protein NEDD1 (Neural precursor cell expressed developmentally down-regulated protein 1) (NEDD-1)	NEDD1	660	18,80	7,27	4	4
Q8TE02	Elongator complex protein 5 (Dermal papilla-derived protein 6) (S-phase 2 protein)	ELP5 C17orf81 DERP6 HSPC002 MSTP071	316	16,85	18,67	3	4
Q92547	DNA topoisomerase 2-binding protein 1 (DNA topoisomerase II-beta-binding protein 1) (TopBP1) (DNA topoisomerase II-binding protein 1)	TOPBP1 KIAA0259	1522	18,53	3,81	3	4
Q92734	Protein TFG (TRK-fused gene protein)	TFG	400	16,66	17,50	3	4
Q96GY3	Protein lin-37 homolog (Antolefinin)	LIN37 MSTP064	246	18,04	17,89	3	4
Q9BW27	Nuclear pore complex protein Nup85 (85 kDa nucleoporin) (FROUNT) (Nucleoporin Nup75) (Nucleoporin Nup85) (Pericentrin-1)	NUP85 NUP75 PCNT1	656	17,97	6,40	3	4
Q9BX63	Fanconi anemia group J protein (Protein FACJ) (EC 3.6.4.13) (ATP-dependent RNA helicase BRIP1) (BRCA1-associated C-terminal helicase 1)	BRIP1 BACH1 FANCI	1249	14,76	4,40	4	4
Q9BXF6	Rab11 family-interacting protein 5 (Rab11-FIP5) (Gamma-SNAP-associated factor 1) (Gaf-1) (Phosphoprotein pp75)	RAB11FIP5 GAF1 KIAA0857 RIP11	653	20,48	8,42	3	4
Q9H0J9	Poly [ADP-ribose] polymerase 12 (PARP-12) (EC 2.4.2.30) (ADP-ribosyltransferase diphtheria toxin-like 12) (ARTD12)	PARP12 ZC3HDC1	701	16,43	9,84	4	4
Q9HAW4	Claspin (hClaspin)	CLSPN	1339	16,92	4,26	4	4
Q9NQC7	Ubiquitin carboxyl-terminal hydrolase CYLD (EC 3.4.19.12) (Deubiquitinating enzyme CYLD) (Ubiquitin thioesterase CYLD)	CYLD CYLD1 KIAA0849 HSPC057	956	14,62	5,23	4	4
Q9NTJ3	Structural maintenance of chromosomes protein 4 (SMC protein 4) (SMC-4) (Chromosome-associated polypeptide C) (hCAP-C) (XCAP-C homolog)	SMC4 CAPC SMC4L1	1288	15,39	4,89	4	4
Q9UGU0	Transcription factor 20 (TCF-20) (Nuclear factor SPBP) (Protein AR1) (Stromelysin-1 PDGF-responsive element-binding protein) (SPRE-binding protein)	TCF20 KIAA0292 SPBP	1960	19,75	2,35	2	4
Q9UM11	Fizzy-related protein homolog (Fzr) (CDC20-like protein 1) (Cdh1/Hct1 homolog) (hCDH1)	FZR1 CDH1 FYR FZR KIAA1242	496	19,08	15,32	4	4
Q9UN86	Ras GTPase-activating protein-binding protein 2 (G3BP-2) (GAP SH3 domain-binding protein 2)	G3BP2 KIAA0660	482	17,44	13,69	4	4
Q9UPQ9	Trinucleotide repeat-containing gene 6B protein	TNRC6B KIAA1093	1833	16,80	2,18	3	4
Q9Y2K1	Zinc finger and BTB domain-containing protein 1	ZBTB1 KIAA0997	713	17,40	7,99	4	4
Q9Y4B6	Protein VPRBP (DDB1- and CUL4-associated factor 1) (HIV-1 Vpr-binding protein) (VprBP) (Vpr-interacting protein)	VPRBP DCAF1 KIAA0800 RIP	1507	17,01	4,38	4	4

Q9Y4X0	AMME syndrome candidate gene 1 protein	AMMECR1	333	14,26	14,41	4	4
Q9Y520	Protein PRRC2C (BAT2 domain-containing protein 1) (HBV X-transactivated gene 2 protein) (HBV XAg-transactivated protein 2)	PRRC2C BAT2D1 BAT2L2 KIAA1096 XTP2	2896	17,74	1,80	3	4
O00139	Kinesin-like protein KIF2A (Kinesin-2) (hK2)	KIF2A KIF2 KNS2	706	13,43	5,95	3	3
O15084	Serine/threonine-protein phosphatase 6 regulatory ankyrin repeat subunit A (PP6-ARS-A) (Serine/threonine-protein phosphatase 6 regulatory subunit ARS-A)	ANKRD28 KIAA0379	1053	14,76	5,60	3	3
O15164	Transcription intermediary factor 1-alpha (TIF1-alpha) (EC 6.3.2.-) (E3 ubiquitin-protein ligase TRIM24) (RING finger protein 82)	TRIM24 RNF82 TIF1 TIF1A	1050	10,44	3,81	3	3
O43164	E3 ubiquitin-protein ligase Praja-2 (Praja2) (EC 6.3.2.-) (RING finger protein 131)	PJA2 KIAA0438 RNF131	708	14,37	5,93	2	3
O43474	Krueppel-like factor 4 (Epithelial zinc finger protein EZF) (Gut-enriched krueppel-like factor)	KLF4 EZF GKLF	513	12,19	10,53	3	3
O94806	Serine/threonine-protein kinase D3 (EC 2.7.11.13) (Protein kinase C nu type) (Protein kinase EPK2) (nPKC-nu)	PRKD3 EPK2 PRKCN	890	10,99	3,48	2	3
O94887	FERM, RhoGEF and pleckstrin domain-containing protein 2 (FERM domain including RhoGEF) (FIR) (Pleckstrin homology domain-containing family C member 3)	FARP2 KIAA0793 PLEKHC3	1054	13,16	3,70	2	3
O94967	WD repeat-containing protein 47 (Neuronal enriched MAP interacting protein) (Nemitin)	WDR47 KIAA0893	919	12,88	5,88	3	3
P14859	POU domain, class 2, transcription factor 1 (NF-A1) (Octamer-binding protein 1) (Oct-1) (Octamer-binding transcription factor 1) (OTF-1)	POU2F1 OCT1 OTF1	743	13,56	8,21	3	3
P17676	CCAAT/enhancer-binding protein beta (C/EBP beta) (Liver activator protein) (LAP) (Liver-enriched inhibitory protein) (LIP)	CEBPB TCF5 PP9092	345	14,85	8,99	2	3
P28066	Proteasome subunit alpha type-5 (EC 3.4.25.1) (Macropain zeta chain) (Multicatalytic endopeptidase complex zeta chain) (Proteasome zeta chain)	PSMA5	241	13,97	21,99	3	3
P28290	Sperm-specific antigen 2 (Cleavage signal-1 protein) (CS-1) (Ki-ras-induced actin-interacting protein)	SSFA2 CS1 KIAA1927 KRAP	1259	14,31	3,73	2	3
P28715	DNA repair protein complementing XP-G cells (EC 3.1.-.-) (DNA excision repair protein ERCC-5)	ERCC5 ERCC2 XPG XPGC	1186	15,07	2,78	2	3
P39880	Homeobox protein cut-like 1 (CCAAT displacement protein) (CDP) (Homeobox protein cux-1)	CUX1 CUTL1	1505	11,15	2,13	2	3
P41134	DNA-binding protein inhibitor ID-1 (Class B basic helix-loop-helix protein 24) (bHLHb24)	ID1 BHLHB24 ID	155	12,08	30,32	3	3

P49841	Glycogen synthase kinase-3 beta (GSK-3 beta) (EC 2.7.11.26) (Serine/threonine-protein kinase GSK3B) (EC 2.7.11.1)	GSK3B	420	11,73	12,62	3	3
P49959	Double-strand break repair protein MRE11A (Meiotic recombination 11 homolog 1) (MRE11 homolog 1)	MRE11A HNGS1 MRE11	708	12,25	6,21	3	3
P50552	Vasodilator-stimulated phosphoprotein (VASP)	VASP	380	13,12	12,89	3	3
P50750	Cyclin-dependent kinase 9 (EC 2.7.11.22) (EC 2.7.11.23) (C-2K) (Cell division cycle 2-like protein kinase 4) (Cell division protein kinase 9)	CDK9 CDC2L4 TAK	372	14,12	13,44	3	3
P54278	Mismatch repair endonuclease PMS2 (EC 3.1.-.-) (DNA mismatch repair protein PMS2) (PMS1 protein homolog 2)	PMS2 PMSL2	862	12,39	4,99	3	3
P55081	Microfibrillar-associated protein 1	MFAP1	439	15,17	14,35	3	3
P57740	Nuclear pore complex protein Nup107 (107 kDa nucleoporin) (Nucleoporin Nup107)	NUP107	925	10,26	5,30	3	3
P78362	SRSF protein kinase 2 (EC 2.7.11.1) (SFRS protein kinase 2) (Serine/arginine-rich protein-specific kinase 2) (SR-protein-specific kinase 2)	SRPK2	688	12,04	5,23	2	3
P84090	Enhancer of rudimentary homolog	ERH	104	14,70	26,92	2	3
Q12769	Nuclear pore complex protein Nup160 (160 kDa nucleoporin) (Nucleoporin Nup160)	NUP160 KIAA0197 NUP120	1436	12,02	3,06	3	3
Q13042	Cell division cycle protein 16 homolog (Anaphase-promoting complex subunit 6) (APC6) (CDC16 homolog) (CDC16Hs) (Cyclosome subunit 6)	CDC16 ANAPC6	620	14,21	8,71	3	3
Q13586	Stromal interaction molecule 1	STIM1 GOK	685	14,15	6,86	3	3
Q14457	Beclin-1 (Coiled-coil myosin-like BCL2-interacting protein) (Protein GT197)	BECN1 GT197	450	11,18	6,89	3	3
Q14978	Nucleolar and coiled-body phosphoprotein 1 (140 kDa nucleolar phosphoprotein) (Nopp140) (Hepatitis C virus NS5A-transactivated protein 13)	NOLC1 KIAA0035 NS5ATP13	699	10,10	2,86	2	3
Q15369	Transcription elongation factor B polypeptide 1 (Elongin 15 kDa subunit) (Elongin-C) (EloC)	TCEB1	112	14,38	30,36	2	3
Q53SF7	Cordon-bleu protein-like 1	COBLL1 KIAA0977	1204	11,29	4,90	3	3
Q5VZE5	N-alpha-acetyltransferase 35, NatC auxiliary subunit (Embryonic growth-associated protein homolog) (Protein MAK10 homolog)	NAA35 EGAP MAK10	725	13,78	7,03	3	3
Q6BDS2	UHRF1-binding protein 1 (ICBP90-binding protein 1) (Ubiquitin-like containing PHD and RING finger domains 1-binding protein 1)	UHRF1BP1 C6orf107	1440	11,45	3,47	3	3

Appendix

Q8N5C8	TGF-beta-activated kinase 1 and MAP3K7-binding protein 3 (Mitogen-activated protein kinase kinase kinase 7-interacting protein 3)	TAB3 MAP3K7IP3	712	13,16	9,69	3	3
Q8TDB6	E3 ubiquitin-protein ligase DTX3L (EC 6.3.2.-) (B-lymphoma- and BAL-associated protein) (Protein deltex-3-like) (Rhysin-2) (Rhysin2)	DTX3L BBAP	740	11,75	6,89	3	3
Q8WVB6	Chromosome transmission fidelity protein 18 homolog (hCTF18) (CHL12)	CHTF18 C16orf41 CTF18	975	12,37	3,79	2	3
Q92576	PHD finger protein 3	PHF3 KIAA0244	2039	12,54	2,35	3	3
Q92879	CUGBP Elav-like family member 1 (CELF-1) (50 kDa nuclear polyadenylated RNA-binding protein) (Bruno-like protein 2)	CELF1 BRUNOL2 CUGBP CUGBP1 NAB50	486	12,69	8,02	3	3
Q96EB1	Elongator complex protein 4 (hELP4) (PAX6 neighbor gene protein)	ELP4 C11orf19 PAXNEB	424	10,86	13,44	3	3
Q96M27	Protein PRRC1 (Proline-rich and coiled-coil-containing protein 1)	PRRC1	445	13,13	10,34	3	3
Q96N46	Tetratricopeptide repeat protein 14 (TPR repeat protein 14)	TTC14 KIAA1980 UNQ5813/PRO19630	770	11,31	6,23	3	3
Q96S38	Ribosomal protein S6 kinase delta-1 (S6K-delta-1) (EC 2.7.11.1) (52 kDa ribosomal protein S6 kinase)	RPS6KC1 RPK118	1066	13,54	5,25	3	3
Q9BU76	Multiple myeloma tumor-associated protein 2 (hMMTAG2)	MMTAG2 C1orf35	263	12,13	9,89	2	3
Q9BUL9	Ribonuclease P protein subunit p25 (RNase P protein subunit p25) (EC 3.1.26.5)	RPP25	199	13,54	23,12	2	3
Q9C0F1	Centrosomal protein of 44 kDa (Cep44) (HBV PreS1-transactivated protein 3) (PS1TP3)	CEP44 KIAA1712	390	13,94	18,46	3	3
Q9H0H5	Rac GTPase-activating protein 1 (Male germ cell RacGap) (MgcRacGAP) (Protein CYK4 homolog) (CYK4) (HsCYK-4)	RACGAP1 KIAA1478 MGCRACGAP	632	13,51	7,12	3	3
Q9NPI6	mRNA-decapping enzyme 1A (EC 3.-.-.-) (Smad4-interacting transcriptional co-activator) (Transcription factor SMIF)	DCP1A SMIF	582	13,48	10,82	3	3
Q9NS91	E3 ubiquitin-protein ligase RAD18 (EC 6.3.2.-) (Postreplication repair protein RAD18) (hHR18) (hRAD18) (RING finger protein 73)	RAD18 RNF73	495	11,53	9,09	3	3
Q9NY27	Serine/threonine-protein phosphatase 4 regulatory subunit 2	PPP4R2 SBB157	417	16,57	10,79	2	3
Q9P2B4	CTTNBP2 N-terminal-like protein	CTTNBP2NL KIAA1433	639	11,93	6,26	2	3
Q9UGR2	Zinc finger CCCH domain-containing protein 7B (Rotavirus 'X'-associated non-structural protein) (RoXaN)	ZC3H7B KIAA1031	993	10,30	3,93	3	3
Q9UJX2	Cell division cycle protein 23 homolog (Anaphase-promoting complex subunit 8) (APC8) (Cyclosome subunit 8)	CDC23 ANAPC8	597	12,64	6,37	3	3

Q9UK76	Hematological and neurological expressed 1 protein (Androgen-regulated protein 2)	HN1 ARM2	154	14,05	54,55	3	3
Q9UMZ2	Synergina gamma (AP1 subunit gamma-binding protein 1) (Gamma-synergina)	SYNRG AP1GBP1 SYNG	1314	12,18	4,26	3	3
Q9UN79	Transcription factor SOX-13 (Islet cell antigen 12) (SRY (Sex determining region Y)-box 13) (Type 1 diabetes autoantigen ICA12)	SOX13	622	13,66	8,84	3	3
Q9UQ88	Cyclin-dependent kinase 11A (EC 2.7.11.22) (Cell division cycle 2-like protein kinase 2) (Cell division protein kinase 11A)	CDK11A CDC2L2 CDC2L3 PITSLREB	783	11,14	6,77	3	3
Q9Y2K5	R3H domain-containing protein 2	R3HDM2 KIAA1002	976	15,98	4,61	2	3
Q9Y2U8	Inner nuclear membrane protein Man1 (LEM domain-containing protein 3)	LEMD3 MAN1	911	12,52	6,26	3	3
Q9Y2X7	ARF GTPase-activating protein GIT1 (ARF GAP GIT1) (Cool-associated and tyrosine-phosphorylated protein 1) (CAT-1) (CAT1)	GIT1	761	11,91	7,36	3	3
Q9Y388	RNA-binding motif protein, X-linked 2	RBMX2 CGI-79	322	10,31	9,32	3	3
Q9Y4A5	Transformation/transcription domain-associated protein (350/400 kDa PCAF-associated factor) (PAF350/400) (STAF40) (Tra1 homolog)	TRRAP PAF400	3859	11,39	1,27	3	3
Q9Y5Q8	General transcription factor 3C polypeptide 5 (TF3C-epsilon) (Transcription factor IIIC 63 kDa subunit) (TFIIIC 63 kDa subunit)	GTF3C5 CDABP0017	519	11,68	8,86	3	3
O15037	Protein KHNYN (KH and NYN domain-containing protein)	KHNYN KIAA0323	678	8,48	5,01	2	2
O43379	WD repeat-containing protein 62	WDR62 C19orf14	1518	7,82	1,84	2	2
O43809	Cleavage and polyadenylation specificity factor subunit 5 (Cleavage and polyadenylation specificity factor 25 kDa subunit)	NUDT21 CFIM25 CPSF25 CPSF5	227	9,03	14,10	2	2
O75128	Protein cordon-bleu	COBL KIAA0633	1261	7,06	2,78	2	2
P04049	RAF proto-oncogene serine/threonine-protein kinase (EC 2.7.11.1) (Proto-oncogene c-RAF) (cRaf) (Raf-1)	RAF1 RAF	648	7,00	3,09	2	2
P06730	Eukaryotic translation initiation factor 4E (eIF-4E) (eIF4E) (eIF-4F 25 kDa subunit) (mRNA cap-binding protein)	EIF4E EIF4EL1 EIF4F	217	7,35	11,98	2	2
P13674	Prolyl 4-hydroxylase subunit alpha-1 (4-PH alpha-1) (EC 1.14.11.2) (Procollagen-proline,2-oxoglutarate-4-dioxygenase subunit alpha-1)	P4HA1 P4HA	534	8,55	4,68	2	2
P30153	Serine/threonine-protein phosphatase 2A 65 kDa regulatory subunit A alpha isoform (Medium tumor antigen-associated 61 kDa protein)	PPP2R1A	589	9,12	6,11	2	2

Appendix

P35249	Replication factor C subunit 4 (Activator 1 37 kDa subunit) (A1 37 kDa subunit) (Activator 1 subunit 4) (Replication factor C 37 kDa subunit) (RF-C 37 kDa subunit) (RFC37)	RFC4	363	6,96	10,19	2	2
P35250	Replication factor C subunit 2 (Activator 1 40 kDa subunit) (A1 40 kDa subunit) (Activator 1 subunit 2) (RFC2	354	7,31	8,47	2	2
P37198	Nuclear pore glycoprotein p62 (62 kDa nucleoporin) (Nucleoporin Nup62)	NUP62	522	9,41	6,51	2	2
P41162	ETS translocation variant 3 (ETS domain transcriptional repressor PE1) (PE-1) (Mitogenic Ets transcriptional suppressor)	ETV3 METS PE1	512	6,98	6,05	2	2
P46100	Transcriptional regulator ATRX (EC 3.6.4.12) (ATP-dependent helicase ATRX) (X-linked helicase II) (X-linked nuclear protein) (XNP) (Znf-HX)	ATRX RAD54L XH2	2492	7,65	1,20	2	2
P49815	Tuberin (Tuberous sclerosis 2 protein)	TSC2 TSC4	1807	9,46	1,88	2	2
P51610	Host cell factor 1 (HCF) (HCF-1) (C1 factor) (CFF) (VCAF) (VP16 accessory protein)	HCFC1 HCF1 HFC1	2035	7,41	1,43	2	2
P52732	Kinesin-like protein KIF11 (Kinesin-like protein 1) (Kinesin-like spindle protein HKSP) (Kinesin-related motor protein Eg5)	KIF11 EG5 KNSL1 TRIP5	1056	9,17	3,31	2	2
P55198	Protein AF-17 (ALL1-fused gene from chromosome 17 protein)	MLLT6 AF17	1093	6,87	3,11	2	2
P61962	DDB1- and CUL4-associated factor 7 (WD repeat-containing protein 68) (WD repeat-containing protein An11 homolog)	DCAF7 HAN11 WDR68	342	8,64	8,48	2	2
P78344	Eukaryotic translation initiation factor 4 gamma 2 (eIF-4-gamma 2) (eIF-4G 2) (eIF4G 2) (Death-associated protein 5) (DAP-5) (p97)	EIF4G2 DAP5 OK/SW-cl.75	907	9,37	4,85	2	2
Q02241	Kinesin-like protein KIF23 (Kinesin-like protein 5) (Mitotic kinesin-like protein 1)	KIF23 KNSL5 MKLP1	960	6,77	2,60	2	2
Q10570	Cleavage and polyadenylation specificity factor subunit 1 (Cleavage and polyadenylation specificity factor 160 kDa subunit) (CPSF 160 kDa subunit)	CPSF1 CPSF160	1443	7,91	2,36	2	2
Q12778	Forkhead box protein O1 (Forkhead box protein O1A) (Forkhead in rhabdomyosarcoma)	FOXO1 FKHR FOXO1A	655	8,84	7,18	2	2
Q12834	Cell division cycle protein 20 homolog (p55CDC)	CDC20	499	9,07	7,01	2	2
Q13148	TAR DNA-binding protein 43 (TDP-43)	TARDBP TDP43	414	9,33	10,14	2	2
Q14257	Reticulocalbin-2 (Calcium-binding protein ERC-55) (E6-binding protein) (E6BP)	RCN2 ERC55	317	9,79	11,04	2	2
Q147X3	N-alpha-acetyltransferase 30 (EC 2.3.1.88) (N-acetyltransferase 12) (N-acetyltransferase MAK3 homolog) (NatC catalytic subunit)	NAA30 C14orf35 MAK3 NAT12	362	7,79	6,63	2	2

Q16543	Hsp90 co-chaperone Cdc37 (Hsp90 chaperone protein kinase-targeting subunit) (p50Cdc37) [Cleaved into: Hsp90 co-chaperone Cdc37, N-terminally processed]	CDC37 CDC37A	378	8,91	7,41	2	2
Q2M389	WASH complex subunit 7	KIAA1033	1173	7,19	2,30	2	2
Q5VUA4	Zinc finger protein 318 (Endocrine regulatory protein)	ZNF318 HRIHFB2436	2279	7,54	1,54	2	2
Q5VZL5	Zinc finger MYM-type protein 4 (Zinc finger protein 262)	ZMYM4 KIAA0425 ZNF262	1548	7,58	1,81	2	2
Q6PGN9	Proline/serine-rich coiled-coil protein 1	PSRC1 DDA3 FP3214	363	7,25	7,44	2	2
Q76FK4	Nucleolar protein 8 (Nucleolar protein Nop132)	NOL8 C9orf34 NOP132	1167	7,06	2,83	2	2
Q7Z739	YTH domain family protein 3	YTHDF3	585	9,74	4,96	2	2
Q86XZ4	Spermatogenesis-associated serine-rich protein 2 (Serine-rich spermatocytes and round spermatid 59 kDa protein) (p59scr)	SPATS2 SCR59 SPATA10 Nbla00526	545	9,46	5,50	2	2
Q8IVH2	Forkhead box protein P4 (Fork head-related protein-like A)	FOXP4 FKHLA	680	8,61	7,94	2	2
Q8IYH5	ZZ-type zinc finger-containing protein 3	ZZZ3	903	8,24	2,99	2	2
Q8N684	Cleavage and polyadenylation specificity factor subunit 7 (Cleavage and polyadenylation specificity factor 59 kDa subunit) (CFIm59) (CPSF 59 kDa subunit)	CPSF7	471	6,85	5,10	2	2
Q8NEM2	SHC SH2 domain-binding protein 1	SHCBP1	672	8,16	5,36	2	2
Q8NI35	InaD-like protein (Inadl protein) (hINADL) (Pals1-associated tight junction protein) (Protein associated to tight junctions)	INADL PATJ	1801	9,04	2,00	2	2
Q8WWN8	Arf-GAP with Rho-GAP domain, ANK repeat and PH domain-containing protein 3 (Centaurin-delta-3) (Cnt-d3)	ARAP3 CENTD3	1544	6,51	2,66	2	2
Q8WXI9	Transcriptional repressor p66-beta (GATA zinc finger domain-containing protein 2B) (p66/p68)	GATAD2B KIAA1150	593	7,77	6,07	2	2
Q92793	CREB-binding protein (EC 2.3.1.48)	CREBBP CBP	2442	7,62	1,06	2	2
Q96EY1	DnaJ homolog subfamily A member 3, mitochondrial (DnaJ protein Tid-1) (hTid-1) (Hepatocellular carcinoma-associated antigen 57)	DNAJA3 HCA57 TID1	480	8,27	5,83	2	2
Q96SB4	SRSF protein kinase 1 (EC 2.7.11.1) (SFRS protein kinase 1) (Serine/arginine-rich protein-specific kinase 1) (SR-protein-specific kinase 1)	SRPK1	655	6,71	2,90	2	2
Q96T37	Putative RNA-binding protein 15 (One-twenty two protein 1) (RNA-binding motif protein 15)	RBM15 OTT OTT1	977	7,72	2,97	2	2

Appendix

Q9BUH8	Brain-enriched guanylate kinase-associated protein	BEGAIN KIAA1446	593	8,40	5,73	2	2
Q9C0C7	Activating molecule in BECN1-regulated autophagy protein 1	AMBRA1 KIAA1736	1298	9,02	3,24	2	2
Q9H1A4	Anaphase-promoting complex subunit 1 (APC1) (Cyclosome subunit 1) (Mitotic checkpoint regulator) (Testis-specific gene 24 protein)	ANAPC1 TSG24	1944	7,46	2,52	2	2
Q9H211	DNA replication factor Cdt1 (Double parked homolog) (DUP)	CDT1	546	6,74	6,41	2	2
Q9H4B6	Protein salvador homolog 1 (45 kDa WW domain protein) (hWW45)	SAV1 WW45	383	8,85	12,53	2	2
Q9H4I2	Zinc fingers and homeoboxes protein 3 (Triple homeobox protein 1) (Zinc finger and homeodomain protein 3)	ZHX3 KIAA0395 TIX1	956	7,93	3,24	2	2
Q9HCD6	Protein TANC2 (Tetratricopeptide repeat, ankyrin repeat and coiled-coil domain-containing protein 2)	TANC2 KIAA1148 KIAA1636	1990	7,08	1,16	2	2
Q9P0U4	CpG-binding protein (CXXC-type zinc finger protein 1) (PHD finger and CXXC domain-containing protein 1)	CXXC1 CFP1 CGBP PCCX1 PHF18	656	8,73	6,55	2	2
Q9UJX4	Anaphase-promoting complex subunit 5 (APC5) (Cyclosome subunit 5)	ANAPC5 APC5	755	9,26	3,84	2	2
Q9UNY4	Transcription termination factor 2 (EC 3.6.4.-) (Lodestar homolog) (RNA polymerase II termination factor) (Transcription release factor 2) (F2) (HuF2)	TTF2	1162	12,31	3,27	2	2
Q9UPP1	Histone lysine demethylase PHF8 (EC 1.14.11.27) (PHD finger protein 8)	PHF8 KIAA1111 ZNF422	1060	7,29	2,74	2	2
Q9Y478	5'-AMP-activated protein kinase subunit beta-1 (AMPK subunit beta-1) (AMPKb)	PRKAB1 AMPK	270	9,64	11,85	2	2
Q9Y5A9	YTH domain family protein 2 (CLL-associated antigen KW-14) (High-glucose-regulated protein 8) (Renal carcinoma antigen NY-REN-2)	YTHDF2 HGRG8	579	10,10	5,18	2	2
Q9Y5T5	Ubiquitin carboxyl-terminal hydrolase 16 (EC 3.4.19.12) (Deubiquitinating enzyme 16) (Ubiquitin thioesterase 16)	USP16 MSTP039	823	8,77	4,62	2	2

11.2 Appendix II. List of the 458 hits found in GST-PLK1-PBD-UBI pulldown.

This list excludes proteins also present in the GST control sample. Hits were sorted by decreasing number of peptide spectrum mass (PSM). Coverage, number of peptides identified and number of PSM are shown for each protein identified.

Uniprot ID	Protein names	Gene names	Length	Score	Coverage (%)	# Peptides	# PSM
O95071	E3 ubiquitin-protein ligase UBR5 (EC 6.3.2.-) (E3 ubiquitin-protein ligase, HECT domain-containing 1)	UBR5 EDD EDD1 HYD KIAA0896	2799	503,99	37,91	67	128
P07437	Tubulin beta chain (Tubulin beta-5 chain)	TUBB TUBB5 OK/SW-cl.56	444	473,10	78,38	24	122
P45974	Ubiquitin carboxyl-terminal hydrolase 5 (EC 3.4.19.12) (Deubiquitinating enzyme 5) (Isopeptidase T) (Ubiquitin thioesterase 5)	USP5 ISOT	858	430,74	53,96	33	111
P68032	Actin, alpha cardiac muscle 1 (Alpha-cardiac actin)	ACTC1 ACTC	377	268,05	35,28	10	76
Q13509	Tubulin beta-3 chain (Tubulin beta-4 chain) (Tubulin beta-III)	TUBB3 TUBB4	450	276,52	43,11	16	70
O75592	Probable E3 ubiquitin-protein ligase MYCBP2 (EC 6.3.2.-) (Myc-binding protein 2) (Pam/highwire/rpm-1 protein)	MYCBP2 KIAA0916 PAM	4640	196,08	15,41	43	49
Q7Z6Z7	E3 ubiquitin-protein ligase HUWE1 (EC 6.3.2.-) (ARF-binding protein 1) (ARF-BP1) (HECT, UBA and WWE domain-containing protein 1)	HUWE1 KIAA0312 KIAA1578 URB1 HSPC272	4374	182,80	16,85	43	49
Q92995	Ubiquitin carboxyl-terminal hydrolase 13 (EC 3.4.19.12) (Deubiquitinating enzyme 13) (Isopeptidase T-3) (ISOT-3)	USP13 ISOT3	863	174,62	50,41	28	46
Q9UPU5	Ubiquitin carboxyl-terminal hydrolase 24 (EC 3.4.19.12) (Deubiquitinating enzyme 24)	USP24 KIAA1057	2620	164,23	22,14	36	44
Q9BQE3	Tubulin alpha-1C chain (Alpha-tubulin 6) (Tubulin alpha-6 chain)	TUBA1C TUBA6	449	172,79	67,26	20	41
O00750	Phosphatidylinositol 4-phosphate 3-kinase C2 domain-containing subunit beta (PI3K-C2-beta)	PIK3C2B	1634	146,13	28,34	30	37
Q9Y6I4	Ubiquitin carboxyl-terminal hydrolase 3 (EC 3.4.19.12) (Deubiquitinating enzyme 3)	USP3	520	144,80	47,50	19	37
Q9BUF5	Tubulin beta-6 chain (Tubulin beta class V)	TUBB6	446	127,29	47,76	13	35
Q96S55	ATPase WRNIP1 (EC 3.6.1.3) (Werner helicase-interacting protein 1)	WRNIP1 WHIP	665	127,30	47,37	18	32

Appendix

P49792	E3 SUMO-protein ligase RanBP2 (EC 6.3.2.-) (358 kDa nucleoporin) (Nuclear pore complex protein Nup358) (Nucleoporin Nup358)	RANBP2 NUP358	3224	120,00	14,39	26	31
P68366	Tubulin alpha-4A chain (Alpha-tubulin 1) (Testis-specific alpha-tubulin) (Tubulin H2-alpha)	TUBA4A TUBA1	448	128,07	55,13	17	31
O00159	Unconventional myosin-Ic (Myosin I beta) (MMI-beta) (MMIb)	MYO1C	1063	95,97	29,92	21	26
Q9Y4E8	Ubiquitin carboxyl-terminal hydrolase 15 (EC 3.4.19.12) (Deubiquitinating enzyme 15) (Ubiquitin thioesterase 15)	USP15 KIAA0529	981	97,06	32,01	22	25
O60271	C-Jun-amino-terminal kinase-interacting protein 4 (JIP-4) (JNK-interacting protein 4) (Cancer/testis antigen 89) (CT89)	SPAG9 HSS KIAA0516 MAPK8IP4 SYD1 HLC6	1321	87,62	23,62	22	24
Q13137	Calcium-binding and coiled-coil domain-containing protein 2 (Antigen nuclear dot 52 kDa protein) (Nuclear domain 10 protein NDP52)	CALCOCO2 NDP52	446	98,61	48,65	14	23
Q96N67	Dedicator of cytokinesis protein 7	DOCK7 KIAA1771	2140	84,39	15,56	22	23
Q9UJX2	Cell division cycle protein 23 homolog (Anaphase-promoting complex subunit 8) (APC8) (Cyclosome subunit 8)	CDC23 ANAPC8	597	87,88	44,05	19	23
P31689	DnaJ homolog subfamily A member 1 (DnaJ protein homolog 2) (HSDJ) (Heat shock 40 kDa protein 4) (Heat shock protein J2) (HSJ-2)	DNAJA1 DNAJ2 HDJ2 HSJ2 HSPF4	397	86,79	48,11	12	22
Q9H1A4	Anaphase-promoting complex subunit 1 (APC1) (Cyclosome subunit 1) (Mitotic checkpoint regulator) (Testis-specific gene 24 protein)	ANAPC1 TSG24	1944	80,62	15,95	18	22
Q15751	Probable E3 ubiquitin-protein ligase HERC1 (EC 6.3.2.-) (HECT domain and RCC1-like domain-containing protein 1) (p532) (p619)	HERC1	4861	72,56	8,33	19	19
Q7Z569	BRCA1-associated protein (EC 6.3.2.-) (BRAP2) (Impedes mitogenic signal propagation) (IMP)	BRAP RNF52	592	81,01	37,50	15	19
Q96EP0	E3 ubiquitin-protein ligase RNF31 (EC 6.3.2.-) (HOIL-1-interacting protein) (HOIP)	RNF31 ZIBRA	1072	69,80	30,04	17	19
Q9Y5T5	Ubiquitin carboxyl-terminal hydrolase 16 (EC 3.4.19.12) (Deubiquitinating enzyme 16)	USP16 MSTP039	823	73,53	29,04	15	19
O95714	E3 ubiquitin-protein ligase HERC2 (EC 6.3.2.-) (HECT domain and RCC1-like domain-containing protein 2)	HERC2	4834	65,44	6,43	17	18
Q12965	Unconventional myosin-Ie (Myosin-Ic) (Unconventional myosin 1E)	MYO1E MYO1C	1108	72,11	22,83	17	18
Q9C0C2	182 kDa tankyrase-1-binding protein	TNKS1BP1 KIAA1741 TAB182	1729	81,75	15,21	15	18
Q9Y4E5	Zinc finger protein 451 (Coactivator for steroid receptors)	ZNF451 COASTER KIAA0576 KIAA1702	1061	67,59	21,87	13	18
Q13045	Protein flightless-1 homolog	FLII FLIL	1269	67,26	22,77	16	17

Q53GT1	Kelch-like protein 22	KLHL22	634	67,13	33,28	12	17
Q6Y7W6	PERQ amino acid-rich with GYF domain-containing protein 2 (GRB10-interacting GYF protein 2)	GIGYF2 KIAA0642 PERQ2 TNRC15	1299	62,24	18,55	14	16
Q7Z5K2	Wings apart-like protein homolog (Friend of EBNA2 protein)	WAPAL FOE KIAA0261 WAPL	1190	61,94	19,08	14	16
Q9UJX3	Anaphase-promoting complex subunit 7 (APC7) (Cyclosome subunit 7)	ANAPC7 APC7	599	63,50	33,22	14	16
Q13042	Cell division cycle protein 16 homolog (Anaphase-promoting complex subunit 6) (APC6)	CDC16 ANAPC6	620	61,67	34,68	14	15
Q9UJX5	Anaphase-promoting complex subunit 4 (APC4) (Cyclosome subunit 4)	ANAPC4 APC4	808	58,11	21,29	14	15
P52272	Heterogeneous nuclear ribonucleoprotein M (hnRNP M)	HNRNPM HNRPM NAGR1	730	49,65	24,66	12	14
P53621	Coatomer subunit alpha (Alpha-coat protein) (Alpha-COP) (HEP-COP) (HEPCOP) [Cleaved into: Xenin (Xenopsin-related peptide); Proxenin]	COPA	1224	53,71	18,06	14	14
Q93008	Probable ubiquitin carboxyl-terminal hydrolase FAF-X (EC 3.4.19.12) (Deubiquitinating enzyme FAF-X) (Fat facets in mammals) (hFAM)	USP9X DFFRX FAM USP9	2570	53,20	7,32	12	14
Q9UBN7	Histone deacetylase 6 (HD6) (EC 3.5.1.98)	HDAC6 KIAA0901 JM21	1215	49,84	14,90	10	14
Q9UM54	Unconventional myosin-VI (Unconventional myosin-6)	MYO6 KIAA0389	1294	55,55	12,36	11	14
O60566	Mitotic checkpoint serine/threonine-protein kinase BUB1 beta (EC 2.7.11.1) (MAD3/BUB1-related protein kinase) (hBUBR1)	BUB1B BUBR1 MAD3L SSK1	1050	53,71	15,62	10	13
O60784	Target of Myb protein 1	TOM1	492	57,17	39,23	11	13
P08729	Keratin, type II cytoskeletal 7 (Cytokeratin-7) (CK-7) (Keratin-7) (K7) (Sarcolectin) (Type-II keratin Kb7)	KRT7 SCL	469	47,01	24,52	10	13
P13639	Elongation factor 2 (EF-2)	EEF2 EF2	858	50,90	22,73	12	13
P25391	Laminin subunit alpha-1 (Laminin A chain) (Laminin-1 subunit alpha) (Laminin-3 subunit alpha) (S-laminin subunit alpha) (S-LAM alpha)	LAMA1 LAMA	3075	49,67	7,06	12	13
P31327	Carbamoyl-phosphate synthase [ammonia], mitochondrial (EC 6.3.4.16) (Carbamoyl-phosphate synthetase I) (CPSase I)	CPS1	1500	56,15	13,00	10	13
P35580	Myosin-10 (Cellular myosin heavy chain, type B) (Myosin heavy chain 10) (Myosin heavy chain, non-muscle IIb)	MYH10	1976	55,17	7,29	10	13
Q13586	Stromal interaction molecule 1	STIM1 GOK	685	53,83	25,40	11	13
Q8TD16	Protein bicaudal D homolog 2 (Bic-D 2)	BICD2 KIAA0699	824	50,47	25,36	13	13

Appendix

Q9UJ41	Rab5 GDP/GTP exchange factor (RAP1) (Rabaptin-5-associated exchange factor for Rab5) (Rabex-5)	RABGEF1 RABEX5	708	57,69	24,72	12	13
Q12834	Cell division cycle protein 20 homolog (p55CDC)	CDC20	499	45,55	29,66	7	12
P13861	cAMP-dependent protein kinase type II-alpha regulatory subunit	PRKAR2A PKR2 PRKAR2	404	43,08	35,40	10	11
P21580	Tumor necrosis factor alpha-induced protein 3 (TNF alpha-induced protein 3) (EC 3.4.19.12) (EC 6.3.2.-) (OTU domain-containing protein 7C)	TNFAIP3 OTUD7C	790	38,62	17,72	10	11
P22626	Heterogeneous nuclear ribonucleoproteins A2/B1 (hnRNP A2/B1)	HNRNPA2B1 HNRNPA2B1	353	46,98	33,14	7	11
P30260	Cell division cycle protein 27 homolog (Anaphase-promoting complex subunit 3) (APC3) (CDC27 homolog) (CDC27Hs) (H-NUC)	CDC27 ANAPC3 DOS1430E D17S978E	824	44,51	21,12	11	11
P31943	Heterogeneous nuclear ribonucleoprotein H (hnRNP H) [Cleaved into: Heterogeneous nuclear ribonucleoprotein H, N-terminally processed]	HNRNPH1 HNRPH HNRPH1	449	43,28	27,84	8	11
P62140	Serine/threonine-protein phosphatase PP1-beta catalytic subunit (PP-1B) (PPP1CD) (EC 3.1.3.16) (EC 3.1.3.53)	PPP1CB	327	41,04	40,67	8	11
Q14192	Four and a half LIM domains protein 2 (FHL-2) (LIM domain protein DRAL) (Skeletal muscle LIM-protein 3) (SLIM-3)	FHL2 DRAL SLIM3	279	41,57	50,54	9	11
Q86VP1	Tax1-binding protein 1 (TRAF6-binding protein)	TAX1BP1 T6BP PRO0105	789	38,84	12,55	9	11
Q9NYL9	Tropomodulin-3 (Ubiquitous tropomodulin) (U-Tmod)	TMOD3	352	40,40	38,07	9	11
O14964	Hepatocyte growth factor-regulated tyrosine kinase substrate (Hrs) (Protein pp110)	HGS HRS	777	35,23	19,31	10	10
O60884	DnaJ homolog subfamily A member 2 (Cell cycle progression restoration gene 3 protein) (Dnj3) (Dj3) (HIRA-interacting protein 4)	DNAJA2 CPR3 HIRIP4	412	40,95	33,98	7	10
P14866	Heterogeneous nuclear ribonucleoprotein L (hnRNP L)	HNRNPL HNRPL P/OKcl.14	589	44,63	30,73	7	10
P36578	60S ribosomal protein L4 (60S ribosomal protein L1)	RPL4 RPL1	427	36,50	23,42	9	10
Q14204	Cytoplasmic dynein 1 heavy chain 1 (Cytoplasmic dynein heavy chain 1) (Dynein heavy chain, cytosolic)	DYNC1H1 DHC1 DNCH1 DNCL DNECL DYHC KIAA0325	4646	32,55	3,47	10	10
Q8N556	Actin filament-associated protein 1 (110 kDa actin filament-associated protein) (AFAP-110)	AFAP1 AFAP	730	32,45	22,60	10	10
Q96PM5	RING finger and CHY zinc finger domain-containing protein 1 (EC 6.3.2.-) (Androgen receptor N-terminal-interacting protein)	RCHY1 ARNIP CHIMP PIRH2 RNF199 ZNF363	261	39,18	49,43	8	10
Q9UJX4	Anaphase-promoting complex subunit 5 (APC5) (Cyclosome subunit 5)	ANAPC5 APC5	755	36,90	14,83	8	10

O15371	Eukaryotic translation initiation factor 3 subunit D (eIF3d) (Eukaryotic translation initiation factor 3 subunit 7) (eIF-3-zeta) (eIF3 p66)	EIF3D EIF3S7	548	35,59	21,17	7	9
O43795	Unconventional myosin-Ib (MYH-1c) (Myosin I alpha) (MMI-alpha) (MMIa)	MYO1B	1136	35,14	12,85	9	9
O95425	Supervillin (Archvillin) (p205/p250)	SVIL	2214	37,25	7,27	9	9
P04843	Dolichyl-diphosphooligosaccharide--protein glycosyltransferase subunit 1 (EC 2.4.99.18)	RPN1	607	36,62	22,24	8	9
P09493	Tropomyosin alpha-1 chain (Alpha-tropomyosin) (Tropomyosin-1)	TPM1 C15orf13 TMSA	284	32,37	17,25	6	9
P46777	60S ribosomal protein L5	RPL5 MSTP030	297	31,58	29,97	7	9
P52292	Importin subunit alpha-1 (Karyopherin subunit alpha-2) (RAG cohort protein 1) (SRP1-alpha)	KPNA2 RCH1 SRP1	529	32,70	21,74	7	9
Q13470	Non-receptor tyrosine-protein kinase TNK1 (EC 2.7.10.2) (CD38 negative kinase 1)	TNK1	666	35,50	18,17	7	9
Q14145	Kelch-like ECH-associated protein 1 (Cytosolic inhibitor of Nrf2) (INrf2) (Kelch-like protein 19)	KEAP1 INRF2 KIAA0132 KLHL19	624	39,04	27,56	8	9
Q8WUF5	RelA-associated inhibitor (Inhibitor of ASPP protein) (Protein iASPP) (NFKB-interacting protein 1) (PPP1R13B-like protein)	PPP1R13L IASPP NKIP1 PPP1R13BL RAI	828	34,48	19,32	9	9
Q9BYM8	RanBP-type and C3HC4-type zinc finger-containing protein 1 (EC 6.3.2.-) (HBV-associated factor 4)	RBCK1 C20orf18 RNF54 UBCE7IP3 XAP3 XAP4	510	34,27	21,57	7	9
O14545	TRAF-type zinc finger domain-containing protein 1 (Protein FLN29)	TRAFFD1 FLN29	582	31,07	23,71	8	8
O15020	Spectrin beta chain, non-erythrocytic 2 (Beta-III spectrin) (Spinocerebellar ataxia 5 protein)	SPTBN2 KIAA0302 SCA5	2390	31,23	3,85	7	8
P04792	Heat shock protein beta-1 (HspB1) (28 kDa heat shock protein)	HSPB1 HSP27 HSP28	205	26,44	51,22	5	8
P22314	Ubiquitin-like modifier-activating enzyme 1 (Protein A1S9) (Ubiquitin-activating enzyme E1)	UBA1 A1S9T UBE1	1058	32,23	7,84	5	8
P52907	F-actin-capping protein subunit alpha-1 (CapZ alpha-1)	CAPZA1	286	30,11	31,12	5	8
P62195	26S protease regulatory subunit 8 (26S proteasome AAA-ATPase subunit RPT6) (Proteasome 26S subunit ATPase 5)	PSMC5 SUG1	406	28,12	21,92	7	8
P78347	General transcription factor II-I (GTFII-I) (TFII-I) (Bruton tyrosine kinase-associated protein 135) (BAP-135) (BTK-associated protein 135)	GTF2I BAP135 WBSCR6	998	31,23	10,02	7	8
Q02880	DNA topoisomerase 2-beta (EC 5.99.1.3) (DNA topoisomerase II, beta isozyme)	TOP2B	1626	30,65	8,24	8	8
Q12905	Interleukin enhancer-binding factor 2 (Nuclear factor of activated T-cells 45 kDa)	ILF2 NF45 PRO3063	390	29,93	26,67	6	8

Appendix

Q15276	Rab GTPase-binding effector protein 1 (Rabaptin-4) (Rabaptin-5) (Rabaptin-5alpha) (Renal carcinoma antigen NY-REN-17)	RABEP1 RAB5EP RABPT5 RABPT5A	862	31,21	11,48	7	8
Q16531	DNA damage-binding protein 1 (DDB p127 subunit) (DNA damage-binding protein a) (DDBa) (Damage-specific DNA-binding protein 1)	DDB1 XAP1	1140	27,31	10,96	8	8
Q5M775	Cytospin-B (Nuclear structure protein 5) (NSP5) (Sperm antigen HCMOGT-1) (Sperm antigen with calponin homology and coiled-coil domains 1)	SPECC1 CYTSB NSP5	1068	33,22	12,27	8	8
Q6GQQ9	OTU domain-containing protein 7B (EC 3.4.19.12) (Cellular zinc finger anti-NF-kappa-B protein)	OTUD7B ZA20D1	843	29,92	13,64	8	8
Q6P2Q9	Pre-mRNA-processing-splicing factor 8 (220 kDa U5 snRNP-specific protein) (PRP8 homolog) (Splicing factor Prp8) (p220)	PRPF8 PRPC8	2335	28,23	5,35	7	8
Q92841	Probable ATP-dependent RNA helicase DDX17 (EC 3.6.4.13) (DEAD box protein 17) (DEAD box protein p72) (RNA-dependent helicase p72)	DDX17	729	31,05	16,05	8	8
Q96I18	Leucine-rich repeat and calponin homology domain-containing protein 3	LRCH3	777	30,62	18,79	7	8
Q9BY89	Uncharacterized protein KIAA1671	KIAA1671	1806	30,12	6,70	7	8
O75128	Protein cordon-bleu	COBL KIAA0633	1261	24,78	6,19	6	7
O95831	Apoptosis-inducing factor 1, mitochondrial (EC 1.1.1.-) (Programmed cell death protein 8)	AIFM1 AIF PDCD8	613	24,24	14,19	7	7
P13010	X-ray repair cross-complementing protein 5 (EC 3.6.4.-) (86 kDa subunit of Ku antigen) (ATP-dependent DNA helicase 2 subunit 2)	XRCC5 G22P2	732	25,88	15,44	6	7
P15880	40S ribosomal protein S2 (40S ribosomal protein S4) (Protein LLRep3)	RPS2 RPS4	293	26,33	21,50	5	7
P35606	Coatomer subunit beta' (Beta'-coat protein) (Beta'-COP) (p102)	COPB2	906	24,86	11,70	6	7
P40939	Trifunctional enzyme subunit alpha, mitochondrial (78 kDa gastrin-binding protein) (TP-alpha)	HADHA HADH	763	26,87	15,86	7	7
P47756	F-actin-capping protein subunit beta (CapZ beta)	CAPZB	277	24,59	27,80	6	7
Q6WCQ1	Myosin phosphatase Rho-interacting protein (M-RIP) (Rho-interacting protein 3) (RIP3) (p116Rip)	MPRIIP KIAA0864 MRIP RHOIP3	1025	29,54	13,17	7	7
Q86SQ0	Pleckstrin homology-like domain family B member 2 (Protein LL5-beta)	PHLDB2 LL5B	1253	29,00	11,01	7	7
Q86XP3	ATP-dependent RNA helicase DDX42 (EC 3.6.4.13) (DEAD box protein 42) (RNA helicase-like protein) (RHELP)	DDX42	938	26,67	16,63	6	7
Q8IYW5	E3 ubiquitin-protein ligase RNF168 (hRNF168) (EC 6.3.2.-) (RING finger protein 168)	RNF168	571	30,76	16,29	5	7

Q8N3C0	Activating signal cointegrator 1 complex subunit 3 (EC 3.6.4.12) (ASC-1 complex subunit p200)	ASCC3 HELIC1	2202	27,17	4,86	6	7
Q96EY1	DnaJ homolog subfamily A member 3, mitochondrial (DnaJ protein Tid-1) (hTid-1)	DNAJA3 HCA57 TID1	480	27,11	22,71	6	7
Q96RL1	BRCA1-A complex subunit RAP80 (Receptor-associated protein 80) (Retinoid X receptor-interacting protein 110)	UIMC1 RAP80 RXRIP110	719	25,02	14,46	6	7
Q99460	26S proteasome non-ATPase regulatory subunit 1 (26S proteasome regulatory subunit RPN2)	PSMD1	953	29,95	14,48	7	7
Q9NS91	E3 ubiquitin-protein ligase RAD18 (EC 6.3.2.-) (Postreplication repair protein RAD18) (hHR18) (RAD18 RNF73	495	23,78	15,96	6	7
Q9P275	Ubiquitin carboxyl-terminal hydrolase 36 (EC 3.4.19.12) (Deubiquitinating enzyme 36) (Ubiquitin thioesterase 36)	USP36 KIAA1453	1121	28,26	5,80	5	7
Q9UJX6	Anaphase-promoting complex subunit 2 (APC2) (Cyclosome subunit 2)	ANAPC2 APC2 KIAA1406	822	26,21	11,80	7	7
Q9UMS4	Pre-mRNA-processing factor 19 (Nuclear matrix protein 200) (PRP19/PSO4 homolog) (hPso4) (Senescence evasion factor)	PRPF19 NMP200 PRP19 SNEV	504	32,18	27,98	5	7
O00571	ATP-dependent RNA helicase DDX3X (EC 3.6.4.13) (DEAD box protein 3, X-chromosomal)	DDX3X DBX DDX3	662	23,84	12,24	6	6
O15037	Protein KHNYN (KH and NYN domain-containing protein)	KHNYN KIAA0323	678	21,96	8,55	4	6
O15143	Actin-related protein 2/3 complex subunit 1B (Arp2/3 complex 41 kDa subunit) (p41-ARC)	ARPC1B ARC41	372	24,04	26,88	5	6
O43242	26S proteasome non-ATPase regulatory subunit 3 (26S proteasome regulatory subunit RPN3)	PSMD3	534	23,03	17,04	6	6
O43684	Mitotic checkpoint protein BUB3	BUB3	328	20,77	21,04	5	6
O43823	A-kinase anchor protein 8 (AKAP-8) (A-kinase anchor protein 95 kDa) (AKAP 95)	AKAP8 AKAP95	692	23,40	12,86	5	6
O75533	Splicing factor 3B subunit 1 (Pre-mRNA-splicing factor SF3b 155 kDa subunit) (SF3b155) (Spliceosome-associated protein 155) (SAP 155)	SF3B1 SAP155	1304	22,39	6,52	6	6
O75643	U5 small nuclear ribonucleoprotein 200 kDa helicase (EC 3.6.4.13) (Activating signal cointegrator 1 complex subunit 3-like 1)	SNRNP200 ASCC3L1 HELIC2 KIAA0788	2136	22,88	3,98	6	6
P08174	Complement decay-accelerating factor (CD antigen CD55)	CD55 CR DAF	381	24,70	14,96	3	6
P18124	60S ribosomal protein L7	RPL7	248	22,10	26,21	5	6
P35613	Basigin (5F7) (Collagenase stimulatory factor) (Extracellular matrix metalloproteinase inducer) (EMMPRIN)	BSG UNQ6505/PRO21383	385	23,24	21,82	4	6

Appendix

P38159	RNA-binding motif protein, X chromosome (Glycoprotein p43) (Heterogeneous nuclear ribonucleoprotein G) (hnRNP G)	RBMX HNRPG RBMXP1	391	22,83	17,90	5	6
P42566	Epidermal growth factor receptor substrate 15 (Protein Eps15) (Protein AF-1p)	EPS15 AF1P	896	22,19	9,93	5	6
P42704	Leucine-rich PPR motif-containing protein, mitochondrial (130 kDa leucine-rich protein) (LRP 130) (GP130)	LRPPRC LRP130	1394	21,27	6,03	6	6
P57740	Nuclear pore complex protein Nup107 (107 kDa nucleoporin) (Nucleoporin Nup107)	NUP107	925	24,35	12,22	6	6
P62158	Calmodulin (CaM)	CALM1 CALM CAM CAM1; CALM2 CAM2 CAMB; CALM3 CALML2 CAM3 CAMC CAMIII	149	24,03	28,86	3	6
P62424	60S ribosomal protein L7a (PLA-X polypeptide) (Surfeit locus protein 3)	RPL7A SURF-3 SURF3	266	22,34	15,04	4	6
P78527	DNA-dependent protein kinase catalytic subunit (DNA-PK catalytic subunit) (DNA-PKcs) (EC 2.7.11.1) (DNPK1) (p460)	PRKDC HYRC HYRC1	4128	21,48	1,84	6	6
Q08380	Galectin-3-binding protein (Basement membrane autoantigen p105) (Lectin galactoside-binding soluble 3-binding protein)	LGALS3BP M2BP	585	21,53	16,92	5	6
Q12849	G-rich sequence factor 1 (GRSF-1)	GRSF1	480	21,63	19,17	5	6
Q12906	Interleukin enhancer-binding factor 3 (Double-stranded RNA-binding protein 76) (DRBP76) (M-phase phosphoprotein 4) (MPP4)	ILF3 DRBF MPHOSPH4 NF90	894	21,22	9,84	5	6
Q13200	26S proteasome non-ATPase regulatory subunit 2 (26S proteasome regulatory subunit RPN1) (26S proteasome regulatory subunit S2)	PSMD2 TRAP2	908	22,26	9,03	5	6
Q13751	Laminin subunit beta-3 (Epiligrin subunit bata) (Kalinin B1 chain) (Kalinin subunit beta) (LAMB3 LAMNB1	1172	25,50	10,15	6	6
Q15646	2'-5'-oligoadenylate synthase-like protein (2'-5'-OAS-related protein) (2'-5'-OAS-RP) (59 kDa 2'-5'-oligoadenylate synthase-like protein)	OASL TRIP14	514	22,00	15,56	5	6
Q3ZCQ8	Mitochondrial import inner membrane translocase subunit TIM50	TIMM50 TIM50 PRO1512	353	20,62	20,68	5	6
Q5JSZ5	Protein PRRC2B (HLA-B-associated transcript 2-like 1) (Proline-rich coiled-coil protein 2B)	PRRC2B BAT2L BAT2L1 KIAA0515	2229	23,79	4,13	5	6
Q7RTP6	Protein-methionine sulfoxide oxidase MICAL3 (EC 1.14.13.-) (Molecule interacting with CasL protein 3) (MICAL-3)	MICAL3 KIAA0819 KIAA1364	2002	20,82	4,00	6	6
Q8IW35	Centrosomal protein of 97 kDa (Cep97) (Leucine-rich repeat and IQ domain-containing protein 2)	CEP97 LRRIQ2	865	20,57	11,33	6	6

Q8NCE2	Myotubularin-related protein 14 (EC 3.1.3.-) (HCV NS5A-transactivated protein 4 splice variant A-binding protein 1)	MTMR14 C3orf29	650	21,07	14,31	6	6
Q8TC07	TBC1 domain family member 15 (GTPase-activating protein RAB7) (GAP for RAB7) (Rab7-GAP)	TBC1D15	691	22,77	12,74	6	6
Q8WUM0	Nuclear pore complex protein Nup133 (133 kDa nucleoporin) (Nucleoporin Nup133)	NUP133	1156	26,78	9,34	6	6
Q9NQC7	Ubiquitin carboxyl-terminal hydrolase CYLD (EC 3.4.19.12) (Deubiquitinating enzyme CYLD) (Ubiquitin thioesterase CYLD)	CYLD CYLD1 KIAA0849 HSPC057	956	20,57	8,37	6	6
Q9UBC2	Epidermal growth factor receptor substrate 15-like 1 (Eps15-related protein) (Eps15R)	EPS15L1 EPS15R	864	25,72	14,24	6	6
Q9UNM6	26S proteasome non-ATPase regulatory subunit 13 (26S proteasome regulatory subunit RPN9)	PSMD13	376	23,23	17,82	4	6
Q9Y5B9	FACT complex subunit SPT16 (Chromatin-specific transcription elongation factor 140 kDa subunit) (FACT 140 kDa subunit)	SUPT16H FACT140 FACTP140	1047	22,97	6,78	6	6
O00165	HCLS1-associated protein X-1 (HS1-associating protein X-1) (HAX-1) (HS1-binding protein 1) (HSP1BP-1)	HAX1 HS1BP1	279	20,22	19,00	3	5
O15511	Actin-related protein 2/3 complex subunit 5 (Arp2/3 complex 16 kDa subunit) (p16-ARC)	ARPC5 ARC16	151	23,26	30,46	3	5
O75323	Protein NipSnap homolog 2 (NipSnap2) (Glioblastoma-amplified sequence)	GBAS NIPSNAP2	286	19,29	30,77	5	5
O75821	Eukaryotic translation initiation factor 3 subunit G (eIF3g) (Eukaryotic translation initiation factor 3 RNA-binding subunit)	EIF3G EIF3S4	320	19,34	13,44	4	5
P05141	ADP/ATP translocase 2 (ADP,ATP carrier protein 2) (ADP,ATP carrier protein, fibroblast isoform) (Adenine nucleotide translocator 2)	SLC25A5 ANT2	298	19,91	13,09	3	5
P11388	DNA topoisomerase 2-alpha (EC 5.99.1.3) (DNA topoisomerase II, alpha isozyme)	TOP2A TOP2	1531	20,47	4,18	4	5
P12236	ADP/ATP translocase 3 (ADP,ATP carrier protein 3) (ADP,ATP carrier protein, isoform T2) (ANT 2) (Adenine nucleotide translocator 3) (ANT 3)	SLC25A6 ANT3 CDABP0051	298	20,55	22,15	4	5
P13987	CD59 glycoprotein (1F5 antigen) (20 kDa homologous restriction factor) (HRF-20) (HRF20) (MAC-inhibitory protein) (MAC-IP)	CD59 MIC11 MIN1 MIN2 MIN3 MSK21	128	18,50	18,75	2	5
P14923	Junction plakoglobin (Catenin gamma) (Desmoplakin III) (Desmoplakin-3)	JUP CTNNG DP3	745	17,11	9,40	4	5
P27105	Erythrocyte band 7 integral membrane protein (Protein 7.2b) (Stomatin)	STOM BND7 EPB72	288	19,37	24,65	4	5
P27708	CAD protein [Includes: Glutamine-dependent carbamoyl-phosphate synthase (EC 6.3.5.5);	CAD	2225	20,95	4,85	5	5
P35268	60S ribosomal protein L22 (EBER-associated protein) (EAP) (Epstein-Barr virus small RNA-associated protein)	RPL22	128	18,05	50,78	4	5

Appendix

P43686	26S protease regulatory subunit 6B (26S proteasome AAA-ATPase subunit RPT3) (MB67-interacting protein) (MIP224)	PSMC4 MIP224 TBP7	418	18,75	18,42	3	5
P46087	Putative ribosomal RNA methyltransferase NOP2 (EC 2.1.1.-) (Nucleolar protein 1) (Nucleolar protein 2 homolog)	NOP2 NOL1	812	17,74	10,22	5	5
P49411	Elongation factor Tu, mitochondrial (EF-Tu) (P43)	TUFM	452	17,56	14,60	5	5
P60842	Eukaryotic initiation factor 4A-I (eIF-4A-I) (eIF4A-I) (EC 3.6.4.13) (ATP-dependent RNA helicase eIF4A-1)	EIF4A1 DDX2A EIF4A	406	18,86	14,53	4	5
P62269	40S ribosomal protein S18 (Ke-3) (Ke3)	RPS18 D6S218E	152	18,09	21,71	4	5
P62888	60S ribosomal protein L30	RPL30	115	19,04	50,43	4	5
Q03013	Glutathione S-transferase Mu 4 (EC 2.5.1.18) (GST class-mu 4) (GST-Mu2) (GSTM4-4)	GSTM4	218	19,16	29,82	5	5
Q07020	60S ribosomal protein L18	RPL18	188	16,96	25,53	4	5
Q08499	cAMP-specific 3',5'-cyclic phosphodiesterase 4D (EC 3.1.4.53) (DPDE3) (PDE43)	PDE4D DPDE3	809	19,07	11,74	5	5
Q13347	Eukaryotic translation initiation factor 3 subunit I (eIF3I) (Eukaryotic translation initiation factor 3 subunit 2)	EIF3I EIF3S2 TRIP1	325	19,42	35,69	5	5
Q15046	Lysine--tRNA ligase (EC 6.1.1.6) (Lysyl-tRNA synthetase) (LysRS)	KARS KIAA0070	597	19,66	17,09	5	5
Q15650	Activating signal cointegrator 1 (ASC-1) (Thyroid receptor-interacting protein 4) (TR-interacting protein 4) (TRIP-4)	TRIP4	581	20,37	18,24	5	5
Q8IUH3	RNA-binding protein 45 (Developmentally-regulated RNA-binding protein 1) (RB-1) (RNA-binding motif protein 45)	RBM45 DRB1 DRBP1	476	19,06	12,18	4	5
Q8NHV4	Protein NEDD1 (Neural precursor cell expressed developmentally down-regulated protein 1) (NEDD-1)	NEDD1	660	19,07	6,82	4	5
Q96GX5	Serine/threonine-protein kinase greatwall (GW) (GWL) (hGWL) (EC 2.7.11.1) (Microtubule-associated serine/threonine-protein kinase-like)	MASTL GW GWL THC2	879	19,40	6,14	4	5
Q96R06	Sperm-associated antigen 5 (Astrin) (Deepest) (Mitotic spindle-associated protein p126) (MAP126)	SPAG5	1193	19,46	7,54	5	5
Q96SB3	Neurabin-2 (Neurabin-II) (Protein phosphatase 1 regulatory subunit 9B) (Spinophilin)	PPP1R9B PPP1R6	815	19,58	6,99	4	5
Q9BPW8	Protein NipSnap homolog 1 (NipSnap1)	NIPSNAP1	284	19,00	32,39	5	5
Q9Y230	RuvB-like 2 (EC 3.6.4.12) (48 kDa TATA box-binding protein-interacting protein) (48 kDa TBP-interacting protein)	RUVBL2 INO80J TIP48 TIP49B CGI-46	463	17,47	13,61	5	5

O00232	26S proteasome non-ATPase regulatory subunit 12 (26S proteasome regulatory subunit RPN5) (26S proteasome regulatory subunit p55)	PSMD12	456	14,24	7,89	3	4
O00267	Transcription elongation factor SPT5 (hSPT5) (DRB sensitivity-inducing factor 160 kDa subunit) (DSIF p160)	SUPT5H SPT5 SPT5H	1087	16,27	5,89	3	4
O00622	Protein CYR61 (CCN family member 1) (Cysteine-rich angiogenic inducer 61) (Insulin-like growth factor-binding protein 10) (IBP-10)	CYR61 CCN1 GIG1 IGFBP10	381	16,83	19,42	3	4
O14979	Heterogeneous nuclear ribonucleoprotein D-like (hnRNP D-like) (hnRNP DL) (AU-rich element RNA-binding factor) (JKT41-binding protein)	HNRNPDL HNRPDL JKTBP	420	13,80	9,05	3	4
O43143	Putative pre-mRNA-splicing factor ATP-dependent RNA helicase DHX15 (EC 3.6.4.13) (ATP-dependent RNA helicase #46)	DHX15 DBP1 DDX15	795	14,05	8,81	4	4
O43175	D-3-phosphoglycerate dehydrogenase (3-PGDH) (EC 1.1.1.95)	PHGDH PGDH3	533	13,33	9,19	4	4
O60506	Heterogeneous nuclear ribonucleoprotein Q (hnRNP Q) (Glycine- and tyrosine-rich RNA-binding protein) (GRY-RBP)	SYNCRIP HNRPQ NSAP1	623	14,54	9,15	4	4
O60573	Eukaryotic translation initiation factor 4E type 2 (eIF-4E type 2) (eIF4E type 2)	EIF4E2 EIF4EL3	245	13,35	22,86	4	4
O75044	SLIT-ROBO Rho GTPase-activating protein 2 (srGAP2) (Formin-binding protein 2) (Rho GTPase-activating protein 34)	SRGAP2 ARHGAP34 FNBP2 KIAA0456 SRGAP2A	1071	16,58	7,56	4	4
O94875	Sorbin and SH3 domain-containing protein 2 (Arg/Abl-interacting protein 2) (ArgBP2) (Sorbin)	SORBS2 ARGBP2 KIAA0777	1100	14,03	6,82	4	4
O94966	Ubiquitin carboxyl-terminal hydrolase 19 (EC 3.4.19.12) (Deubiquitinating enzyme 19) (Ubiquitin thioesterase 19)	USP19 KIAA0891 ZMYND9	1318	15,63	5,99	4	4
O95817	BAG family molecular chaperone regulator 3 (BAG-3) (Bcl-2-associated athanogene 3) (Bcl-2-binding protein Bis) (Docking protein CAIR-1)	BAG3 BIS	575	18,89	10,96	3	4
P05386	60S acidic ribosomal protein P1	RPLP1 RRP1	114	15,28	66,67	3	4
P08195	4F2 cell-surface antigen heavy chain (4F2hc) (4F2 heavy chain antigen) (Lymphocyte activation antigen 4F2 large subunit)	SLC3A2 MDU1	630	12,78	8,41	4	4
P17980	26S protease regulatory subunit 6A (26S proteasome AAA-ATPase subunit RPT5) (Proteasome 26S subunit ATPase 3)	PSMC3 TBP1	439	12,76	10,48	3	4
P35637	RNA-binding protein FUS (75 kDa DNA-pairing protein) (Oncogene FUS) (Oncogene TLS) (POMp75) (Translocated in liposarcoma protein)	FUS TLS	526	16,01	15,97	4	4

Appendix

P35998	26S protease regulatory subunit 7 (26S proteasome AAA-ATPase subunit RPT1) (Proteasome 26S subunit ATPase 2) (Protein MSS1)	PSMC2 MSS1	433	15,97	15,47	4	4
P42677	40S ribosomal protein S27 (Metallopan-stimulin 1) (MPS-1)	RPS27 MPS1	84	12,99	29,76	2	4
P46736	Lys-63-specific deubiquitinase BRCC36 (EC 3.4.19.-) (BRCA1-A complex subunit BRCC36) (BRCA1/BRCA2-containing complex subunit 3)	BRCC3 BRCC36 C6.1A CXorf53	316	15,28	17,09	4	4
P46781	40S ribosomal protein S9	RPS9	194	12,49	16,49	4	4
P46782	40S ribosomal protein S5 [Cleaved into: 40S ribosomal protein S5, N-terminally processed]	RPS5	204	17,33	28,43	4	4
P48643	T-complex protein 1 subunit epsilon (TCP-1-epsilon) (CCT-epsilon)	CCT5 CCTE KIAA0098	541	14,60	12,20	4	4
P50416	Carnitine O-palmitoyltransferase 1, liver isoform (CPT1-L) (EC 2.3.1.21) (Carnitine O-palmitoyltransferase I, liver isoform) (CPT I)	CPT1A CPT1	773	15,34	8,80	4	4
P51532	Transcription activator BRG1 (EC 3.6.4.-) (ATP-dependent helicase SMARCA4) (BRG1-associated factor 190A) (BAF190A)	SMARCA4 BAF190A BRG1 SNF2B SNF2L4	1647	17,42	3,46	4	4
P51610	Host cell factor 1 (HCF) (HCF-1) (C1 factor) (CFF) (VCAF) (VP16 accessory protein)	HCFC1 HCF1 HFC1	2035	15,05	2,36	3	4
P56192	Methionine--tRNA ligase, cytoplasmic (EC 6.1.1.10) (Methionyl-tRNA synthetase) (MetRS)	MARS	900	15,06	11,11	4	4
P61160	Actin-related protein 2 (Actin-like protein 2)	ACTR2 ARP2	394	14,65	12,18	4	4
P61981	14-3-3 protein gamma (Protein kinase C inhibitor protein 1) (KCIP-1) [Cleaved into: 14-3-3 protein gamma, N-terminally processed]	YWHAG	247	13,55	26,32	4	4
P62333	26S protease regulatory subunit 10B (26S proteasome AAA-ATPase subunit RPT4) (Proteasome 26S subunit ATPase 6)	PSMC6 SUG2	389	14,13	13,62	3	4
P62753	40S ribosomal protein S6 (Phosphoprotein NP33)	RPS6 OK/SW-cl.2	249	13,03	21,29	4	4
P62805	Histone H4	HIST1H4A H4	103	12,78	38,83	4	4
P63167	Dynein light chain 1, cytoplasmic (8 kDa dynein light chain) (DLC8) (Dynein light chain LC8-type 1)	DYNLL1 DLC1 DNCL1 DNCLC1 HDLC1	89	16,90	50,56	3	4
P63220	40S ribosomal protein S21	RPS21	83	15,42	39,76	3	4
P78406	mRNA export factor (Rae1 protein homolog) (mRNA-associated protein mrnp 41)	RAE1 MRNP41	368	15,54	21,20	4	4
P84098	60S ribosomal protein L19	RPL19	196	14,91	17,35	3	4
Q00587	Cdc42 effector protein 1 (Binder of Rho GTPases 5) (Serum protein MSE55)	CDC42EP1 BORG5 CEP1 MSE55	391	16,54	16,37	3	4

Q02878	60S ribosomal protein L6 (Neoplasm-related protein C140) (Tax-responsive enhancer element-binding protein 107) (TaxREB107)	RPL6 TXREB1	288	12,76	14,93	4	4
Q05086	Ubiquitin-protein ligase E3A (EC 6.3.2.-) (E6AP ubiquitin-protein ligase) (Human papillomavirus E6-associated protein)	UBE3A E6AP EPVE6AP HPVE6A	875	19,06	8,34	4	4
Q06830	Peroxiredoxin-1 (EC 1.11.1.15) (Natural killer cell-enhancing factor A) (NKEF-A) (Proliferation-associated gene protein) (PAG)	PRDX1 PAGA PAGB TDPX2	199	12,78	29,65	4	4
Q08050	Forkhead box protein M1 (Forkhead-related protein FKHL16) (Hepatocyte nuclear factor 3 forkhead homolog 11) (HFH-11)	FOXM1 FKHL16 HFH11 MPP2 WIN	763	15,66	9,96	4	4
Q12769	Nuclear pore complex protein Nup160 (160 kDa nucleoporin) (Nucleoporin Nup160)	NUP160 KIAA0197 NUP120	1436	13,52	5,36	4	4
Q12789	General transcription factor 3C polypeptide 1 (TF3C-alpha) (TFIIIC box B-binding subunit) (Transcription factor IIIC 220 kDa subunit)	GTF3C1	2109	13,43	4,69	4	4
Q12904	Aminoacyl tRNA synthase complex-interacting multifunctional protein 1 (Multisynthase complex auxiliary component p43)	AIMP1 EMAP2 SCYE1	312	12,75	17,31	2	4
Q13151	Heterogeneous nuclear ribonucleoprotein A0 (hnRNP A0)	HNRNPA0 HNRPA0	305	15,15	21,31	4	4
Q13247	Serine/arginine-rich splicing factor 6 (Pre-mRNA-splicing factor SRP55) (Splicing factor, arginine/serine-rich 6)	SRSF6 SFRS6 SRP55	344	14,05	8,72	3	4
Q14596	Next to BRCA1 gene 1 protein (Cell migration-inducing gene 19 protein) (Membrane component chromosome 17 surface marker 2) (NBR1 1A13B KIAA0049 M17S2 MIG19	966	15,69	7,14	3	4
Q14839	Chromodomain-helicase-DNA-binding protein 4 (CHD-4) (EC 3.6.4.12) (ATP-dependent helicase CHD4)	CHD4	1912	17,91	4,03	4	4
Q15233	Non-POU domain-containing octamer-binding protein (NonO protein) (54 kDa nuclear RNA- and DNA-binding protein)	NONO NRB54	471	14,68	12,10	4	4
Q16576	Histone-binding protein RBBP7 (Histone acetyltransferase type B subunit 2)	RBBP7 RBAP46	425	14,69	14,12	4	4
Q16666	Gamma-interferon-inducible protein 16 (Ifi-16) (Interferon-inducible myeloid differentiation transcriptional activator)	IFI16 IFNGIP1	785	12,54	7,13	4	4
Q86TC9	Myopalladin (145 kDa sarcomeric protein)	MYPN MYOP	1320	15,43	5,45	3	4
Q92547	DNA topoisomerase 2-binding protein 1 (DNA topoisomerase II-beta-binding protein 1) (TopBP1)	TOPBP1 KIAA0259	1522	13,61	4,40	4	4
Q92783	Signal transducing adapter molecule 1 (STAM-1)	STAM STAM1	540	18,16	17,59	4	4

Appendix

Q96PK6	RNA-binding protein 14 (Paraspeckle protein 2) (PSP2) (RNA-binding motif protein 14) (RRM-containing coactivator activator/modulator)	RBM14 SIP	669	16,66	10,16	3	4
Q99623	Prohibitin-2 (B-cell receptor-associated protein BAP37) (D-prohibitin) (Repressor of estrogen receptor activity)	PHB2 BAP REA	299	13,62	18,06	4	4
Q9H5N1	Rab GTPase-binding effector protein 2 (Rabaptin-5beta)	RABEP2 RABPT5B	569	16,68	9,14	4	4
Q9NVV4	Poly(A) RNA polymerase, mitochondrial (PAP) (EC 2.7.7.19) (PAP-associated domain-containing protein 1) (Polynucleotide adenylyltransferase)	MTPAP PAPD1	582	17,51	14,60	4	4
Q9NWF9	E3 ubiquitin-protein ligase RNF216 (EC 6.3.2.-) (RING finger protein 216) (Triad domain-containing protein 3)	RNF216 TRIAD3 UBCE7IP1 ZIN	866	16,85	6,35	4	4
Q9P0K7	Ankycorbin (Ankyrin repeat and coiled-coil structure-containing protein) (Novel retinal pigment epithelial cell protein)	RAI14 KIAA1334 NORPEG	980	13,51	4,39	4	4
Q9P2J5	Leucine--tRNA ligase, cytoplasmic (EC 6.1.1.4) (Leucyl-tRNA synthetase) (LeuRS)	LARS KIAA1352	1176	12,89	6,29	4	4
Q9UDY2	Tight junction protein ZO-2 (Tight junction protein 2) (Zona occludens protein 2) (Zonula occludens protein 2)	TJP2 X104 ZO2	1190	14,14	4,54	4	4
Q9UK59	Lariat debranching enzyme (EC 3.1.-.-)	DBR1	544	14,45	10,29	4	4
Q9ULJ8	Neurabin-1 (Neurabin-I) (Neural tissue-specific F-actin-binding protein I) (Protein phosphatase 1 regulatory subunit 9A)	PPP1R9A KIAA1222	1098	14,18	4,92	4	4
Q9UQE7	Structural maintenance of chromosomes protein 3 (SMC protein 3) (SMC-3) (Basement membrane-associated chondroitin proteoglycan)	SMC3 BAM BMH CSPG6 SMC3L1	1217	14,06	3,94	3	4
Q9Y4B5	Protein SOGA2 (Coiled-coil domain-containing protein 165)	SOGA2 CCDC165 KIAA0802	1905	13,69	3,31	4	4
Q9Y4C2	Protein FAM115A	FAM115A KIAA0738	921	13,96	5,75	4	4
Q9Y608	Leucine-rich repeat flightless-interacting protein 2 (LRR FLII-interacting protein 2)	LRRFIP2	721	17,19	5,83	3	4
Q9Y678	Coatomer subunit gamma-1 (Gamma-1-coat protein) (Gamma-1-COP)	COPG1 COPG	874	14,12	8,24	3	4
O00541	Pescadillo homolog	PES1	588	10,47	5,78	3	3
O00592	Podocalyxin (GCTM-2 antigen) (Gp200) (Podocalyxin-like protein 1) (PC) (PCLP-1)	PODXL PCLP PCLP1	558	11,31	7,53	2	3
O15027	Protein transport protein Sec16A (SEC16 homolog A)	SEC16A KIAA0310 SEC16 SEC16L	2179	9,80	1,51	3	3
O15144	Actin-related protein 2/3 complex subunit 2 (Arp2/3 complex 34 kDa subunit) (p34-ARC)	ARPC2 ARC34 PRO2446	300	10,46	16,00	3	3

O15372	Eukaryotic translation initiation factor 3 subunit H (eIF3h) (Eukaryotic translation initiation factor 3 subunit 3) (eIF-3-gamma) (eIF3 p40 subunit)	EIF3H EIF3S3	352	9,80	13,35	3	3
O60216	Double-strand-break repair protein rad21 homolog (hHR21) (Nuclear matrix protein 1) (NXP-1) (SCC1 homolog)	RAD21 HR21 KIAA0078 NXP1	631	10,68	7,29	2	3
O75052	Carboxyl-terminal PDZ ligand of neuronal nitric oxide synthase protein (C-terminal PDZ ligand of neuronal nitric oxide synthase protein)	NOS1AP CAPON KIAA0464	506	11,47	7,91	3	3
O76021	Ribosomal L1 domain-containing protein 1 (CATX-11) (Cellular senescence-inhibited gene protein) (Protein PBK1)	RSL1D1 CATX11 CSIG PBK1 L12	490	10,27	8,57	3	3
O95816	BAG family molecular chaperone regulator 2 (BAG-2) (Bcl-2-associated athanogene 2)	BAG2	211	11,13	19,43	3	3
P00533	Epidermal growth factor receptor (EC 2.7.10.1) (Proto-oncogene c-ErbB-1)	EGFR ERBB ERBB1 HER1	1210	11,48	4,05	3	3
P07858	Cathepsin B (EC 3.4.22.1) (APP secretase) (APPS) (Cathepsin B1) [Cleaved into: Cathepsin B light chain; Cathepsin B heavy chain]	CTSB CPSB	339	10,62	13,86	3	3
POC2W1	F-box/SPRY domain-containing protein 1 (F-box only protein 45) (hFbxo45)	FBXO45 FBX45	286	9,17	11,89	3	3
P13674	Prolyl 4-hydroxylase subunit alpha-1 (4-PH alpha-1) (EC 1.14.11.2) (Procollagen-proline,2-oxoglutarate-4-dioxygenase subunit alpha-1)	P4HA1 P4HA	534	10,38	6,93	3	3
P14868	Aspartate--tRNA ligase, cytoplasmic (EC 6.1.1.12) (Aspartyl-tRNA synthetase) (AspRS) (Cell proliferation-inducing gene 40 protein)	DARS PIG40	501	10,91	8,38	3	3
P16070	CD44 antigen (CDw44) (Epican) (Extracellular matrix receptor III) (ECMR-III) (GP90 lymphocyte homing/adhesion receptor) (HUTCH-I)	CD44 LHR MDU2 MDU3 MIC4	742	10,50	5,26	3	3
P26373	60S ribosomal protein L13 (Breast basic conserved protein 1)	RPL13 BBC1 OK/SW-cl.46	211	10,72	16,11	3	3
P26447	Protein S100-A4 (Calvasculin) (Metastasin) (Placental calcium-binding protein) (Protein Mts1) (S100 calcium-binding protein A4)	S100A4 CAPL MTS1	101	9,18	28,71	3	3
P27824	Calnexin (IP90) (Major histocompatibility complex class I antigen-binding protein p88) (p90)	CANX	592	9,54	8,61	3	3
P31930	Cytochrome b-c1 complex subunit 1, mitochondrial (Complex III subunit 1) (Core protein I)	UQCRC1	480	9,15	12,50	3	3
P39019	40S ribosomal protein S19	RPS19	145	9,46	22,07	3	3
P41212	Transcription factor ETV6 (ETS translocation variant 6) (ETS-related protein Tel1) (Tel)	ETV6 TEL TEL1	452	9,81	9,73	3	3
P41743	Protein kinase C iota type (EC 2.7.11.13) (Atypical protein kinase C-lambda/iota) (PRKC-lambda/iota) (aPKC-lambda/iota) (nPKC-iota)	PRKCI DXS1179E	596	10,56	10,57	3	3

Appendix

P46060	Ran GTPase-activating protein 1 (RanGAP1)	RANGAP1 KIAA1835 SD	587	10,16	5,62	3	3
P46776	60S ribosomal protein L27a	RPL27A	148	10,20	15,54	2	3
P47755	F-actin-capping protein subunit alpha-2 (CapZ alpha-2)	CAPZA2	286	12,84	16,43	3	3
P50914	60S ribosomal protein L14 (CAG-ISL 7)	RPL14	215	10,55	15,35	3	3
P51116	Fragile X mental retardation syndrome-related protein 2	FXR2 FMR1L2	673	10,76	9,06	3	3
P52701	DNA mismatch repair protein Msh6 (hMSH6) (G/T mismatch-binding protein) (GTBP) (GTMBP) (MutS-alpha 160 kDa subunit) (p160)	MSH6 GTBP	1360	11,40	4,04	3	3
P54132	Bloom syndrome protein (EC 3.6.4.12) (DNA helicase, RecQ-like type 2) (RecQ2) (RecQ protein-like 3)	BLM RECQ2 RECQL3	1417	10,86	4,16	3	3
P55036	26S proteasome non-ATPase regulatory subunit 4 (26S proteasome regulatory subunit RPN10) (26S proteasome regulatory subunit S5A)	PSMD4 MCB1	377	12,84	11,41	3	3
P56537	Eukaryotic translation initiation factor 6 (eIF-6) (B(2)GCN homolog) (B4 integrin interactor) (CAB) (p27(BBP))	EIF6 EIF3A ITGB4BP OK/SW-cl.27	245	11,48	18,78	3	3
P57678	Gem-associated protein 4 (Gemin-4) (Component of gems 4) (p97)	GEMIN4	1058	10,70	7,75	3	3
P61247	40S ribosomal protein S3a (v-fos transformation effector protein) (Fte-1)	RPS3A FTE1 MFTL	264	11,05	16,29	3	3
P61313	60S ribosomal protein L15	RPL15 EC45 TCBAP0781	204	9,88	10,29	2	3
P62910	60S ribosomal protein L32	RPL32 PP9932	135	10,17	27,41	3	3
P63010	AP-2 complex subunit beta (AP105B) (Adapter-related protein complex 2 subunit beta) (Adaptor protein complex AP-2 subunit beta)	AP2B1 ADTB2 CLAPB1	937	15,27	8,75	3	3
Q02241	Kinesin-like protein KIF23 (Kinesin-like protein 5) (Mitotic kinesin-like protein 1)	KIF23 KNSL5 MKLP1	960	9,68	6,46	3	3
Q02543	60S ribosomal protein L18a	RPL18A	176	11,33	20,45	3	3
Q07157	Tight junction protein ZO-1 (Tight junction protein 1) (Zona occludens protein 1) (Zonula occludens protein 1)	TJP1 ZO1	1748	10,27	2,12	3	3
Q09028	Histone-binding protein RBBP4 (Chromatin assembly factor 1 subunit C) (CAF-1 subunit C) (Chromatin assembly factor I p48 subunit)	RBBP4 RBAP48	425	11,38	11,29	3	3
Q12888	Tumor suppressor p53-binding protein 1 (53BP1) (p53-binding protein 1) (p53BP1)	TP53BP1	1972	11,64	4,01	3	3
Q13162	Peroxiredoxin-4 (EC 1.11.1.15) (Antioxidant enzyme AOE372) (AOE37-2) (Peroxiredoxin IV) (PRDX4	271	11,17	16,24	2	3

Q13409	Cytoplasmic dynein 1 intermediate chain 2 (Cytoplasmic dynein intermediate chain 2) (Dynein intermediate chain 2, cytosolic)	DYNC112 DNCI2 DNCIC2	638	9,42	3,76	2	3
Q13615	Myotubularin-related protein 3 (EC 3.1.3.48) (FYVE domain-containing dual specificity protein phosphatase 1) (FYVE-DSP1)	MTMR3 KIAA0371 ZFYVE10	1198	11,61	4,42	3	3
Q14137	Ribosome biogenesis protein BOP1 (Block of proliferation 1 protein)	BOP1 KIAA0124	746	10,89	7,91	3	3
Q14244	Enscosin (Epithelial microtubule-associated protein of 115 kDa) (E-MAP-115) (Microtubule-associated protein 7) (MAP-7)	MAP7	749	9,06	3,20	2	3
Q14974	Importin subunit beta-1 (Importin-90) (Karyopherin subunit beta-1) (Nuclear factor p97)	KPNB1 NTF97	876	9,93	4,91	3	3
Q15029	116 kDa U5 small nuclear ribonucleoprotein component (Elongation factor Tu GTP-binding domain-containing protein 2) (SNU114 homolog) (hsNU114)	EFTUD2 KIAA0031 SNRP116	972	10,46	5,04	3	3
Q15365	Poly(rC)-binding protein 1 (Alpha-CP1) (Heterogeneous nuclear ribonucleoprotein E1) (hnRNP E1)	PCBP1	356	10,83	15,17	3	3
Q15648	Mediator of RNA polymerase II transcription subunit 1 (Activator-recruited cofactor 205 kDa component) (ARC205)	MED1 ARC205 CRSP1 CRSP200 DRIP205	1581	12,15	2,34	2	3
Q2NL82	Pre-rRNA-processing protein TSR1 homolog	TSR1 KIAA1401	804	10,66	7,46	3	3
Q6AWC2	Protein WWC2 (BH-3-only member B) (WW domain-containing protein 2)	WWC2 BOMB	1192	11,80	4,87	2	3
Q6PGQ7	Protein aurora borealis (HsBora)	BORA C13orf34	559	11,85	6,26	2	3
Q7KZF4	Staphylococcal nuclease domain-containing protein 1 (100 kDa coactivator) (EBNA2 coactivator p100)	SND1 TDRD11	910	13,17	5,38	3	3
Q7Z5Y7	BTB/POZ domain-containing protein KCTD20	KCTD20 C6orf69	419	10,43	12,65	3	3
Q8IY81	pre-rRNA processing protein FTSJ3 (EC 2.1.1.-) (2'-O-ribose RNA methyltransferase SPB1 homolog) (Protein ftsj homolog 3)	FTSJ3 SB92	847	11,11	5,19	2	3
Q8IY92	Structure-specific endonuclease subunit SLX4 (BTB/POZ domain-containing protein 12)	SLX4 BTBD12 KIAA1784 KIAA1987	1834	10,35	2,45	2	3
Q8N1F7	Nuclear pore complex protein Nup93 (93 kDa nucleoporin) (Nucleoporin Nup93)	NUP93 KIAA0095	819	11,03	5,01	3	3
Q8TDD1	ATP-dependent RNA helicase DDX54 (EC 3.6.4.13) (ATP-dependent RNA helicase DP97) (DEAD box RNA helicase 97 kDa)	DDX54	881	11,05	6,24	3	3
Q8TEB1	DDB1- and CUL4-associated factor 11 (WD repeat-containing protein 23)	DCAF11 WDR23 GL014 PRO2389	546	13,21	8,97	3	3

Appendix

Q96DE5	Anaphase-promoting complex subunit 16 (APC16) (Cyclosome subunit 16)	ANAPC16 C10orf104	110	10,98	39,09	3	3
Q96T88	E3 ubiquitin-protein ligase UHRF1 (EC 6.3.2.-) (Inverted CCAAT box-binding protein of 90 kDa) (Nuclear protein 95)	UHRF1 ICBP90 NP95 RNF106	793	12,40	5,55	3	3
Q9H098	Protein FAM107B	FAM107B C10orf45	131	10,59	19,08	3	3
Q9H6R0	Putative ATP-dependent RNA helicase DHX33 (EC 3.6.4.13) (DEAH box protein 33)	DHX33 DDX33	707	10,55	5,66	3	3
Q9NWM3	CUE domain-containing protein 1	CUEDC1	386	15,31	20,47	3	3
Q9NX58	Cell growth-regulating nucleolar protein	LYAR PNAS-5	379	10,99	14,51	3	3
Q9P0U4	CpG-binding protein (CXXC-type zinc finger protein 1) (PHD finger and CXXC domain-containing protein 1)	CXXC1 CFP1 CGBP PCCX1 PHF18	656	10,83	7,77	3	3
Q9UPQ3	Arf-GAP with GTPase, ANK repeat and PH domain- containing protein 1 (AGAP-1) (Centaurin-gamma-2) (Cnt-g2)	AGAP1 CENTG2 KIAA1099	857	11,67	4,67	3	3
Q9Y265	RuvB-like 1 (EC 3.6.4.12) (49 kDa TATA box-binding protein-interacting protein) (49 kDa TBP-interacting protein)	RUVBL1 INO80H NMP238 TIP49 TIP49A	456	10,84	9,65	3	3
Q9Y5Q9	General transcription factor 3C polypeptide 3 (Transcription factor IIIC 102 kDa subunit) (TFIIIC 102 kDa subunit) (TFIIIC102)	GTF3C3	886	11,39	5,53	3	3
A1L390	Pleckstrin homology domain-containing family G member 3 (PH domain-containing family G member 3)	PLEKHG3 KIAA0599	1219	7,23	3,69	2	2
O00231	26S proteasome non-ATPase regulatory subunit 11 (26S proteasome regulatory subunit RPN6) (26S proteasome regulatory subunit S9)	PSMD11	422	7,97	5,92	2	2
O00411	DNA-directed RNA polymerase, mitochondrial (MtrPOL) (EC 2.7.7.6)	POLRMT	1230	7,00	2,85	2	2
O00483	NADH dehydrogenase [ubiquinone] 1 alpha subcomplex subunit 4 (Complex I-MLRQ) (CI-MLRQ)	NDUFA4	81	6,11	27,16	2	2
O00567	Nucleolar protein 56 (Nucleolar protein 5A)	NOP56 NOL5A	594	8,20	4,21	2	2
O15381	Nuclear valosin-containing protein-like (NVLp) (Nuclear VCP-like protein)	NVL	856	7,07	3,50	2	2
O43491	Band 4.1-like protein 2 (Generally expressed protein 4.1) (4.1G)	EPB41L2	1005	5,94	3,28	2	2
O60232	Sjogren syndrome/scleroderma autoantigen 1 (Autoantigen p27)	SSSCA1	199	10,00	15,08	2	2
O60716	Catenin delta-1 (Cadherin-associated Src substrate) (CAS) (p120 catenin) (p120(ctn)) (p120(cas))	CTNND1 KIAA0384	968	6,36	4,03	2	2
O75146	Huntingtin-interacting protein 1-related protein (HIP1-related protein) (Huntingtin-interacting protein 12) (HIP-12)	HIP1R HIP12 KIAA0655	1068	6,91	2,34	2	2

O75808	Calpain-15 (EC 3.4.22.-) (Small optic lobes homolog)	CAPN15 SOLH	1086	7,23	2,39	2	2
O75822	Eukaryotic translation initiation factor 3 subunit J (eIF3j) (Eukaryotic translation initiation factor 3 subunit 1) (eIF-3-alpha) (eIF3 p35)	EIF3J EIF3S1 PRO0391	258	7,49	13,18	2	2
O95633	Follistatin-related protein 3 (Follistatin-like protein 3) (Follistatin-related gene protein)	FSTL3 FLRG UNQ674/PRO1308	263	7,38	9,51	2	2
O95782	AP-2 complex subunit alpha-1 (100 kDa coated vesicle protein A) (Adapter-related protein complex 2 subunit alpha-1)	AP2A1 ADTAA CLAPA1	977	6,98	6,04	2	2
P00367	Glutamate dehydrogenase 1, mitochondrial (GDH 1) (EC 1.4.1.3)	GLUD1 GLUD	558	7,90	6,99	2	2
P01891	HLA class I histocompatibility antigen, A-68 alpha chain (Aw-68) (HLA class I histocompatibility antigen, A-28 alpha chain)	HLA-A HLAA	365	7,60	7,40	2	2
P05362	Intercellular adhesion molecule 1 (ICAM-1) (Major group rhinovirus receptor) (CD antigen CD54)	ICAM1	532	7,30	6,02	2	2
P08574	Cytochrome c1, heme protein, mitochondrial (Complex III subunit 4) (Complex III subunit IV) (Cytochrome b-c1 complex subunit 4)	CYC1	325	6,67	14,77	2	2
P09622	Dihydrolipoyl dehydrogenase, mitochondrial (EC 1.8.1.4) (Dihydrolipoamide dehydrogenase) (Glycine cleavage system L protein)	DLD GCSL LAD PHE3	509	6,68	8,84	2	2
P09913	Interferon-induced protein with tetratricopeptide repeats 2 (IFIT-2) (ISG-54 K) (Interferon-induced 54 kDa protein)	IFIT2 CIG-42 G10P2 IFI54 ISG54	472	6,58	5,08	2	2
P11177	Pyruvate dehydrogenase E1 component subunit beta, mitochondrial (PDHE1-B) (EC 1.2.4.1)	PDHB PHE1B	359	6,98	9,47	2	2
P13073	Cytochrome c oxidase subunit 4 isoform 1, mitochondrial (Cytochrome c oxidase polypeptide IV)	COX4I1 COX4	169	6,35	14,20	2	2
P14314	Glucosidase 2 subunit beta (80K-H protein) (Glucosidase II subunit beta) (Protein kinase C substrate 60.1 kDa protein heavy chain) (PKCSH)	PRKCSH G19P1	528	7,64	7,39	2	2
P14618	Pyruvate kinase PKM (EC 2.7.1.40) (Cytosolic thyroid hormone-binding protein) (CTHBP) (Opa-interacting protein 3) (OIP-3)	PKM OIP3 PK2 PK3 PKM2	531	7,00	4,52	2	2
P15374	Ubiquitin carboxyl-terminal hydrolase isozyme L3 (UCH-L3) (EC 3.4.19.12) (Ubiquitin thioesterase L3)	UCHL3	230	6,40	14,35	2	2
P16615	Sarcoplasmic/endoplasmic reticulum calcium ATPase 2 (SERCA2) (SR Ca(2+)-ATPase 2) (EC 3.6.3.8) (Calcium pump 2)	ATP2A2 ATP2B	1042	7,01	2,30	2	2
P18621	60S ribosomal protein L17 (60S ribosomal protein L23) (PD-1)	RPL17	184	5,92	13,04	2	2
P22087	rRNA 2'-O-methyltransferase fibrillarin (EC 2.1.1.-) (34 kDa nucleolar scleroderma antigen)	FBL FIB1 FLRN	321	8,30	11,84	2	2

Appendix

P25789	Proteasome subunit alpha type-4 (EC 3.4.25.1) (Macropain subunit C9) (Multicatalytic endopeptidase complex subunit C9)	PSMA4 HC9 PSC9	261	6,53	12,26	2	2
P28066	Proteasome subunit alpha type-5 (EC 3.4.25.1) (Macropain zeta chain) (Multicatalytic endopeptidase complex zeta chain)	PSMA5	241	9,12	17,01	2	2
P29728	2'-5'-oligoadenylate synthase 2 ((2-5')oligo(A) synthase 2) (2-5A synthase 2) (EC 2.7.7.84) (p69 OAS / p71 OAS) (p69OAS / p71OAS)	OAS2	719	7,19	4,17	2	2
P36542	ATP synthase subunit gamma, mitochondrial (F-ATPase gamma subunit)	ATP5C1 ATP5C ATP5CL1	298	7,05	7,72	2	2
P36776	Lon protease homolog, mitochondrial (EC 3.4.21.-) (LONHs) (Lon protease-like protein) (LONP)	LONP1 PRSS15	959	6,66	6,67	2	2
P46778	60S ribosomal protein L21	RPL21	160	7,71	16,25	2	2
P46783	40S ribosomal protein S10	RPS10	165	8,94	17,58	2	2
P50402	Emerin	EMD EDMD STA	254	8,63	9,84	2	2
P51114	Fragile X mental retardation syndrome-related protein 1 (hFXR1p)	FXR1	621	8,94	7,25	2	2
P51571	Translocon-associated protein subunit delta (TRAP-delta) (Signal sequence receptor subunit delta) (SSR-delta)	SSR4 TRAPD	173	6,10	13,29	2	2
P51665	26S proteasome non-ATPase regulatory subunit 7 (26S proteasome regulatory subunit RPN8) (26S proteasome regulatory subunit S12)	PSMD7 MOV34L	324	7,91	12,65	2	2
P52732	Kinesin-like protein KIF11 (Kinesin-like protein 1) (Kinesin-like spindle protein HKSP) (Kinesin-related motor protein Eg5)	KIF11 EG5 KNSL1 TRIP5	1056	9,35	3,60	2	2
P53396	ATP-citrate synthase (EC 2.3.3.8) (ATP-citrate (pro-S)-lyase) (ACL) (Citrate cleavage enzyme)	ACLY	1101	6,36	1,82	2	2
P53618	Coatomer subunit beta (Beta-coat protein) (Beta-COP)	COPB1 COPB MSTP026	953	6,65	3,46	2	2
P54136	Arginine-tRNA ligase, cytoplasmic (EC 6.1.1.19) (Arginyl-tRNA synthetase) (ArgRS)	RARS	660	6,41	4,70	2	2
P55084	Trifunctional enzyme subunit beta, mitochondrial (TP-beta) [Includes: 3-ketoacyl-CoA thiolase (EC 2.3.1.16)]	HADHB MSTP029	474	7,46	5,27	2	2
P55735	Protein SEC13 homolog (SEC13-like protein 1) (SEC13-related protein)	SEC13 D3S1231E SEC13L1 SEC13R	322	8,94	9,94	2	2
P55884	Eukaryotic translation initiation factor 3 subunit B (eIF3b) (Eukaryotic translation initiation factor 3 subunit 9) (Prt1 homolog)	EIF3B EIF3S9	814	7,95	4,05	2	2
P59998	Actin-related protein 2/3 complex subunit 4 (Arp2/3 complex 20 kDa subunit) (p20-ARC)	ARPC4 ARC20	168	6,11	11,31	2	2
P60981	Destrin (Actin-depolymerizing factor) (ADF)	DSTN ACTDP DSN	165	8,22	17,58	2	2

P61254	60S ribosomal protein L26	RPL26	145	6,17	11,72	2	2
P61513	60S ribosomal protein L37a	RPL37A	92	7,96	32,61	2	2
P61964	WD repeat-containing protein 5 (BMP2-induced 3-kb gene protein)	WDR5 BIG3	334	8,42	12,87	2	2
P62081	40S ribosomal protein S7	RPS7	194	7,82	26,80	2	2
P62306	Small nuclear ribonucleoprotein F (snRNP-F) (Sm protein F) (Sm-F) (SmF)	SNRPF PBSCF	86	7,95	55,81	2	2
P62318	Small nuclear ribonucleoprotein Sm D3 (Sm-D3) (snRNP core protein D3)	SNRPD3	126	9,03	24,60	2	2
P62841	40S ribosomal protein S15 (RIG protein)	RPS15 RIG	145	8,92	28,28	2	2
P62854	40S ribosomal protein S26	RPS26	115	7,31	18,26	2	2
P62857	40S ribosomal protein S28	RPS28	69	6,37	33,33	2	2
P62899	60S ribosomal protein L31	RPL31	125	6,15	18,40	2	2
P62906	60S ribosomal protein L10a (CSA-19) (Neural precursor cell expressed developmentally down-regulated protein 6) (NEDD-6)	RPL10A NEDD6	217	8,52	13,36	2	2
P62917	60S ribosomal protein L8	RPL8	257	7,81	10,51	2	2
P63208	S-phase kinase-associated protein 1 (Cyclin-A/CDK2-associated protein p19) (Organ of Corti protein 2) (OCP-2)	SKP1 EMC19 OCP2 SKP1A TCEB1L	163	8,14	15,95	2	2
P68400	Casein kinase II subunit alpha (CK II alpha) (EC 2.7.11.1)	CSNK2A1 CK2A1	391	8,30	8,95	2	2
P78524	Suppression of tumorigenicity 5 protein (DENN domain-containing protein 2B) (HeLa tumor suppression 1)	ST5 DENND2B HTS1	1137	8,50	3,61	2	2
P81605	Dermcidin (EC 3.4.-.-) (Preproteolysin) [Cleaved into: Survival-promoting peptide; DCD-1]	DCD AIDD DSEP	110	6,75	20,00	2	2
P82933	28S ribosomal protein S9, mitochondrial (MRP-S9) (S9mt)	MRPS9 RPMS9	396	8,39	7,07	2	2
P83731	60S ribosomal protein L24 (60S ribosomal protein L30)	RPL24	157	7,08	13,38	2	2
P84090	Enhancer of rudimentary homolog	ERH	104	9,24	26,92	2	2
Q00325	Phosphate carrier protein, mitochondrial (Phosphate transport protein) (PTP) (Solute carrier family 25 member 3)	SLC25A3 PHC OK/SW-cl.48	362	7,29	7,73	2	2
Q12797	Aspartyl/asparaginyl beta-hydroxylase (EC 1.14.11.16) (Aspartate beta-hydroxylase) (ASP beta-hydroxylase)	ASPH	758	6,66	8,05	2	2

Appendix

Q13155	Aminoacyl tRNA synthase complex-interacting multifunctional protein 2 (Multisynthase complex auxiliary component p38)	AIMP2 JTV1 PRO0992	320	8,03	13,13	2	2
Q13257	Mitotic spindle assembly checkpoint protein MAD2A (HsMAD2) (Mitotic arrest deficient 2-like protein 1) (MAD2-like protein 1)	MAD2L1 MAD2	205	8,03	15,61	2	2
Q13283	Ras GTPase-activating protein-binding protein 1 (G3BP-1) (EC 3.6.4.12) (EC 3.6.4.13) (ATP-dependent DNA helicase VIII)	G3BP1 G3BP	466	7,92	7,08	2	2
Q13765	Nascent polypeptide-associated complex subunit alpha (NAC-alpha) (Alpha-NAC)	NACA HSD48	215	7,94	13,02	2	2
Q14152	Eukaryotic translation initiation factor 3 subunit A (eIF3a) (Eukaryotic translation initiation factor 3 subunit 10)	EIF3A EIF3S10 KIAA0139	1382	7,45	2,03	2	2
Q14157	Ubiquitin-associated protein 2-like (Protein NICE-4)	UBAP2L KIAA0144 NICE4	1087	8,93	3,04	2	2
Q14498	RNA-binding protein 39 (Hepatocellular carcinoma protein 1) (RNA-binding motif protein 39)	RBM39 HCC1 RNPC2	530	9,19	5,28	2	2
Q14697	Neutral alpha-glucosidase AB (EC 3.2.1.84) (Alpha-glucosidase 2) (Glucosidase II subunit alpha)	GANAB G2AN KIAA0088	944	7,33	4,66	2	2
Q15003	Condensin complex subunit 2 (Barren homolog protein 1) (Chromosome-associated protein H) (hCAP-H) (Non-SMC condensin I complex subunit)	NCAPH BRRN BRRN1 CAPH KIAA0074	741	6,24	4,99	2	2
Q15019	Septin-2 (Neural precursor cell expressed developmentally down-regulated protein 5) (NEDD-5)	SEPT2 DIFF6 KIAA0158 NEDD5	361	7,50	8,31	2	2
Q15369	Transcription elongation factor B polypeptide 1 (Elongin 15 kDa subunit) (Elongin-C) (EloC)	TCEB1	112	9,08	30,36	2	2
Q16204	Coiled-coil domain-containing protein 6 (Papillary thyroid carcinoma-encoded protein) (Protein H4)	CCDC6 D10S170 TST1	474	7,22	6,54	2	2
Q16891	Mitochondrial inner membrane protein (Cell proliferation-inducing gene 4/52 protein) (Mitofilin) (p87/89)	IMMT HMP MINOS2 PIG4 PIG52	758	7,19	6,99	2	2
Q5BKZ1	DBIRD complex subunit ZNF326 (Zinc finger protein 326) (Zinc finger protein interacting with mRNPs and DBC1)	ZNF326 ZIRD	582	7,70	8,25	2	2
Q5T4S7	E3 ubiquitin-protein ligase UBR4 (EC 6.3.2.-) (600 kDa retinoblastoma protein-associated factor) (N-recogin-4)	UBR4 KIAA0462 KIAA1307 RBAF600 ZUBR1	5183	6,17	0,89	2	2
Q5W0B1	RING finger protein 219	RNF219 C13orf7	726	6,57	3,72	2	2
Q6NZI2	Polymerase I and transcript release factor (Cavin-1)	PTRF FKSG13	390	8,89	10,77	2	2
Q6PD62	RNA polymerase-associated protein CTR9 homolog (SH2 domain-binding protein 1)	CTR9 KIAA0155 SH2BP1	1173	8,01	3,32	2	2
Q6PJ61	F-box only protein 46 (F-box only protein 34-like)	FBXO46 FBX46 FBXO34L	603	8,15	7,79	2	2

Q6UWZ7	BRCA1-A complex subunit Abraxas (Coiled-coil domain-containing protein 98) (Protein FAM175A)	FAM175A ABRA1 CCDC98 UNQ496/PRO1013	409	7,07	5,87	2	2
Q6ZW31	Rho GTPase-activating protein SYDE1 (Synapse defective protein 1 homolog 1) (Protein syd-1 homolog 1)	SYDE1	735	6,80	3,54	2	2
Q7KZ85	Transcription elongation factor SPT6 (hSPT6) (Histone chaperone suppressor of Ty6) (Tat-cotransactivator 2 protein) (Tat-CT2 protein)	SUPT6H KIAA0162 SPT6H	1726	8,24	3,19	2	2
Q7RTV0	PHD finger-like domain-containing protein 5A (PHD finger-like domain protein 5A) (Splicing factor 3B-associated 14 kDa protein) (SF3b14b)	PHF5A	110	8,87	26,36	2	2
Q86V81	THO complex subunit 4 (Tho4) (Ally of AML-1 and LEF-1) (Aly/REF export factor) (Transcriptional coactivator Aly/REF)	ALYREF ALY BEF THOC4	257	9,52	15,18	2	2
Q86VM9	Zinc finger CCCH domain-containing protein 18 (Nuclear protein NHN1)	ZC3H18 NHN1	953	9,73	4,41	2	2
Q86YT6	E3 ubiquitin-protein ligase MIB1 (EC 6.3.2.-) (DAPK-interacting protein 1) (DIP-1) (Mind bomb homolog 1)	MIB1 DIP1 KIAA1323 ZZANK2	1006	7,58	3,28	2	2
Q8IVM0	Coiled-coil domain-containing protein 50 (Protein Ymer)	CCDC50 C3orf6	306	7,52	7,52	2	2
Q8N2S1	Latent-transforming growth factor beta-binding protein 4 (LTBP-4)	LTBP4	1624	7,57	3,20	2	2
Q8N3V7	Synaptopodin	SYNPO KIAA1029	929	8,30	4,95	2	2
Q8NCA5	Protein FAM98A	FAM98A	519	11,58	13,29	2	2
Q8NHZ8	Anaphase-promoting complex subunit CDC26 (Anaphase-promoting complex subunit 12) (APC12) (Cell division cycle protein 26 homolog)	CDC26 ANAPC12 C9orf17	85	7,70	42,35	2	2
Q8WV41	Sorting nexin-33 (SH3 and PX domain-containing protein 3)	SNX33 SH3PX3 SH3PXD3C SNX30	574	8,47	7,84	2	2
Q8WXI9	Transcriptional repressor p66-beta (GATA zinc finger domain-containing protein 2B) (p66/p68)	GATAD2B KIAA1150	593	6,69	3,88	2	2
Q93009	Ubiquitin carboxyl-terminal hydrolase 7 (EC 3.4.19.12) (Deubiquitinating enzyme 7)	USP7 HAUSP	1102	6,75	3,63	2	2
Q96CW1	AP-2 complex subunit mu (AP-2 mu chain) (Adapter-related protein complex 2 subunit mu) (Adaptin-mu2)	AP2M1 CLAPM1 KIAA0109	435	6,13	8,51	2	2
Q96DI7	U5 small nuclear ribonucleoprotein 40 kDa protein (U5 snRNP 40 kDa protein) (U5-40K) (38 kDa-splicing factor)	SNRNP40 PRP8BP SFP38 WDR57	357	9,19	16,25	2	2
Q96HS1	Serine/threonine-protein phosphatase PGAM5, mitochondrial (EC 3.1.3.16) (Bcl-XL-binding protein v68) (Phosphoglycerate mutase family member 5)	PGAM5	289	7,64	7,96	2	2
Q9BPX5	Actin-related protein 2/3 complex subunit 5-like protein (Arp2/3 complex 16 kDa subunit 2) (ARC16-2)	ARPC5L	153	7,02	15,03	2	2

Appendix

Q9BQ67	Glutamate-rich WD repeat-containing protein 1	GRWD1 KIAA1942 WDR28	446	6,36	11,66	2	2
Q9BUJ2	Heterogeneous nuclear ribonucleoprotein U-like protein 1 (Adenovirus early region 1B-associated protein 5) (E1B-55 kDa-associated protein 5)	HNRNPUL1 E1BAP5 HNRNPUL1	856	7,64	3,27	2	2
Q9BVP2	Guanine nucleotide-binding protein-like 3 (E2-induced gene 3 protein) (Novel nucleolar protein 47) (NNP47)	GNL3 E2IG3 NS	549	6,67	5,65	2	2
Q9BYG3	MKI67 FHA domain-interacting nucleolar phosphoprotein (Nucleolar phosphoprotein Nopp34)	NIFK MKI67IP NOPP34	293	7,07	9,56	2	2
Q9GZL7	Ribosome biogenesis protein WDR12 (WD repeat-containing protein 12)	WDR12	423	5,83	7,33	2	2
Q9GZS3	WD repeat-containing protein 61 (Meiotic recombination REC14 protein homolog) (SKI8 homolog) (Ski8)	WDR61	305	6,76	12,13	2	2
Q9H0A0	N-acetyltransferase 10 (EC 2.3.1.-)	NAT10 ALP KIAA1709	1025	8,60	2,93	2	2
Q9H1I8	Activating signal cointegrator 1 complex subunit 2 (ASC-1 complex subunit p100) (Trip4 complex subunit p100)	ASCC2 ASC1P100	757	7,68	4,76	2	2
Q9H6R4	Nucleolar protein 6 (Nucleolar RNA-associated protein) (Nrap)	NOL6	1146	6,32	3,93	2	2
Q9H6R7	WD repeat-containing protein C2orf44	C2orf44 PP384	721	7,45	2,77	2	2
Q9H6X2	Anthrax toxin receptor 1 (Tumor endothelial marker 8)	ANTXR1 ATR TEM8	564	6,11	3,90	2	2
Q9H936	Mitochondrial glutamate carrier 1 (GC-1) (Glutamate/H(+) symporter 1) (Solute carrier family 25 member 22)	SLC25A22 GC1	323	8,62	8,67	2	2
Q9H9J4	Ubiquitin carboxyl-terminal hydrolase 42 (EC 3.4.19.12) (Deubiquitinating enzyme 42) (Ubiquitin thioesterase 42)	USP42	1324	7,64	2,79	2	2
Q9HC36	RNA methyltransferase-like protein 1 (EC 2.1.1.-)	RNMTL1 HC90	420	6,76	9,05	2	2
Q9NVP1	ATP-dependent RNA helicase DDX18 (EC 3.6.4.13) (DEAD box protein 18) (Myc-regulated DEAD box protein) (MrDb)	DDX18	670	6,68	5,37	2	2
Q9NXW2	DnaJ homolog subfamily B member 12	DNAJB12	375	6,74	8,80	2	2
Q9UGI0	Ubiquitin thioesterase ZRANB1 (EC 3.4.19.12) (TRAF-binding domain-containing protein) (hTrabid)	ZRANB1 TRABID	708	7,04	6,21	2	2
Q9UHD2	Serine/threonine-protein kinase TBK1 (EC 2.7.11.1) (NF-kappa-B-activating kinase) (T2K) (TANK-binding kinase 1)	TBK1 NAK	729	7,86	5,21	2	2
Q9UM13	Anaphase-promoting complex subunit 10 (APC10) (Cyclosome subunit 10)	ANAPC10 APC10	185	6,00	9,73	2	2

Q9UQ80	Proliferation-associated protein 2G4 (Cell cycle protein p38-2G4 homolog) (hG4-1) (ErbB3-binding protein 1)	PA2G4 EBP1	394	6,84	5,84	2	2
Q9Y277	Voltage-dependent anion-selective channel protein 3 (VDAC-3) (hVDAC3) (Outer mitochondrial membrane protein porin 3)	VDAC3	283	7,27	12,01	2	2
Q9Y2W1	Thyroid hormone receptor-associated protein 3 (Thyroid hormone receptor-associated protein complex 150 kDa component) (Trap150)	THRAP3 TRAP150	955	6,63	3,14	2	2
Q9Y305	Acyl-coenzyme A thioesterase 9, mitochondrial (Acyl-CoA thioesterase 9) (EC 3.1.2.-) (Acyl-CoA thioester hydrolase 9)	ACOT9 CGI-16	439	6,56	7,52	2	2
Q9Y3U8	60S ribosomal protein L36	RPL36	105	6,98	20,00	2	2
Q9Y512	Sorting and assembly machinery component 50 homolog (Transformation-related gene 3 protein) (TRG-3)	SAMM50 SAM50 CGI-51 TRG3	469	7,16	7,89	2	2
Q9Y5A9	YTH domain family protein 2 (CLL-associated antigen KW-14) (High-glucose-regulated protein 8) (Renal carcinoma antigen NY-REN-2)	YTHDF2 HGRG8	579	7,53	4,84	2	2
Q9Y6N5	Sulfide:quinone oxidoreductase, mitochondrial	SQRDL CGI-44	450	6,16	7,78	2	2

11.3 Appendix III. List of the 115 hits identified in both the GST-PLK1-PBD wild-type and the GST-PLK1-PBD-UBI mutant.

Hits were sorted by decreasing number of peptide spectrum mass (PSM) in the GST-PLK1-PBD-UBI sample. Coverage, number of peptides identified and number of PSM are shown for both experiments. PSM differential results in the difference between PSM of GST-PLK1-PBD-UBI and GST-PLK1-PBD. For each protein specifically, high PSM differential correlates with high binding towards the ubiquitinated form of PLK1.

Uniprot ID	Protein names	GST-PLK1-PBD			GST-PLK1-PBD-UBI			PSM differential
		Cov	# Pep	# PSM	Cov	# Pep	# PSM	
O95071	E3 ubiquitin-protein ligase UBR5	6,65	11	11	37,91	67	128	117
P45974	Ubiquitin carboxyl-terminal hydrolase 5	11,89	6	6	53,96	33	111	105
Q92995	Ubiquitin carboxyl-terminal hydrolase 13	3,71	2	2	50,41	28	46	44
O00750	Phosphatidylinositol 4-phosphate 3-kinase C2 domain-containing subunit beta	5,81	4	4	28,34	30	37	33
Q13509	Tubulin beta-3 chain	48,89	17	42	43,11	16	70	28
Q96S55	ATPase WRNIP1	27,52	12	13	47,37	18	32	19
Q9H1A4	Anaphase-promoting complex subunit 1	2,16	3	4	15,95	18	22	18
Q7Z569	BRCA1-associated protein	4,56	2	2	37,50	15	19	17
Q9UJX2	Cell division cycle protein 23 homolog	15,58	6	7	44,05	19	23	16
Q9BUF5	Tubulin beta-6 chain	44,84	13	22	47,76	13	35	13
Q9YST5	Ubiquitin carboxyl-terminal hydrolase 16	17,38	10	10	29,04	15	19	9
Q13045	Protein flightless-1 homolog	10,72	8	8	22,77	16	17	9
P31327	Carbamoyl-phosphate synthase [ammonia], mitochondrial	5,07	3	4	13,00	10	13	9
Q13586	Stromal interaction molecule 1	8,03	3	4	25,40	11	13	9
Q9UJX3	Anaphase-promoting complex subunit 7	17,86	7	8	33,22	14	16	8
Q13042	Cell division cycle protein 16 homolog	23,23	8	8	34,68	14	15	7
Q9UJX4	Anaphase-promoting complex subunit 5	7,81	3	3	14,83	8	10	7
Q12834	Cell division cycle protein 20 homolog	16,03	5	6	29,66	7	12	6
Q13200	26S proteasome non-ATPase regulatory subunit 2	2,64	2	2	9,03	5	6	4
Q96RL1	BRCA1-A complex subunit RAP80	13,91	4	4	14,46	6	7	3
Q9NQC7	Ubiquitin carboxyl-terminal hydrolase CYLD	2,72	2	3	8,37	6	6	3
O14964	Hepatocyte growth factor-regulated tyrosine kinase substrate	12,61	7	8	19,31	10	10	2
O75128	Protein cordon-bleu	4,12	4	5	6,19	6	7	2

Q96EY1	DnaJ homolog subfamily A member 3, mitochondrial	10,00	4	5	22,71	6	7	2
Q9NS91	E3 ubiquitin-protein ligase RAD18	13,13	5	5	15,96	6	7	2
O15037	Protein KHNYN	6,34	3	4	8,55	4	6	2
Q8NCE2	Myotubularin-related protein 14	11,38	4	4	14,31	6	6	2
P17980	26S protease regulatory subunit 6A	7,74	2	2	10,48	3	4	2
Q93008	Probable ubiquitin carboxyl-terminal hydrolase FAF-X	8,72	13	13	7,32	12	14	1
P62805	Histone H4	27,18	3	3	38,83	4	4	1
Q92547	DNA topoisomerase 2-binding protein 1	4,34	3	3	4,40	4	4	1
Q7Z6Z7	E3 ubiquitin-protein ligase HUWE1	16,44	43	49	16,85	43	49	0
Q8NHV4	Protein NEDD1	8,64	5	5	6,82	4	5	0
P51610	Host cell factor 1	3,49	3	4	2,36	3	4	0
Q00587	Cdc42 effector protein 1	21,48	4	4	16,37	3	4	0
P13674	Prolyl 4-hydroxylase subunit alpha-1	11,05	3	3	6,93	3	3	0
Q8N1F7	Nuclear pore complex protein Nup93	5,86	3	3	5,01	3	3	0
P52732	Kinesin-like protein KIF11	3,69	2	2	3,60	2	2	0
Q53GT1	Kelch-like protein 22	35,65	14	18	33,28	12	17	-1
O14545	TRAF-type zinc finger domain-containing protein 1	25,09	8	9	23,71	8	8	-1
Q96II8	Leucine-rich repeat and calponin homology domain-containing protein 3	23,17	9	9	18,79	7	8	-1
Q3ZCQ8	Mitochondrial import inner membrane translocase subunit TIM50	22,95	6	7	20,68	5	6	-1
O60573	Eukaryotic translation initiation factor 4E type 2	27,35	5	5	22,86	4	4	-1
P41743	Protein kinase C iota type	14,26	4	4	10,57	3	3	-1
Q02241	Kinesin-like protein KIF23	6,56	4	4	6,46	3	3	-1
P14618	Pyruvate kinase PKM	8,66	3	3	4,52	2	2	-1
P50402	Emerin	21,65	3	3	9,84	2	2	-1
Q15019	Septin-2	15,79	3	3	8,31	2	2	-1
Q15369	Transcription elongation factor B polypeptide 1	30,36	2	3	30,36	2	2	-1
Q8N3V7	Synaptopodin	6,57	3	3	4,95	2	2	-1
Q8WXI9	Transcriptional repressor p66-beta	8,09	3	3	3,88	2	2	-1
Q9Y5A9	YTH domain family protein 2	7,08	3	3	4,84	2	2	-1
O60566	Mitotic checkpoint serine/threonine-protein kinase BUB1 beta	19,52	13	15	15,62	10	13	-2
P30260	Cell division cycle protein 27 homolog	22,33	12	13	21,12	11	11	-2
O43684	Mitotic checkpoint protein BUB3	37,50	6	8	21,04	5	6	-2
P60842	Eukaryotic initiation factor 4A-I	25,62	7	7	14,53	4	5	-2
P47755	F-actin-capping protein subunit alpha-2	33,57	5	5	16,43	3	3	-2
Q9P0U4	CpG-binding protein	11,89	5	5	7,77	3	3	-2
P28066	Proteasome subunit alpha type-5	17,01	3	4	17,01	2	2	-2
P36776	Lon protease homolog, mitochondrial	9,18	4	4	6,67	2	2	-2

Appendix

P84090	Enhancer of rudimentary homolog	26,92	2	4	26,92	2	2	-2
Q93009	Ubiquitin carboxyl-terminal hydrolase 7	5,63	4	4	3,63	2	2	-2
Q9BQE3	Tubulin alpha-1C chain	70,38	20	44	67,26	20	41	-3
Q7Z5K2	Wings apart-like protein homolog	26,13	19	19	19,08	14	16	-3
Q14192	Four and a half LIM domains protein 2	52,69	10	14	50,54	9	11	-3
P57740	Nuclear pore complex protein Nup107	16,54	9	9	12,22	6	6	-3
Q8IW35	Centrosomal protein of 97 kDa	20,23	9	9	11,33	6	6	-3
Q9P0K7	Ankycorbin	10,61	7	7	4,39	4	4	-3
Q9Y678	Coatomer subunit gamma-1	15,68	7	7	8,24	3	4	-3
P63010	AP-2 complex subunit beta	12,27	6	6	8,75	3	3	-3
Q6Y7W6	PERQ amino acid-rich with GYF domain-containing protein 2	25,56	16	20	18,55	14	16	-4
P53621	Coatomer subunit alpha	21,65	16	18	18,06	14	14	-4
O43175	D-3-phosphoglycerate dehydrogenase	23,83	8	8	9,19	4	4	-4
Q12769	Nuclear pore complex protein Nup160	9,54	7	8	5,36	4	4	-4
Q92783	Signal transducing adapter molecule 1	26,85	7	8	17,59	4	4	-4
P54132	Bloom syndrome protein	9,03	7	7	4,16	3	3	-4
Q9UQE7	Structural maintenance of chromosomes protein 3	10,02	9	9	3,94	3	4	-5
Q15003	Condensin complex subunit 2	14,84	6	7	4,99	2	2	-5
Q9UK59	Lariat debranching enzyme	20,40	8	10	10,29	4	4	-6
Q14697	Neutral alpha-glucosidase AB	12,18	6	8	4,66	2	2	-6
Q5W0B1	RING finger protein 219	17,08	8	8	3,72	2	2	-6
P68366	Tubulin alpha-4A chain	58,26	19	38	55,13	17	31	-7
Q13409	Cytoplasmic dynein 1 intermediate chain 2	29,94	9	10	3,76	2	3	-7
O60716	Catenin delta-1	14,46	8	9	4,03	2	2	-7
O43823	A-kinase anchor protein 8	26,59	12	14	12,86	5	6	-8
Q09028	Histone-binding protein RBBP4	51,06	10	11	11,29	3	3	-8
Q8WUF5	RelA-associated inhibitor	29,35	17	18	19,32	9	9	-9
Q96GX5	Serine/threonine-protein kinase greatwall	19,91	12	14	6,14	4	5	-9
O60216	Double-strand-break repair protein rad21 homolog	27,10	9	12	7,29	2	3	-9
Q7KZ85	Transcription elongation factor SPT6	11,88	11	11	3,19	2	2	-9
O60271	C-Jun-amino-terminal kinase-interacting protein 4	33,08	31	34	23,62	22	24	-10
P42566	Epidermal growth factor receptor substrate 15	32,03	15	16	9,93	5	6	-10
P78347	General transcription factor II-I	24,75	17	19	10,02	7	8	-11
Q86TC9	Myopalladin	16,21	13	15	5,45	3	4	-11
Q12888	Tumor suppressor p53-binding protein 1	11,97	13	14	4,01	3	3	-11
Q14974	Importin subunit beta-1	26,37	13	14	4,91	3	3	-11
Q14498	RNA-binding protein 39	30,19	12	13	5,28	2	2	-11
P35606	Coatomer subunit beta	33,11	18	19	11,70	6	7	-12
Q86SQ0	Pleckstrin homology-like domain family B member 2	20,51	18	19	11,01	7	7	-12

Q8WUM0	Nuclear pore complex protein Nup133	22,75	16	18	9,34	6	6	-12
Q5T4S7	E3 ubiquitin-protein ligase UBR4	4,98	13	14	0,89	2	2	-12
Q08499	cAMP-specific 3',5'-cyclic phosphodiesterase 4D	22,99	14	18	11,74	5	5	-13
Q14839	Chromodomain-helicase-DNA-binding protein 4	13,81	15	17	4,03	4	4	-13
Q16204	Coiled-coil domain-containing protein 6	26,79	10	15	6,54	2	2	-13
O15027	Protein transport protein Sec16A	10,37	10	17	1,51	3	3	-14
P52701	DNA mismatch repair protein Msh6	18,75	16	17	4,04	3	3	-14
P00533	Epidermal growth factor receptor	17,11	13	18	4,05	3	3	-15
P68400	Casein kinase II subunit alpha	47,83	13	18	8,95	2	2	-16
Q9Y2W1	Thyroid hormone receptor-associated protein 3	20,52	15	18	3,14	2	2	-16
Q9UBC2	Epidermal growth factor receptor substrate 15-like 1	39,00	20	24	14,24	6	6	-18
Q9UDY2	Tight junction protein ZO-2	20,92	15	22	4,54	4	4	-18
O00267	Transcription elongation factor SPT5	34,41	22	23	5,89	3	4	-19
P09913	Interferon-induced protein with tetratricopeptide repeats 2	43,01	16	23	5,08	2	2	-21
Q5JSZ5	Protein PRRC2B	16,42	24	29	4,13	5	6	-23
Q14157	Ubiquitin-associated protein 2-like	36,89	22	43	3,04	2	2	-41

**Molecular mechanisms of PLK1 recognition by CUL3/KLHL22
E3-ubiquitin ligase controlling mitotic progression**

Résumé

L'ubiquitination est une modification post-traductionnelle impliquée dans de nombreux mécanismes cellulaires. L'E3-ubiquitine ligase CULLIN 3 (CUL3) est un régulateur essentiel de la progression mitotique, ubiquitinant d'importants régulateurs mitotiques et contrôlant leur localisation subcellulaire. Plus particulièrement, notre travail décrit le rôle de la nouvelle E3-ligase CUL3/KLHL22 dans la régulation de l'activité localisée de Polo-like kinase 1 (PLK1) et de ce fait dans l'établissement d'une progression mitotique précise. Néanmoins, les mécanismes moléculaires qui régissent la reconnaissance de son substrat par CUL3 demeurent inconnus. L'activité catalytique de PLK1 ne semble pas être nécessaire à son interaction avec KLHL22, mais aussi bien son domaine kinase que Polo-box (PBD) suffisent à co-purifier KLHL22. Des mutations au niveau du motif DFG, situé en amont du domaine kinase, et du tryptophane 414 au sein du PBD semblent influencer sur la reconnaissance de KLHL22. Les résultats obtenus montrent les premières indications biochimiques du mode d'interaction du complexe CUL3/KLHL22/PLK1.

Mots clés : mitose, ubiquitin, Cullin, kinases, protéines BTB-Kelch CUL3, PLK1, KLHL22.

Résumé en anglais

Ubiquitination is a post-translational modification involved in many cellular processes. The E3 ubiquitin-ligase based on CULLIN 3 protein (CUL3) is an essential regulator of mitotic division in human cells by ubiquitinating several important mitotic regulators and controlling their subcellular localization. In particular, our work described the role of novel CUL3/KLHL22 E3-ligase in regulation of localized activity of Polo-like kinase 1 (PLK1) and thereby faithful mitotic progression. However, the molecular mechanisms of substrate recognition by CUL3 remain unknown. The catalytic activity of PLK1 may not be required for binding KLHL22 but both the kinase and the Polo-box domains are sufficient to co-purify KLHL22. Mutating the DFG motif within the kinase domain and the tryptophan 414 within the PBD influence the binding to KLHL22. These results provide first insights into molecular mechanisms of CUL3/KLHL22/PLK1 complex.

Keywords : mitosis, ubiquitin, Cullin, kinases, BTB-Kelch proteins CUL3, PLK1, KLHL22.